

**THE GENERAL EVALUATION OF THE NODAL  
SYNTHESIS METHOD IN NUCLEAR REACTOR  
TRANSIENT ANALYSIS**

by

**Weng-Sheng Kuo**

B.S., Chung Cheng Institute of Technology, Taiwan, ROC (1981)

M.S., National Tsing Hwa University, Taiwan, ROC (1986)

S.M., Massachusetts Institute of Technology (1991)

Nucl.E., Massachusetts Institute of Technology (1991)

Submitted to the Department of Nuclear Engineering  
in partial fulfillment of the requirements for the degree of

**DOCTOR OF PHILOSOPHY**

at the

**MASSACHUSETTS INSTITUTE OF TECHNOLOGY**

December 1993

©Weng-Sheng Kuo, MCMXCIII. All rights reserved.

The author hereby grants to MIT permission to reproduce and  
to distribute copies of this thesis document in whole or in part.

Author ..... *J* .....  
Department of Nuclear Engineering  
December 21, 1993

Certified by ..... *J* ..... Allan F. Henry  
Professor of Nuclear Engineering  
Thesis Supervisor

Certified by ..... *J* ..... David D. Lanning  
Professor of Nuclear Engineering  
Thesis Reader

Accepted by ..... *J* ..... Allan F. Henry  
MASSACHUSETTS INSTITUTE  
OF TECHNOLOGY Chairman, Departmental Committee on Graduate Students

APR 26 1994

LIBRARIES

Science

# **THE GENERAL EVALUATION OF THE NODAL SYNTHESIS METHOD IN NUCLEAR REACTOR TRANSIENT ANALYSIS**

by

**Weng-Sheng Kuo**

Submitted to the Department of Nuclear Engineering  
on December 21, 1993, in partial fulfillment of the  
requirements for the degree of  
**DOCTOR OF PHILOSOPHY**

## **Abstract**

This thesis evaluates the nodal synthesis method for nuclear reactor transient analysis. The basic idea of the nodal synthesis method is to expand the time-dependent neutron fluxes as a linear combination of a set of pre-computed static trial functions with unknown time-dependent mixing coefficients. The mixing coefficients are then obtained from a weighted-residual approach. The main purpose is to investigate the feasibility of the nodal synthesis model for real- or near real-time application to tightly coupled cores such as the MIT Research Reactor.

The approach consists of two portions. First, the theoretical nodal synthesis model, which is based on the coarse-mesh, finite-difference neutron diffusion equations with discontinuity factors, is studied. The neutron fluxes are expanded and substituted into those governing equations, and then the mixing coefficients are calculated by the weighted-residual method. Several one-dimensional, steady-state and transient test problems are analyzed to evaluate the accuracy and computational efficiency of the theoretical nodal synthesis model.

The second part is the validation of an approach which can be taken to determine the few-group nodal parameters for the application of the experimental nodal synthesis method to transient studies involving the MIT Research Reactor. The approach uses the Monte-Carlo code MCNP to generate few-group nodal cross sections and discontinuity factors for the triangular-z nodal diffusion code QUARTZ. A simple test problem was analyzed to demonstrate the procedure.

The main findings are that (1) the nodal synthesis model can reproduce reference neutron-flux distributions with an average error in total reactor power of about 1-2 %; (2) the computing speed for the nodal synthesis model is not fast enough for practical applications; and (3) good statistical behavior and the determination of accurate group-to-group scattering cross sections are two key factors for the complete validation of the MCNP-QUARTZ procedure.

Thesis Supervisor: Allan F. Henry  
Title: Professor of Nuclear Engineering

## **Acknowledgments**

The author would like to sincerely appreciate his thesis supervisor, Prof. Allan F. Henry. Without his guidance and encouragement, this thesis can not be completed.

Thanks are given to Prof. David D. Lanning for reading the thesis.

The author is also in debt to Dr. John A. Bernard for his financial support.

Special thanks are also given to the Department of Energy for sponsoring author's research project.

The author would also like to thank the Institute of Nuclear Energy Research of the Atomic Energy Commission at Taiwan for their sponsor and support.

Finally, the author would like to thank his wife, Rong-Hwa Feng, for her consistent backup, endless patience, and sometimes stringent pushing.

# Table of Contents

<b>Abstract</b>	<b>2</b>
<b>Acknowledgement</b>	<b>3</b>
<b>Table of Contents</b>	<b>4</b>
<b>List of Figures</b>	<b>9</b>
<b>List of Tables</b>	<b>13</b>
<b>Chapter 1 Introduction</b>	<b>15</b>
1.1 Overview . . . . .	15
1.2 Objective and Approach . . . . .	18
1.2.1 Objective . . . . .	18
1.2.2 Theoretical Nodal Synthesis Approach . . . . .	18
1.2.3 Experimental Nodal Synthesis Approach . . . . .	19
1.3 Thesis Organization . . . . .	21
<b>Chapter 2 Theoretical Nodal Synthesis Approach</b>	<b>22</b>
2.1 Introduction . . . . .	22
2.2 Nodal Equations Having the CMFD Form . . . . .	22
2.2.1 The Equations . . . . .	22
2.2.2 The Boundary Conditions . . . . .	27
2.3 Derivation of the General Nodal Synthesis Model . . . . .	30
2.4 Derivation of the Collapsed-Group Nodal Synthesis Model . . . . .	35
2.5 Numerical Methods for Solving the Nodal Synthesis Equations . . . . .	37
2.5.1 Steady-State Solution . . . . .	37

2.5.2	Transient Solution . . . . .	39
2.6	Methods for Updating the Discontinuity Factors . . . . .	42
2.7	Summary . . . . .	43
<b>Chapter 3 Implementaion of the Nodal Synthesis Models to One-Dimensional Computer Codes</b>		<b>44</b>
3.1	Introduction . . . . .	44
3.2	SYN1T: One-Dimensional General Nodal Synthesis Code . . . . .	46
3.2.1	General Characteristics . . . . .	46
3.2.2	CMFD Discontinuity Factors . . . . .	52
3.2.3	Zero-Flux Boundary Correction Factors . . . . .	52
3.2.4	Thermal-Hydraulic Model . . . . .	54
3.2.5	Cross-Section Feedback Mechanism . . . . .	55
3.2.6	Variable Rod-Position Problems . . . . .	56
3.2.7	Convergence Test for Steady-State Problems . . . . .	60
3.2.8	Transient Problems . . . . .	61
3.2.9	Total Reactivity . . . . .	61
3.3	SYN1CG: One-Dimensional Collapsed-Group Nodal Synthesis Code . . . . .	62
3.4	Summary . . . . .	68
<b>Chapter 4 One-Dimensional Numerical Tests of the Theoretical Nodal Synthesis Models</b>		<b>69</b>
4.1	Introduction . . . . .	69
4.2	Tests of the General Nodal Synthesis Model . . . . .	69
4.2.1	Steady-State Problems . . . . .	69
4.2.1.1	Variable Inlet Coolant Temperature Problem . . . . .	70
4.2.1.2	Variable Rod-Position Problem 1 – Fully-Rodded Case . .	81
4.2.1.3	Variable Rod-Position Problem 2 – Partially-Rodded Case	88
4.2.2	Transient Problem . . . . .	97
4.3	Tests of the Collapsed-Group Nodal Synthesis Model . . . . .	112
4.3.1	Steady-State Problem . . . . .	112
4.3.2	Transient Problem . . . . .	113
4.4	Comparison of the Nodal Synthesis Models . . . . .	121

4.4.1 Accuracy . . . . .	121
4.4.2 Computing Efficiency . . . . .	124
4.5 Summary . . . . .	126
<b>Chapter 5 Review of the Experimental Nodal Synthesis Model and Application to MITR-II Transient Studies</b>	<b>127</b>
5.1 Introduction . . . . .	127
5.2 Review of the Experimental Nodal Synthesis Model . . . . .	128
5.2.1 Governing Equations . . . . .	128
5.2.2 Solution Method . . . . .	129
5.3 Application of the Experimental Nodal Synthesis Model to MITR-II Transient Studies . . . . .	130
5.4 Summary . . . . .	131
<b>Chapter 6 Determination of Few-Group Nodal Parameters for the Experimental Nodal Synthesis Model</b>	<b>132</b>
6.1 Introduction . . . . .	132
6.2 Description of MITR-II . . . . .	133
6.3 Description of the MCNP Monte-Carlo Code . . . . .	137
6.4 Description of the QUARTZ Nodal Code . . . . .	138
6.5 Determination of Few-Group Nodal Parameters for QUARTZ . . . . .	139
6.5.1 MCNP Model . . . . .	139
6.5.2 Homogenized Cross Sections . . . . .	154
6.5.3 CMFD Discontinuity Factors . . . . .	156
6.5.4 Albedo Values . . . . .	157
6.6 Self-Consistency Tests of the Nodal Parameters . . . . .	158
6.7 Summary . . . . .	159
<b>Chapter 7 Demonstration of the MCNP-QUARTZ Procedure with a Test Problem</b>	<b>160</b>
7.1 Introduction . . . . .	160
7.2 Description of the Test Problem . . . . .	160
7.3 Determination of Two-Group Nodal Parameters . . . . .	162

7.4 Results and Analysis . . . . .	163
7.5 Summary . . . . .	170
<b>Chapter 8 Summary, Conclusions, and Recommendations</b>	<b>171</b>
8.1 Summary . . . . .	171
8.2 Conclusions . . . . .	172
8.2.1 Theoretical Nodal Synthesis Models . . . . .	172
8.2.2 Experimental Nodal Synthesis Model . . . . .	172
8.3 Recommendations for Future Work . . . . .	173
<b>References</b>	<b>174</b>
<b>Appendix A CMFD-DF3: A Program to Extract CMFD Discontinuity Factors from the QUANDRY Restart File</b>	
A.1 Introduction . . . . .	178
A.2 Program Listing of CMFD-DF3 . . . . .	180
<b>Appendix B ZFXBCC: A Program to Extract Zero-Flux Boundary Correction Factors from the QUANDRY Restart File</b>	
B.1 Introduction . . . . .	185
B.2 Program Listing of ZFXBC . . . . .	187
<b>Appendix C Test Problem Specifications for the Theoretical Nodal Synthesis Models</b>	
C.1 Steady-State Variable Inlet Coolant Temperature Problem . . . . .	202
C.2 Steady-State Variable Rod-Position Problem 1 – Fully-Rodded Case . . . . .	205
C.3 Steady-State Variable Rod-Position Problem 2 – Partially-Rodded Case . . . . .	207
C.4 Transient Variable Inlet Coolant Temperature Problem . . . . .	210
<b>Appendix D MCNP Input Data for the Test Problem</b>	
D.1 Input Data for Tallying Cell Fluxes and Cross Sections . . . . .	215
D.2 Input Data for Tallying Surface Fluxes . . . . .	219
D.3 Input Data for Tallying Surface Currents . . . . .	224
<b>Appendix E Cross Sections, Fluxes, Currents, and CMFD Discontinuity</b>	

<b>Factors for the Test Problem</b>	<b>229</b>
E.1 Nodal Fluxes . . . . .	230
E.2 Two-Group Cross Sections . . . . .	234
E.3 Surface Fluxes . . . . .	240
E.4 Surface Currents . . . . .	247
E.5 CMFD Discontinuity Factors . . . . .	254
<b>Appendix F Scattering Cross Sections for the Test Problem</b>	<b>261</b>
F.1 Introduction . . . . .	262
F.1 Set A . . . . .	263
F.2 Set B . . . . .	265
F.3 Set C . . . . .	267
<b>Appendix G QUARTZ Input Data for the Test Problem</b>	<b>269</b>

# List of Figures

2-1 Schematic node layout . . . . .	25
2-2 CMFD discontinuity factors . . . . .	28
3-1 General Flow Diagram of Nodal Synthesis Calculations . . . . .	45
3-2 Flow diagram of SYN1T (Part 1) . . . . .	47
3-3 Flow diagram of SYN1T (Part 2) . . . . .	48
3-4 Flow diagram of SYN1T (Part 3) . . . . .	49
3-5 A 3-node diagram showing the node-fully-rodded problem . . . . .	57
3-6 A 3-node diagram showing the node-partially-rodded problem . . . . .	59
3-7 Flow diagram of SYN1CG (Part 1) . . . . .	63
3-8 Flow diagram of SYN1CG (Part 2) . . . . .	64
3-9 Flow diagram of SYN1CG (Part 3) . . . . .	65
4-1 Relative error in normalized power density for steady-state case A . . . . .	71
4-2 Thermal fluxes of bracketing states and intermediate state for steady-state case B-1 . . . . .	73
4-3 Thermal fluxes of bracketing states and intermediate state for steady-state case B-2 . . . . .	74
4-4 Thermal fluxes of bracketing states and intermediate state for steady-state case B-3 . . . . .	75
4-5 Relative error in normalized power density for steady-state case B-1 . . . . .	76
4-6 Normalized nodal power density for steady-state case B-2 . . . . .	77
4-7 Relative error in normalized power density for steady-state case B-2 . . . . .	78
4-8 Normalized nodal power density for steady-state case B-3 . . . . .	79
4-9 Relative error in normalized power density for steady-state case B-3 . . . . .	80

4-10 Variable rod-position problem – fully-rodded case . . . . .	81
4-11 Normalized nodal power density for steady-state case C-1 . . . . .	83
4-12 Relative error in normalized nodal power density for steady-state case C-1 . .	83
4-13 Normalized nodal power density for steady-state case C-2 . . . . .	84
4-14 Relative error in normalized nodal power density for steady-state case C-2 .	84
4-15 Normalized nodal power density for steady-state case C-3 . . . . .	85
4-16 Relative error in normalized nodal power density for steady-state case C-3 .	85
4-17 Thermal fluxes of bracketing states and reference state for steady-state case series C . . . . .	86
4-18 Variable rod-position problem – partially-rodded case . . . . .	88
4-19 Normalized nodal power density for steady-state case D-1 . . . . .	90
4-20 Absolute error in normalized nodal power density for steady-state case D-1	90
4-21 Relative error in normalized nodal power density for steady-state case D-1 .	91
4-22 Normalized nodal power density for steady-state case D-2 . . . . .	92
4-23 Absolute error in normalized nodal power density for steady-state case D-2	92
4-24 Relative error in normalized nodal power density for steady-state case D-2 .	93
4-25 Normalized nodal power density for steady-state case D-3 . . . . .	94
4-26 Absolute error in normalized nodal power density for steady-state case D-3	94
4-27 Relative error in normalized nodal power density for steady-state case D-3 .	95
4-28 Thermal fluxes of bracketing states and reference state for steady-state case D-1 . . . . .	96
4-29 Thermal fluxes of bracketing states and reference state for steady-state cases D-1 and D-2 . . . . .	96
4-30 Total reactor power for transient case E-2 . . . . .	100
4-31 Relative error in total reactor power for transient case E-2 . . . . .	100
4-32 Total reactivity for transient case E-2 . . . . .	101
4-33 Absolute error in total reactivity for transient case E-2 . . . . .	101
4-34 Relative error in nodal power density for transient case E-2 . . . . .	102
4-35 Total reactor power for transient case E-3 . . . . .	103
4-36 Relative error in total reactor power for transient case E-3 . . . . .	103
4-37 Total reactivity for transient case E-3 . . . . .	104
4-38 Absolute error in total reactivity for transient case E-3 . . . . .	104

4-39 Relative error in nodal power density for transient case E-3 . . . . .	105
4-40 Total reactor power for transient case E-4 . . . . .	106
4-41 Relative error in total reactor power for transient case E-4 . . . . .	106
4-42 Total reactivity for transient case E-4 . . . . .	107
4-43 Absolute error in total reactivity for transient case E-4 . . . . .	107
4-44 Relative error in nodal power density for transient case E-4 . . . . .	108
4-45 Total reactor power for transient case E-6 . . . . .	109
4-46 Relative error in total reactor power for transient case E-6 . . . . .	109
4-47 Total reactivity for transient case E-6 . . . . .	110
4-48 Absolute error in total reactivity for transient case E-6 . . . . .	110
4-49 Relative error in nodal power density for transient case E-6 . . . . .	111
4-50 Relative error in normalized power density for steady-state case A-CG . .	112
4-51 Total reactor power for transient case E-2CG . . . . .	115
4-52 Relative error in total reactor power for transient case E-2CG . . . . .	115
4-53 Total reactivity for transient case E-2CG . . . . .	116
4-54 Absolute error in total reactivity for transient case E-2CG . . . . .	116
4-55 Relative error in nodal power density for transient case E-2CG . . . . .	117
4-56 Total reactor power for transient case E-3CG . . . . .	118
4-57 Relative error in total reactor power for transient case E-3CG . . . . .	118
4-58 Total reactivity for transient case E-3CG . . . . .	119
4-59 Absolute error in total reactivity for transient case E-3CG . . . . .	119
4-60 Relative error in nodal power density for transient case E-3CG . . . . .	120
4-61 Comparison of error in reactor power for cases E-2CG and E-2 . . . . .	122
4-62 Comparison of error in reactivity for cases E-2CG and E-2 . . . . .	122
4-63 Comparison of error in reactor power for cases E-3CG and E-3 . . . . .	123
4-64 Comparison of error in reactivity for cases E-3CG and E-3 . . . . .	123
4-65 Computing efficiency for nodal synthesis models . . . . .	125
4-66 Percentage of matrix computing time in total CPU time for a transient cal- culation . . . . .	125
6-1 Artist's view of the MITR-II reactor facility . . . . .	134
6-2 Vertical cross-section of the MITR-II . . . . .	135

6-3	MITR-II core configuration . . . . .	136
6-4	Cross-sectional view of MCNP model for MITR-II core number 2 . . . . .	140
6-5	Vertical view of MCNP model for MITR-II core number 2 . . . . .	141
6-6	Steps in the development of the MCNP in-core model for MITR-II . . . . .	143
6-7	Steps in the development of the MCNP out-of-core model for MITR-II . . . . .	144
6-8	Steps in the development of the MCNP supplement model for MITR-II . . . . .	145
6-9	Three-dimensional view of the QUARTZ triangular-z geometry model for MITR-II . . . . .	146
6-10	Two-dimensional slice of a 3-D QUARTZ triangular-z mesh layout for MITR-II	147
6-11	Cross-sectional view of MCNP in-core model . . . . .	148
6-12	Vertical view of MCNP in-core model . . . . .	149
6-13	Cross-sectional view of MCNP out-of-core model . . . . .	150
6-14	Vertical view of MCNP out-of-core model . . . . .	151
6-15	Cross-sectional view of MCNP supplement model . . . . .	152
6-16	Vertical view of MCNP supplement model . . . . .	153
6-17	MCNP net current on triangular-z nodal faces . . . . .	156
7-1	Configuration of a demonstration problem for MCNP-QUARTZ computation procedure . . . . .	161
7-2	Relative error in group-flux for test case A . . . . .	164
7-3	Relative error in group-flux for test case B . . . . .	165
7-4	Relative error in group-flux for test case C . . . . .	166
7-5	Statistical uncertainty in reference MCNP group-flux . . . . .	167
7-6	Relative differences between the local boundary condition constants and the average constants . . . . .	169
A-1	Flow diagram of CMFD-DF3 . . . . .	179
B-1	Flow diagram of ZFXBC . . . . .	186

# List of Tables

2.1	$\alpha$ 's and $\beta$ 's for standard boundary conditions . . . . .	29
2.2	Comparison of the linear system for the nodal synthesis models . . . . .	36
3.1	SYN1T program units (Part 1) . . . . .	50
3.2	SYN1T program units (Part 2) . . . . .	51
3.3	SYN1CG program units (Part 1) . . . . .	66
3.4	SYN1CG program units (Part 2) . . . . .	67
4.1	Test cases for steady-state variable inlet coolant temperature problem . . .	70
4.2	Thermal fluxes of bracketing states and intermediate state for steady-state case A . . . . .	71
4.3	Neutron multiplication factor for steady-state case A . . . . .	72
4.4	Neutron multiplication factors for steady-state case series B . . . . .	74
4.5	Test cases for variable rod-position problem 1 – fully-rodded case . . . . .	81
4.6	Neutron multiplication factors for steady-state case series C . . . . .	86
4.7	Ratios of discontinuity factors for steady-state case C-2 . . . . .	87
4.8	Test cases for variable rod-position problem 2 – partially-rodded case . . . . .	88
4.9	Neutron multiplication factors for steady-state case series D . . . . .	95
4.10	Test cases for inlet coolant temperature transient problem . . . . .	98
4.11	Summary of synthesis results for inlet coolant temperature transient problem	99
4.12	Neutron multiplication factor for steady-state case A-CG . . . . .	113
4.13	Transient test cases for collapsed-group synthesis model . . . . .	113
4.14	Summary of transient results for collapsed-group synthesis model . . . . .	114
7.1	QUARTZ test cases for demonstration problem . . . . .	163
7.2	$K_{\text{eff}}$ for QUARTZ test cases . . . . .	163

**A.1 Structure of the QUANDRY restart file . . . . . 179**

# Chapter 1

## Introduction

### 1.1 Overview

The fast and accurate determination of the instantaneous, three-dimensional, spatial core power distribution and the total core reactivity can contribute significantly to the safety and control of a large commercial nuclear power plant. The more accurately the power distribution is obtained, the more optimally a plant can be operated. Also, the faster the power distribution and the reactivity are determined, the easier the power plant can be controlled.

Conventionally, the power distribution and the reactivity are calculated by the diffusion-theory approximation to the rigorous Boltzman transport theory, which is impractical for use on a routine basis. Before the maturation of the nodal diffusion models, finite-difference methods for solving the diffusion equations were used. Although they can generate very accurate results, the requirement of very fine meshes (on the order of 1 cm) renders three-dimensional computations very expensive. Today, modern nodal methods are applied in the nuclear industry, and the finite-difference techniques are used only for benchmarking.

The modern nodal methods can use relatively large meshes or nodes (about the size of a fuel assembly, on the order of 20 cm), and the computing speed is about two orders of magnitudes faster than for the finite-difference methods [S-1]. This improvement in computing efficiency is due to a substantial reduction in the size of the system of equations to be solved. For a given accuracy, the nodal methods require only several thousand nodes, whereas the finite-difference methods need several million meshes! The basic strategy of nodal methods is to derive nodal balance equations and nodal coupling equations, and

then solve these two sets of equations iteratively. The nodal balance equations involve node-averaged fluxes and surface-averaged currents. The nodal coupling equations provide the relationships between the node-averaged fluxes and the surface-averaged currents. In solving the coupling equations, the spatial shapes of the transverse leakages are not known, and various assumptions can be made. Procedures used to solve these coupling equations lead to the classification of the modern nodal method into two separate branches: analytic nodal methods [S-1] and the polynomial nodal methods [S-2, Z-1].

In the analytic nodal method, a quadratic shape of the transverse leakage is generally used and the coupling equations are solved analytically. However, the complexity in solving these equations restricts the application of the analytic nodal method to two neutron energy groups. On the other hand, in the modern polynomial nodal method, a special polynomial expansion technique is used to solve the coupling equations and the restriction to two energy groups is relaxed. Furthermore, a special non-linear iteration scheme is often employed in the polynomial nodal method. This scheme consists of solving the coarse-mesh finite-difference (CMFD) equations for the node-averaged fluxes, solving the coupling equations for the surface-averaged currents and fluxes, and introducing correction factors, namely the CMFD discontinuity factors, in the coupling equations so that reference leakages can be reproduced. Both the analytic and polynomial nodal methods give comparable results.

Unlike the modern nodal methods, which were introduced into reactor calculations in the early 1980's, the origin of the synthesis methods [K-1, S-3, Y-1] can be traced back to the early 1960's. The underlying idea of synthesis methods is the expansion of time-dependent flux shapes as a series of trial functions. The governing equations are derived using a variational principle or the weighted-residual method.

Most of the early synthesis methods blended two-dimensional expansion functions and solved for one-dimensional, time-dependent mixing coefficients, since at that time, three-dimensional computation capabilities were not available. However, with the introduction of the nodal methods, relatively cheap and accurate three-dimensional calculations became available, and point-synthesis techniques that blend three-dimensional flux shapes have become possible. In 1992, a point-synthesis method based on the analytic nodal method [L-1] was developed at MIT. The accuracy of this model was acceptable. However, its computing efficiency was very poor. On the other hand, use of the point synthesis approximation to infer reactivity and flux shape from the readings of neutron flux detectors shows promise

of great success [J-1]. Numerical tests of the method have shown that very accurate values of flux shapes and reactivity can be reconstructed in real-time. We shall refer to these two approaches as the “theoretical” and “experimental” nodal point synthesis models.

## 1.2 Objective and Approach

### 1.2.1 Objective

The objective of this thesis is to evaluate the potential of the “theoretical” and the “experimental” nodal synthesis models for real-time nuclear reactor simulations of tightly coupled cores such as the MIT Research Reactor. The accuracy of calculated time-dependent power distributions and total reactivity, as determined by the theoretical point synthesis model, along with the computing efficiency are investigated numerically. For evaluating the experimental point synthesis model, the validity of an approach which can be used to generate the two-group nodal parameters for the application to the transient studies for the MIT Research Reactor is investigated.

### 1.2.2 Theoretical Nodal Synthesis Approach

The approach is two-fold. First, a “theoretical” nodal synthesis model is developed. A set of nodal equations having the coarse mesh finite difference (CMFD) form [H-1], corrected by discontinuity factors, is derived. Then, two different versions of “theoretical” nodal synthesis models are derived from these CMFD equations by the weighted-residual method. In the “general” nodal synthesis model, the flux shape  $\phi^g(x, y, z, t)$  is approximated by a linear combination of several pre-computed steady-state expansion functions  $\varphi_n^g(x, y, z, t)$ , with unknown group-dependent mixing coefficients  $T_n^g(t)$ :

$$\begin{bmatrix} \phi^1(x, y, z, t) \\ \vdots \\ \phi^G(x, y, z, t) \end{bmatrix} \approx \sum_{n=1}^N \begin{bmatrix} \varphi_n^1(x, y, z) & 0 \cdots & 0 \\ \vdots & \ddots & \vdots \\ 0 & 0 \cdots & \varphi_n^G(x, y, z) \end{bmatrix} \begin{bmatrix} T_n^1(t) \\ \vdots \\ T_n^G(t) \end{bmatrix}, \quad (1.1)$$

where,

G = total number of neutron energy groups,

N = total number of expansion functions,

g = group index,

n = expansion function index.

Then in the “collapsed-group” nodal synthesis model [H-2], the group-dependence of the mixing coefficients is relaxed:

$$\begin{bmatrix} \phi^1(x, y, z, t) \\ \vdots \\ \phi^G(x, y, z, t) \end{bmatrix} \approx \sum_{n=1}^N \begin{bmatrix} \varphi_n^1(x, y, z) \\ \vdots \\ \varphi_n^G(x, y, z) \end{bmatrix} T_n(t). \quad (1.2)$$

Several hypothetical one-dimensional problems are used to test these two models. The test cases include the steady-state variable inlet coolant temperature problem, the steady-state variable control-rod position problem, and the time-dependent variable inlet coolant temperature problem. Several methods are devised to update the discontinuity factors for the transient case in order to study the effect of the discontinuity factors on the accuracy of the models. The reference solutions are obtained from QUANDRY [S-1], an analytic nodal diffusion code developed at MIT.

### 1.2.3 Experimental Nodal Synthesis Approach

The second approach is an extension of previous work done by Robert Jacqmin [J-1]. In his “experimental” nodal synthesis model, “direct outputs from the neutron-flux detectors” were used to obtain mixing coefficients  $T_n^g(t)$  or  $T_n(t)$  using the relationship

$$C^{(j)}(t) = \int_{V^{(j)}} dx dy dz \sum_{g=1}^G \Sigma^{g,(j)}(x, y, z, t) \phi^g(x, y, z, t), \quad j = 1, 2, \dots, J, \quad (1.3)$$

where  $\phi^g(x, y, z, t)$  is approximated by Equation (1.1) or (1.2) and where

- $J$  = total number of neutron-flux detectors,
- $V^{(j)}$  = volume of the  $j$ -th detector,
- $C^{(j)}(t)$  = signal returned by the  $j$ -th detector, i.e., the counting rate,
- $\Sigma^{g,(j)}(x, y, z, t)$  = response function, or the homogenized cross-section for the  $j$ -th detector.

Note that in this model, either the “general” nodal synthesis expansion, Equation (1.1), or the “collapsed-group” nodal synthesis expansion, Equation (1.2), can be applied.

In Jacqmin’s research experimental detector readings were not available, and the signals were provided by output from the QUANDRY code. This “semi-experimental” nodal synthesis model applied to the analysis of some rather severe PWR transients produced results

which were in excellent agreement with reference calculations. Moreover, the computing speed was faster than real-time.

In the present research, an approach is devised to determine few-group nodal parameters from a Monte Carlo model and to reproduce reference results by a three-dimensional triangular-z nodal code, QUARTZ, developed by DeLorey [D-1]. The approach is demonstrated with a simple test problem.

### **1.3 Thesis Organization**

The thesis is divided into eight chapters. In Chapter 2, the theory of the general nodal synthesis model is described. First, multi-group nodal equations having the CMFD form corrected by discontinuity factors are derived. Then, the general nodal synthesis equations are obtained by the weighted-residual method. The simplified collapsed-group nodal synthesis model is also developed. In addition, the numerical methods used for solving the steady-state and time-dependent governing equations are reviewed.

In Chapter 3, two one-dimensional computer codes developed to solve the general and collapsed-group nodal synthesis models are presented. Detailed descriptions of the key parts of these codes are given.

In Chapter 4, test results for the general nodal synthesis model and the collapsed-group nodal synthesis model are presented along with a discussion of accuracy and computing efficiency.

In Chapter 5, Jacqmin's experimental nodal synthesis model is reviewed, and the application of this model to the MIT Research Reactor (MITR) transient studies is discussed.

In Chapter 6, an approach which can be used to determine the few-group nodal cross sections and CMFD discontinuity factors for the MITR transient analysis is described.

In Chapter 7, a simple test problem is set up and analyzed to demonstrate the validity of the approach outlined in Chapter 6.

Finally, in Chapter 8, the research is summarized, major conclusions are drawn, and recommendations for future work are made.

# **Chapter 2**

## **Theoretical Nodal Synthesis Approach**

### **2.1 Introduction**

This chapter describes the development of the general nodal synthesis model and the collapsed-group nodal synthesis model. These theoretical synthesis models are derived on the basis of nodal equations having the CMFD form, corrected by discontinuity factors. Although the numerical tests covered in Chapter 4 are for one-dimensional problems only, the models are developed on a three-dimensional Cartesian geometry in this Chapter for generality. Section 2.2 presents the CMFD-form nodal equations. Section 2.3 deals with the development of the general nodal synthesis model. Section 2.4 derives the collapsed-group synthesis model. Section 2.5 reviews the numerical methods applied to solving the synthesis equations. Finally, the treatment of the discontinuity factors is included in Section 2.6.

### **2.2 Nodal Equations Having the CMFD Form**

#### **2.2.1 The Equations**

We begin with the time-dependent, multigroup neutron and precursor equations as follows:

$$\begin{aligned} \frac{1}{v_g} \frac{\partial \phi_g(\underline{r}, t)}{\partial t} &= -\nabla \cdot \underline{J}_g(\underline{r}, t) - \Sigma_g(\underline{r}, t)\phi_g(\underline{r}, t) + \sum_{\substack{g'=1 \\ g' \neq g}}^G \Sigma_{gg'}(\underline{r}, t)\phi_{g'}(\underline{r}, t) + \\ &\quad \sum_{g'=1}^G \frac{1}{\gamma}(1-\beta)\chi_{pg}\nu\Sigma_{fg'}(\underline{r}, t)\phi_{g'}(\underline{r}, t) + \sum_{i=1}^D \lambda_i \chi_{di}^g C_i(\underline{r}, t) \end{aligned} \quad (2.1)$$

$$\begin{aligned} \frac{\partial C_d(\underline{r}, t)}{\partial t} &= \beta_d \frac{1}{\gamma} \sum_{g=1}^G \nu \Sigma_{fg}(\underline{r}, t)\phi_g(\underline{r}, t) - \lambda_d C_d(\underline{r}, t) \\ g &= 1, \dots, G, d = 1, \dots, D \end{aligned} \quad (2.2)$$

where,

- $G$  = total number of neutron energy groups,
- $D$  = total number of delayed neutron precursor families,
- $v_g$  = neutron velocity for group  $g$ ,
- $\phi_g(\underline{r}, t)$  = scalar neutron flux density in group  $g$ ,
- $J_g(\underline{r}, t)$  = net neutron current density in group  $g$ ,
- $\Sigma_g(\underline{r}, t)$  = macroscopic total cross section for group  $g$  minus the in-group scattering cross section,
- $\gamma$  = the critical eigenvalue ( $k_{eff}$ ),
- $\chi_{pg}$  = prompt fission neutron spectrum for group  $g$ ,
- $\nu$  = average number of neutrons emitted per fission,
- $\Sigma_{fg}(\underline{r}, t)$  = macroscopic fission cross section for group  $g$ ,
- $\Sigma_{gg'}(\underline{r}, t)$  = macroscopic scattering cross section from group  $g'$  to  $g$ ,
- $\lambda_i$  = decay constant for delayed neutron precursor family  $i$ ,
- $\chi_{di}^g$  = delayed neutron spectrum for family  $i$  in group  $g$ ,
- $C_i(\underline{r}, t)$  = density of delayed neutron precursors in family  $i$ ,
- $\beta_d$  = fractional yield of delayed neutron precursors in family  $d$  per fission,
- $\beta$  = total fractional yield of delayed neutron precursors per fission,  $\sum_{d=1}^D \beta_d$ .

Next, by integrating Equations (2.1) and (2.2) over the volume of a Cartesian node  $(i, j, k)$ , we have

$$\frac{1}{v_g} \frac{\partial \overline{\phi}_g^{ijk}(t)}{\partial t} = -\frac{1}{V^{ijk}} \sum_{p=1}^6 \int_{S_p} \underline{J}_g(\underline{r}, t) \cdot \underline{n}_p dS - \overline{\Sigma}_g^{ijk}(t) \overline{\phi}_g^{ijk}(t) + \sum_{\substack{g'=1 \\ g' \neq g}}^G \overline{\Sigma}_{gg'}^{ijk}(t) \overline{\phi}_{g'}^{ijk}(t) + \sum_{g'=1}^G \frac{1}{\gamma} (1-\beta) \chi_{pg} \nu \overline{\Sigma}_{fg'}^{ijk}(t) \overline{\phi}_{g'}^{ijk}(t) + \sum_{m=1}^D \lambda_m \chi_{dm}^g \overline{C}_m^{ijk}(t) \quad (2.3)$$

$$\frac{\partial \overline{C}_d^{ijk}(t)}{\partial t} = \beta_d \frac{1}{\gamma} \sum_{g=1}^G \nu \overline{\Sigma}_{fg}^{ijk}(t) \overline{\phi}_g^{ijk}(t) - \lambda_d \overline{C}_d^{ijk}(t) \quad (2.4)$$

$g = 1, \dots, G, d = 1, \dots, D$

where,

$V^{ijk}$  = volume of a node,

$S_p$  = surface area of a face p,

$\underline{n}_p$  = outward-directed normal vector on a face p,

and,

$$\begin{aligned} \overline{\phi}_g^{ijk}(t) &= \frac{1}{V^{ijk}} \int_{V^{ijk}} \phi_g(\underline{r}, t) dV, \\ \overline{\Sigma}_g^{ijk}(t) &= \frac{1}{V^{ijk} \overline{\phi}_g^{ijk}(t)} \int_{V^{ijk}} \Sigma_g(\underline{r}, t) \phi_g(\underline{r}, t) dV, \\ \nu \overline{\Sigma}_g^{ijk}(t) &= \frac{1}{V^{ijk} \overline{\phi}_g^{ijk}(t)} \int_{V^{ijk}} \nu \Sigma_g(\underline{r}, t) \phi_g(\underline{r}, t) dV, \\ \overline{\Sigma}_{gg'}^{ijk}(t) &= \frac{1}{V^{ijk} \overline{\phi}_{g'}^{ijk}(t)} \int_{V^{ijk}} \nu \Sigma_{gg'}(\underline{r}, t) \phi_{g'}(\underline{r}, t) dV, \\ \overline{C}_d^{ijk}(t) &= \frac{1}{V^{ijk}} \int_{V^{ijk}} C_d(\underline{r}, t) dV. \end{aligned}$$

The general layout of a Cartesian node system is shown in Figure 2-1.

Then, applying Fick's law and introducing the CMFD discontinuity factors, we can relate the face-averaged currents with the node-averaged fluxes in an exact manner [H-1].

The procedure is described below.

Fick's law is written as

$$\underline{J}_g(\underline{r}, t) \approx -D_g(\underline{r}, t) \nabla \phi_g(\underline{r}, t) \quad (2.5)$$

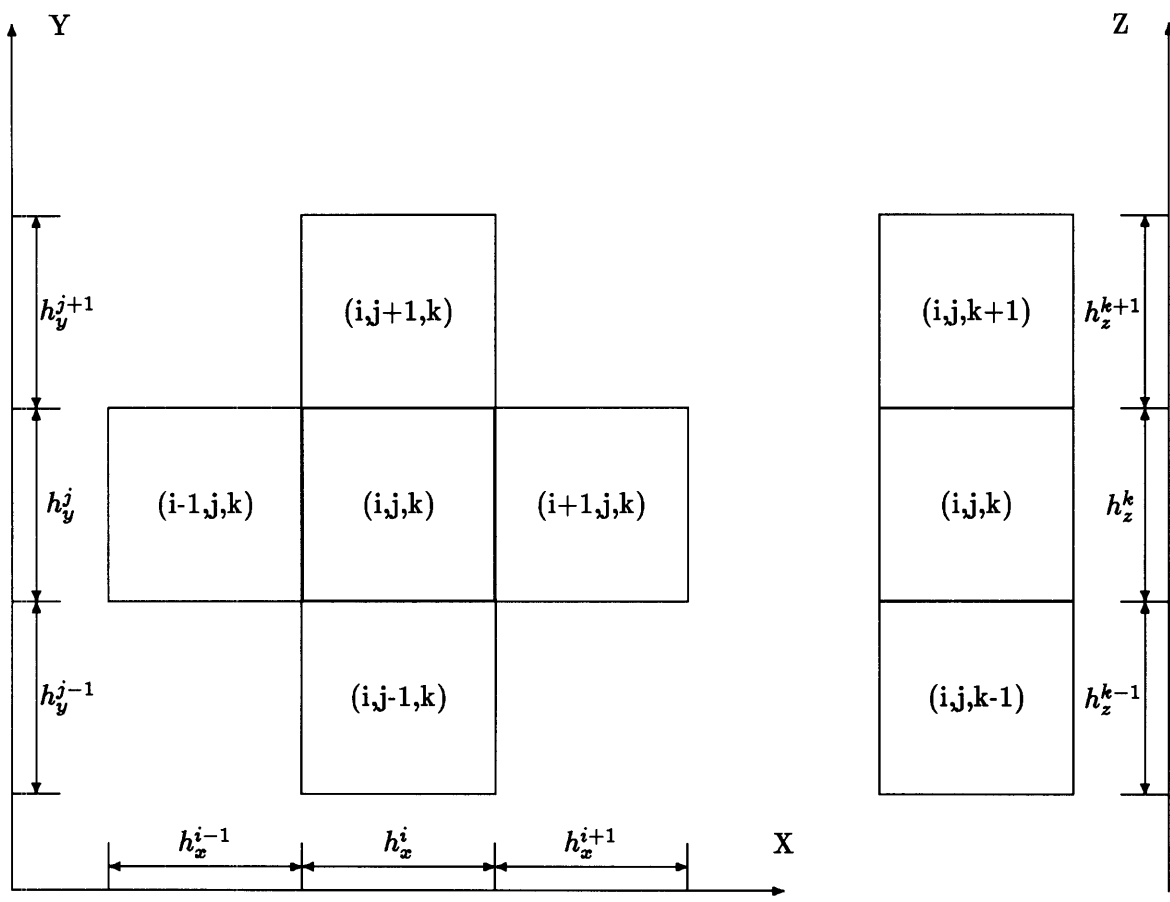


Figure 2-1: Schematic node layout

where  $D_g(\underline{r}, t)$  is the neutron diffusion coefficient for group-g.

Integrating this Equation over a face-p of node (i,j,k) with the assumption that the flux varies linearly from the center of the node to its surface, we obtain the following expression

$$\bar{J}_{gp}^l(t) \approx -\bar{D}_g^l(t) \frac{\bar{\phi}_{gp}^l(t) - \bar{\phi}_g^l(t)}{\frac{h_l^p}{2}} \quad (2.6)$$

where,

$$\bar{J}_{gp}^l(t) = \frac{1}{S_p} \int_{S_p} \underline{J}_g(\underline{r}, t) \cdot \underline{n}_p dS, \quad (2.7)$$

$$\bar{\phi}_{gp}^l(t) = \frac{1}{S_p} \int_{S_p} \phi_g(\underline{r}, t) dS, \quad (2.8)$$

and,

$h_l^p$  = width of node-l in the direction normal to face-p,

$l$  = a short-hand index representing node (i,j,k).

Similarly for node-m ( $m$  being a short-hand index representing a node that is adjacent to node-l), adjacent to node-l at face-q (face-p is exactly the same as face-q, except that for node-m, it is differently indexed), we can write

$$\bar{J}_{gq}^m(t) \approx -\bar{D}_g^m(t) \frac{\bar{\phi}_{gq}^m(t) - \bar{\phi}_g^m(t)}{\frac{h_m^q}{2}}. \quad (2.9)$$

Using the continuity condition of the net current density across the interface (i.e., face-p or face-q) between the nodes  $l$  and  $m$ , and introducing the concept of the CMFD discontinuity factors, we combine Equation (2.6) with (2.9) to form

$$\begin{aligned} \bar{J}_{gp}^l(t) &= -\bar{D}_g^l(t) \frac{\frac{\bar{\phi}_{gp}^l(t)}{f_{glm}^l(t)} - \bar{\phi}_g^l(t)}{\frac{h_l^p}{2}} \\ &= -\bar{D}_g^m(t) \frac{\bar{\phi}_g^m(t) - \frac{\bar{\phi}_{gq}^m(t)}{f_{glm}^m(t)}}{\frac{h_m^q}{2}} \end{aligned} \quad (2.10)$$

where  $f_{glm}^l(t)$  is the CMFD discontinuity factor applied on the node- $l$  side of the interface between nodes  $l$  and  $m$ , and  $f_{glm}^m(t)$  is the CMFD discontinuity factor applied on the node- $m$  side of the interface (see Figure 2-2).

Eliminating the face-averaged flux,  $\bar{\phi}_{gp}^l(t)$  or  $\bar{\phi}_{gq}^m(t)$ , from Equation (2.10), we obtain the following coupling relation between the face-averaged current and the node-averaged flux

$$\bar{J}_{gp}^l(t) = 2 \left[ \frac{h_l^p}{\bar{D}_g^l(t)} + \frac{f_{glm}^m(t)}{f_{glm}^l(t)} \frac{h_m^q}{\bar{D}_g^m(t)} \right]^{-1} \left[ \bar{\phi}_g^l(t) - \frac{f_{glm}^m(t)}{f_{glm}^l(t)} \bar{\phi}_g^m(t) \right]. \quad (2.11)$$

By substituting Equation (2.11) into Equation (2.3), and using the relation between face-averaged and face-integrated current density as given in Equation (2.7), we can obtain a set of the general, time-dependent nodal equations having the CMFD form, associated with the time-dependent precursor equations

$$\begin{aligned} \frac{1}{v_g} \frac{\partial \bar{\phi}_g^l(t)}{\partial t} &= - \sum_{p=1}^6 \frac{2S_p}{V^l} \left[ \frac{h_l^p}{\bar{D}_g^l(t)} + \frac{f_{glm}^m(t)}{f_{glm}^l(t)} \frac{h_m^q}{\bar{D}_g^m(t)} \right]^{-1} \left[ \bar{\phi}_g^l(t) - \frac{f_{glm}^m(t)}{f_{glm}^l(t)} \bar{\phi}_g^m(t) \right] - \\ &\quad \Sigma_g^l(t) \bar{\phi}_g^l(t) + \sum_{\substack{g'=1 \\ g' \neq g}}^G \bar{\Sigma}_{gg'}^l(t) \bar{\phi}_{g'}^l(t) + \sum_{g'=1}^G \frac{1}{\gamma} (1-\beta) \chi_{pg} \bar{\nu} \bar{\Sigma}_{fg'}^l(t) \bar{\phi}_{g'}^l(t) + \\ &\quad \sum_{i=1}^D \lambda_i \chi_{di}^g \bar{C}_i^l(t) \end{aligned} \quad (2.12)$$

$$\begin{aligned} \frac{\partial \bar{C}_i^l(t)}{\partial t} &= \beta_i \frac{1}{\gamma} \sum_{g=1}^G \bar{\nu} \bar{\Sigma}_{fg}^l(t) \bar{\phi}_g^l(t) - \lambda_i \bar{C}_i^l(t) \\ g &= 1, \dots, G, d = 1, \dots, D. \end{aligned} \quad (2.13)$$

Note that the node indices  $l$  and  $m$  depend on the face indices  $p$  and  $q$ , respectively.

## 2.2.2 The Boundary Conditions

Different boundary conditions can be specified with the following relation applied to a node  $l$  having an external surface  $p$

$$\alpha_g \bar{J}_{gp}^l(t) - \beta_g \bar{\phi}_{gp}^l(t) = 0 \quad (2.14)$$

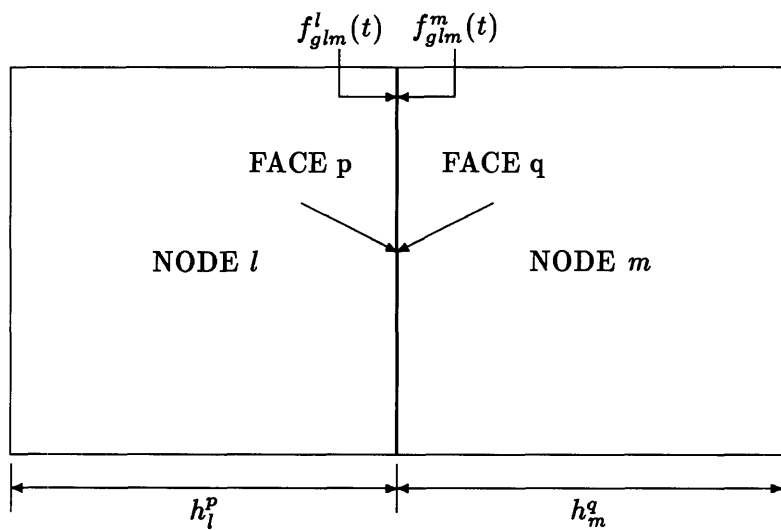


Figure 2-2: CMFD discontinuity factors

where  $\alpha$ 's and  $\beta$ 's for the most common boundary conditions are collected in Table 2.1. This Equation is used to derive a coupling relation for boundary faces as follow

$$\bar{J}_{gp}^l(t) = 2 \left[ \frac{h_l^p}{\bar{D}_g^l(t)} \beta_g + \frac{2 \alpha_g}{f_{glm}^l(t)} \right]^{-1} \beta_g \bar{\phi}_g^l(t). \quad (2.15)$$

Table 2.1:  $\alpha$ 's and  $\beta$ 's for standard boundary conditions [G-1]

Boundary condition	$\alpha$	$\beta$
Zero flux	0	1
Zero current	1	0
Zero incoming current	2	1
Albedo	1	$\left(\frac{\underline{J} \cdot \underline{n}}{\phi}\right)^a$

---

<sup>a</sup> $\underline{J}$  is the net current vector,  $\underline{n}$  is an outward-directed normal on the boundary faces, and  $\phi$  is the flux on the boundary surfaces.

### 2.3 Derivation of the General Nodal Synthesis Model

Before deriving the general nodal synthesis equations, it is convenient to cast the CMFD-nodal and precursor equations (Equations (2.12) and (2.13)) into a compact matrix form

$$\begin{aligned} \mathbf{V}^{-1} \frac{\partial \Phi^l(t)}{\partial t} &= - \sum_{p=1}^6 \Omega_p \mathbf{D}_{lm}^p(t) [\Phi^l(t) - \mathbf{r}_{lm}(t) \Phi^m(t)] - \mathbf{A}^l(t) \Phi^l(t) + \\ &\quad \frac{1}{\gamma} (1 - \beta) \underline{\chi}_p \mathbf{F}^{l\mathbf{T}}(t) \Phi^l(t) + \sum_{i=1}^D \lambda_i \underline{\chi}_{di} \bar{\bar{C}}_i^l(t) \end{aligned} \quad (2.16)$$

$$\frac{\partial \bar{\bar{C}}_i^l(t)}{\partial t} = \beta_i \frac{1}{\gamma} \mathbf{F}^{l\mathbf{T}}(t) \Phi^l(t) - \lambda_i \bar{\bar{C}}_i^l(t) \quad (2.17)$$

$l, m = 1, \dots, NIJK$

where,

$NIJK$  = total number of nodes,

$$\Phi^l(t) = \begin{bmatrix} \bar{\bar{\phi}}_1^l(t) \\ \vdots \\ \bar{\bar{\phi}}_G^l(t) \end{bmatrix},$$

$$\mathbf{V}^{-1} = \begin{bmatrix} \frac{1}{V_1} & 0 & 0 \\ 0 & \ddots & 0 \\ 0 & 0 & \frac{1}{V_G} \end{bmatrix},$$

$$\underline{\chi}_p = \begin{bmatrix} \chi_{p1} \\ \vdots \\ \chi_{pG} \end{bmatrix},$$

$$\underline{\chi}_{di} = \begin{bmatrix} \chi_{di}^1 \\ \vdots \\ \chi_{di}^G \end{bmatrix},$$

$$\mathbf{F}^{l\mathbf{T}}(t) = \begin{bmatrix} \nu \bar{\Sigma}_{f1}^l(t) \\ \dots \\ \nu \bar{\Sigma}_{fG}^l(t) \end{bmatrix},$$

$$\begin{aligned}
\Omega &= \frac{2S_p}{V^l}, \\
\mathbf{A}^l(t) &= \begin{bmatrix} \bar{\Sigma}_1^l(t) & -\bar{\Sigma}_{12}^l(t) & \cdots & -\bar{\Sigma}_{1G}^l(t) \\ -\bar{\Sigma}_{21}^l(t) & \bar{\Sigma}_2^l(t) & & \vdots \\ -\bar{\Sigma}_{G1}^l(t) & \cdots & \bar{\Sigma}_G^l(t) \end{bmatrix}, \\
\mathbf{r}_{lm}(t) &= \begin{pmatrix} [0] & & & (\text{boundary surfaces}) \\ \begin{bmatrix} r_{1lm}(t) & 0 & 0 \\ 0 & \ddots & 0 \\ 0 & 0 & r_{Glm}(t) \end{bmatrix} & & (\text{interior surfaces}) \end{pmatrix}, \\
r_{glm}(t) &= \frac{f_{glm}^m(t)}{f_{glm}^l(t)}, \\
\mathbf{D}_{lm}^p(t) &= \begin{pmatrix} \left[ \begin{bmatrix} h_l^p \\ \bar{D}_1^l(t) \end{bmatrix} \beta_1 + \frac{2\alpha_1}{f_{1lm}^l(t)} \right]^{-1} \beta_1 & 0 & 0 \\ 0 & \ddots & 0 \\ 0 & 0 & \left[ \begin{bmatrix} h_l^p \\ \bar{D}_G^l(t) \end{bmatrix} \beta_G + \frac{2\alpha_G}{f_{Glm}^l(t)} \right]^{-1} \beta_G \end{pmatrix} \\
&\quad (\text{boundary surfaces}) \\
\mathbf{D}_{lm}^p(t) &= \begin{pmatrix} \left[ \begin{bmatrix} h_l^p \\ \bar{D}_1^l(t) \end{bmatrix} + \frac{r_{1lm}(t)}{\bar{D}_1^l(t)} h_m^q \right]^{-1} & 0 & 0 \\ 0 & \ddots & 0 \\ 0 & 0 & \left[ \begin{bmatrix} h_l^p \\ \bar{D}_G^l(t) \end{bmatrix} + \frac{r_{Glm}(t)}{\bar{D}_G^l(t)} h_m^q \right]^{-1} \end{pmatrix} \\
&\quad (\text{interior surfaces})
\end{pmatrix}.
\end{aligned}$$

In the general nodal synthesis method, the node-averaged neutron flux is approximated as a linear combination of a set of pre-computed expansion functions  $\bar{\psi}_{n,g}^l$ , with unknown mixing coefficients  $T_{n,g}(t)$ ; which for a given n and g, are the same for all nodes

$$\begin{bmatrix} \bar{\phi}_1^l(t) \\ \vdots \\ \bar{\phi}_G^l(t) \end{bmatrix} \approx \sum_{n=1}^N \begin{bmatrix} \bar{\psi}_{n,1}^l & 0 & 0 \\ 0 & \ddots & 0 \\ 0 & 0 & \bar{\psi}_{n,G}^l \end{bmatrix} \begin{bmatrix} T_{n,1}(t) \\ \vdots \\ T_{n,G}(t) \end{bmatrix}, \quad (2.18)$$

or, in matrix form

$$\Phi^l(t) \approx \sum_{n=1}^N \Psi_n^l T_n(t) \quad l = 1, \dots, NIJK. \quad (2.19)$$

The expansion indicated by Equation (2.19) is substituted into Equations (2.16) and (2.17), the former is premultiplied by the diagonal matrix  $\mathbf{W}_n^l$  and the latter is premultiplied by  $\mathbf{W}_n^l \chi_{di}$ ; then both results are summed over all nodes. The matrix  $\mathbf{W}_n^l$ , defined by

$$\mathbf{W}_n^l = \begin{bmatrix} W_{n,1}^l & 0 & 0 \\ 0 & \ddots & 0 \\ 0 & 0 & W_{n,G}^l \end{bmatrix} \quad (2.20)$$

consists of pre-computed, group weighting functions.

This procedure is repeated for N different weighting functions, resulting in the set of equations

$$\underline{\tau}_n \frac{d}{dt} \mathbf{T}(t) = -[\mathbf{L}_n(t) + \mathbf{A}_n(t)] \mathbf{T}(t) + \frac{1}{\gamma} (1 - \beta) \mathbf{F}_{pn}^T(t) \mathbf{T}(t) + \sum_{i=1}^D \lambda_i \mathbf{C}_{i,n}(t) \quad (2.21)$$

$$\frac{d}{dt} \mathbf{C}_{i,n}(t) = \frac{1}{\gamma} \beta \mathbf{F}_{di,n}^T(t) \mathbf{T}(t) - \lambda_i \mathbf{C}_{i,n}(t) \quad (2.22)$$

$i = 1, \dots, D, n = 1, \dots, N$

where,

$$\begin{aligned}
\mathbf{T}(t) &= \begin{bmatrix} T_1(t) \\ \vdots \\ T_N(t) \end{bmatrix}, \\
\mathbf{C}_{i,n}(t) &= \left\langle \mathbf{W}_n^l \underline{\chi}_{di} \bar{G}_i^l(t) \right\rangle^a \\
\boldsymbol{\tau}_n &= \left[ \left\langle \mathbf{W}_n^l \mathbf{V}^{-1} \Psi_1^l \right\rangle \dots \left\langle \mathbf{W}_n^l \mathbf{V}^{-1} \Psi_N^l \right\rangle \right], \\
\mathbf{L}_n(t) &= \begin{bmatrix} \left\langle \mathbf{W}_n^l \sum_p \Omega_p \mathbf{D}_{lm}^p(t) [\Psi_1^l - \mathbf{r}_{lm}(t) \Psi_1^m] \right\rangle \\ \vdots \\ \left\langle \mathbf{W}_n^l \sum_p \Omega_p \mathbf{D}_{lm}^p(t) [\Psi_N^l - \mathbf{r}_{lm}(t) \Psi_N^m] \right\rangle \end{bmatrix}^T, \\
\mathbf{A}_n(t) &= \left[ \left\langle \mathbf{W}_n^l \mathbf{A}^l(t) \Psi_1^l \right\rangle \dots \left\langle \mathbf{W}_n^l \mathbf{A}^l(t) \Psi_N^l \right\rangle \right], \\
\mathbf{F}_{pn}^T(t) &= \left[ \left\langle \mathbf{W}_n^l \underline{\chi}_p \mathbf{F}^{lT}(t) \Psi_1^l \right\rangle \dots \left\langle \mathbf{W}_n^l \underline{\chi}_p \mathbf{F}^{lT}(t) \Psi_N^l \right\rangle \right], \\
\mathbf{F}_{d_{i,n}}^T(t) &= \left[ \left\langle \mathbf{W}_n^l \underline{\chi}_{di} \mathbf{F}^{lT}(t) \Psi_1^l \right\rangle \dots \left\langle \mathbf{W}_n^l \underline{\chi}_{di} \mathbf{F}^{lT}(t) \Psi_N^l \right\rangle \right].
\end{aligned}$$

---

<sup>a</sup> $\langle X^l V^l \rangle \equiv \sum_{i=1}^{NIJK} X^l V^l$ . We can also collect all the nodal-fluxes into a huge matrix of dimension NIJK and derive the synthesis equations. This alternative approach will give the same final form of the governing equations as that given by the present method. However, its efficiency is poorer than the present method [H-3].

The expansion functions are obtained from steady-state nodal calculations for some intermediate reactor conditions which closely bracket the range of expected transient conditions. The weight functions may be the adjoint neutron fluxes corresponding to some pre-selected, reference condition or may be just the expansion functions themselves (Galerkin weighting). The weight functions are also generated from the same nodal code used to produce the expansion functions. The choice of expansion functions relies on the understanding of the physics of the problems. However, experience in applying the synthesis method to the steady-state neutron diffusion equations shows that, in general, four or five expansion functions per group are sufficient to reconstruct acceptable neutron flux distribution [H-2].

The nodal synthesis method reduces the number of independent variables in a transient problem from four (i.e., 3 space and 1 time variables) to only one (time). Equations (2.21) and (2.22) represent a set of coupled ordinary differential equations of only one independent variable. The solutions  $\mathbf{T}(t)$  and  $\mathbf{C}_{i,n}(t)$  can be solved using conventional

numerical methods as addressed in Section 2.5.

Once the mixing coefficients are computed, the neutron flux distribution at various times during a reactor transient can be reconstructed from Equation (2.19).

Before developing the Collapsed-group nodal synthesis model, we can reconstruct Equations (2.21) and (2.22) into a “super-matrix” form as follows

$$\underline{\tau} \frac{d}{dt} \mathbf{T}(t) = -\mathbf{H}(t) \mathbf{T}(t) + \frac{1}{\gamma} (1 - \beta) \mathbf{F}_P(t) \mathbf{T}(t) + \sum_{i=1}^D \lambda_i \mathbf{C}_i(t) \quad (2.23)$$

$$\begin{aligned} \frac{d}{dt} \mathbf{C}_i(t) &= \frac{1}{\gamma} \beta_i \mathbf{F}_{di}(t) \mathbf{T}(t) - \lambda_i \mathbf{C}_i(t) \\ i &= 1, \dots, D \end{aligned} \quad (2.24)$$

where  $\underline{\tau}$ ,  $\mathbf{H}(t)$ ,  $\mathbf{F}_P(t)$ , and  $\mathbf{F}_{di}(t)$  are  $N \times N$  matrices, and their elements are themselves  $G \times G$  matrices.  $\mathbf{T}(t)$ ,  $\mathbf{C}_i(t)$  are  $N$ -element column vectors, and their elements are themselves  $G$ -element vectors.

Note that the total loss matrix  $\mathbf{H}(t)$  includes the leakage matrices,  $\mathbf{L}_n(t)$ , and the absorption matrices,  $\mathbf{A}_n(t)$ . Equations (2.23) and (2.24) are equivalent to  $G \times N$  coupled differential equations in the mixing coefficients  $T_{n,g}(t)$  and weighted precursor concentrations  $\langle \mathbf{W}_n^l \chi_{di}^g \bar{\mathbf{C}}_i^l(t) \rangle$ , respectively.

This simple structure of Equations (2.23) and (2.24) allows us to compare the general synthesis model with the collapsed-group synthesis model and discuss the numerical methods without losing generality.

## 2.4 Derivation of the Collapsed-Group Nodal Synthesis Model

In the collapsed-group nodal synthesis model, the neutron flux is expanded as

$$\begin{bmatrix} \bar{\phi}_1^l(t) \\ \vdots \\ \bar{\phi}_G^l(t) \end{bmatrix} \approx \begin{bmatrix} \bar{\psi}_{1,1}^l & \bar{\psi}_{1,2}^l & \cdots & \bar{\psi}_{1,N}^l \\ \vdots & \vdots & \vdots & \vdots \\ \bar{\psi}_{G,1}^l & \bar{\psi}_{G,2}^l & \cdots & \bar{\psi}_{G,N}^l \end{bmatrix} \begin{bmatrix} T_1(t) \\ \vdots \\ T_N(t) \end{bmatrix} \quad (2.25)$$

or, in terms of a matrix form

$$\Phi^l(t) \approx \Psi^l \mathbf{T}(t). \quad (2.26)$$

Note that the group-dependence of the mixing coefficients in relaxed in the collapsed-group synthesis method. Setting up the weighting matrix as

$$\mathbf{W}^l = \begin{bmatrix} W_{1,1}^l & W_{1,2}^l & \cdots & W_{1,G}^l \\ \vdots & \vdots & \vdots & \vdots \\ W_{N,1}^l & W_{N,2}^l & \cdots & W_{N,G}^l \end{bmatrix} \quad (2.27)$$

and following the same procedure as that used to derive the general nodal synthesis equations, we obtain

$$\tau \frac{d}{dt} \mathbf{T}(t) = -\mathbf{H}(t) \mathbf{T}(t) + \frac{1}{\gamma} (1 - \beta) \mathbf{F}_P(t) \mathbf{T}(t) + \sum_{i=1}^D \lambda_i \mathbf{C}_i(t) \quad (2.28)$$

$$\frac{d}{dt} \mathbf{C}_i(t) = \frac{1}{\gamma} \beta_i \mathbf{F}_{di}(t) \mathbf{T}(t) - \lambda_i \mathbf{C}_i(t) \quad (2.29)$$

$$i = 1, \dots, D.$$

Note that the structures of Equations (2.28) and (2.29) are exactly the same as those of Equations (2.23) and (2.24), respectively. However, the collapsed-group nodal synthesis equations constitute a different linear system from the general synthesis model. Table 2.2 compares the difference between these two models. It can be seen that the size of the linear system for the collapsed-group synthesis model reduces by a factor of  $G^2$  as compared with

the general synthesis model.

Table 2.2: Comparison of the linear system for the nodal synthesis models

Item	General Synthesis Model	Collapsed-group Synthesis Model
$\Psi$	$G \times G$ matrix	$G \times N$ matrix
$W$	$G \times G$ matrix	$N \times G$ matrix
$T$	$(N \times G)$ -element vector	$N$ -element vector
$C_i$	$(N \times G)$ -element vector	$N$ -element vector
$H$	$(N G) \times (N G)$ matrix	$N \times N$ matrix
$A$	$(N G) \times (N G)$ matrix	$N \times N$ matrix
$F_p$	$(N G) \times (N G)$ matrix	$N \times N$ matrix
$F_{di}$	$(N G) \times (N G)$ matrix	$N \times N$ matrix
Linear System	$(N G) \times (N G)$	$N \times N$

## 2.5 Numerical Methods for Solving the Nodal Synthesis Equations

The numerical methods discussed in this section apply to both the general nodal synthesis and the collapsed-group nodal synthesis models. The equations to be solved are the “super-matrix” form of the synthesis equations, i.e., Equations (2.23) and (2.24).

### 2.5.1 Steady-State Solution

For the initial steady state condition, Equations (2.23) and (2.24) reduce to

$$\mathbf{H}_0 \mathbf{T}_0 = \frac{1}{\gamma} \mathbf{F}_0 \mathbf{T}_0 \quad (2.30)$$

where,

$$\mathbf{T}_0 = \mathbf{T}(0),$$

$$\mathbf{H}_0 = \mathbf{H}(0),$$

$$\mathbf{F}_0 = (1 - \beta) \mathbf{F}_p(0) + \sum_{i=1}^D \beta_i \mathbf{F}_{di}(0).$$

Solving Equation (2.30) requires solving a generalized matrix eigenvalue problem with the eigenvalue  $\gamma$  and eigenvector  $\mathbf{T}_0$ . However, the ill-condition nature of the linear system causes standard methods to be unreliable. The power method used by Brooks [B-1] proved to be unstable and was rejected by Lee [L-1]. On the other hand, the QZ method [M-1, G-2] has been successfully applied to the point synthesis model based on the analytic nodal method [L-1]. Therefore, we shall use the QZ method to solve the steady-state synthesis equations.

In general, the QZ method solves the following generalized matrix eigenvalue problem

$$\mathbf{A} \underline{\mathbf{x}} = \lambda \mathbf{B} \underline{\mathbf{x}} \quad (2.31)$$

where,

$\mathbf{A}, \mathbf{B}$  = general square matrices,  
 $\lambda$  = eigenvalue,  
 $\underline{x}$  = eigenvector.

The principle of the QZ method is to transform the eigenvalue problem, Equation (2.31), into a unitarily equivalent problem

$$\mathbf{Q} \mathbf{A} \mathbf{Z} \underline{y} = \lambda \mathbf{Q} \mathbf{B} \mathbf{Z} \underline{y} \quad (2.32)$$

where  $\mathbf{Q}$  and  $\mathbf{Z}$  are two unitary matrices such that  $\mathbf{Q} \mathbf{A} \mathbf{Z}$  and  $\mathbf{Q} \mathbf{B} \mathbf{Z}$  are both upper triangular matrices.

The algorithm consists of four steps:

1.  $\mathbf{A}$  is reduced to upper Hessenburg form and at the same time  $\mathbf{B}$  is reduced to upper triangular form.
2.  $\mathbf{A}$  is reduced to quasi-triangular form.
3. The reduced  $\mathbf{A}$  is transformed into triangular form and eigenvalues are extracted.
4. The eigenvalues are obtained from the triangular matrices and the eigenvectors are then transformed back into the original coordinate system.

### 2.5.2 Transient Solution

Different numerical methods are used to solve the neutron equation, Equation (2.23), and the precursor equation, Equation (2.24). Equation (2.23) is differenced using the  $\theta$ -method [S-1, V-1] as

$$\begin{aligned} \frac{1}{\Delta t_s} \tau (\mathbf{T}_{s+1} - \mathbf{T}_s) = & - [\theta \mathbf{H}_{s+1} \mathbf{T}_{s+1} + (1 - \theta) \mathbf{H}_s \mathbf{T}_s] + \\ & \frac{1}{\gamma} (1 - \beta) [\theta \mathbf{F}_{p,s+1} \mathbf{T}_{s+1} + (1 - \theta) \mathbf{F}_{p,s} \mathbf{T}_s] + \\ & \sum_{i=1}^D \lambda_i [\theta_d \mathbf{C}_{i,s+1} + (1 - \theta_d) \mathbf{C}_{i,s}] \end{aligned} \quad (2.33)$$

where,

$$\begin{aligned} \Delta t_s &= t_{s+1} - t_s, \\ \mathbf{T}_s &= \mathbf{T}(t_s), \\ \mathbf{H}_s &= \mathbf{H}(t_s), \\ \mathbf{F}_{p,s} &= \mathbf{F}_p(t_s), \\ \mathbf{C}_{i,s} &= \mathbf{C}_i(t_s), \\ s &= 1, 2, \dots; 0 \leq \theta, \theta_d \leq 1. \end{aligned}$$

Note that the whole time sequence is subdivided into many small time intervals,  $\Delta t_s$ , and the solutions are at times  $t_s$ ,  $s = 1, 2, \dots$  (solution at time  $t_0$  is the steady-state solution). In the  $\theta$ -method, two  $\theta$ 's are used;  $\theta$  is used for the prompt neutron terms, and  $\theta_d$  is for the delayed neutron precursor terms.

To solve Equation (2.24), we integrate over a time interval  $[t_s, t_{s+1}]$ . Making the assumption that the fission rate and precursor concentrations vary linearly in that interval [S-3], we obtain

$$\mathbf{C}_{i,s+1} = \mathbf{C}_{i,s} e^{-\lambda_i \Delta t_s} +$$

$$\begin{aligned} & \frac{\beta_i}{\gamma \lambda_i} \left[ \frac{1 - e^{-\lambda_i \Delta t_s}}{\lambda_i \Delta t_s} - e^{-\lambda_i \Delta t_s} \right] \mathbf{F}_{\text{dis}} \mathbf{T}_s + \\ & \frac{\beta_i}{\gamma \lambda_i} \left[ 1 - \frac{1 - e^{-\lambda_i \Delta t_s}}{\lambda_i \Delta t_s} \right] \mathbf{F}_{\text{di}_{s+1}} \mathbf{T}_{s+1} \end{aligned} \quad (2.34)$$

where,

$$\mathbf{F}_{\text{dis}} = \mathbf{F}_{\text{di}}(t_s).$$

Finally, substituting Equation (2.34) into Equation (2.33) and rearranging, we have

$$\mathbf{LHS}_{s+1} \mathbf{T}_{s+1} = \mathbf{RHSA}_s \mathbf{T}_s + \mathbf{RHSB}_s \mathbf{C}_{i,s} \quad (2.35)$$

where,

$$\begin{aligned} \mathbf{LHS}_{s+1} &= \frac{\tau}{\Delta t_s} + \theta \mathbf{H}_{s+1} - \frac{1-\beta}{\gamma} \theta \mathbf{F}_{\mathbf{p},s+1} - \sum_{i=1}^D \theta_d \frac{\beta_i}{\gamma} \left( 1 - \frac{1 - e^{-\lambda_i \Delta t_s}}{\lambda_i \Delta t_s} \right) \mathbf{F}_{\text{di}_{s+1}}, \\ \mathbf{RHSA}_s &= \frac{\tau}{\Delta t_s} - (1-\theta) \mathbf{H}_s + \frac{1-\beta}{\gamma} (1-\theta) \mathbf{F}_{\mathbf{p},s} + \\ &\quad \sum_{i=1}^D \theta_d \frac{\beta_i}{\gamma} \left( \frac{1 - e^{-\lambda_i \Delta t_s}}{\lambda_i \Delta t_s} - e^{-\lambda_i \Delta t_s} \right) \mathbf{F}_{\text{dis}}, \\ \mathbf{RHSB}_s &= \sum_{i=1}^D \lambda_i [\theta_d (e^{-\lambda_i \Delta t_s} - 1) + 1]. \end{aligned}$$

From Equations (2.35) and (2.34), the mixing coefficients  $\mathbf{T}_s$  and the weighted precursor concentrations  $\mathbf{C}_{i,s}$  at any time  $t_s$  can be calculated. However, to solve Equation (2.35) requires the inverse of matrix  $\mathbf{LHS}_{s+1}$ , and for the same reason as stated in last section, a numerical method that can take care of near-singularity needs to be used. The Singular Value Decomposition (SVD) method [P-1, S-4] was employed by Jacqmin [J-1] and Lee [L-1] in their synthesis models and proved to be very successful. Therefore, in this thesis, we also use the SVD method to solve the transient synthesis equations.

In general, the SVD method decomposes any  $M \times N$  matrix  $\mathbf{A}$  into the product of two orthogonal matrices and a diagonal matrix containing the singular values:

$$(\mathbf{A}) = (\mathbf{U}) \cdot \begin{pmatrix} w_1 & & & \\ & w_2 & & \\ & & \dots & \\ & & & w_N \end{pmatrix} \cdot (\mathbf{V}^T) \quad (2.36)$$

where  $\mathbf{U}$  and  $\mathbf{V}$  are orthogonal matrices and  $w_j, j = 1, \dots, N$  are singular values. Note that there is no restriction to the relationship between  $M$ , the number of rows, and  $N$ , the number of columns, and the problem to be solved is often a linear least-squares system. For a square matrix such as  $\text{LHS}_{s+1}$  in Equation (2.35), the inverse of  $(\mathbf{A})$  is trivial to compute:

$$(\mathbf{A}^{-1}) = (\mathbf{V}) \cdot \begin{pmatrix} \frac{1}{w_1} & & & \\ & \frac{1}{w_2} & & \\ & & \dots & \\ & & & \frac{1}{w_N} \end{pmatrix} \cdot (\mathbf{U}^T). \quad (2.37)$$

The singularity of a linear system can also be diagnosed by the SVD method. A condition number,  $\kappa$ , defined as the ratio of the largest  $w_j$  to the smallest  $w_j$  is often used to detect the singularity of the problem. If  $\mathbf{A}$  has an infinite  $\kappa$ , it is singular, and it is ill-conditioned if  $\kappa$  is very large. If one of the  $w_j$ 's is zero or very small, then its value is dominated by round-off error. Generally, this round-off problem can be avoided by zeroing the very small values of  $w_j$ 's.

Finally, it is essential to note that the matrices  $\mathbf{H}_s$ ,  $\mathbf{F}_{p,s}$ , and  $\mathbf{F}_{dis}$  change implicitly with time via the thermal-hydraulic feedback mechanism or control rod motion. In addition, the change of CMFD discontinuity factors through these feedbacks needs to be characterized. The methods for updating the discontinuity factors are discussed in Section 2.6, while the discussion of thermal-hydraulic feedback and control rod motion is delayed to Chapter 3.

## 2.6 Methods for Updating the Discontinuity Factors

For both steady-state and transient state, the change of the CMFD discontinuity factors needs to be characterized whenever there is a disturbance in flux shape. Two simple methods are proposed to update the CMFD discontinuity factors (f's in short) or the ratios of f's (r's in short) as described below.

### 1. Synthesis Scheme

The f's or r's are synthesized using the mixing coefficients:

$$\xi_{glm}^l = \sum_{n=1}^N |T| \xi_{glm,n}^l \quad (2.38)$$

where,

$N$  = total number of expansion functions,

$T$  = mixing coefficients,  $T_{g,n}$ , or,  $T_n$ ,

$\xi_{glm}^l$  =  $f_{glm}^l$ , or,  $r_{glm}^l$ ,

$\xi_{glm,n}^l$  = a set of pre-computed f's or r's.

The base of this scheme lies in the fact that the mixing coefficients are used to reconstruct the flux shape and thus the CMFD discontinuity factors can also reflect the change of flux shape. Therefore, in analogy with synthesizing the node fluxes, we use the mixing coefficients to synthesize the CMFD discontinuity factors.

### 2. Weighted-Average Scheme

The f's or r's are weighted and averaged by the product of changing mixing coefficients and pre-computed expansion functions:

$$\xi_{glm}^l = \frac{\sum_{n=1}^N |T| \psi_{g,n}^l \xi_{glm,n}^l}{\sum_{n=1}^N |T| \psi_{g,n}^l} \quad (2.39)$$

where  $\psi_{g,n}^l$  is a set of pre-computed expansion functions.

The rationale of this scheme is to add another degree of influence in reconstructing the CMFD discontinuity factors, namely the magnitude of the flux in the mode in question.

These schemes are used in the two one-dimensional nodal synthesis codes (described in Chapter 3) and tested for steady-state and transient problems (described in Chapter 4).

## 2.7 Summary

In this chapter, the general nodal synthesis model and the collapsed-group nodal synthesis model were developed from the CMFD-nodal equations corrected by discontinuity factors. The general nodal synthesis model constitutes an  $NG \times NG$  linear system, while the linear system for the collapsed-group nodal synthesis model has only  $N \times N$  equations. The QZ method is applied to solve the steady-state synthesis equations and the SVD method is used to solve the transient synthesis equations. A simple synthesis scheme and a weighted-average scheme are proposed to update the CMFD discontinuity factors.

## **Chapter 3**

# **Implementaion of the Nodal Synthesis Models to One-Dimensional Computer Codes**

### **3.1 Introduction**

In this chapter, two one-dimensional nodal synthesis codes are developed on the basis of the general nodal synthesis and the collapsed-group nodal synthesis models, respectively. The codes were developed on the MicroVax II machine and were written in standard FORTRAN-77 language. The reference solutions, expansion functions, and CMFD discontinuity factors are all generated by the QUANDRY code [S-1], which is also run on the same machine. The general flow diagram of the nodal synthesis calculation is shown in Figure 3-1. The calculation starts by reading the expansion functions, weight functions, CMFD discontinuity factors, along with the basic input data describing the problem. Next, the matrices of the linear system are computed; the linear system is solved for the mixing coefficients, and the neutron fluxes are reconstructed. Finally, the nodal parameters are updated and the flow returns to the stage of matrix-computing.

Section 3.2 describes the major parts of a one-dimensional general nodal synthesis code, SYN1T, and Section 3.3 outlines SYN1CG, which is a one-dimensional collapsed-group nodal synthesis code.

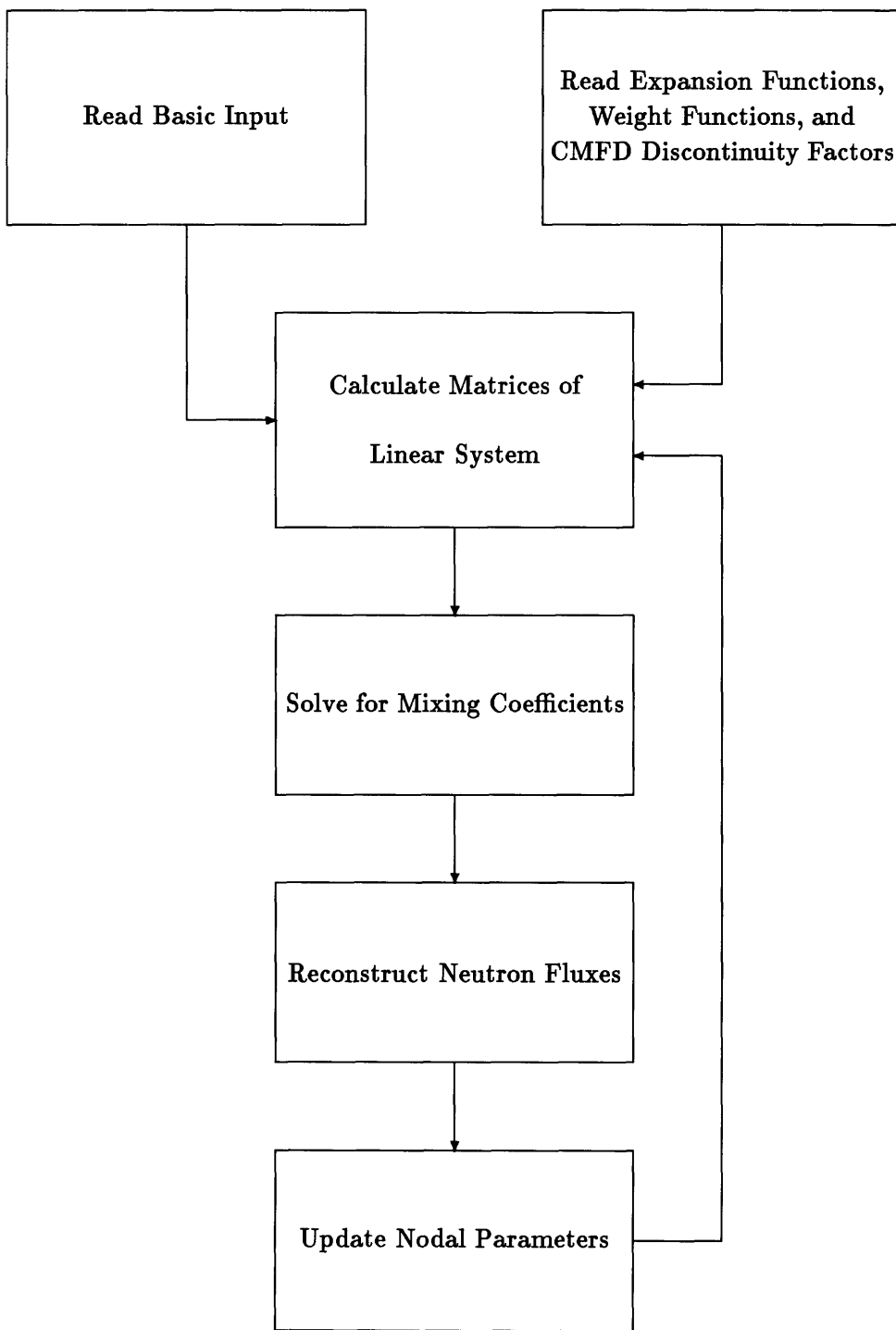


Figure 3-1: General Flow Diagram of Nodal Synthesis Calculations

## **3.2 SYN1T: One-Dimensional General Nodal Synthesis Code**

### **3.2.1 General Characteristics**

SYN1T is a one-dimensional general nodal synthesis code. The code was written in standard FORTRAN 77 language and installed on the MicroVAX II machine. The flow diagrams of SYN1T are illustrated in Figures 3-2, 3-3, and 3-4. The functions of all subroutines are provided in Tables 3.1 and 3.2.

The general characteristics of SYN1T are that:

1. It is based on the general nodal synthesis model.
2. The code is limited to two neutron energy groups and six delayed neutron precursor families.
3. Three different boundary conditions can be used, i.e.,
  - (a) Zero current,
  - (b) Zero flux, and
  - (c) Albedo.
4. SYN1T allows a maximum of 5 auxiliary functions including expansion functions, weight functions, CMFD discontinuity factors, thermal-hydraulic shapes, and zero-flux boundary correction factors (which will be discussed later in this subsection).
5. The expansion functions, weight functions, the CMFD discontinuity factors, the thermal-hydraulic shapes, and the zero-flux boundary correction factors are generated from QUANDRY.
6. It uses the same thermal-hydraulic model, WIGL3 [V-1], as that used by QUANDRY.
7. It uses the same linear cross section feedback model as that used by QUANDRY.
8. SYN1T makes use of the synthesis scheme and the weighted-average scheme to update the CMFD discontinuity factors or their ratios.
9. The steady state eigensystem is solved by the QZ method.
10. The finite-difference transient equations are obtained by the  $\theta$ -method and the time-integrated method, and the matrices are inverted by the SVD method.

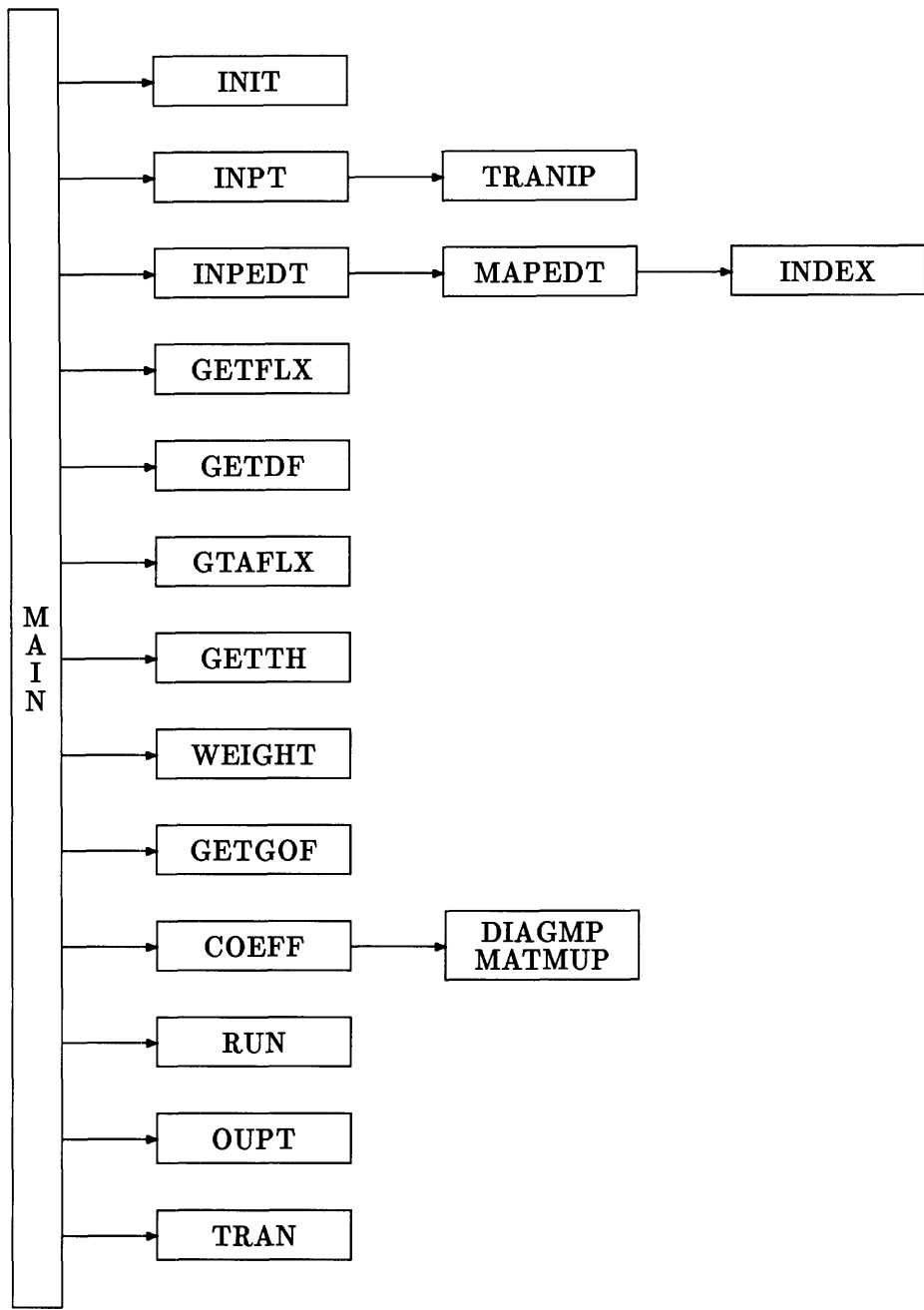


Figure 3-2: Flow diagram of SYN1T (Part 1)

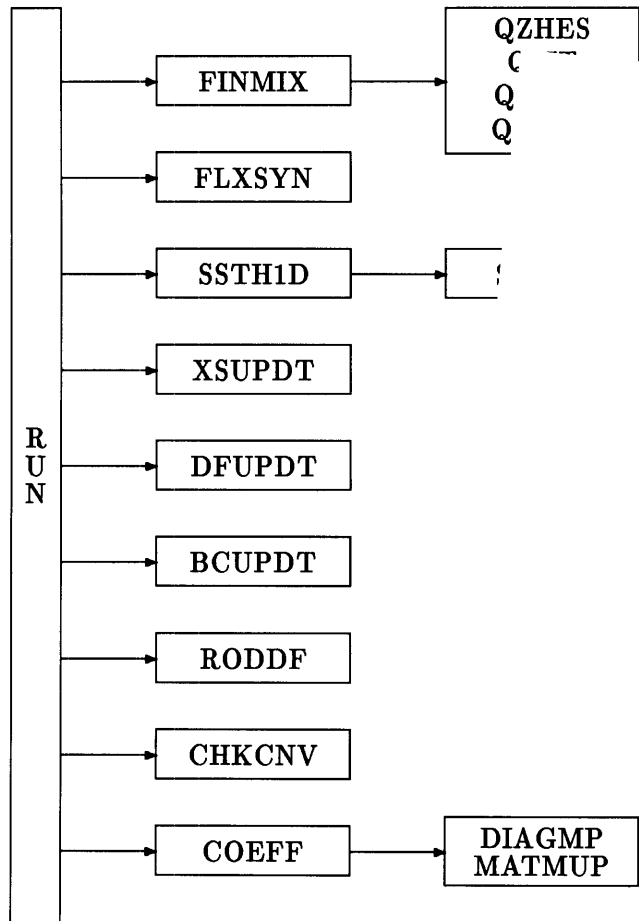
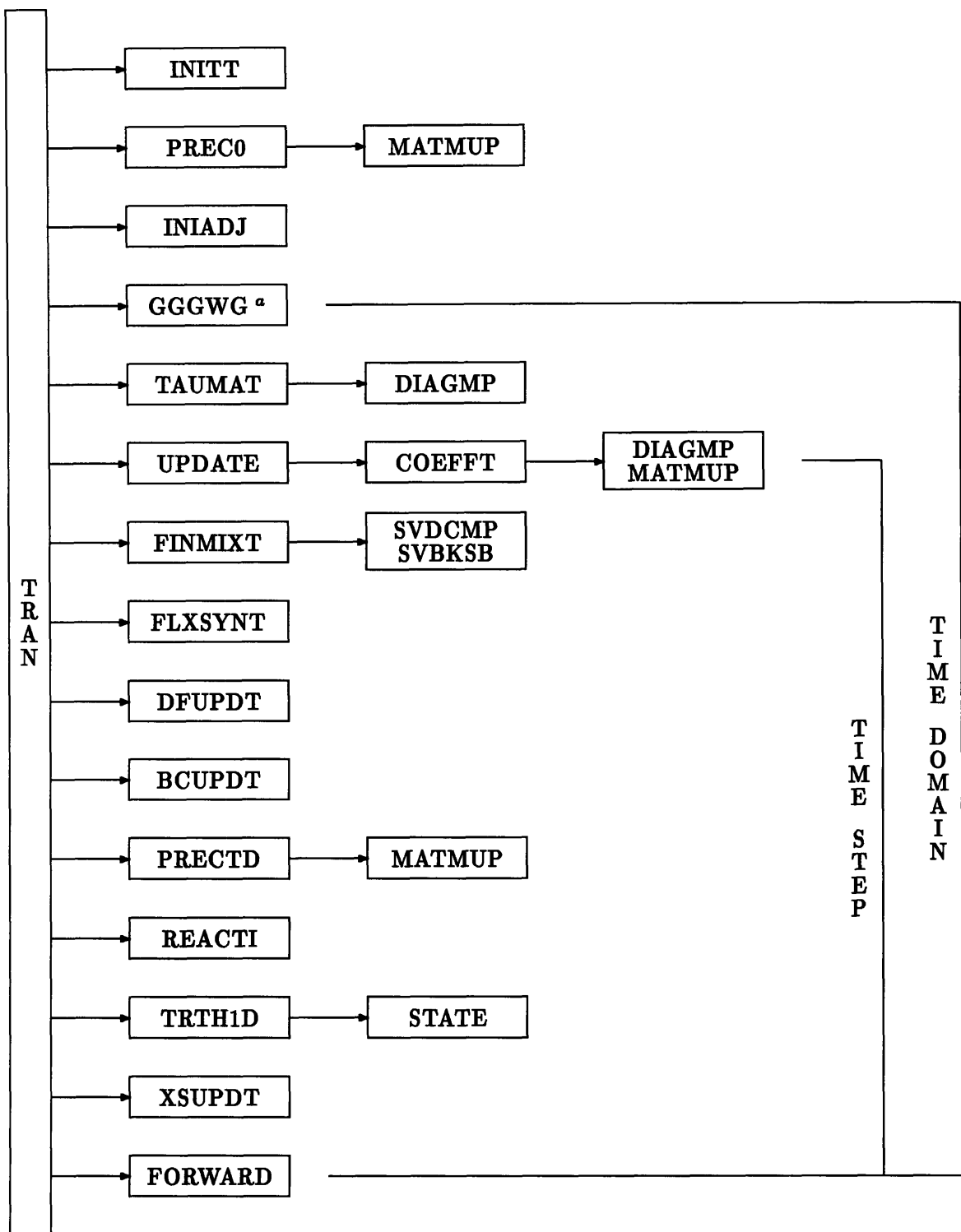


Figure 3-3: Flow diagram of SYN1T (Part 2)



<sup>a</sup>GGGWG represents GETFLX, GETDF, GTAFLX, WEIGHT, and GETGOF.

Figure 3-4: Flow diagram of SYN1T (Part 3)

Table 3.1: SYN1T program units (Part 1)

Program Unit	Function
INIT	Initialize all variables and arrays (G <sup>a</sup> )
INPT	Read input data (G,S)
TRANIP	Read transient input data (T)
INPEDT	Print input data (G)
MAPEDT	Print composition map (G)
INDEX	A dummy subroutine (G)
GETFLX	Read expansion functions (G)
GETDF	Read CMFD discontinuity factors (G)
GTAFLX	Read adjoint fluxes (G)
GETTH	Read thermal-hydraulic shapes (S)
WEIGHT	Set up weight functions (G)
GETGOF	Read zero-flux boundary correction factors (G)
COEFF	Calculate matrices of linear system (S)
DIAGMP	Perform multiplication of two diagonal matrices (G)
MATMUP	Perform multiplication of two general matrices (G)
RUN	Main control subroutine for steady-state problems (S)
OUPT	Print steady-state results (S)
TRAN	Main control subroutine for transient problems (T)
FINMIX	Calculate steady-state mixing coefficients (S)
QZHES	Reduce matrix <b>A</b> to upper Hessenburg form, and reduce matrix <b>B</b> to upper triangular form (S)
QZIT	Find matrices <b>Q</b> and <b>Z</b> (S)
QZVAL	Calculate eigenvalues (S)
QZVEC	Calculate eigenvectors (S)
FLXSYN	Reconstruct steady-state fluxes (S)
SSTH1D	Calculate steady-state thermal-hydraulic data (S)
STATE	Calculate coolant densities (G)
XSUPDT	Update cross sections (G)
DFUPDT	Update CMFD discontinuity factors (G)
BCUPDT	Update zero-flux boundary constants (G)
RODDF	Update CMFD discontinuity factors for fully-rodded nodes, and update CMDF discontinuity factors and cross sections for partially-rodded nodes (S)
CHKCNV	Check convergence of fluxes, criticality, and thermal-hydraulic data (S)

<sup>a</sup>G = General, S = Steady-state, T = Transient.

**Table 3.2: SYN1T program units (Part 2)**

Program Unit	Function
INITT	Restore old matrices and adjust initial $\nu\Sigma_f$ 's to initial steady state critical condition (T <sup>a</sup> )
PREC0	Calculate initial precursor concentrations (T)
INIADJ	Reconstruct initial steady-state adjoint fluxes (T)
REACTI	Calculate reactivity (T)
TAUMAT	Calculate matrix $\underline{\tau}$ (T)
UPDATE	Driver to call COEFFT (T)
COEFFT	Calculate new matrices of linear system (T)
FINMIXT	Calculate transient mixing coefficients (T)
SVDCMP	Decompose matrix $\mathbf{A}$ using SVD method (T)
SVBKSB	Perform backward substitution to find $\mathbf{A}^{-1} \underline{b}$ (T)
FLXSYNT	Reconstruct transient fluxes (T)
PRECTD	Calculate new precursor concentrations (T)
TRTH1D	Calculate transient thermal-hydraulic data (T)
FORWARD	Copy new matrices to old matrices for next time step (T)

<sup>a</sup>T = Transient.

11. SYN1T can solve two kinds of steady state problems, i.e.,
  - (a) Variable inlet coolant temperature, and
  - (b) Variable control rod position.
12. A simple algorithm is used to update the two-group neutron cross sections and the CMFD discontinuity factors for variable rod-position problems. This scheme will be described later in this subsection.
13. SYN1T can solve two kinds of transient problems, i.e.,
  - (a) Variable inlet coolant temperature, and
  - (b) Variable inlet flow rate.
14. SYN1T can output
  - (a) Steady-state eigenvalue,
  - (b) Nodal fluxes,
  - (c) Normalized nodal power densities,

- (d) Nodal thermal-hydraulic parameters,
- (e) Total reactor power, and
- (f) Total reactivity.

### 3.2.2 CMFD Discontinuity Factors

SYN1T requires the input of several sets of reference CMFD discontinuity factors as a basis to compute the “true” CMFD discontinuity factors according to the methods described in Section 2.6. However, QUANDRY does not save the discontinuity factors after a steady-state run. To solve this problem, a simple editing program was written to restore the discontinuity factors from the information kept in QUANDRY’s restart file. The description of this program is included in Appendix A.

### 3.2.3 Zero-Flux Boundary Correction Factors

For problems with zero-flux boundary condition, reference boundary correction factors are required. The rationale can be traced back to the discussion of Section 2.2.2 dealing with boundary condition. Dropping out the node and face indices, we rewrite Equation (2.15) as

$$\bar{J}_g(t) = 2 \left[ \frac{h}{\bar{D}_g(t)} + \frac{2\alpha_g}{\beta_g f_g(t)} \right]^{-1} \bar{\phi}_g(t). \quad (3.1)$$

Note that for zero-flux boundary condition,  $\alpha_g$  is zero but the ratio of  $(\frac{\alpha_g}{\beta_g})$  to  $f_g(t)$  may not be. This fact can be proven via the following steps.

Rearranging Equation (2.14), we obtain

$$\begin{aligned} \bar{\phi}_g(t) &= \frac{\alpha_g}{\beta_g} \bar{J}_g(t) \\ &= \Gamma_g \bar{J}_g(t) \end{aligned} \quad (3.2)$$

where

$$\Gamma_g \equiv \frac{\alpha_g}{\beta_g}.$$

Substituting this relation into Equation (2.10) and rearranging, we have

$$\bar{J}_g(t) = \frac{\bar{\phi}_g(t)}{\frac{h}{2\bar{D}_g(t)} + \frac{\Gamma_g}{f_g(t)}}. \quad (3.3)$$

The boundary correction factor  $\frac{\Gamma_g}{f_g(t)}$  can now be induced from this Equation as

$$\frac{\Gamma_g}{f_g(t)} = \frac{\bar{\phi}_g(t)}{\bar{J}_g(t)} - \frac{h}{2\bar{D}_g(t)}. \quad (3.4)$$

With reference values used in Equation (3.4),  $\frac{\Gamma_g}{f_g(t)}$  may not be zero even though  $\Gamma$  is. As QUANDRY does not explicitly provide this correction factor, a small program was written to compute the zero-flux boundary correction factors from the data stored in the QUANDRY restart file. Appendix B provides a description of this editing program.

The zero-flux boundary correction factors are updated in the same way as the CMFD discontinuity factors:

### 1. Synthesis Scheme

The correction factors are synthesized with a set of continually updated mixing coefficients:

$$\frac{\Gamma_g}{f_{glm}^l} = \sum_{n=1}^N |T_{g,n}| \left( \frac{\Gamma_g}{f_{glm}^l} \right)_n \quad (3.5)$$

where,

$N$  = total number of expansion functions,

$T_{g,n}$  = mixing coefficients,

$\left( \frac{\Gamma_g}{f_{glm}^l} \right)_n$  = a set of pre-computed zero-flux boundary correction factors.

### 2. Weighted-Average Scheme

The correction factors are weighted and averaged by the product of updated mixing

coefficients and pre-computed expansion functions:

$$\frac{\Gamma_g}{f_{g,lm}^l} = \frac{\sum_{n=1}^N |T_{g,n}| \psi_{g,n}^l \left( \frac{\Gamma_g}{f_{g,lm}^l} \right)_n}{\sum_{n=1}^N |T_{g,n}| \psi_{g,n}^l} \quad (3.6)$$

where the  $\psi_{g,n}^l$  are a set of pre-computed expansion functions.

### 3.2.4 Thermal-Hydraulic Model

SYN1T uses the same thermal-hydraulic model, WIGL3, as that used in QUANDRY. For static problems, the average fuel and coolant temperatures in a node are calculated with the steady-state version of WIGL3 model

$$\bar{T}_f^l = \bar{T}_c^l + \frac{V_f^l}{V_c^l} \left( \frac{1}{A_h U} + \frac{1}{A_h h_0} \right) (1 - r) (q''')^l \quad (3.7)$$

$$\bar{T}_c^l = T_b^l + \frac{(q''')^l V_f^l}{2 W_r^l C_c} \quad (3.8)$$

$$T_b^l = 2 \bar{T}_c^{l-1} - T_b^{l-1} \quad (3.9)$$

where,

$\bar{T}_f^l$  = average fuel temperature in node  $l$  (C),

$\bar{T}_c^l$  = average coolant temperature in node  $l$  (C),

$T_b^l$  = inlet (bottom) coolant temperature of node  $l$  (C),

$C_c$  = specific heat of the coolant (erg/g C),

$r$  = fraction of fission power deposited directly into the coolant,

$(q''')^l$  = volumetric energy generation rate in node  $l$  (erg/cm<sup>3</sup>),

$V_c^l$  = volume of coolant in node  $l$  (cm<sup>3</sup>),

$V_f^l$  = volume of fuel in node  $l$  (cm<sup>3</sup>),

$A_h$  = total heat transfer area/coolant volume within a node (cm<sup>-1</sup>),

$h_0$  = convective heat transfer coefficient (erg/s cm<sup>2</sup> C),

$W_r^l$  = coolant mass flow rate in node  $l$  (g/s).

For transient problems, the time-dependent version of WIGL3 model is used:

$$\rho_f V_f^l C_f \frac{d\bar{T}_f^l}{dt} = (1 - r) (q''')^l V_f^l - V_c^l \left[ \frac{1}{A_h U} + \frac{1}{A_h h_0} \left( \frac{W}{W_0} \right)^{0.8} \right]^{-1} (\bar{T}_f^l - \bar{T}_c^l) \quad (3.10)$$

$$V_c^l \left( \frac{\partial(\rho_c H)}{\partial \bar{T}_c} \right) \frac{d\bar{T}_c^l}{dt} = V_c^l \left[ \frac{1}{A_h U} + \frac{1}{A_h h_0} \left( \frac{W}{W_0} \right)^{0.8} \right]^{-1} (\bar{T}_f^l - \bar{T}_c^l) + 2 W_r^l C_c (T_b^l - \bar{T}_c^l) + r (q''')^l V_f^l \quad (3.11)$$

$$T_b^l = 2 \bar{T}_c^{l-1} - T_b^{l-1} \quad (3.12)$$

where,

- $t$  = time (s),
- $\rho_f$  = fuel density ( $\text{g}/\text{cm}^3$ ),
- $\rho_c$  = coolant density ( $\text{g}/\text{cm}^3$ ),
- $C_f$  = specific heat of the fuel ( $\text{erg}/\text{g C}$ ),
- $W_0$  = initial total coolant mass flow rate ( $\text{g}/\text{s}$ ),
- $W$  = total coolant mass flow rate ( $\text{g}/\text{s}$ ),
- $\left( \frac{\partial \rho_c H}{\partial \bar{T}_c} \right)$  = energy required to raise the temperature of a unit volume of coolant one temperature unit ( $\text{erg}/\text{cm}^3 \text{ C}$ ).

Once the nodal coolant temperature (either steady-state or transient) is computed, the nodal coolant density can be calculated as a function of temperature and system pressure.

### 3.2.5 Cross-Section Feedback Mechanism

To account for the change of thermal-hydraulic conditions, the cross sections are updated using the same linear feedback mechanism as that used in QUANDRY, i.e.,

$$\Sigma_\alpha^l(\bar{T}_f, \bar{T}_c, \bar{\rho}_c) = \Sigma_\alpha^l(\bar{T}_{f0}, \bar{T}_{c0}, \bar{\rho}_{c0}) + \left( \frac{\partial \Sigma_\alpha}{\partial \bar{T}_f} \right) (\bar{T}_f^l - \bar{T}_{f0}) + \left( \frac{\partial \Sigma_\alpha}{\partial \bar{T}_c} \right) (\bar{T}_c^l - \bar{T}_{c0}) + \left( \frac{\partial \Sigma_\alpha}{\partial \bar{\rho}_c} \right) (\bar{\rho}_c^l - \bar{\rho}_{c0}) \quad (3.13)$$

where,

- $\bar{T}_{f0}$  = reference fuel temperature (C),  
 $\bar{T}_{c0}$  = reference coolant temperature (C),  
 $\bar{\rho}_{c0}$  = reference coolant density (g/s),  
 $\bar{\rho}_c^l$  = average coolant density in node  $l$  (g/s),  
 $\Sigma_\alpha^l$  = macroscopic cross sections or inverse diffusion coefficients for node  $l$  ( $\text{cm}^{-1}$ ).

For PWR's the coefficients  $\frac{\partial \Sigma_\alpha}{\partial T_c}$  should be taken at constant pressure, while, for BWR's the  $\frac{\partial \Sigma_\alpha}{\partial T_c}$ 's should be at constant moderator density and the  $\frac{\partial \Sigma_\alpha}{\partial \rho_c}$ 's at constant moderator temperature. This linear feedback scheme is applied to both the steady-state and transient problems.

### 3.2.6 Variable Rod-Position Problems

The variable rod-position problems can be divided into two categories: the node-fully-rodded case and the node-partially-rodded case. SYN1T treats these two cases differently. A typical fully-rodded problem can be described with a simple 3-node case as shown in Figure 3-5. The shaded squares represent the fully-rodded nodes and the blank squares represent the unrodded nodes. The intermediate state (or the target state) is the condition we are interested in. States 1 and 2 are two closely bracketed conditions for which the respective expansion functions are generated. The ratios of discontinuity factors for the center node (node 2) can be approximated by the following algorithm

$$r_{g(2)}^- = \frac{(r_{g(1)}^-)_1 \psi_{g,1}^{(1)} + (r_{g(3)}^-)_2 \psi_{g,2}^{(3)}}{\psi_{g,1}^{(1)} + \psi_{g,2}^{(3)}} \quad (3.14)$$

$$r_{g(2)}^+ = \frac{r_{g(1)}^+ \psi_{g,1}^{(1)} + r_{g(3)}^+ \psi_{g,2}^{(3)}}{\psi_{g,1}^{(1)} + \psi_{g,2}^{(3)}} \quad (3.15)$$

$$(3.16)$$

where,

$r_{g(l)}^-$  = ratio of discontinuity factor for node  $l$  on left-hand face,

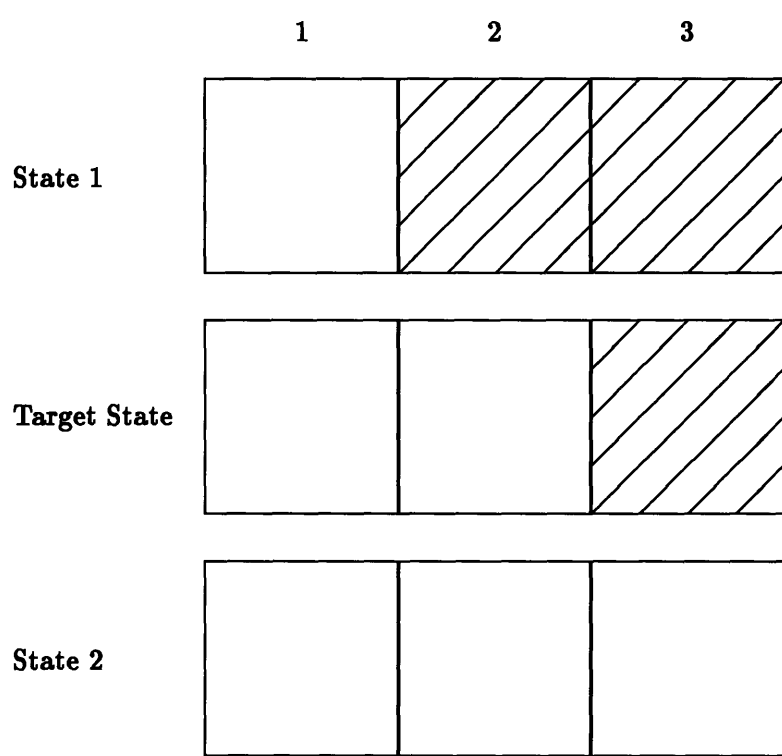


**Figure 3-5: A 3-node diagram showing the node-fully-rodded problem**

- $r_{g(l)}^+$  = ratio of discontinuity factor for node  $l$  on right-hand face,  
 $(r_{g(l)}^-)_n$  = ratio of discontinuity factor for node  $l$  on left-hand face,  
                        associated with state  $n$ ,  
 $(r_{g(l)}^+)_n$  = ratio of discontinuity factor for node  $l$  on left-hand face,  
                        associated with state  $n$ ,  
 $\psi_{g,n}^{(l)}$  = expansion function for node  $l$ , associated with state  $n$ .

In other words, this algorithm uses the reference information on the nodes nearest to the fully-rodded node to compute the approximate values of the ratio of the discontinuity factor. At least two expansion functions are required for this fully-rodded problem.

On the other hand, a typical partially-rodded case is illustrated in Figure 3-6 for a simple 3-node problem. Again, states 1 and 2 represent two closest conditions for which the expansion functions are generated. The target state represents a case where a control rod is halfway inserted in node 2. Unlike the problem of fully-rodded case, the cross sections for this partially-rodded node are not known. Therefore, in addition to the discontinuity factors, the nodal cross sections need to be approximated. A flux and volume weighting scheme, which is similar to that used by Gehin [G-3], is used for updating these parameters:

$$\Sigma_{\alpha,g}^{(2,PRN)} = \frac{(1-R)\Sigma_{\alpha,g}^{(1)}\psi_{g,1}^{(1)} + R\Sigma_{\alpha,g}^{(2,FRN)}\psi_{g,2}^{(1)}}{(1-R)\psi_{g,1}^{(1)} + R\psi_{g,2}^{(1)}} \quad (3.17)$$

$$f_g^{u(2,PRN)} = \frac{(1-R)f_{g(1)}^u\psi_{g,1}^{(1)} + Rf_{g(2,FRN)}^u\psi_{g,2}^{(1)}}{(1-R)\psi_{g,1}^{(1)} + R\psi_{g,2}^{(1)}} \quad (3.18)$$

where,

- $R$  = volume fraction of the rodded portion of the node,  
 $\Sigma_{\alpha,g}^{(2,PRN)}$  = macroscopic cross sections or inverse diffusion coefficients for  
                        the partially-rodded node (PRN),  
 $\Sigma_{\alpha,g}^{(2,FRN)}$  = macroscopic cross sections or inverse diffusion coefficients for  
                        the fully-rodded node (FRN),

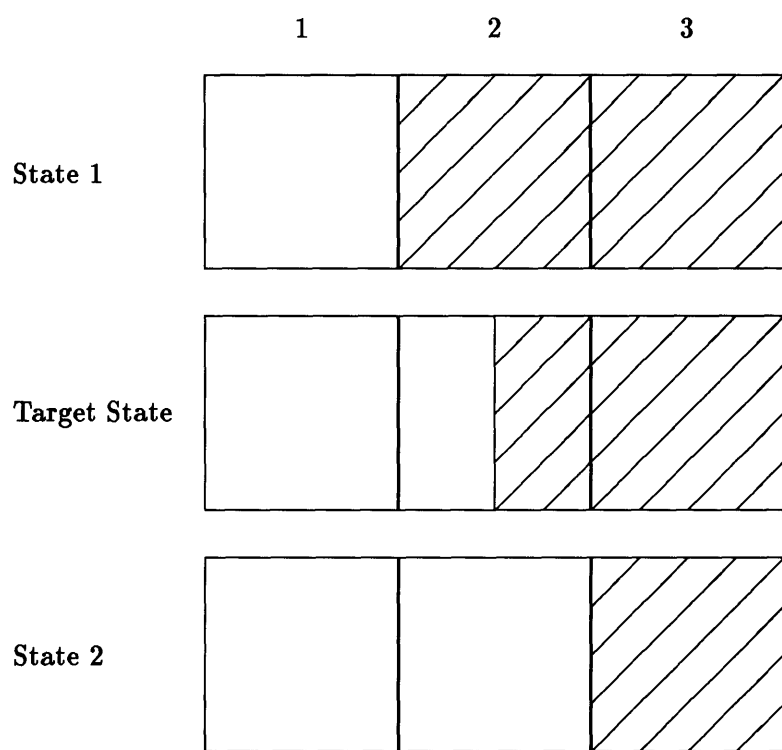


Figure 3-6: A 3-node diagram showing the node-partially-rodded problem

- $\Sigma_{\alpha,g}^{(1)}$  = macroscopic cross sections or inverse diffusion coefficients for node 1,  
 $\psi_{g,n}^{(1)}$  = expansion functions for node 1, associated with state n,  
 $f_g^u(2,PRN)$  = discontinuity factors for the partially-rodded node (PRN), on face u,  
 $f_g^u(2,FRN)$  = discontinuity factors for the fully-rodded node (FRN), on face u,  
 $f_g^u(1)$  = discontinuity factors for node 1, on face u,  
 $u$  = left-hand (-) or right-hand (+) faces.

Note that in Gehin's polynomial nodal model, only the cross sections for the partially-rodded node are computed, whereas in our synthesis model, the discontinuity factors are also updated.

### 3.2.7 Convergence Test for Steady-State Problems

The steady-state problems are solved iteratively until the neutron multiplication factor ( $k_{\text{eff}}$ ), the nodal fluxes, and/or the thermal-hydraulic parameters are converged. The iteration loop includes calculating the initial matrices, solving for the  $k_{\text{eff}}$  and the mixing coefficients, reconstructing the fluxes and calculating the power distribution, calculating the thermal-hydraulic parameters, updating the cross-sections and the discontinuity factors, re-computing the matrices, and so on. Specifically, the nodal fluxes and thermal-hydraulic parameters are converged if

$$\begin{aligned}\epsilon_{1,\max} &\equiv \underset{\text{all nodes, all groups}}{\text{maximum over}} \left( \frac{|\phi_g^{l,t} - \phi_g^{l,t-1}|}{\phi_g^{l,t-1}} \right) \leq \epsilon_{\text{flux}} \\ \epsilon_{2,\max} &\equiv \underset{\text{all nodes}}{\text{maximum over}} \left( \frac{|X^{l,t} - X^{l,t-1}|}{X^{l,t-1}} \right) \leq \epsilon_{\text{thermal}}\end{aligned}$$

where,

- $\epsilon_{1,\max}$  = maximum relative error in the nodal flux,  
 $\epsilon_{2,\max}$  = maximum relative error in the nodal thermal-hydraulic parameters,  
 $\epsilon_{\text{flux}}$  = convergence criterion of nodal flux,  
 $\epsilon_{\text{thermal}}$  = convergence criterion of nodal thermal-hydraulic parameters,  
 $X$  = fuel temperature, coolant temperature, or coolant density,  
 $t$  = iteration number.

### 3.2.8 Transient Problems

SYN1T can solve two kinds of transient problems: variable inlet coolant temperature and variable inlet coolant mass flow rate. These transient forcing functions can be specified as quadratic polynomial in time.

In SYN1T, the entire course of a transient scenario is divided into several time domains. Each time domain is further subdivided into many small equal-sized time steps. During each time domain, expansion functions, weight functions, and discontinuity factors can be reassigned. However, to keep a consistent linear system of equations, the number of expansion functions must be the same throughout the whole transient period.

### 3.2.9 Total Reactivity

The total reactivity during a transient scenario can be computed with the following exact equation [H-2], using a reference adjoint flux  $(\phi_g^*)_0$  as the weight function

$$\begin{aligned} \rho(t) = & 1 + \frac{1}{\sum_l \sum_g (\phi_g^*)_0^l [(1 - \beta)\chi_p^g + \sum_d \chi_d^g \beta_d] \sum_{g'} \bar{\nu} \bar{\Sigma}_{fg'}^l \bar{\phi}_{g'}^l V^l} \left[ \right. \\ & \sum_l \sum_g (\phi_g^*)_0^l \sum_{g'} \bar{\Sigma}_{gg'}^l \bar{\phi}_{g'}^l V^l - \sum_l \sum_g (\phi_g^*)_0^l \bar{\Sigma}_g^l \bar{\phi}_g^l V^l - \\ & \left. \sum_l \sum_g (\phi_g^*)_0^l \sum_p \frac{2S_p}{V^l} \left( \frac{h_l^p}{D_g^l} + \frac{f_{glm}^m}{f_{glm}^l} \frac{h_m^q}{D_g^m} \right)^{-1} \left( \bar{\phi}_g^l - \frac{f_{glm}^m}{f_{glm}^l} \bar{\phi}_g^m \right) V^l \right]. \quad (3.19) \end{aligned}$$

Note that for simplicity, the notation of time-dependence,  $(t)$ , for macroscopic cross sections, nodal fluxes, and discontinuity factors has been dropped out.

### **3.3 SYN1CG: One-Dimensional Collapsed-Group Nodal Synthesis Code**

SYN1CG is a one-dimensional collapsed-group nodal synthesis code. The code is written in standard FORTRAN 77 language and installed on the MicroVAX II machine. In general, SYN1CG is built on SYN1T with the change of matrix structure for many of its subroutines. The flow diagrams of SYN1CG are illustrated in Figures 3-7, 3-8, and 3-9. The functions of all subroutines are provided in Tables 3.3 and 3.4.

The general characteristics of SYN1CG are mostly the same as those of SYN1T:

1. It is based on the collapsed-group nodal synthesis model.
2. The code is limited to two neutron energy groups and six delayed neutron precursor families.
3. Three different boundary conditions can be used, i.e.,
  - (a) Zero current,
  - (b) Zero flux, and
  - (c) Albedo.
4. SYN1CG allows maximum of 5 auxiliary functions including expansion functions, weight functions, CMFD discontinuity factors, thermal-hydraulic shapes, and zero-flux boundary correction factors.
5. The expansion functions, weight functions, the CMFD discontinuity factors, the thermal-hydraulic shapes, and the zero-flux boundary correction factors are generated from QUANDRY.
6. It uses the same thermal-hydraulic model, WIGL3 [V-1], as that used by QUANDRY.
7. It uses the same linear cross section feedback model as that used by QUANDRY.
8. SYN1CG allows the synthesis scheme and the weighted-average scheme to update the CMFD discontinuity factors or their ratios.
9. The steady state eigensystem is solved by the QZ method.

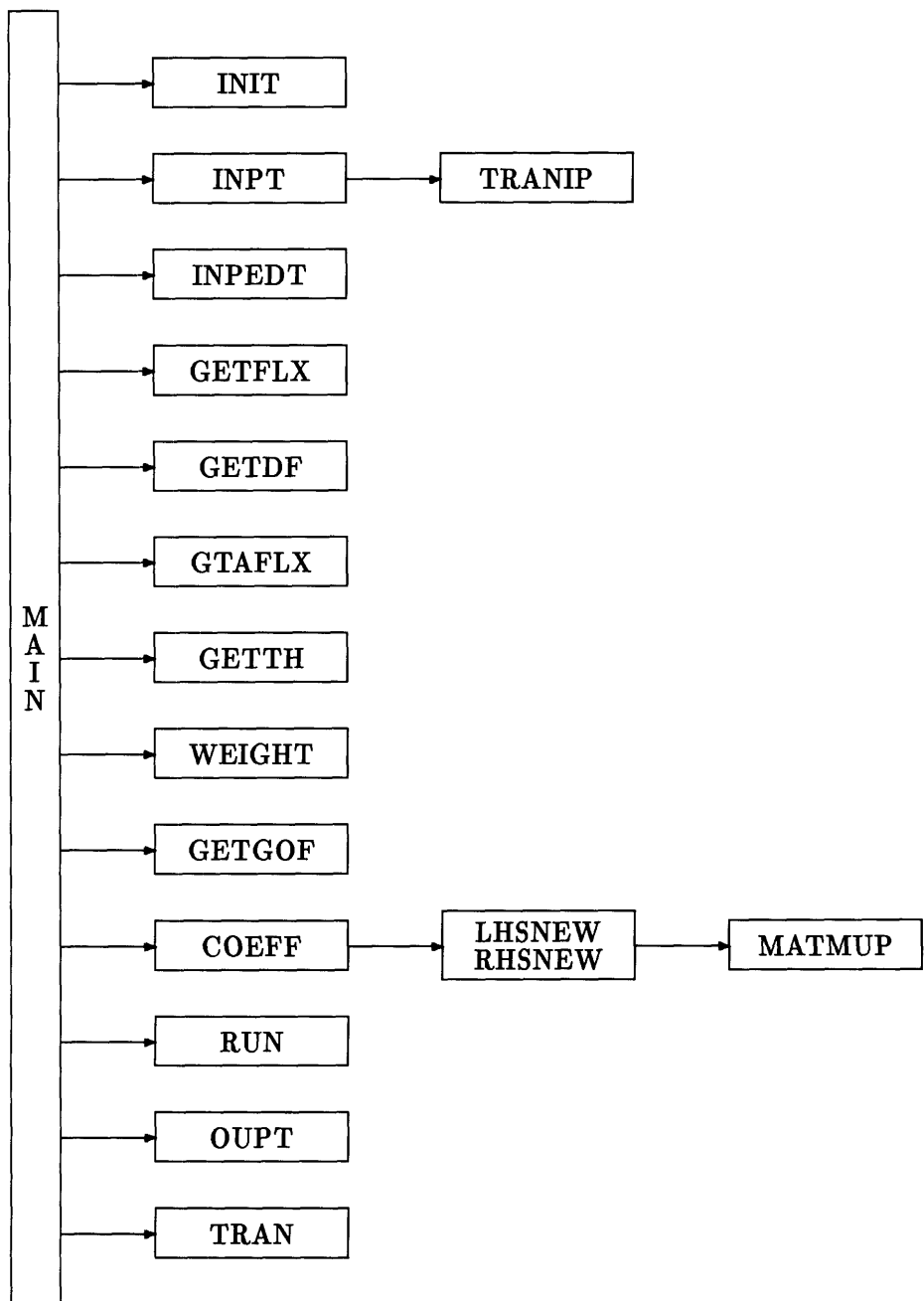


Figure 3-7: Flow diagram of SYN1CG (Part 1)

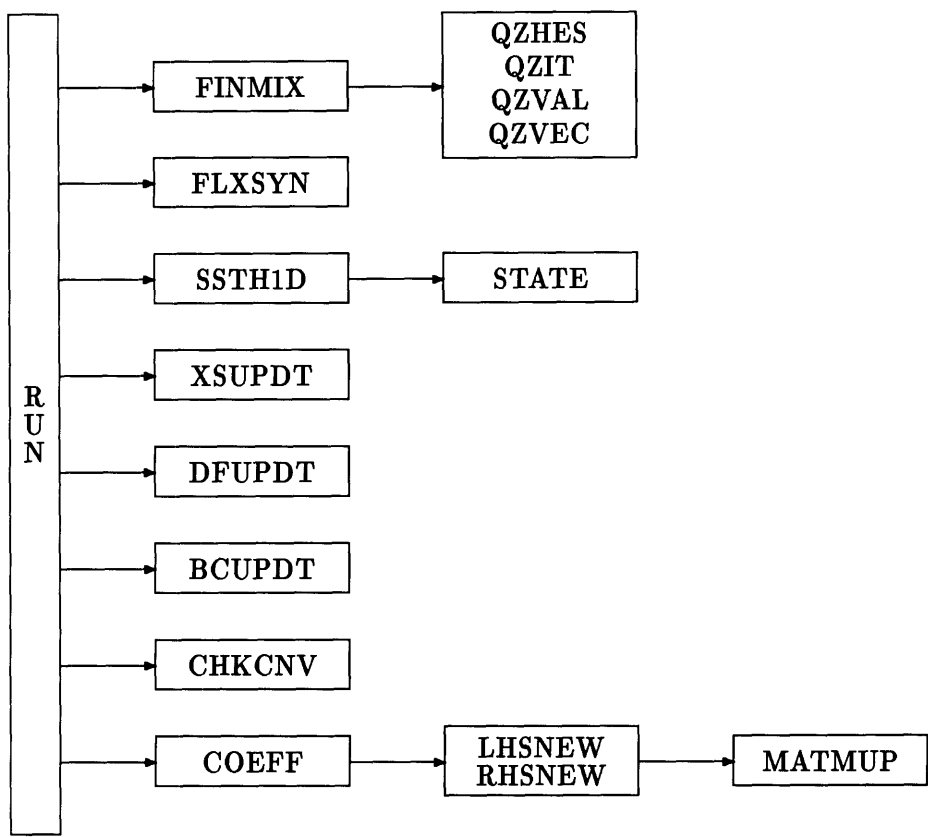
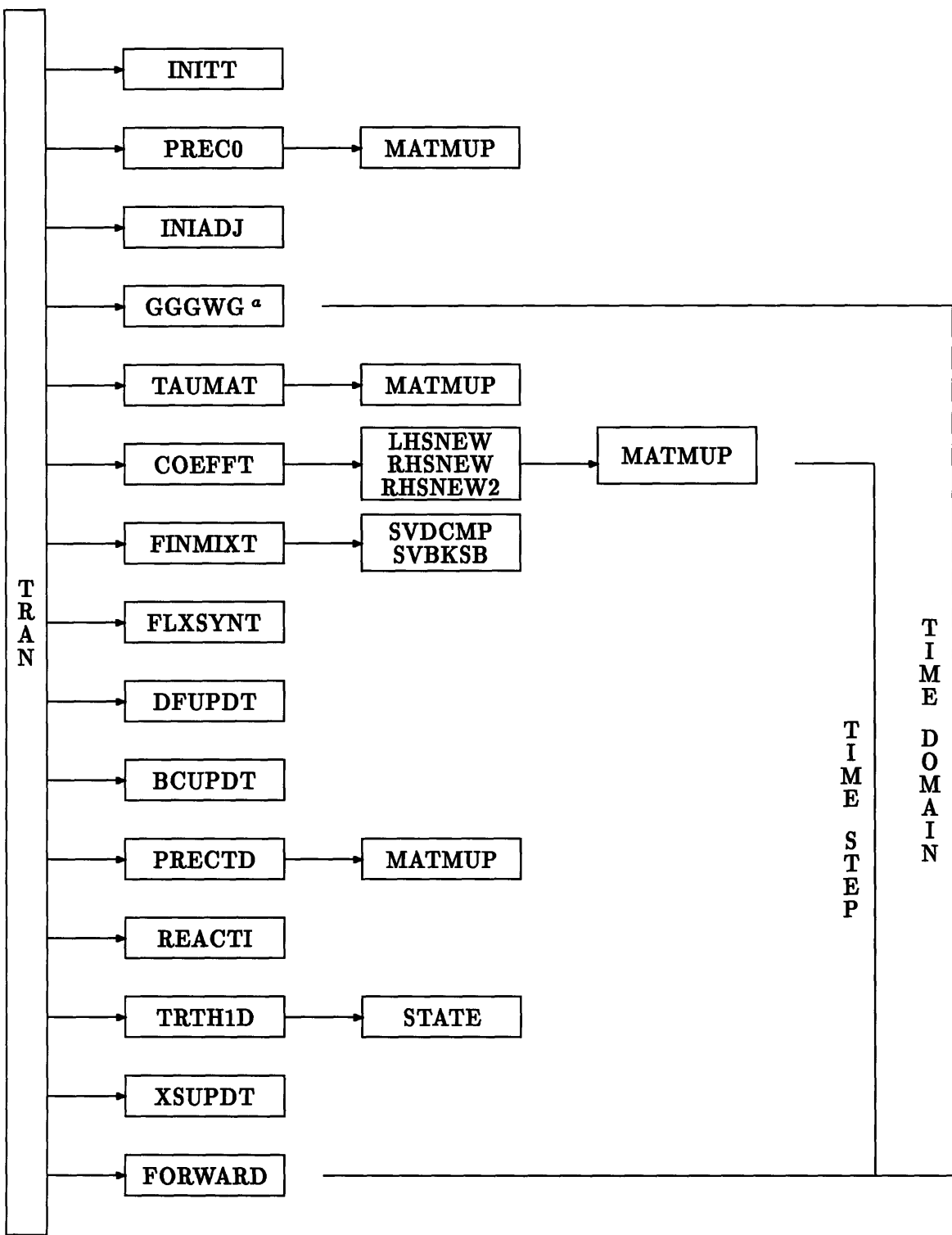


Figure 3-8: Flow diagram of SYN1CG (Part 2)



<sup>a</sup>GGGWG represents GETFLX, GETDF, GTAFLX, WEIGHT, and GETGOF.

Figure 3-9: Flow diagram of SYN1CG (Part 3)

Table 3.3: SYN1CG program units (Part 1)

Program Unit	Function
INIT	Initialize all variables and arrays (G <sup>a</sup> )
INPT	Read input data (G,S)
TRANIP	Read transient input data (T)
INPEDT	Print input data (G)
GETFLX	Read expansion functions (G)
GETDF	Read CMFD discontinuity factors (G)
GTAFLX	Read adjoint fluxes (G)
GETTH	Read thermal-hydraulic shapes (S)
WEIGHT	Set up weight functions (G)
GETGOF	Read zero-flux boundary correction factors (G)
COEFF	Calculate matrices of linear system (S)
LHSNEW	Calculate the total loss matrix (G)
RHSNEW	Calculate the prompt-fission matrix (S)
MATMUP	Perform multiplication of two general matrices (G)
RUN	Main control subroutine for steady-state problems (S)
OUPT	Print steady-state results (S)
TRAN	Main control subroutine for transient problems (T)
FINMIX	Calculate steady-state mixing coefficients (S)
QZHES	Reduce matrix A to upper Hessenburg form, and reduce matrix B to upper triangular form (S)
QZIT	Find matrices Q and Z (S)
QZVAL	Calculate eigenvalues (S)
QZVEC	Calculate eigenvectors (S)
FLXSYN	Reconstruct steady-state fluxes (S)
SSTH1D	Calculate steady-state thermal-hydraulic data (S)
STATE	Calculate coolant densities (G)
XSUPDT	Update cross sections (G)
DFUPDT	Update CMFD discontinuity factors (G)
BCUPDT	Update zero-flux boundary constants (G)
CHKCNV	Check convergence of fluxes, criticality, and thermal-hydraulic data (S)

<sup>a</sup>G = General, S = Steady-state, T = Transient.

Table 3.4: SYN1CG program units (Part 2)

Program Unit	Function
INITT	Restore old matrices and adjust initial $\nu\Sigma_f$ 's to initial steady state critical condition (T <sup>a</sup> )
PREC0	Calculate initial precursor concentrations (T)
INIADJ	Reconstruct initial steady-state adjoint fluxes (T)
REACTI	Calculate reactivity (T)
TAUMAT	Calculate matrix $\tau$ (T)
COEFFT	Calculate new matrices of linear system (T)
RHSNEW2	Calculate the delayed-fission matrix (T)
FINMIXT	Calculate transient mixing coefficients (T)
SVDCMP	Decompose matrix A using SVD method (T)
SVBKSB	Perform backward substitution to find $A^{-1}b$ (T)
FLXSYNT	Reconstruct transient fluxes (T)
PRECTD	Calculate new precursor concentrations (T)
TRTH1D	Calculate transient thermal-hydraulic data (T)
FORWARD	Copy new matrices to old matrices for next time step (T)

<sup>a</sup>T = Transient.

10. The finite-differences transient equations are obtained by the  $\theta$ -method and the time-integrated method, and the matrices are inverted by the SVD method.
11. SYN1CG can only solve steady-state variable inlet coolant temperature problems.
12. SYN1CG can only transient variable inlet coolant temperature or variable inlet coolant mass flow rate problems.
13. SYN1CG can output
  - (a) Steady-state eigenvalue,
  - (b) Nodal fluxes,
  - (c) Normalized nodal power densities,
  - (d) Nodal thermal-hydraulic parameters,
  - (e) Total reactor power, and
  - (f) Total reactivity.

Note that for simplicity, the function of SYN1CG for solving steady-state variable rod-position problems, included for SYN1T, is here absent. The detail description of essential

parts of the code is similar to that given in Section 3.2, and is not repeated here.

### 3.4 Summary

SYN1T and SYN1CG are two one-dimensional computer codes implementing the general nodal synthesis model and the collapsed-group nodal synthesis model, respectively. The key modules of the codes have been described. In Chapter 4, these two codes will be used for several numerical tests of synthesis models.

## **Chapter 4**

# **One-Dimensional Numerical Tests of the Theoretical Nodal Synthesis Models**

### **4.1 Introduction**

In this chapter, several one-dimensional test problems are used to validate the nodal synthesis models. Accuracy and efficiency are discussed, and a comparison of the two synthesis methods is included.

Section 4.2 describes the numerical tests of the general nodal synthesis model. Section 4.3 deals with the tests of the collapsed-group synthesis model. Finally, the comparison of these two synthesis models is included in Section 4.4.

### **4.2 Tests of the General Nodal Synthesis Model**

#### **4.2.1 Steady-State Problems**

Three kinds of test problems are solved by SYN1T to evaluate the accuracy of the general nodal synthesis model. All the test problems were artificially created and simplified so that they do not represent realistic reactor conditions. The following subsections describe the tests in detail.

#### 4.2.1.1 Variable Inlet Coolant Temperature Problem

Four fictitious test cases were studied as listed in Table 4.1. The test model was a one-dimensional 10-node critical core containing 4 different materials and accounting for thermal-hydraulic feedback. All the auxiliary functions and reference solutions were generated by QUANDRY. The weight functions used were all adjoint fluxes. In converging to the consistent thermal hydraulic-neutron flux shapes, CMFD discontinuity factors were updated by synthesizing with mixing coefficients as described in Section 2.6. A complete description of this test model is given in Appendix C.1.

Case A is a “pure” inlet coolant temperature problem in which the expansion functions are determined for the same reactor power as that of the intermediate, critical state to be synthesized. In other words, these two closely bracketing expansion functions are used to synthesize the flux for a third critical reactor state with an intermediate inlet coolant temperature. The thermal fluxes for the two bracketing states as well as for the intermediate state are provided in Table 4.2. The synthesis model generates an excellent solution with the average error in normalized nodal power density of only 0.035%. The error distribution is plotted in Figure 4-1. As shown in the figure, the maximum error of only -0.1% occurs at node 9, which is next to the reflector at node 10. The eigenvalue (neutron multiplication factor) also agrees with the reference solution: As shown in Table 4.3, the  $k_{\text{eff}}$  differs by only 2 parts in a million, which is about the round-off error of the computing system.

Table 4.1: Test cases for steady-state variable inlet coolant temperature problem

Case	Intermediate State	Bracketing States
A	(17.29, 539.19) <sup>a</sup>	(17.29, 555.00), (17.29, 536.91)
B-1	(30.58, 545.22)	(17.29, 555.00), (42.82, 539.19)
B-2	(30.58, 545.22)	(17.29, 555.00), (42.82, 539.19), (35.73, 536.91)
B-3	(30.58, 545.22)	(17.29, 555.00), (17.29, 539.19), (17.29, 536.91)

<sup>a</sup>Reactor state at which the total power is 17.29 MW<sub>t</sub>, and the inlet coolant temperature is 539.19 K.

Case series B is a more general problem in which both the reactor power and the inlet coolant temperature for the intermediate state are different from those for the bracketing states. Cases B-1 to B-3 are three branches of case B to test the sensitivity of the results to

Table 4.2: Thermal fluxes of bracketing states and intermediate state for steady-state case A

Node	(17.29, 555.00) <sup>a</sup>	(17.29, 539.19)	(17.29, 536.91)
1	1.8399e+13 <sup>b</sup>	1.7386e+13	1.7248e+13
2	3.2976e+13	3.2576e+13	3.2512e+13
3	8.4092e+13	8.3923e+13	8.3877e+13
4	1.4016e+14	1.4030e+14	1.4029e+14
5	7.0125e+13	7.0671e+13	7.0741e+13
6	6.3640e+13	6.4283e+13	6.4408e+13
7	1.0954e+14	1.1080e+14	1.1104e+14
8	5.8938e+13	6.0087e+13	6.0194e+13
9	2.1709e+13	2.2117e+13	2.2137e+13
10	1.3364e+13	1.2908e+13	1.2838e+13

<sup>a</sup>Reactor state at which the total power is 17.29 MW<sub>t</sub>, and the inlet coolant temperature is 555 K.

<sup>b</sup>Read as  $1.8399 \times 10^{13}$  n/cm<sup>2</sup> sec.

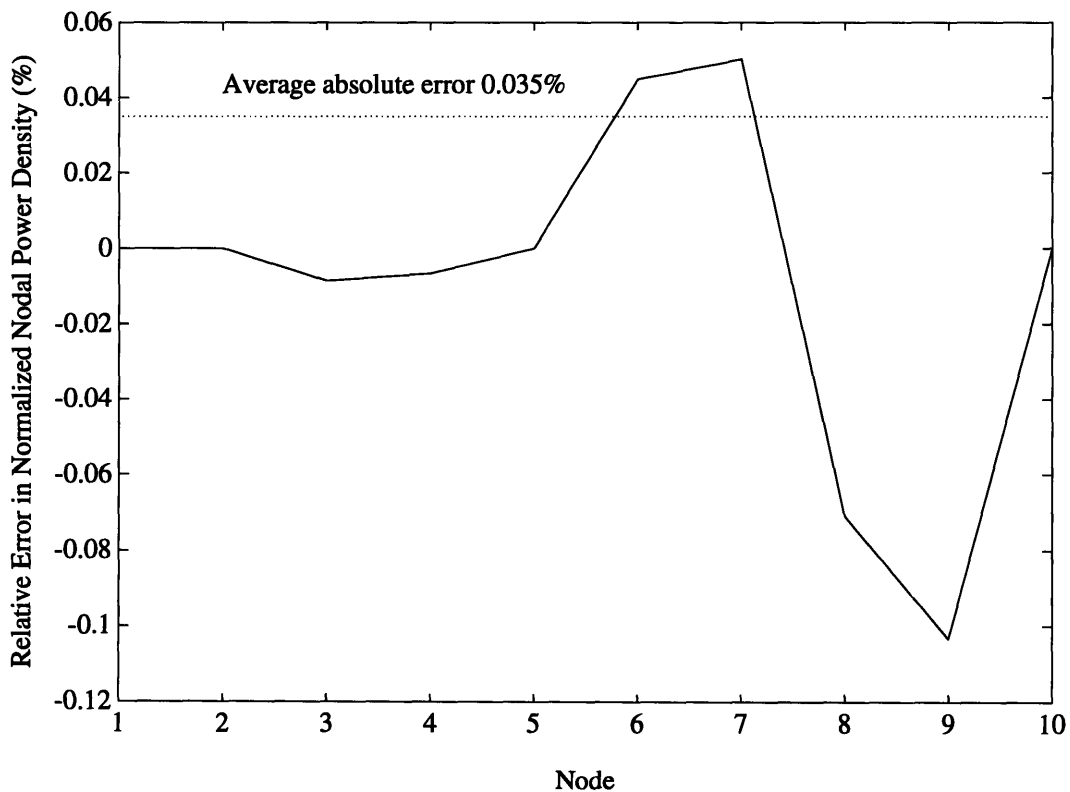


Figure 4-1: Relative error in normalized power density for steady-state case A

Table 4.3: Neutron multiplication factor for steady-state case A

Case	$K_{eff}$
Reference	1.040222
A	1.040220

the use of expansion functions. Case B-1 uses only two bracketing states; case B-2 includes a third state in addition to the two used for case B-1, and case B-3 uses three bracketing states which are all at the same reactor power. Figures 4-2 to 4-4 show the thermal fluxes for those bracketing states as well as for the intermediate state. Note that the legend on the figures, (xx,xx,yy.yyy), represents a reactor state at which the total power is xx.xx MW<sub>t</sub>, and the inlet coolant temperature is yy.yy °K. The error in the synthesized nodal power densities is shown in Figure 4-5 for case B-1, and both the power densities and their errors are shown in Figures 4-6 and 4-7 for case B-2, and Figures 4-8 and 4-9 for case B-3. The synthesized  $k_{eff}$ 's are given in Table 4.4.

Case B-1 gives the best results. The average error in normalized nodal power density is only 0.25%, and the maximum error of 0.86% occurs at node 2, which is next to the reflector at node 1. The eigenvalue differs by only -0.0081%. The synthesized power shape tilts slightly as compared to the reference shape.

For case B-2, it is seen that the use of an extra bracketing state gives a worse solution than that for case B-1. The average error in normalized nodal power density increases to 4.6%, and the maximum error rises to 5.7% at node 2. The error in eigenvalue increases to -0.1%. Note that the power shape tilts more than for case B-1.

Case B-3 gives the worst results of the three cases. The average error in normalized nodal power density increases to 10.5%, and the maximum error goes up to 17% at node 9. The eigenvalue differs by 0.16%. The tilt in the synthesized power shape is opposite to that for cases B-1 and B-2.

The series B studies show that the proper selection of bracketing states for the expansion functions is very important for the accuracy of the general nodal synthesis model. However, there appears to be no systematic way to choose the proper bracketing states. Physical insight may be a useful guide. (In case B-3, the power levels for the two "bracketing" states did not actually bracket the power level for the intermediate state.) However, intuition may

not always work. (In case B-2, one might expect that using more expansion functions would improve the solution, but it did not.) On the other hand, the nodal synthesis model can reproduce the reference solutions, given that the “right” expansion functions.

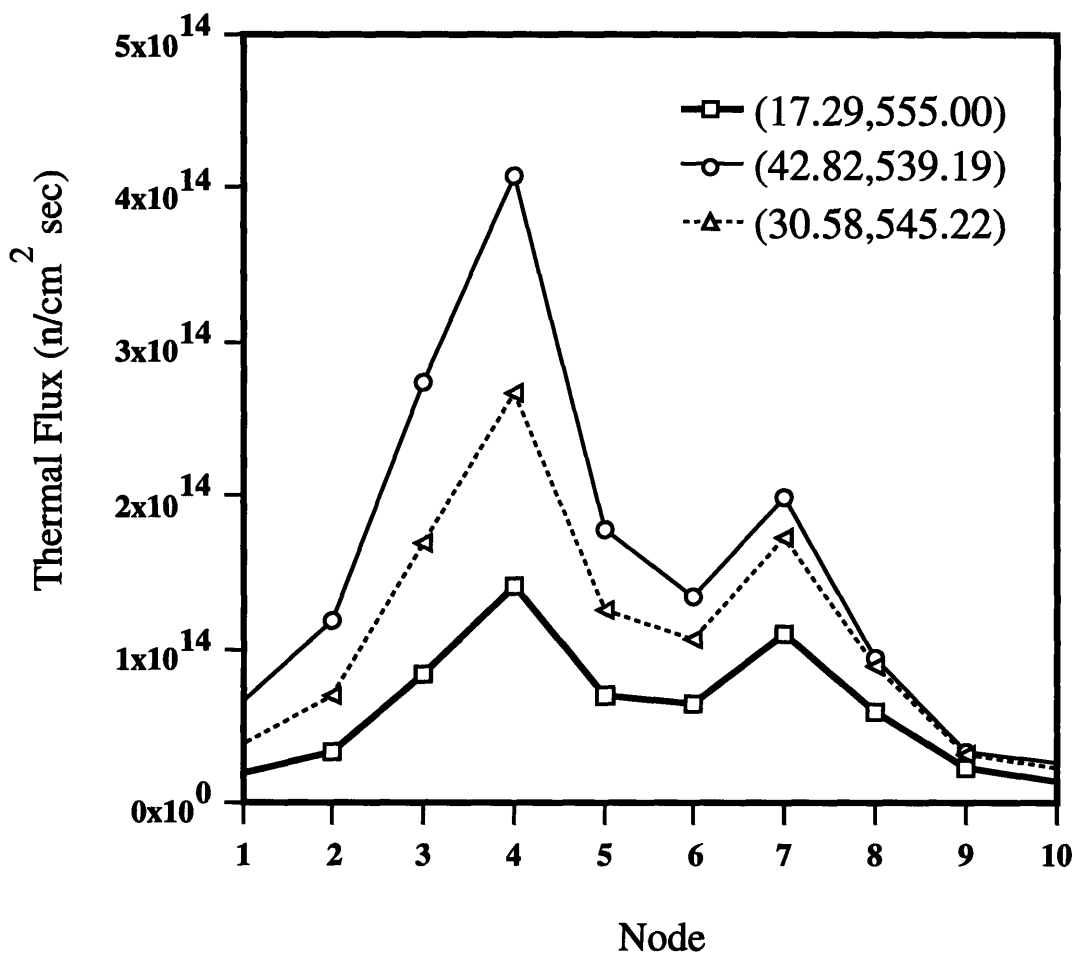


Figure 4-2: Thermal fluxes of bracketing states and intermediate state for steady-state case B-1

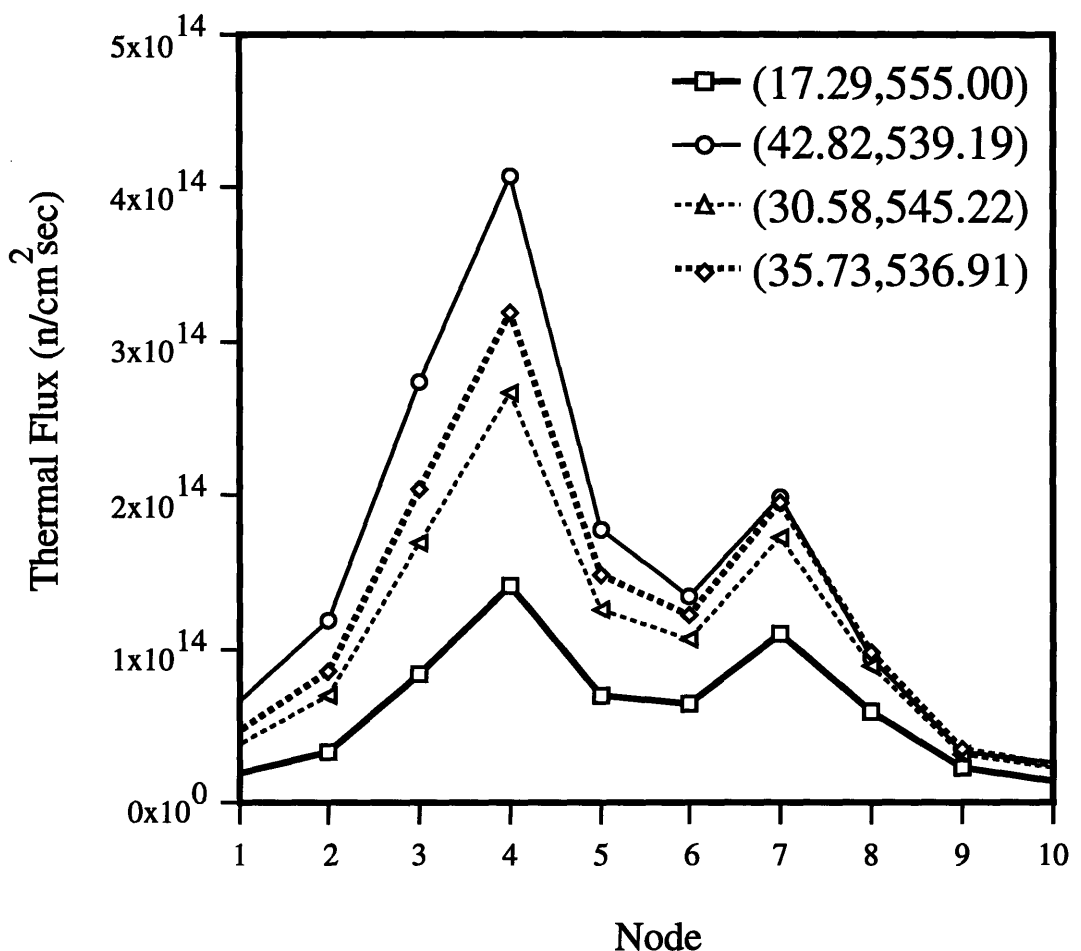


Figure 4-3: Thermal fluxes of bracketing states and intermediate state for steady-state case B-2

Table 4.4: Neutron multiplication factors for steady-state case series B

Case	K <sub>eff</sub>	Relative Error (%)
Reference	1.013592	-
B-1	1.013510	-0.0081
B-2	1.012576	-0.1003
B-3	1.015200	+0.1586

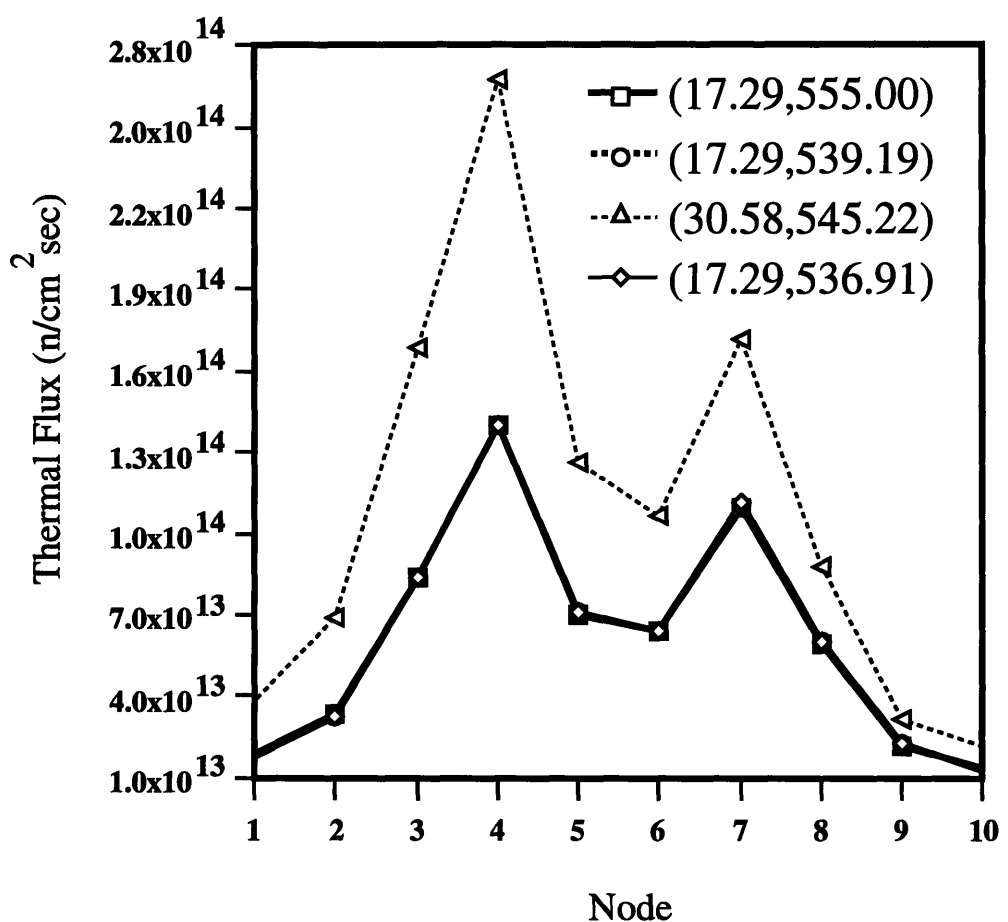


Figure 4-4: Thermal fluxes of bracketing states and intermediate state for steady-state case B-3

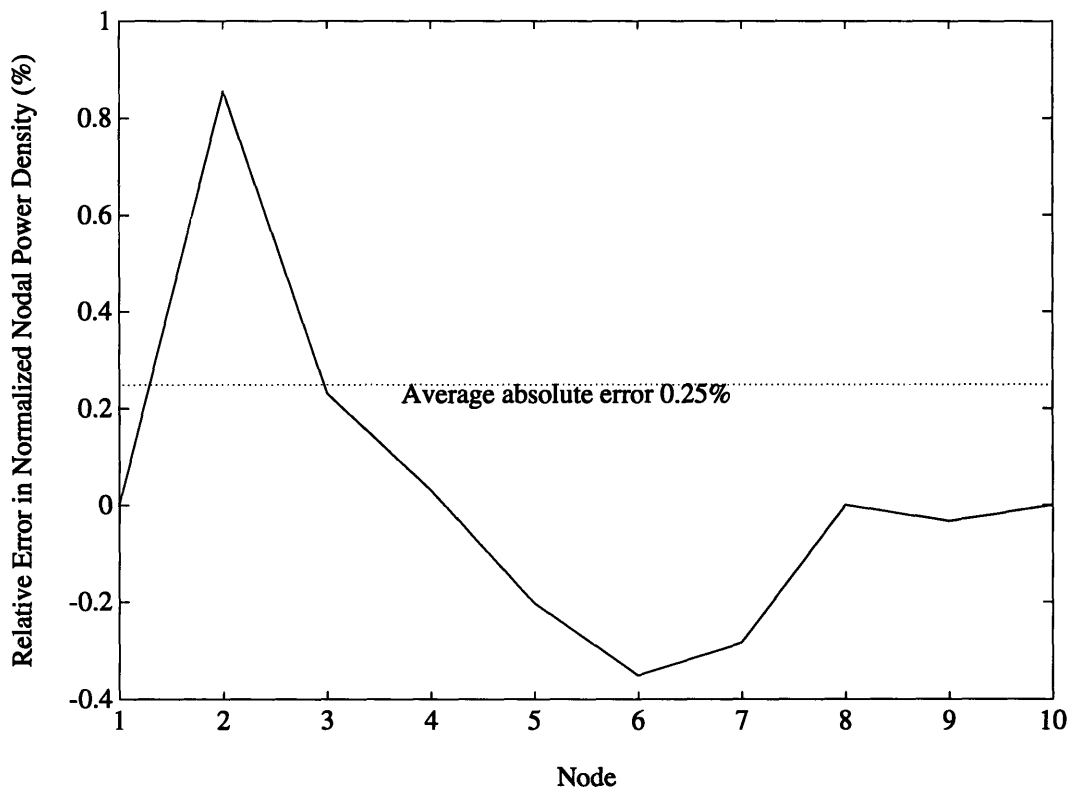


Figure 4-5: Relative error in normalized power density for steady-state case B-1

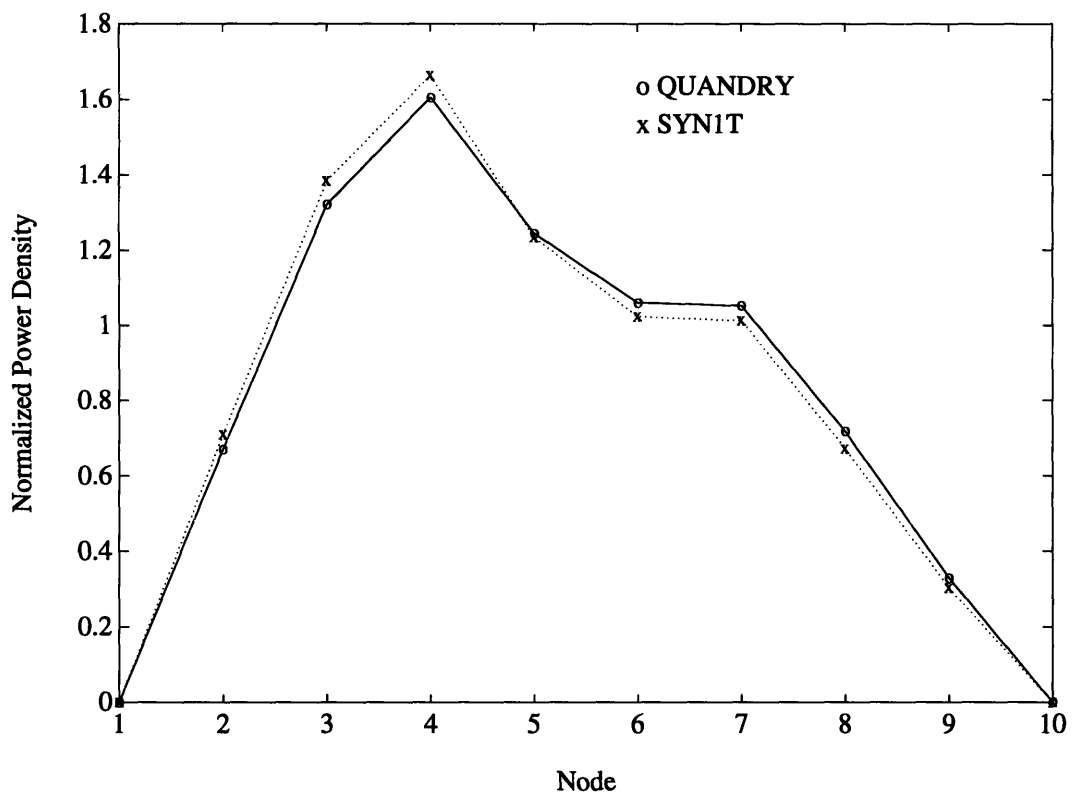


Figure 4-6: Normalized nodal power density for steady-state case B-2

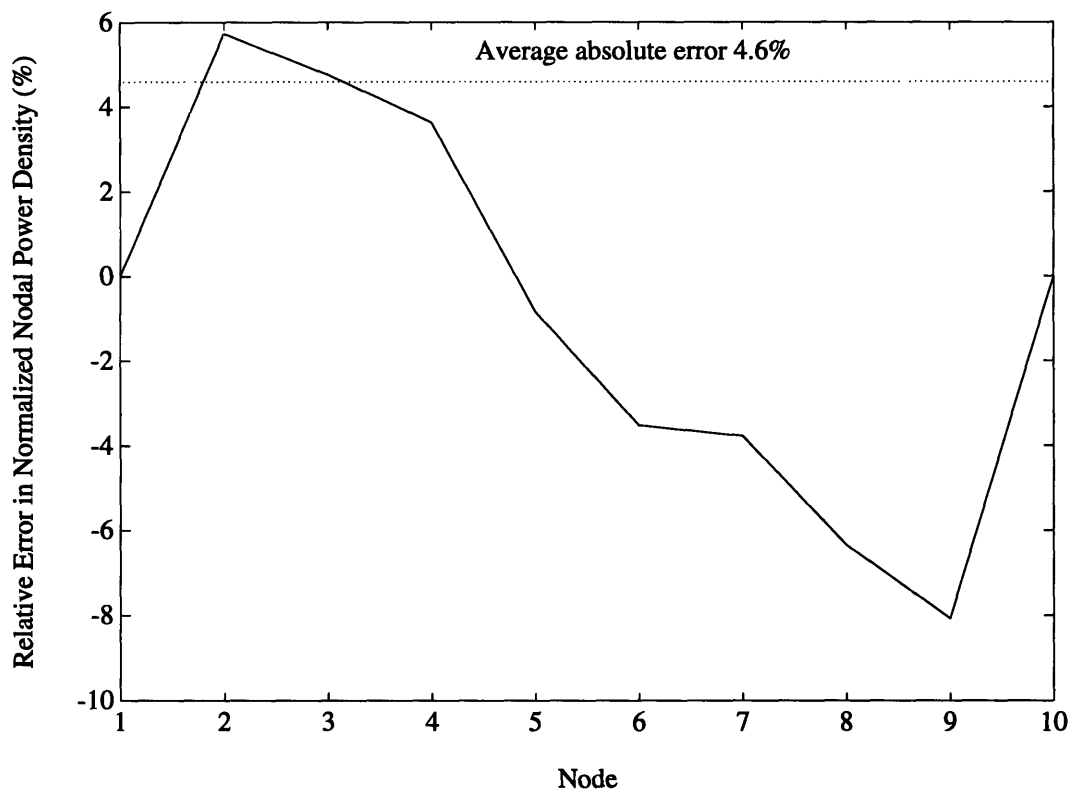


Figure 4-7: Relative error in normalized power density for steady-state case B-2

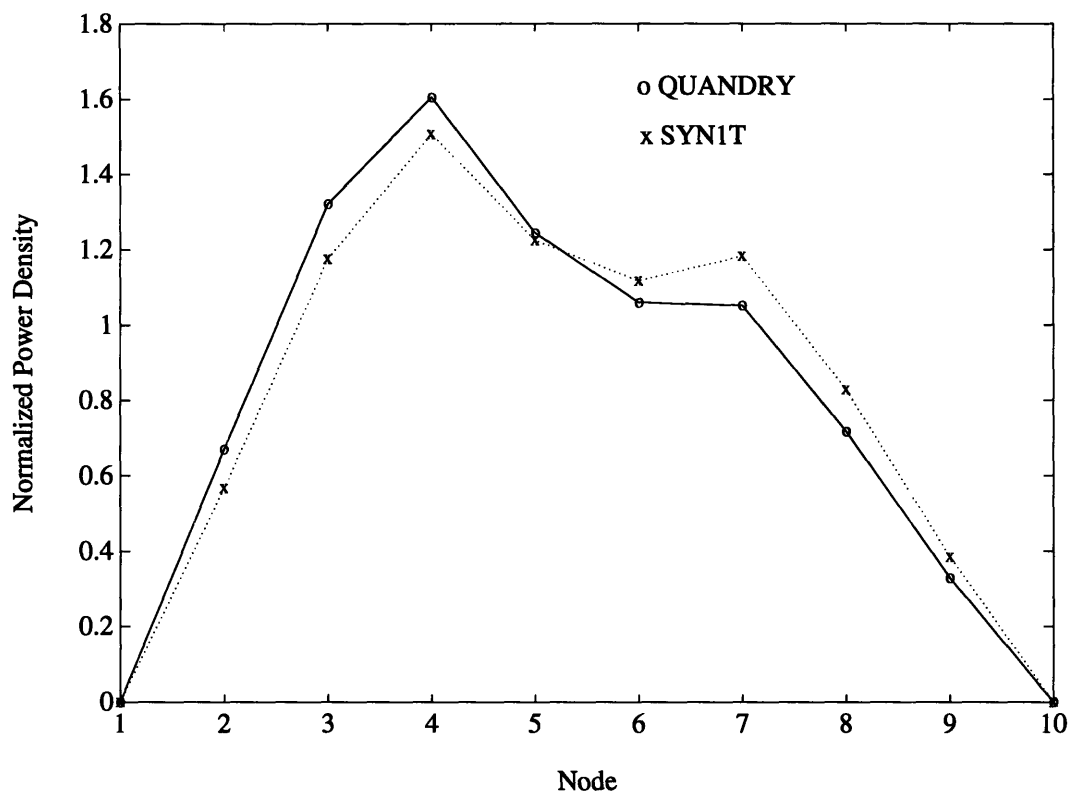


Figure 4-8: Normalized nodal power density for steady-state case B-3

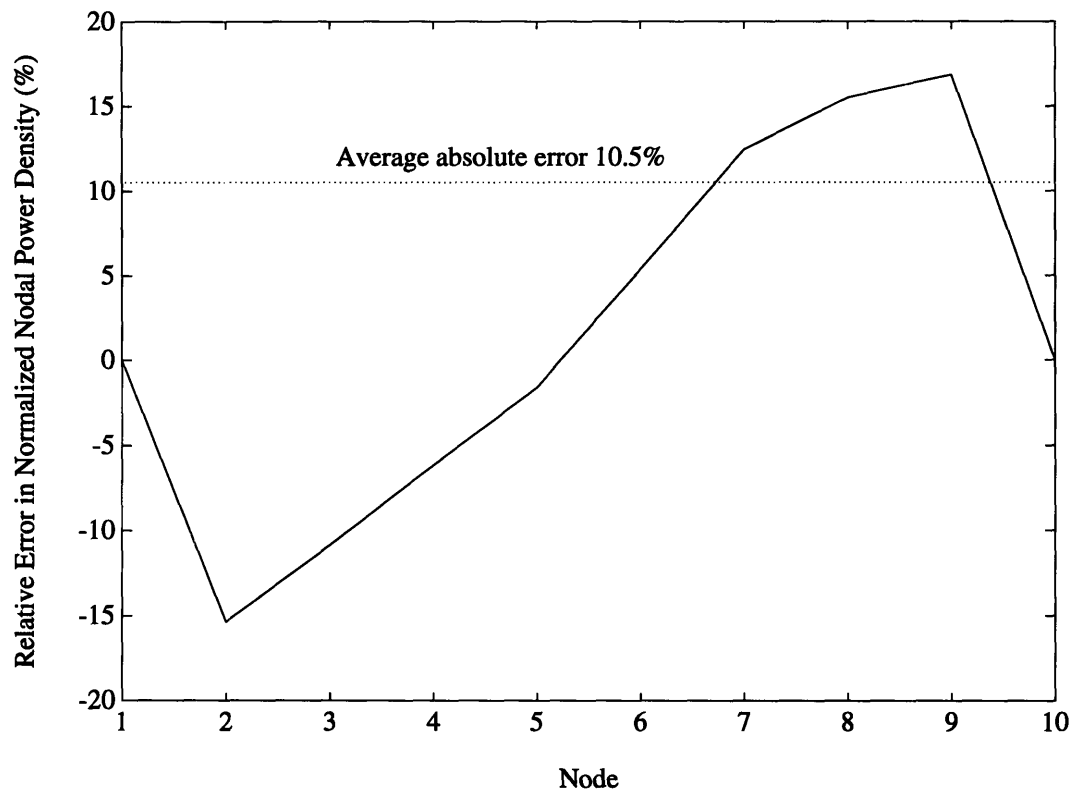


Figure 4-9: Relative error in normalized power density for steady-state case B-3

#### 4.2.1.2 Variable Rod-Position Problem 1 – Fully-Rodded Case

Three test cases were used to study the variable rod-position problem as illustrated in Figure 4-10. The test problem was a critical, one-dimensional, 10-node core containing three materials: reflector at node 1, un-rodded fuel at nodes 2 to 6, and fully-rodded fuel at nodes 7 to 10. Two expansion functions were used for all the test cases as listed in Table 4.5. The problem was run without thermal-hydraulic feedback and weighted with the adjoint fluxes. A complete description of this test problem is given in Appendix C.2.

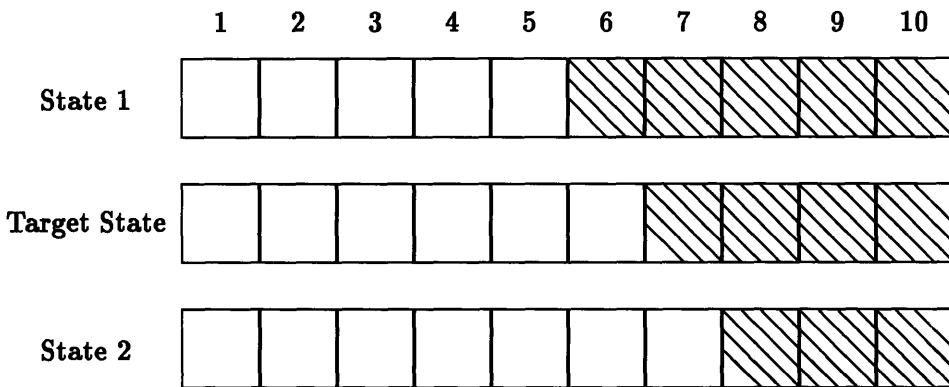


Figure 4-10: Variable rod-position problem – fully-rodded case

Table 4.5: Test cases for variable rod-position problem 1 – fully-rodded case

Case	Expansion Functions	Weight Functions	Treatment to $r$ 's <sup>†</sup> on Problem Faces <sup>‡</sup>
C-1	States 1 and 2 (15 MW <sub>t</sub> )	Adjoint-flux	No special treatment
C-2	States 1 and 2 (15 MW <sub>t</sub> )	Adjoint-flux	Special treatment to $r$ 's of node 7, also similar treatment to $r$ 's on (+) face of node 6, and $r$ 's on (-) face of node 8
C-3	States 1 and 2 (15 MW <sub>t</sub> )	Adjoint-flux	Reference (or exact) $r$ 's

<sup>†</sup> $r$ 's are the short-hand notation for the ratios of discontinuity factors.

<sup>‡</sup>Problem faces include (+) face of node 6, (-) and (+) faces of node 7, and (-) face of node 8.

In case C-1, the ordinary synthesis scheme was used to update the ratios of discontinuity factors ( $r$ 's for short) on all the faces of all the nodes. While in case C-2, in addition to the fact that the flux-averaging method described in Section 3.2.6 was used to update the

ratios of discontinuity factors on both the (−) and (+) faces of node 7 (the problem node), a similar procedure was applied to update the  $r$ 's on the (+) face of node 6, and on the (−) face of node 8. More specifically,  $r$ 's on the (+) face and expansion functions of node 5, as well as  $r$ 's on the (+) face and expansion functions of node 7 were used to obtain the  $r$ 's on the (+) face of node 6. Similarly, the  $r$ 's on the (−) face and expansion functions of node 7, as well as the  $r$ 's on the (−) face and expansion functions of node 9 were used to obtain the  $r$ 's on the (−) face of node 8. In this way, the information on the closest four nodes (nodes 5, 6, 8, and 9) to the problem node (node 7) were used to account for the possible perturbation of the flux shape due to the variation of control rod position. Finally, for case C-3, the exact ratios of discontinuity factors were used and no synthesis was performed to update those values.

The synthesized nodal power densities and their errors are plotted on Figures 4-11 and 4-12 for case C-1, Figures 4-13 and 4-14 for case C-2, and Figures 4-15 and 4-16 for case C-3. The synthesized  $k_{\text{eff}}$ 's are given in Table 4.6. It is very interesting that all three cases produce similar results. The synthesized power shapes are all shifted toward the top of the core with the variation in average errors in normalized power density in the range of 0.24% to 0.69%. The eigenvalues agree with the reference solution with the relative errors in the range of −0.03% to −0.05%. Even doing nothing special to correct the ratios of discontinuity factors on the problem faces (case C-1) generates result very close to case C-3 using the exact ratios of discontinuity factors.

A closer look at the flux shapes as shown in Figure 4-17 shows that the two expansion functions do not totally bracket the reference flux. At node 5, the reference flux falls just outside of the range bounded by these two expansion functions. Furthermore, from node 6 up to 10, the reference state does not have the same flux shape as those two bracketing states. This dissimilarity in flux shape is the essential reason for erroneous synthesized solutions. On the other hand, the method used in case C-2 for correcting the ratios of discontinuity factors on the problem faces works very well. As can be seen in Table 4.7, the maximum relative error is only 0.14%.

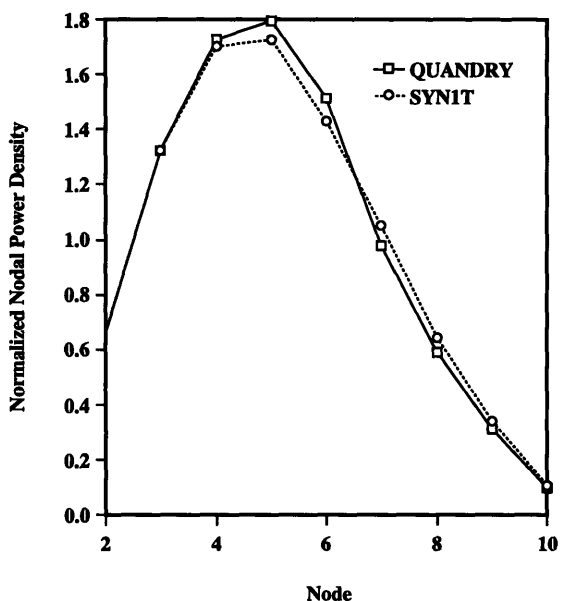


Figure 4-11: Normalized nodal power density for steady-state case C-1

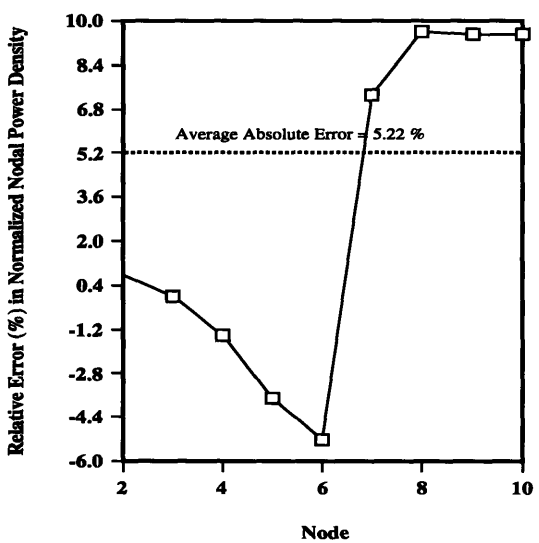


Figure 4-12: Relative error in normalized nodal power density for steady-state case C-1

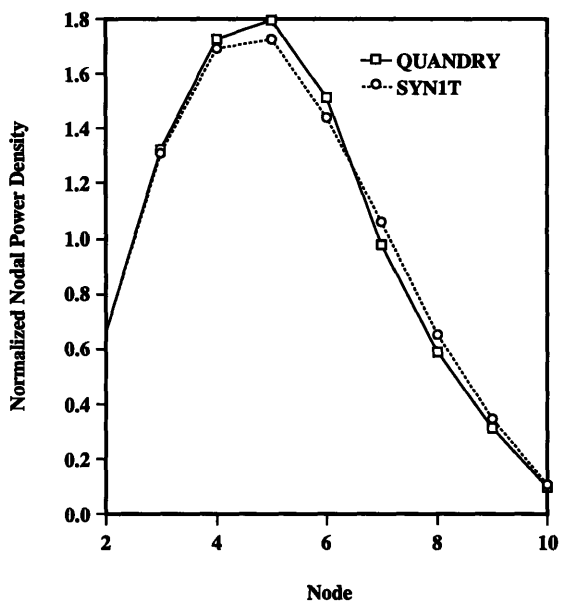


Figure 4-13: Normalized nodal power density for steady-state case C-2

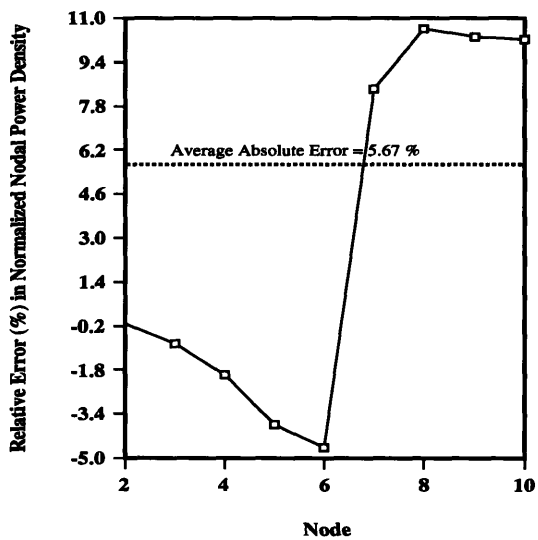


Figure 4-14: Relative error in normalized nodal power density for steady-state case C-2

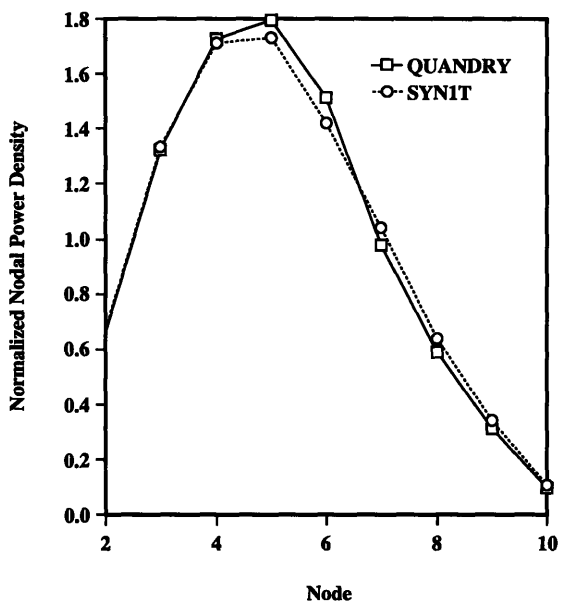


Figure 4-15: Normalized nodal power density for steady-state case C-3

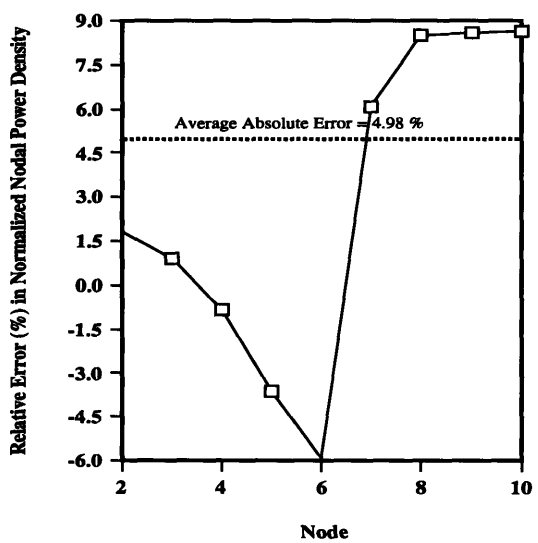


Figure 4-16: Relative error in normalized nodal power density for steady-state case C-3

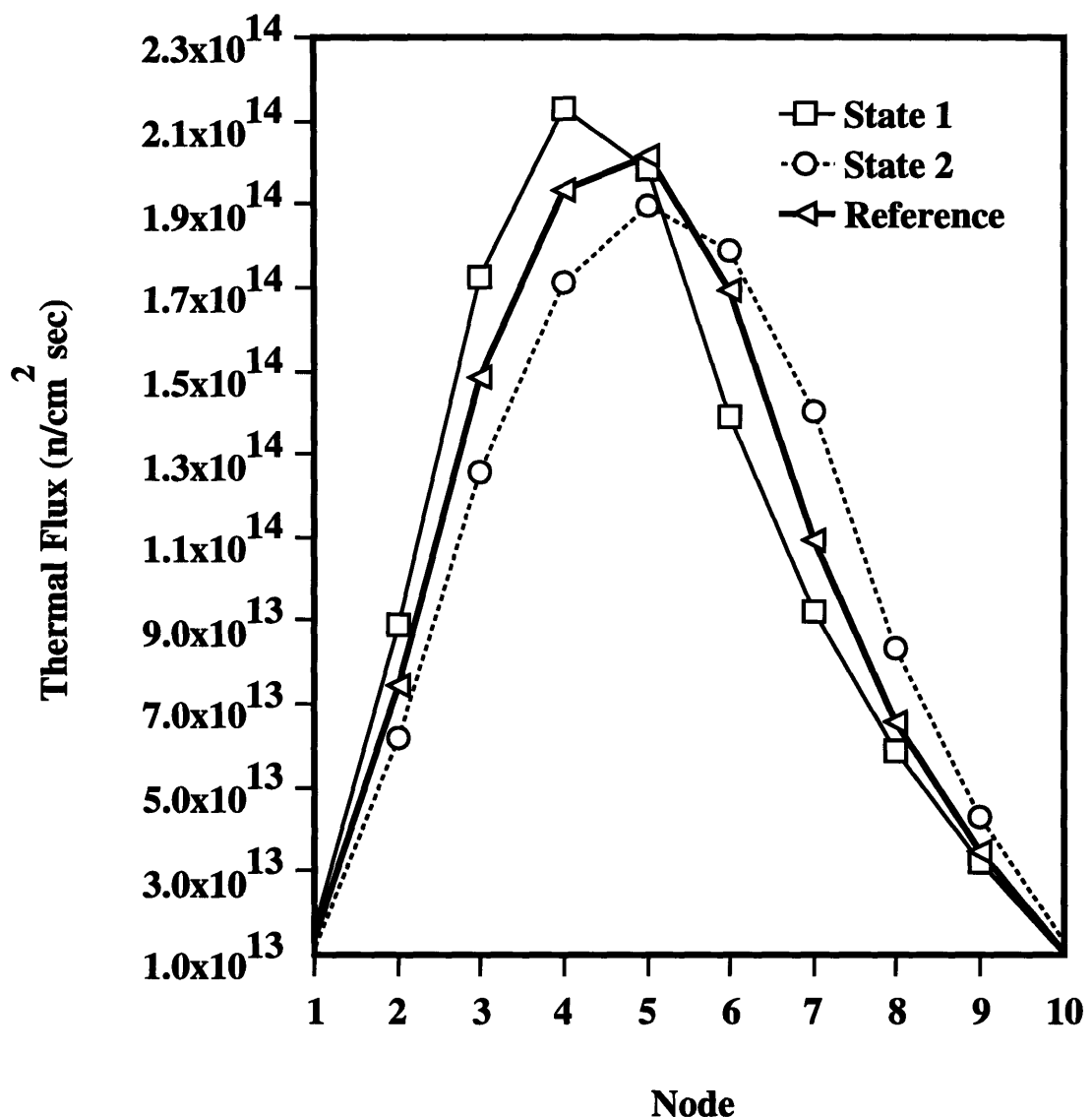


Figure 4-17: Thermal fluxes of bracketing states and reference state for steady-state case series C

Table 4.6: Neutron multiplication factors for steady-state case series C

Case	K <sub>eff</sub>	Relative Error (%)
Reference	1.0118760	-
C-1	1.0115593	-0.0313
C-2	1.0113684	-0.0502
C-3	1.0115007	-0.0371

**Table 4.7: Ratios of discontinuity factors for steady-state case C-2**

Node	Face	Group	Ratios of Discontinuity Factors		
			Case C-2	Reference	Relative Error (%)
6	(+)	1	<b>0.94505</b>	<b>0.94551</b>	<b>-0.0486</b>
		2	<b>0.80069</b>	<b>0.80158</b>	<b>-0.1110</b>
7	(-)	1	<b>1.05830</b>	<b>1.05760</b>	<b>+0.0662</b>
		2	<b>1.24930</b>	<b>1.24750</b>	<b>+0.1443</b>
7	(+)	1	<b>1.00710</b>	<b>1.00780</b>	<b>-0.0695</b>
		2	<b>1.01020</b>	<b>1.01080</b>	<b>-0.0594</b>
8	(-)	1	<b>0.99335</b>	<b>0.99229</b>	<b>+0.1068</b>
		2	<b>0.99042</b>	<b>0.98929</b>	<b>+0.1142</b>

#### 4.2.1.3 Variable Rod-Position Problem 2 – Partially-Rodded Case

The partially-rodded variable rod-position problem was investigated for three test cases. The test problem as illustrated in Figure 4-18 consists of a critical 10-node core with the control rod tip halfway withdrawn from node 6. Nodes 1 to 5 are un-rodded fuel, and nodes 7 to 10 are fully-rodded fuel. Two expansion functions were used for all the test cases as listed in Table 4.8, and the corresponding adjoint fluxes were used as weight functions. A complete description of this test problem is given in Appendix C.3.

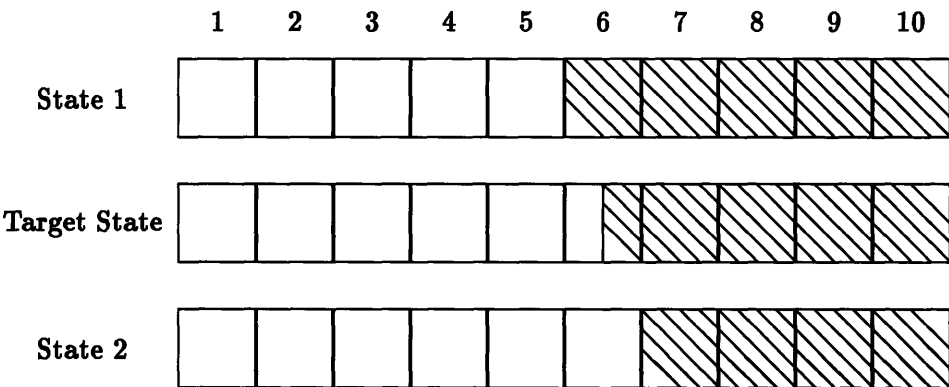


Figure 4-18: Variable rod-position problem – partially-rodded case

Table 4.8: Test cases for variable rod-position problem 2 – partially-rodded case

Case	Expansion Functions	Weight Functions	Thermal Feedback	Special Treatment to Node 6
D-1	States 1 and 2 (10 MW <sub>t</sub> )	Adjoint-flux	No	Section 3.2.6
D-2	States 1 and 2 (10 MW <sub>t</sub> )	Adjoint-flux	Yes	Section 3.2.6
D-3	States 1 and 2 (10 MW <sub>t</sub> )	Adjoint-flux	Yes	Modified Version of Section 3.2.6

Cases D-1 and D-2 used the flux-volume averaging scheme as described in Section 3.2.6 to approximate the cross sections and the discontinuity factors for node 6, while in case D-3, a modified prescription of that described in Section 3.2.6 was used. This modified method uses the synthesized flux rather than the state 1 expansion function in the flux-volume averaging scheme. Case D-1 was run without thermal-hydraulic feedback, whereas cases

D-2 and D-3 were run with temperature and density feedback. All the reference solutions are from 11-node QUANDRY calculations in which node 6 is explicitly divided into two nodes.

The synthesized nodal power densities, absolute errors (differences between normalized power densities divided by 100), and relative errors (fractional differences) are plotted on Figures 4-19, 4-20, and 4-21 for case D-1, Figures 4-22, 4-23, and 4-24 for case D-2, and Figures 4-25, 4-26, and 4-27 for case D-3. The synthesized  $k_{\text{eff}}$ 's are given in Table 4.9.

For case D-1, the power shape shifts slightly toward the top of the core with an average value of absolute error in power density of 2.71%. The relative error reaches the maximum of 35.2% at node 7 and levels off at 31.7% at node 10. These large errors occur at nodes having very low power densities. The eigenvalue agrees well with the reference solution. Case D-2 gives a power shape with an average value of absolute error in power density of 2.58%. Again, the large relative errors occur at low-power nodes. For case D-3, on the other hand, the power shape shifts toward the bottom of the core with an averaged absolute error in power density of 2.94%. The relative errors are decreased as compared with cases D-1 and D-2. However, the eigenvalue is off by  $-0.22\%$ , which is about ten times that for case D-2, and five times that for case D-1.

Just as for the fully-rodded case discussed in the previous subsection, the errors are essentially due to the dissimilarity of the flux shape between the bracketing states and the reference state. This can be seen from Figures 4-28 and 4-29. Nevertheless, the tests show that the nodal synthesis model, using a simple and straightforward method to update the cross sections and the discontinuity factors for the fully-rodded or partially-rodded nodes, can generate reasonably accurate solutions even for the case involving severe perturbations of the flux shape due to variation of control-rod position. However, it also appears that using only two expansion functions for rod-motion problems does not provide sufficient accuracy. For cases more realistic than one-dimensional test problems, it is recommended that at least three bracketing states be used.

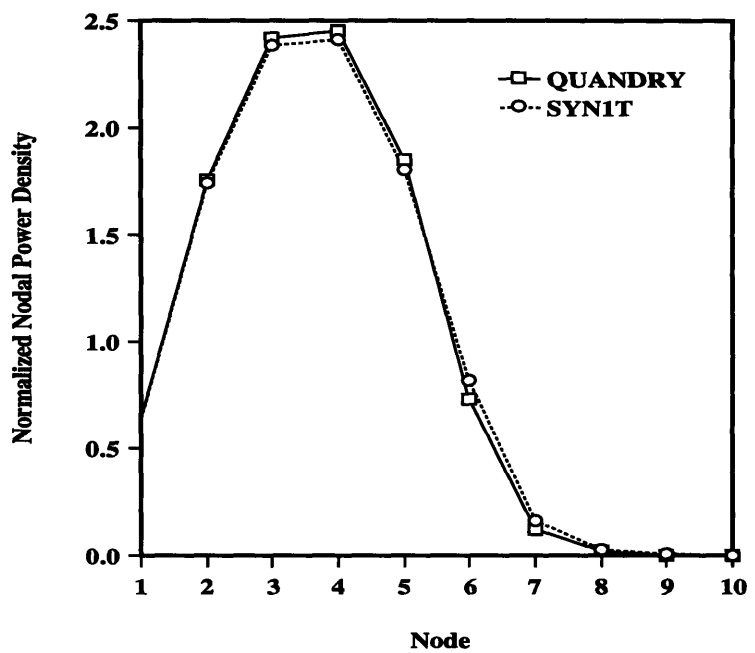


Figure 4-19: Normalized nodal power density for steady-state case D-1

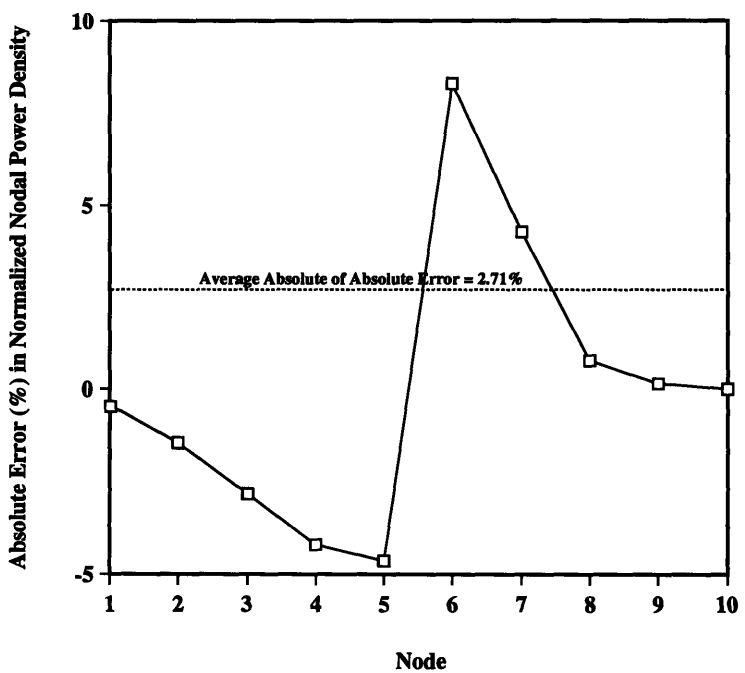


Figure 4-20: Absolute error in normalized nodal power density for steady-state case D-1

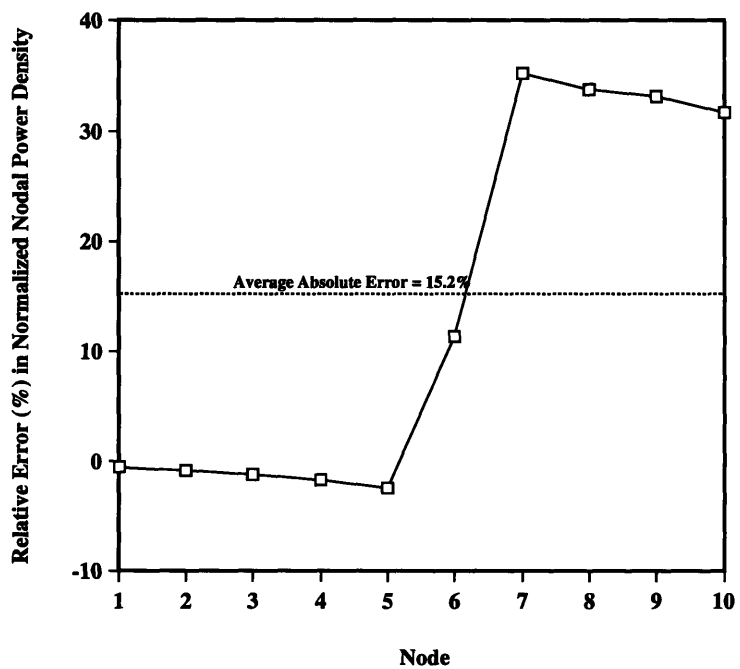


Figure 4-21: Relative error in normalized nodal power density for steady-state case D-1

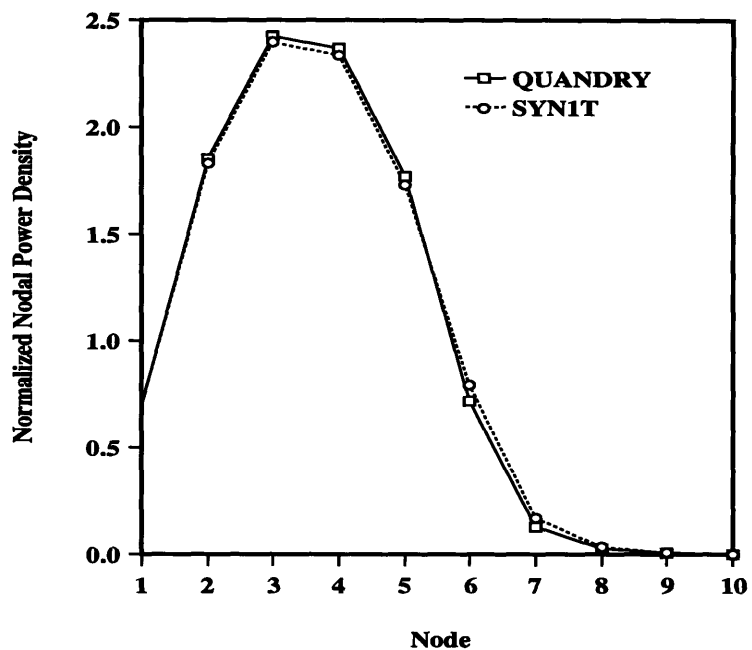


Figure 4-22: Normalized nodal power density for steady-state case D-2

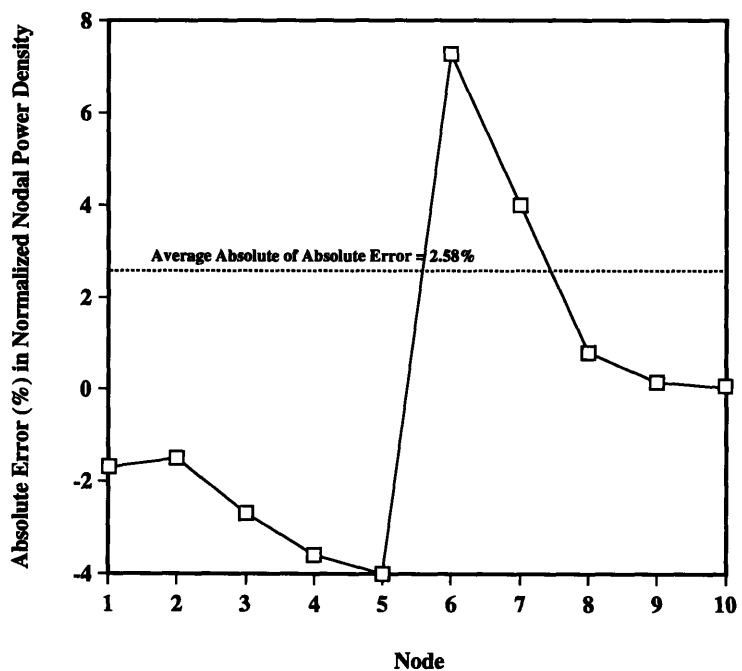


Figure 4-23: Absolute error in normalized nodal power density for steady-state case D-2

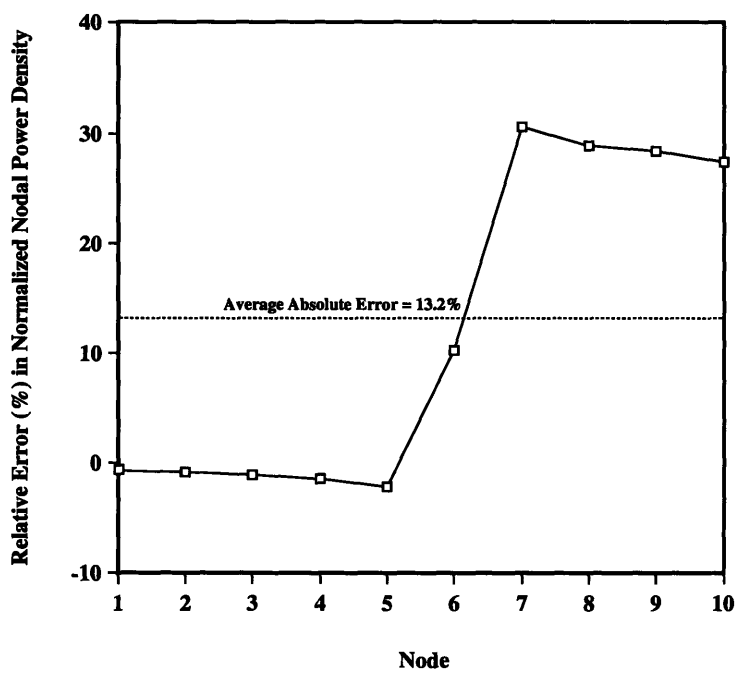


Figure 4-24: Relative error in normalized nodal power density for steady-state case D-2

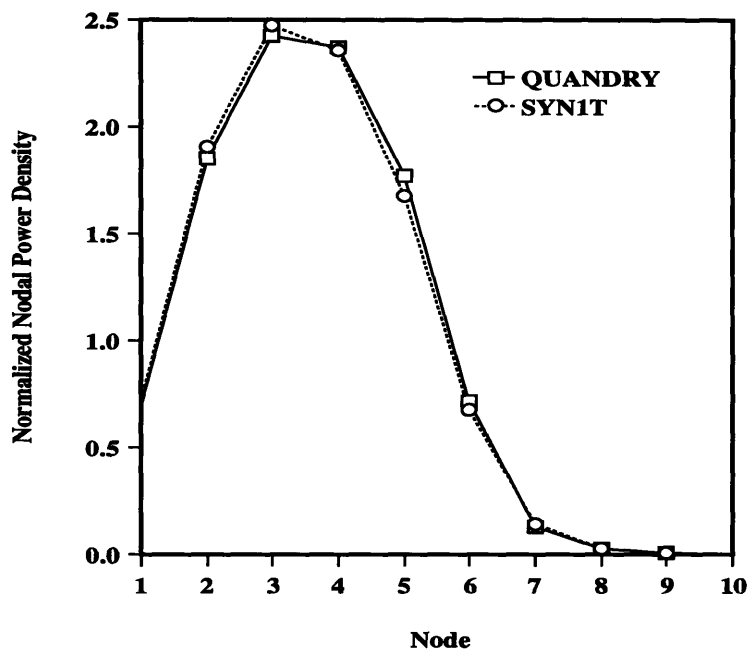


Figure 4-25: Normalized nodal power density for steady-state case D-3

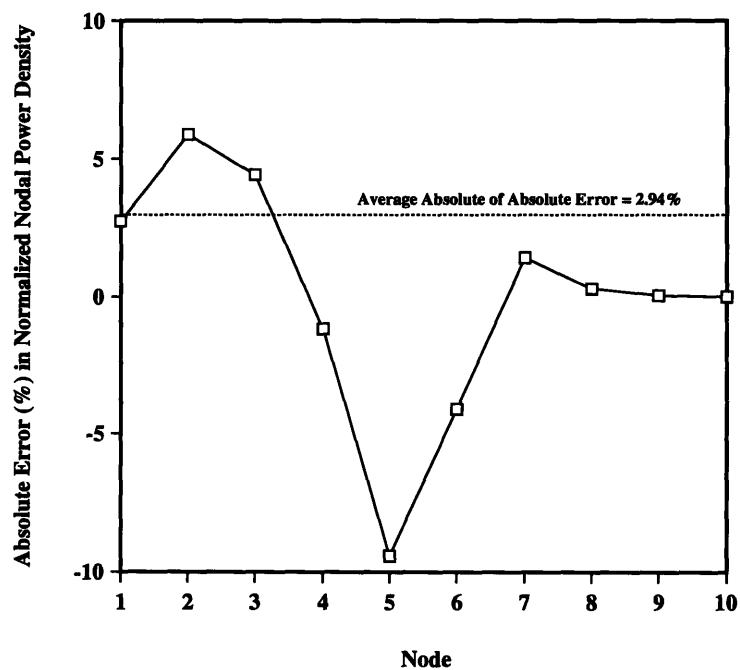


Figure 4-26: Absolute error in normalized nodal power density for steady-state case D-3

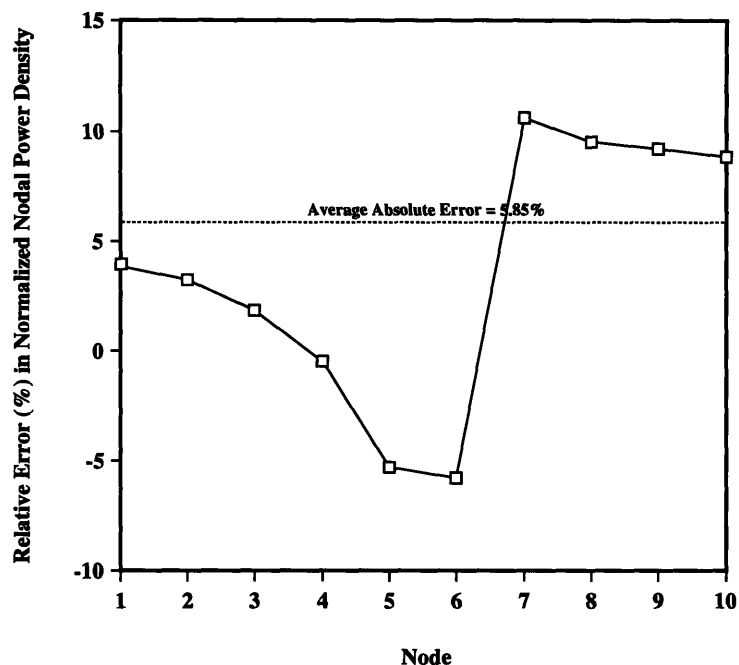


Figure 4-27: Relative error in normalized nodal power density for steady-state case D-3

Table 4.9: Neutron multiplication factors for steady-state case series D

Case	$K_{\text{effective}}$		Relative Error (%)
	SYN1T	Reference	
D-1	0.9752642	0.9756796	-0.043
D-2	0.9504167	0.9506323	-0.023
D-3	0.9485435	0.9506323	-0.220

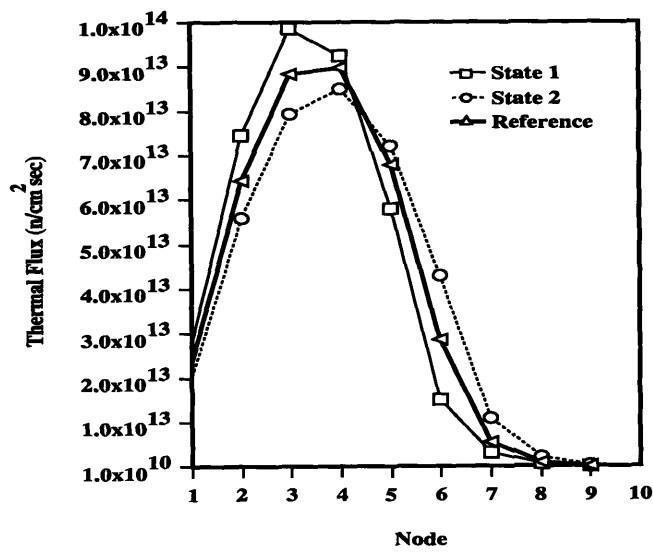


Figure 4-28: Thermal fluxes of bracketing states and reference state for steady-state case D-1

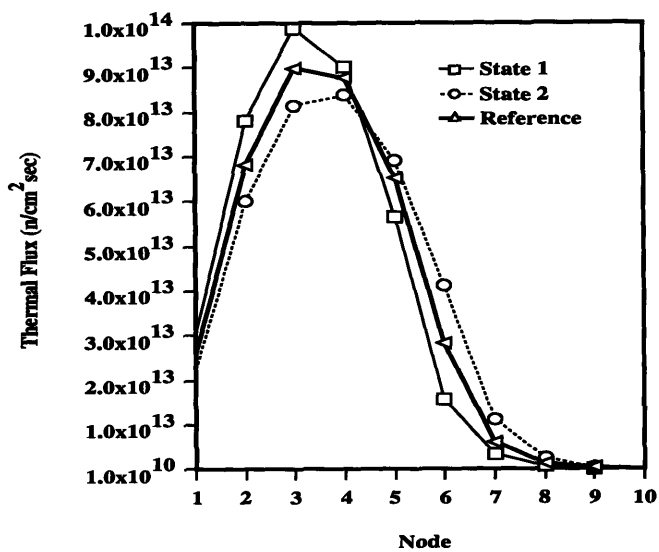


Figure 4-29: Thermal fluxes of bracketing states and reference state for steady-state cases D-1 and D-2

#### 4.2.2 Transient Problem

The test problem is a 10-node reactor core starting at the initial power of  $17.29 \text{ MW}_t$  and inlet coolant temperature of 555 K. The inlet coolant temperature then changes with time according to the following parabolic relation:

$$T_{in}(t) = 555 - 38.826 t + 20.8 t^2. \quad (4.1)$$

The transient begins at 0.0 sec and ends at 1.5 sec with only one delayed-neutron precursor family. A complete description of this test problem is given in Appendix C.4. This transient test is used to investigate the capability of the general nodal synthesis model to reproducing transient solutions, along with the method of updating the discontinuity factors or their ratios, and the computing efficiency.

Six test cases were run as listed in Table 4.10. A summary of the calculational results is provided in Table 4.11. The reactor power and total reactivity are shown on Figures 4-30, 4-31, 4-32, 4-33, and 4-34 for case E-2, on Figures 4-35, 4-36, 4-37, 4-38, and 4-39 for case E-3, on Figures 4-40, 4-41, 4-42, 4-43, and 4-44 for case E-4, and on Figures 4-45, 4-46, 4-47, 4-48, and 4-49 for case E-6.

Several findings are listed below:

1. Updating the discontinuity factors (or f's for short) by pure synthesis scheme greatly improves the accuracy as compared with keeping the f's at the initial steady-state values.
2. Synthesizing the f's rather than the ratios of discontinuity factors (or r's in short) gives the best solution.
3. If the reference f's are not available for synthesizing (e.g., some nodal codes only generate r's instead of f's), the weighted-averaging scheme also gives good results.
4. Using only one expansion function yields relatively good solution for this simple problem. However, this is not generally true for more complex problems.
5. All the cases except E-5 generate very good reactivity values as well as local power distributions. Note that the accuracy of the local power distribution is characterized

by the maximum value of the average error in nodal power density and the maximum value of the maximum error in nodal power density. These are the maximum values over the entire transient period of 1.5 sec.

6. The computing time for synthesis calculations is comparable to that for the reference (QUANDRY) calculations for the cases using two expansion functions. However, for the case with three expansion functions, the computing time doubles.

In summary, the general nodal synthesis method can replicate reference transient results with the right choice of bracketing states and an adequate model of updating the discontinuity factors. However, the computing efficiency must be improved for practical applications.

**Table 4.10: Test cases for inlet coolant temperature transient problem**

Case	Bracketing States	Weight Functions	Updating f's <sup>a</sup> or r's <sup>b</sup>
E-1	(17.29,555.0) <sup>c</sup> , (17.29,539.2)	Adjoint-flux	No (keep at initial f's)
E-2	(17.29,555.0), (17.29,539.2)	Adjoint-flux	Synthesizing f's
E-3	(17.29,555.0), (17.29,539.2), (17.29,536.9)	Adjoint-flux	Synthesizing f's
E-4	(17.29,555.0)	Adjoint-flux	Synthesizing f's
E-5	(17.29,555.0), (17.29,539.2)	Adjoint-flux	Synthesizing r's
E-6	(17.29,555.0), (17.29,539.2)	Adjoint-flux	Weighted-averaging r's

<sup>a</sup>f's: discontinuity factors.

<sup>b</sup>r's: ratios of discontinuity factors.

<sup>c</sup>(xx.xx,yyy.y): bracketing state at which the total reactor power is xx.xx MW<sub>t</sub>, and the inlet coolant temperature is yyy.yy K.

Table 4.11: Summary of synthesis results for inlet coolant temperature transient problem

	Case						Reference
	E-1	E-2	E-3	E-4	E-5	E-6	
Ave Error (%) in Reactor Power	0.942	0.329	0.397	0.717	99.2	0.463	–
Max Error (%) in Reactor Power	3.060	0.999	1.170	1.960	99.4	1.800	–
Ave Error (pcm <sup>a</sup> ) in Reactivity	4.65	3.87	4.95	3.78	5.31e4 <sup>b</sup>	3.04	–
Max Error (pcm) in Reactivity	7.66	5.83	9.88	5.95	5.72e4	4.95	–
Max of Ave Error (%) in Nodal Power Density	1.96	1.96	2.09	1.76	13.5	1.96	–
Max of Max Error (%) in Nodal Power Density	3.67	3.68	4.07	3.03	36.4	3.69	–
Node for Max of Max Error	2	2	2	9	2	2	
Transient Computing Time (sec <sup>c</sup> )	15.88	16.23	34.30	6.90	23.09	18.77	16.75

<sup>a</sup>pcm: percent of a milli,  $10^{-5}$ .

<sup>b</sup>Read as  $5.31 \times 10^4$

<sup>c</sup>MicroVAX II second.

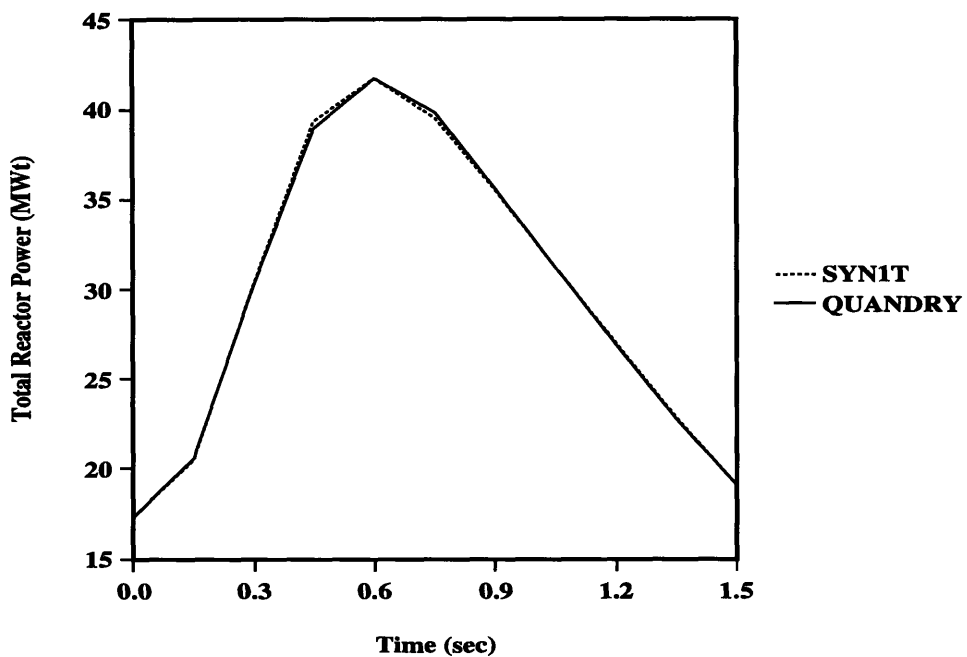


Figure 4-30: Total reactor power for transient case E-2

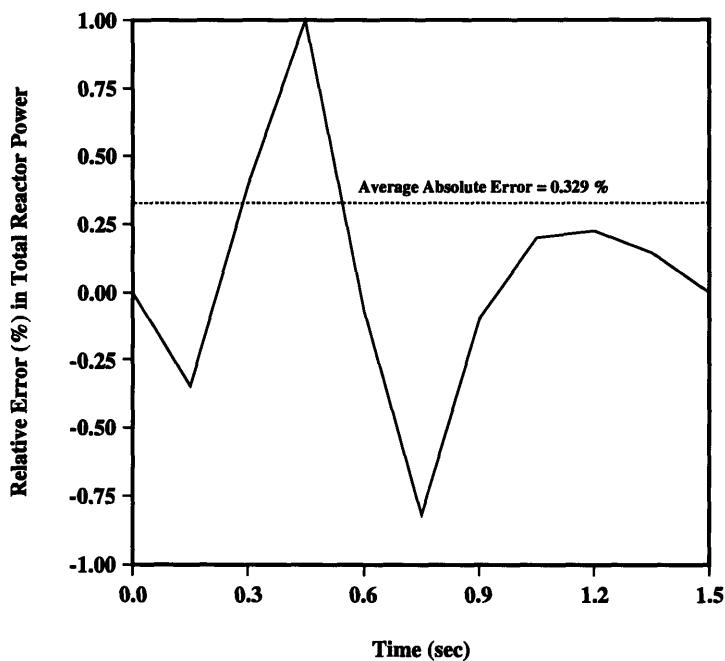


Figure 4-31: Relative error in total reactor power for transient case E-2

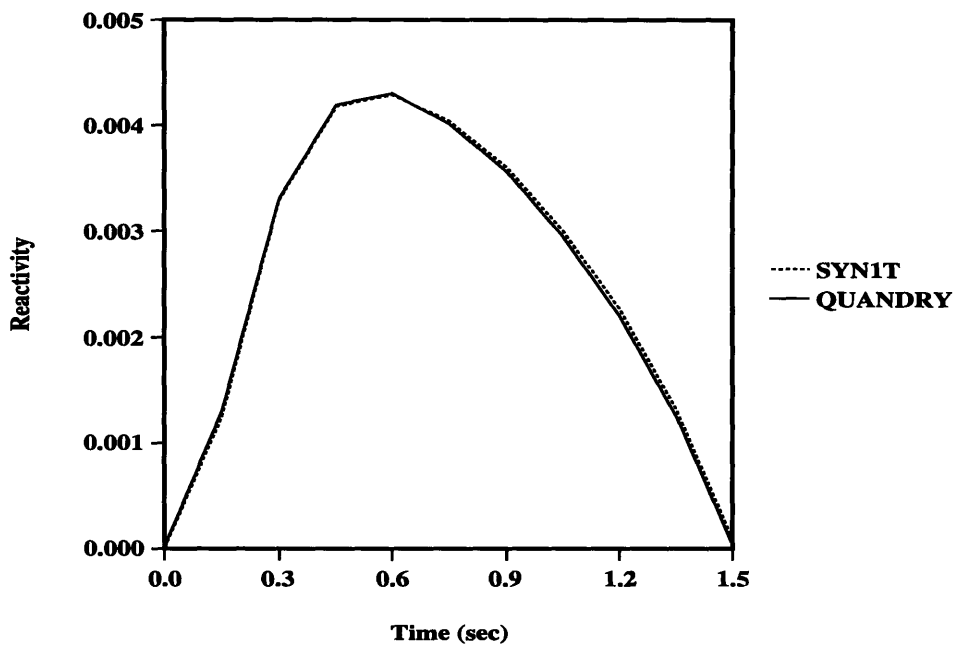


Figure 4-32: Total reactivity for transient case E-2

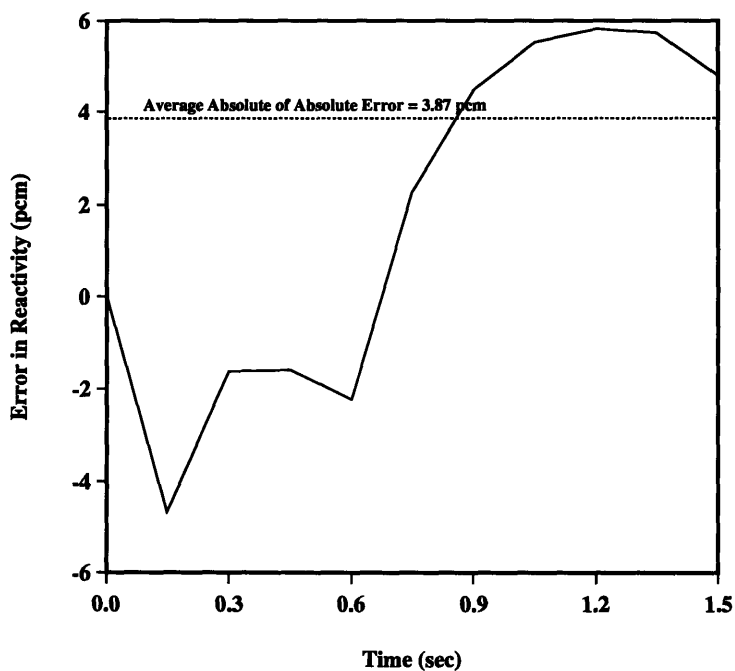


Figure 4-33: Absolute error in total reactivity for transient case E-2

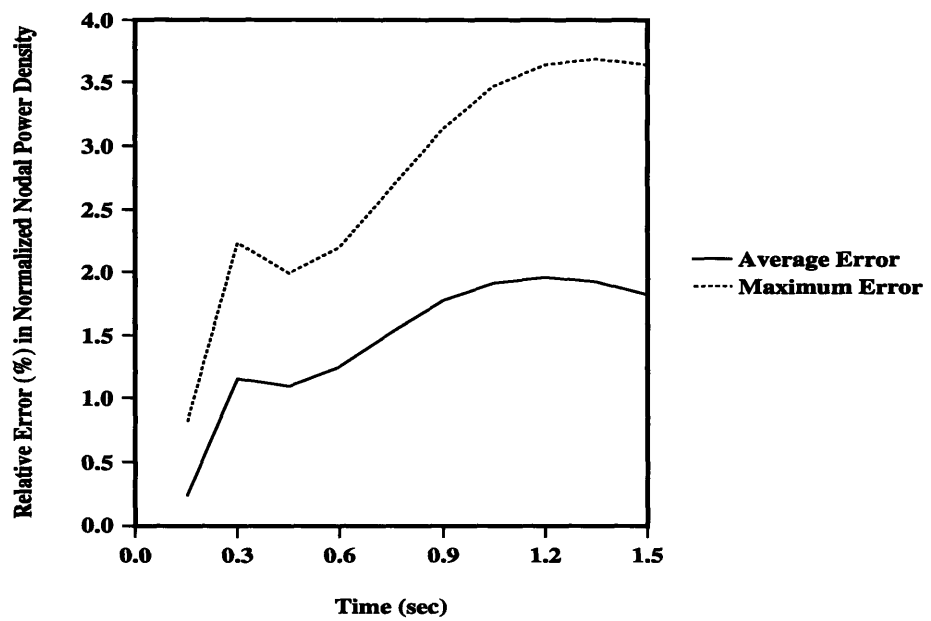


Figure 4-34: Relative error in nodal power density for transient case E-2

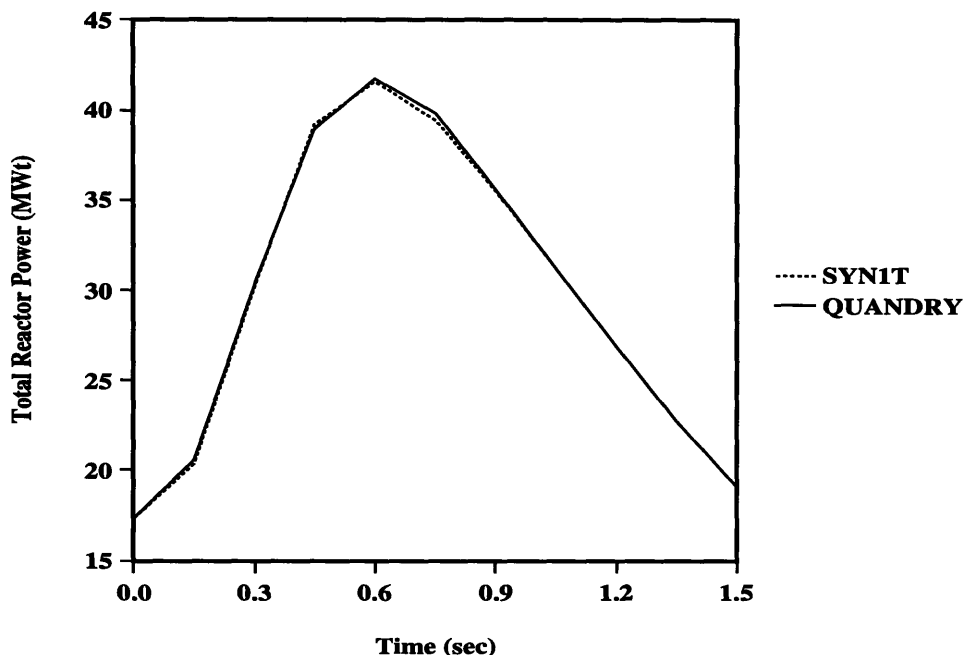


Figure 4-35: Total reactor power for transient case E-3

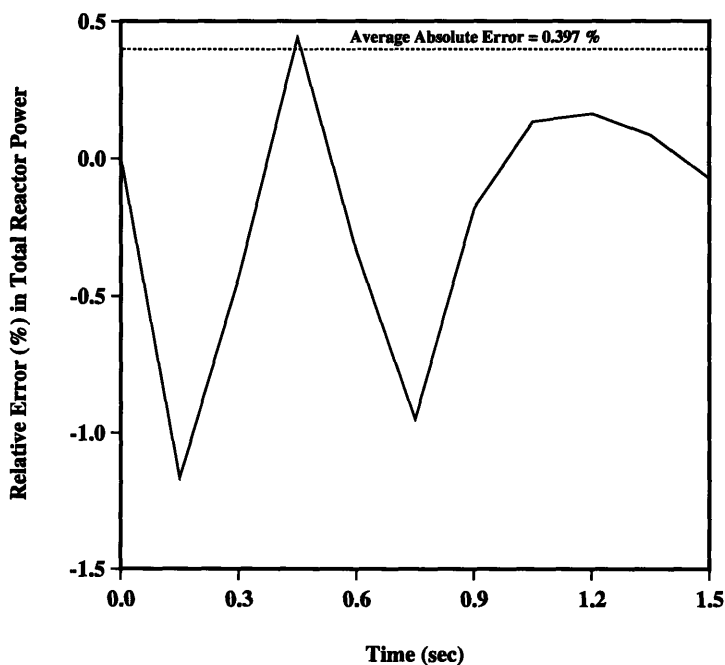


Figure 4-36: Relative error in total reactor power for transient case E-3

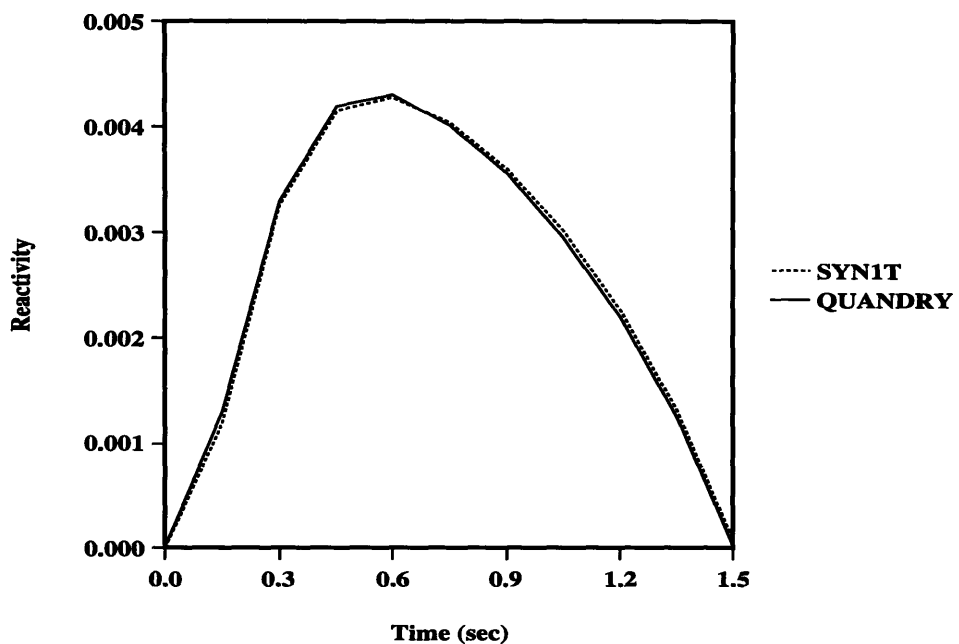


Figure 4-37: Total reactivity for transient case E-3

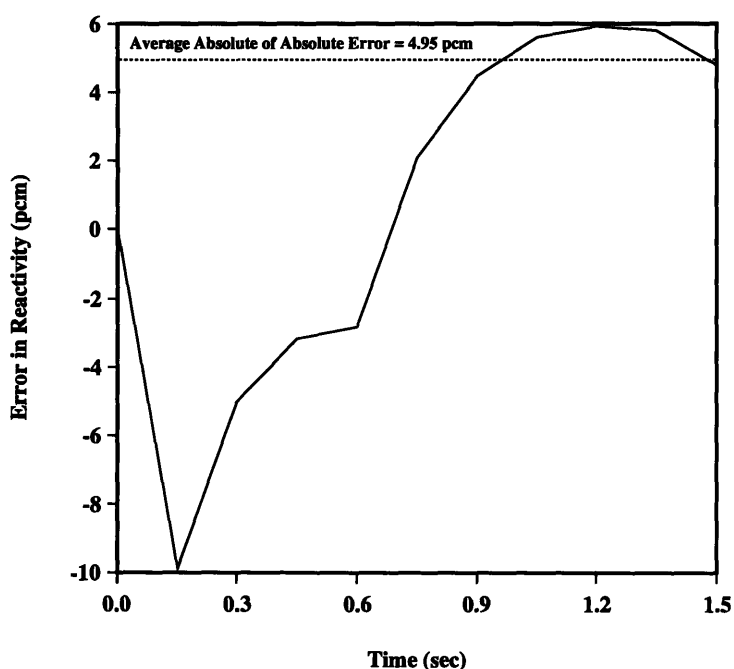


Figure 4-38: Absolute error in total reactivity for transient case E-3

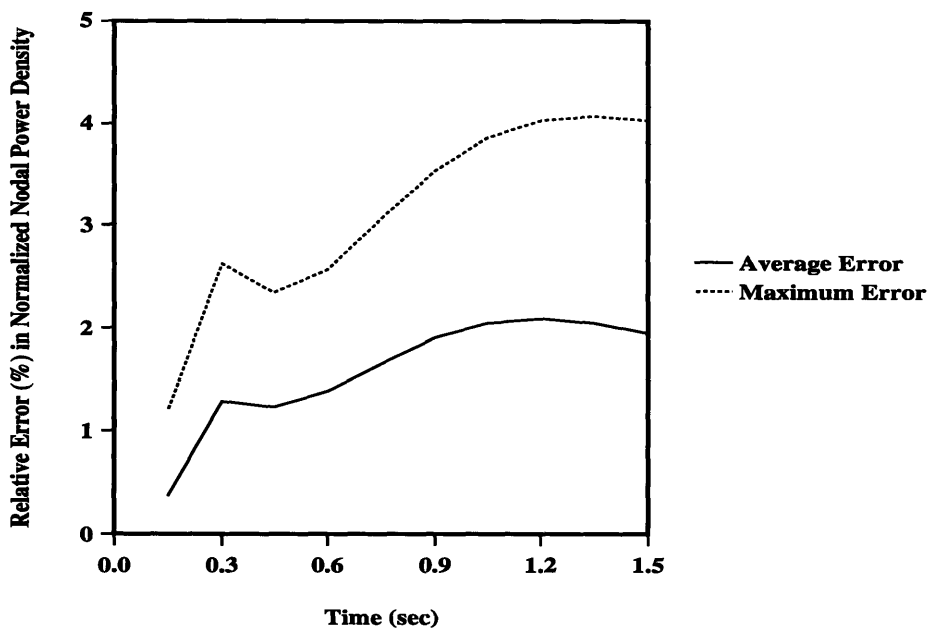


Figure 4-39: Relative error in nodal power density for transient case E-3

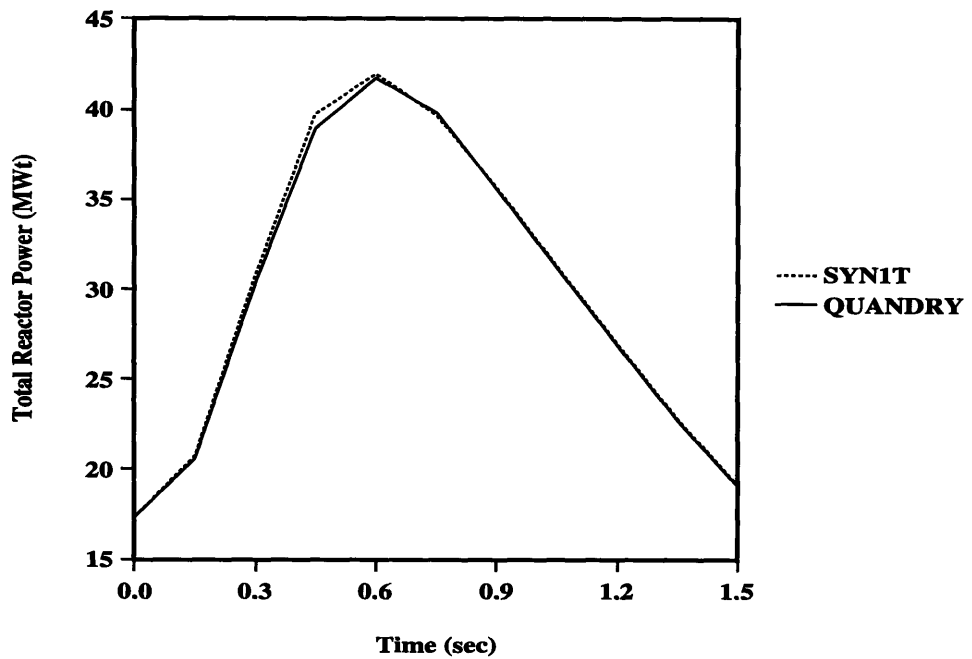


Figure 4-40: Total reactor power for transient case E-4

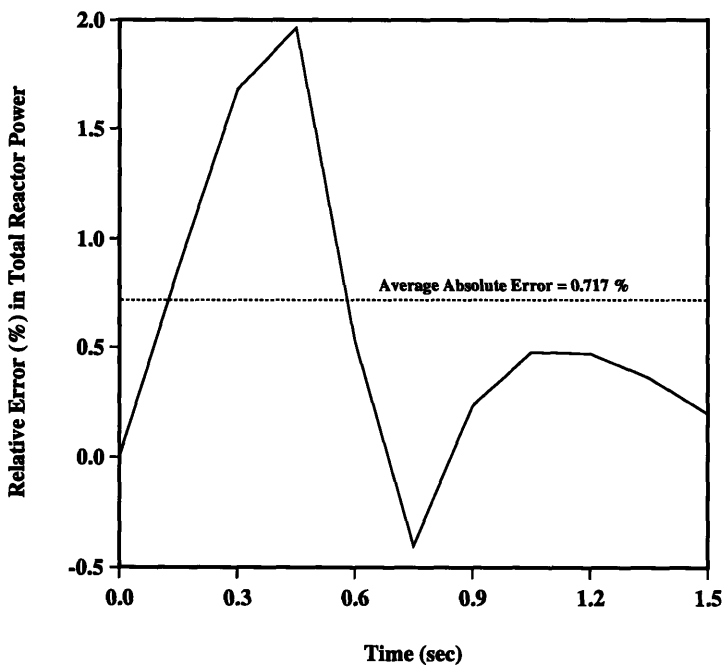


Figure 4-41: Relative error in total reactor power for transient case E-4

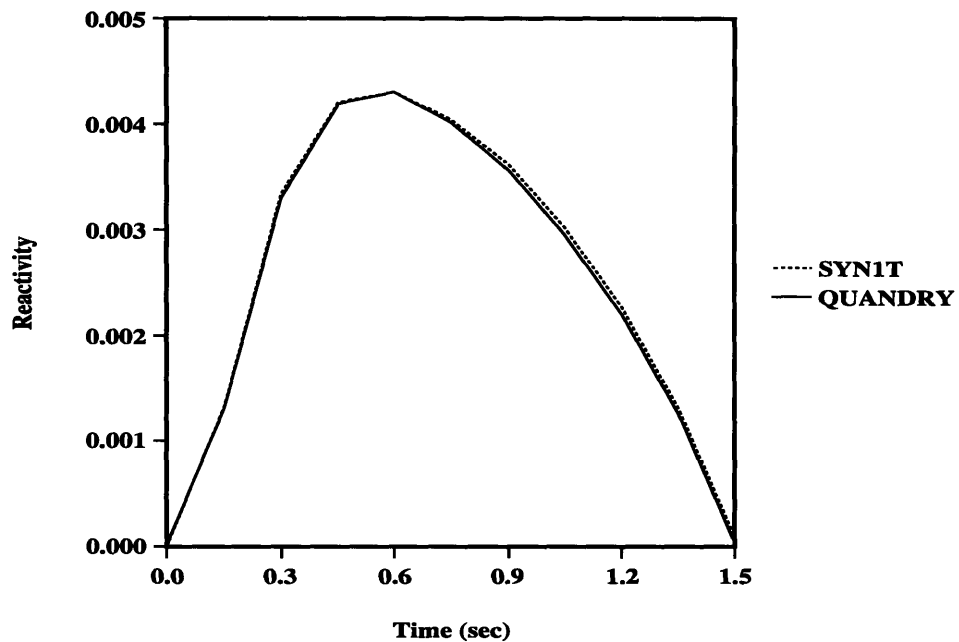


Figure 4-42: Total reactivity for transient case E-4

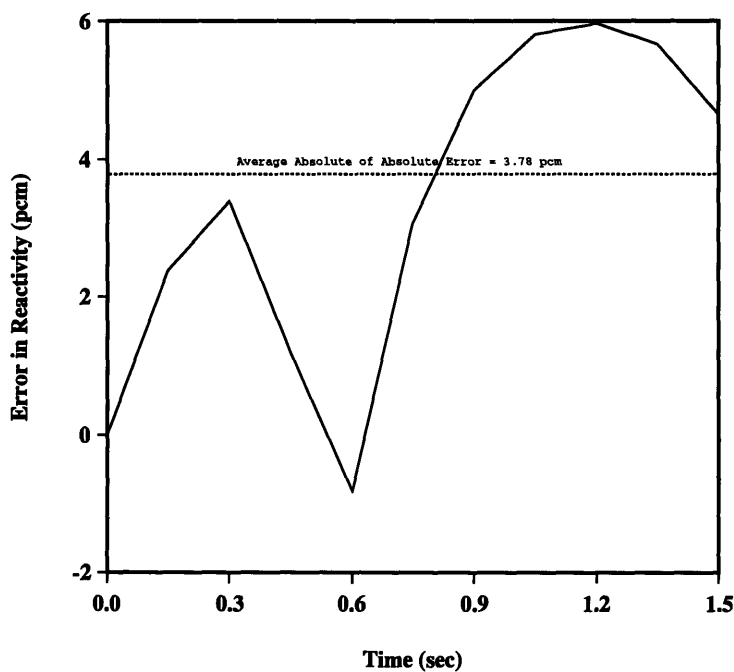


Figure 4-43: Absolute error in total reactivity for transient case E-4

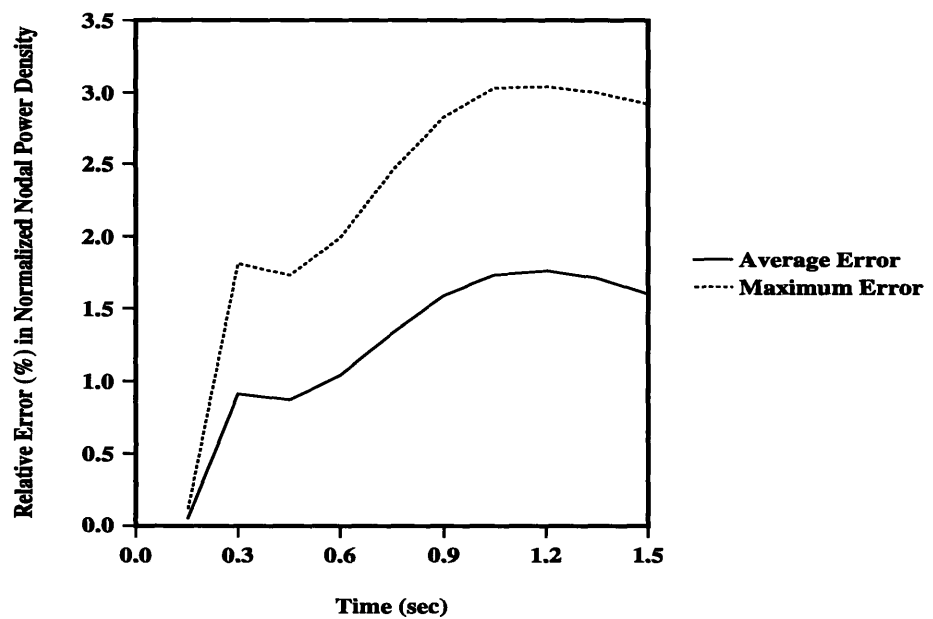


Figure 4-44: Relative error in nodal power density for transient case E-4

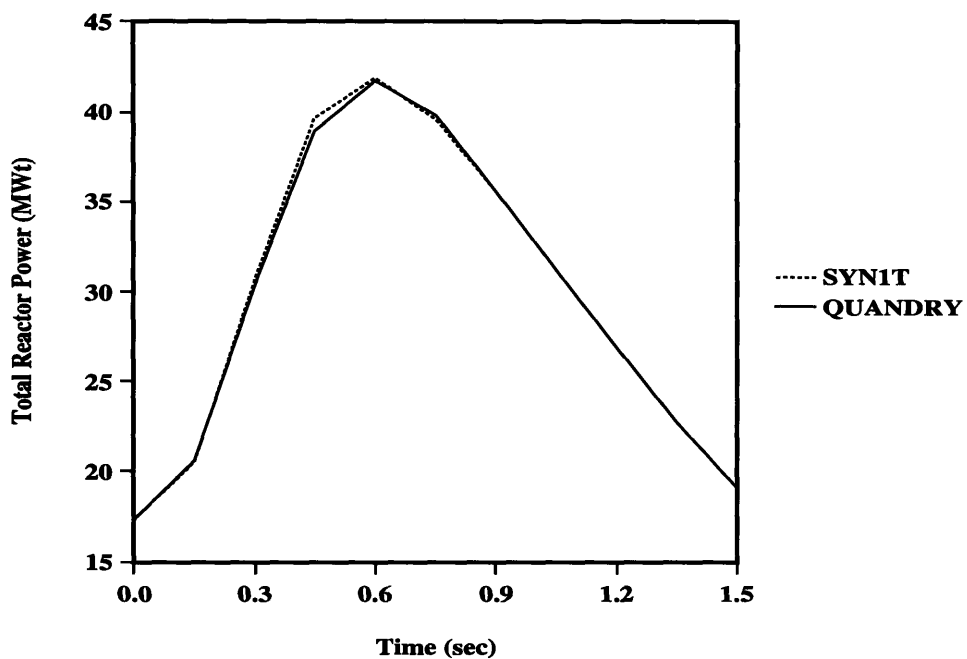


Figure 4-45: Total reactor power for transient case E-6

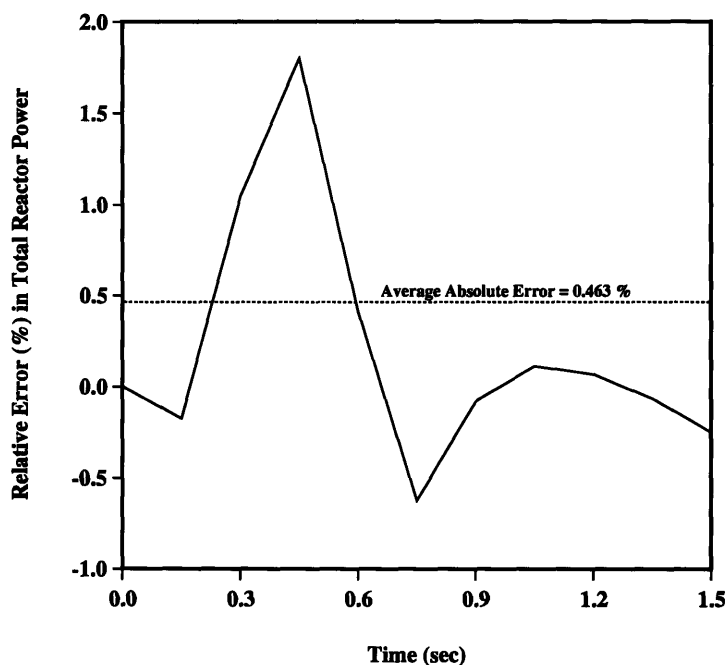


Figure 4-46: Relative error in total reactor power for transient case E-6

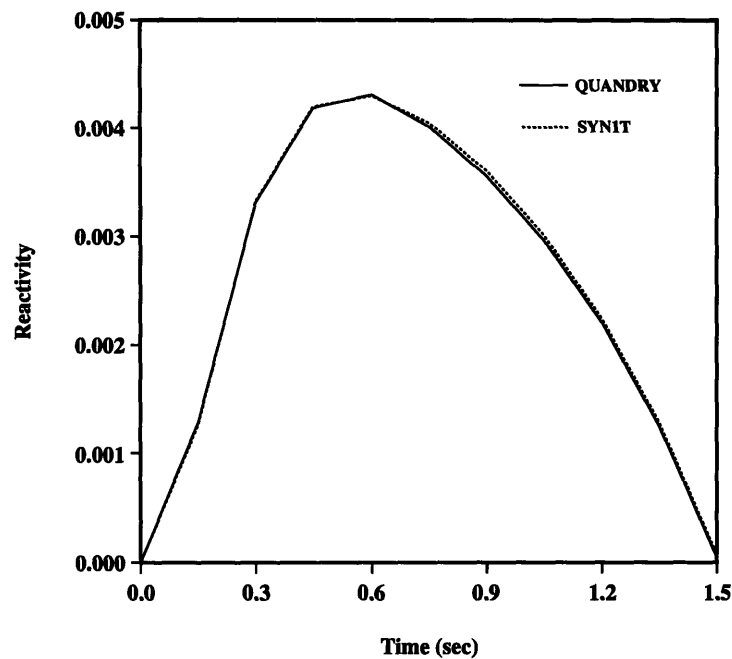


Figure 4-47: Total reactivity for transient case E-6

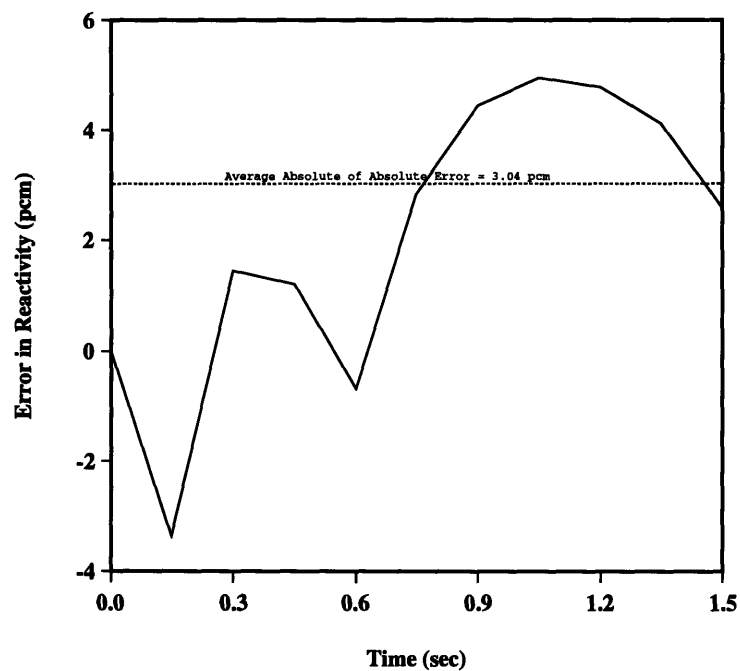


Figure 4-48: Absolute error in total reactivity for transient case E-6

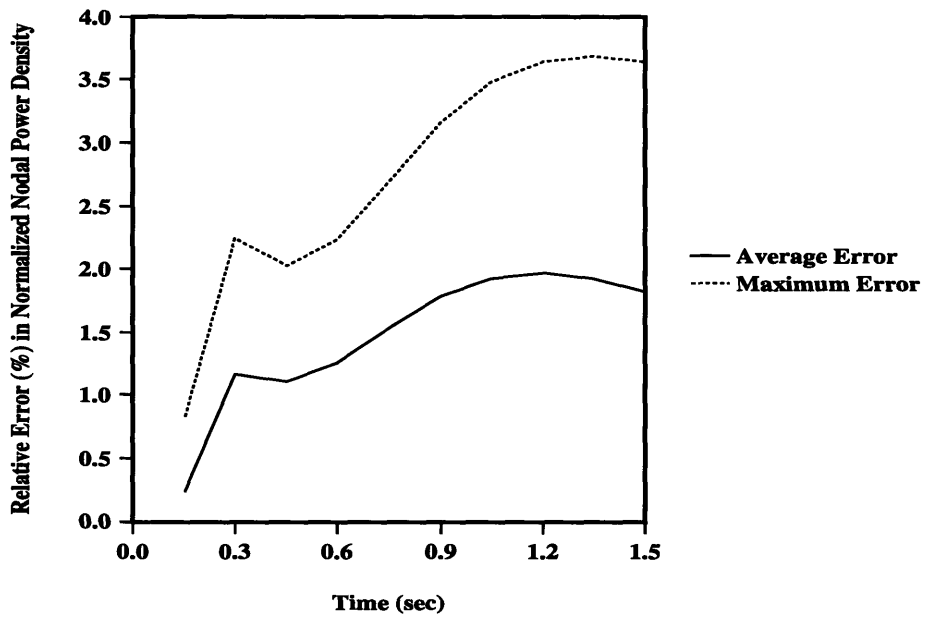


Figure 4-49: Relative error in nodal power density for transient case E-6

## 4.3 Tests of the Collapsed-Group Nodal Synthesis Model

### 4.3.1 Steady-State Problem

The same inlet coolant temperature problem used for case A in Section 4.2.1.1 was used to test the steady-state version of the collapsed-group nodal synthesis model. The results for this test case, namely case A-CG, are summarized in Table 4.12 and Figure 4-50. The synthesis model gives the eigenvalue which differs from the reference solution by only 9 parts in a million. In addition, the power distribution agrees excellently with the reference solution. The average error in normalized nodal power density is only 0.039% and the maximum error of merely -0.1% occurs at node 9, which is next to the reflector.

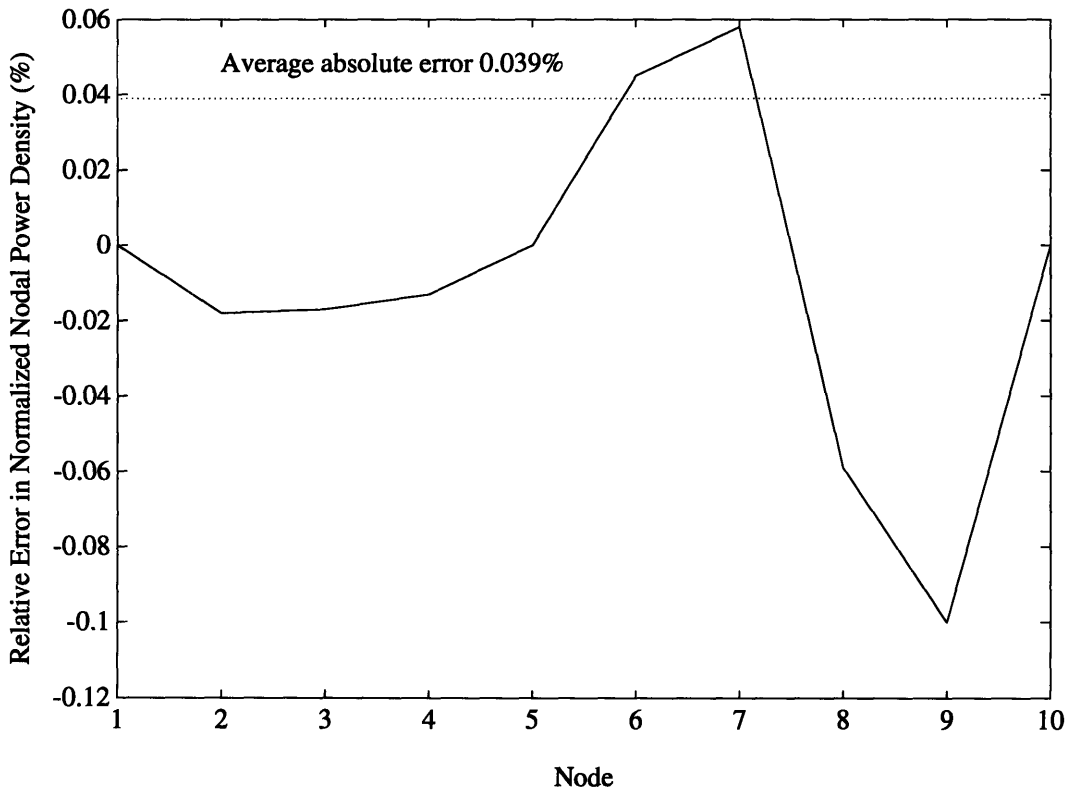


Figure 4-50: Relative error in normalized power density for steady-state case A-CG

Table 4.12: Neutron multiplication factor for steady-state case A-CG

Case	$K_{\text{eff}}$
Reference	1.040222
A-CG	1.040213

#### 4.3.2 Transient Problem

The same 10-node transient problem as that used in Section 4.2.2 was used for studying the transient version of the collapsed-group synthesis model. Only two cases were run as listed in Table 4.13. Note that case E-2CG is the counterpart of case E-2 in Section 4.2.2, and case E-3CG is the counterpart of case E-3, respectively. The calculational results are summarized in Table 4.14. The reactor power and reactivity are shown on Figures 4-51, 4-52, 4-53, 4-54, and 4-55 for case E-2CG, and on Figures 4-56, 4-57, 4-58, 4-59, and 4-60 for case E-3CG.

Both cases provide acceptably accurate results as compared with the reference solutions. The computing efficiency is improved. However, it is only slightly better than that for the reference calculations.

Table 4.13: Transient test cases for collapsed-group synthesis model

Case	Bracketing States	Weight Functions	Updating f's <sup>a</sup> or r's <sup>b</sup>
E-2CG	(17.29,555.0), (17.29,539.2)	Adjoint-flux	Synthesizing f's
E-3CG	(17.29,555.0), (17.29,539.2), (17.29,536.9)	Adjoint-flux	Synthesizing f's

<sup>a</sup>f's: discontinuity factors.

<sup>b</sup>r's: ratios of discontinuity factors.

**Table 4.14: Summary of transient results for collapsed-group synthesis model**

	Case		Reference
	E-2CG	E-3CG	
Ave Error (%) in Reactor Power	0.767	0.767	—
Max Error (%) in Reactor Power	1.870	1.890	—
Ave Error (pcm <sup>a</sup> ) in Reactivity	5.86	5.89	—
Max Error (pcm) in Reactivity	10.4	10.4	—
Max of Ave Error (%) in Nodal Power Density	2.21	2.21	—
Max of Max Error (%) in Nodal Power Density	4.30	4.32	—
Node for Max of Max Error	2	2	
Transient Computing Time (sec <sup>b</sup> )	9.55	12.14	16.75

<sup>a</sup>pcm: percent of a milli,  $10^{-5}$ .

<sup>b</sup>MicroVAX II second.

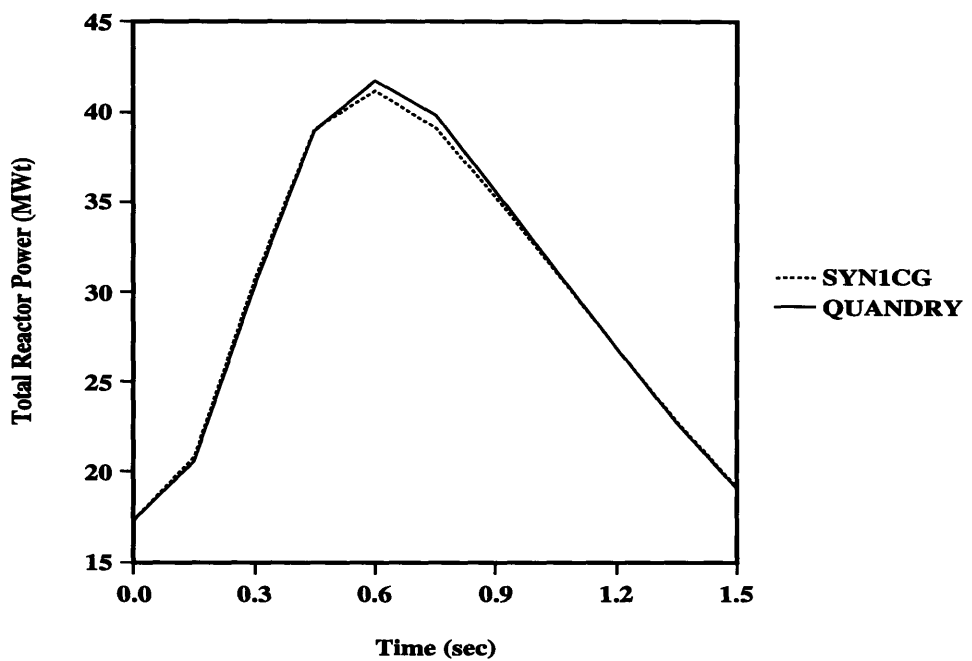


Figure 4-51: Total reactor power for transient case E-2CG

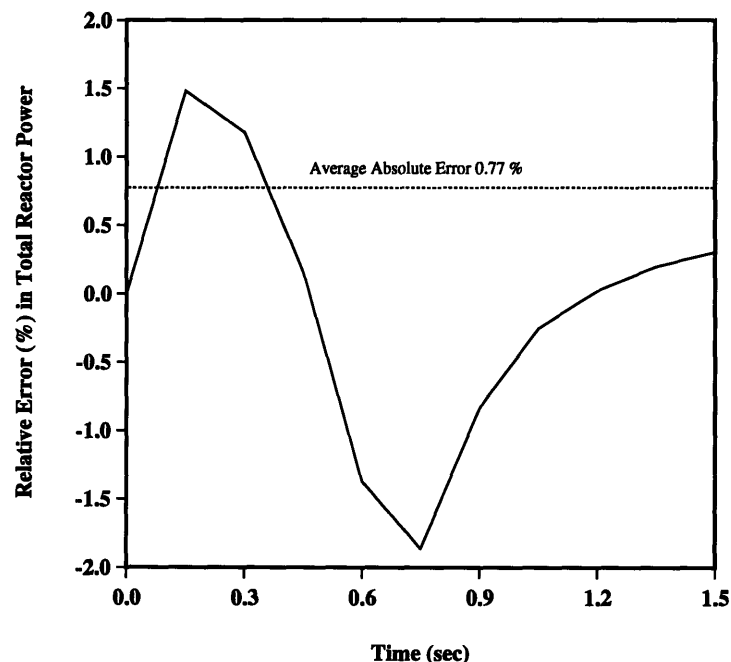


Figure 4-52: Relative error in total reactor power for transient case E-2CG

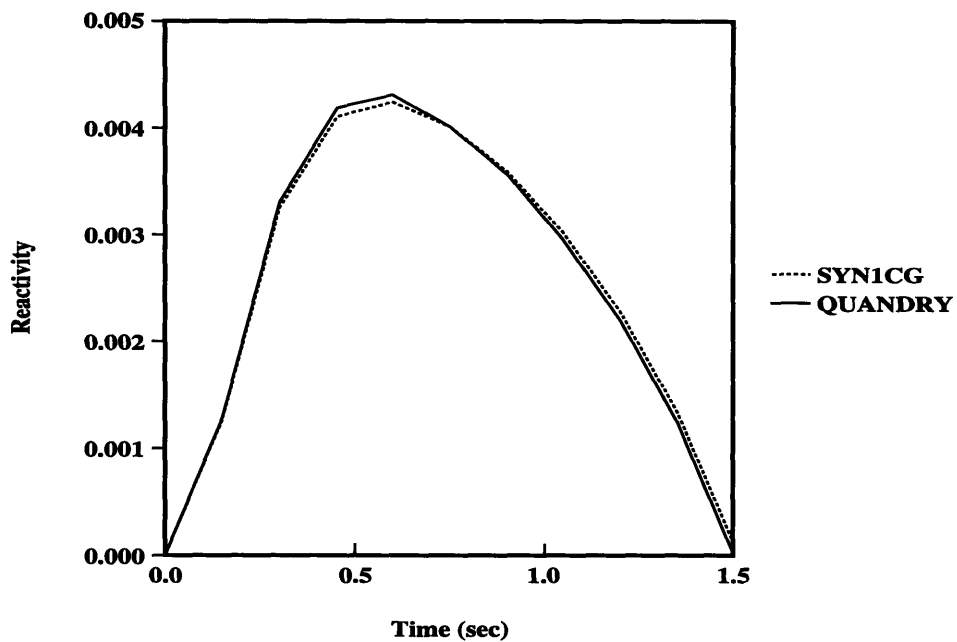


Figure 4-53: Total reactivity for transient case E-2CG

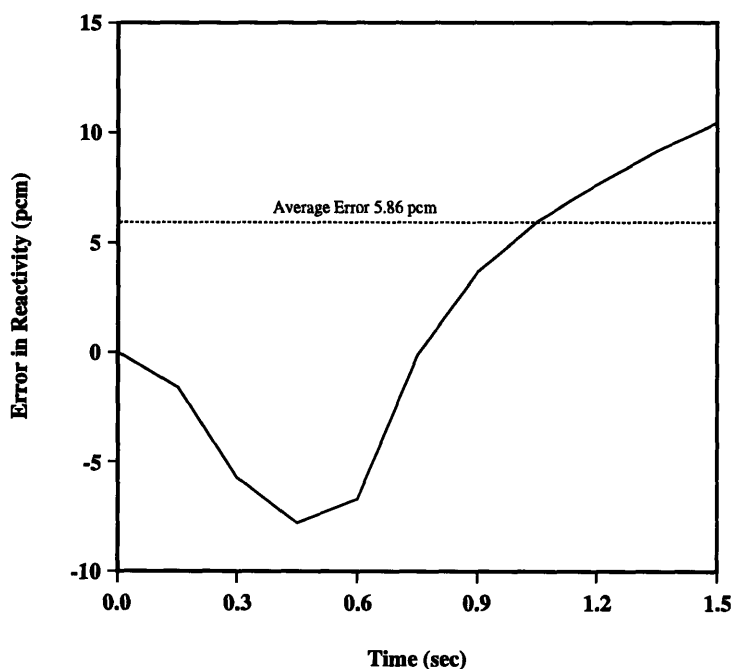


Figure 4-54: Absolute error in total reactivity for transient case E-2CG

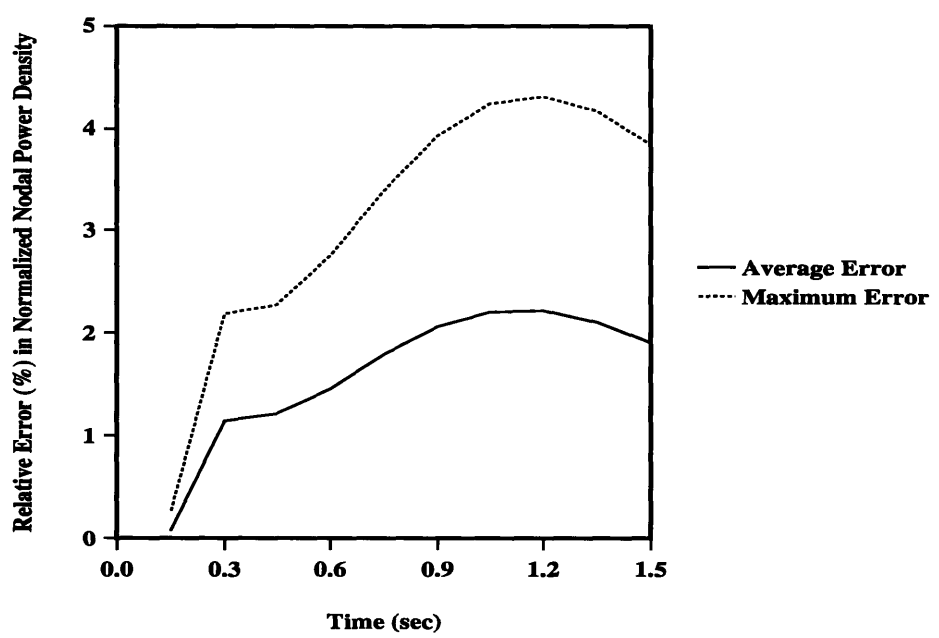


Figure 4-55: Relative error in nodal power density for transient case E-2CG

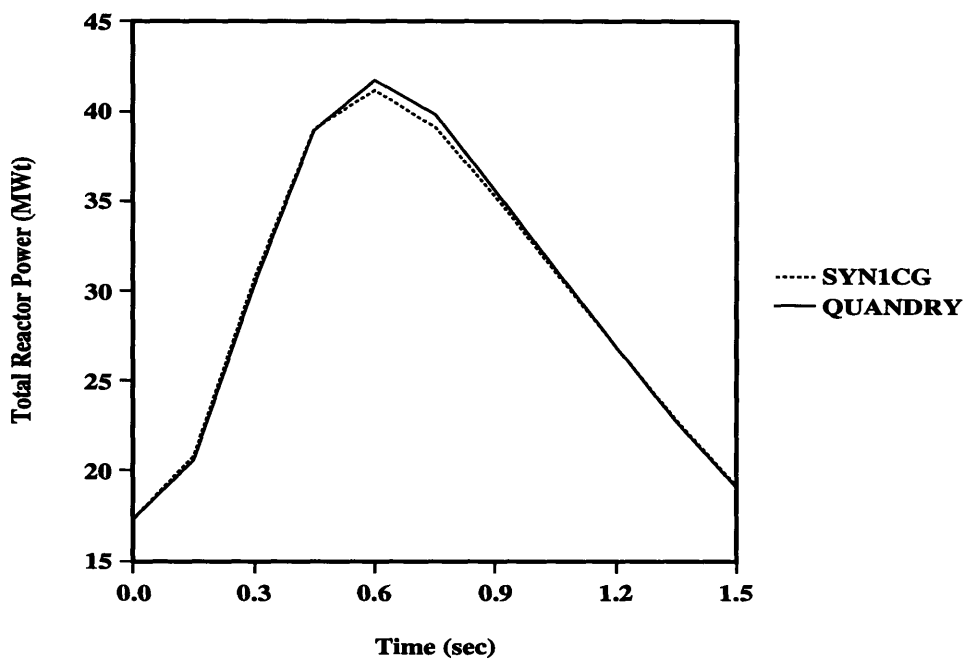


Figure 4-56: Total reactor power for transient case E-3CG

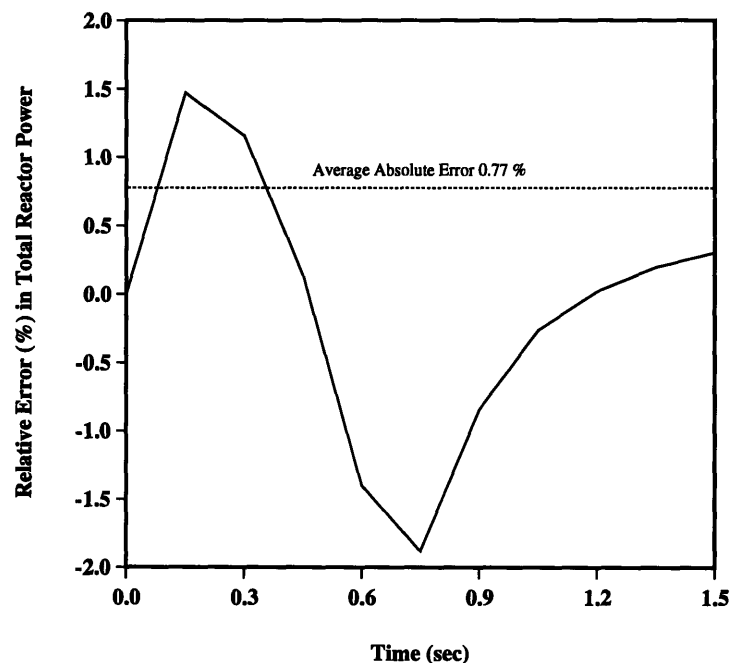


Figure 4-57: Relative error in total reactor power for transient case E-3CG

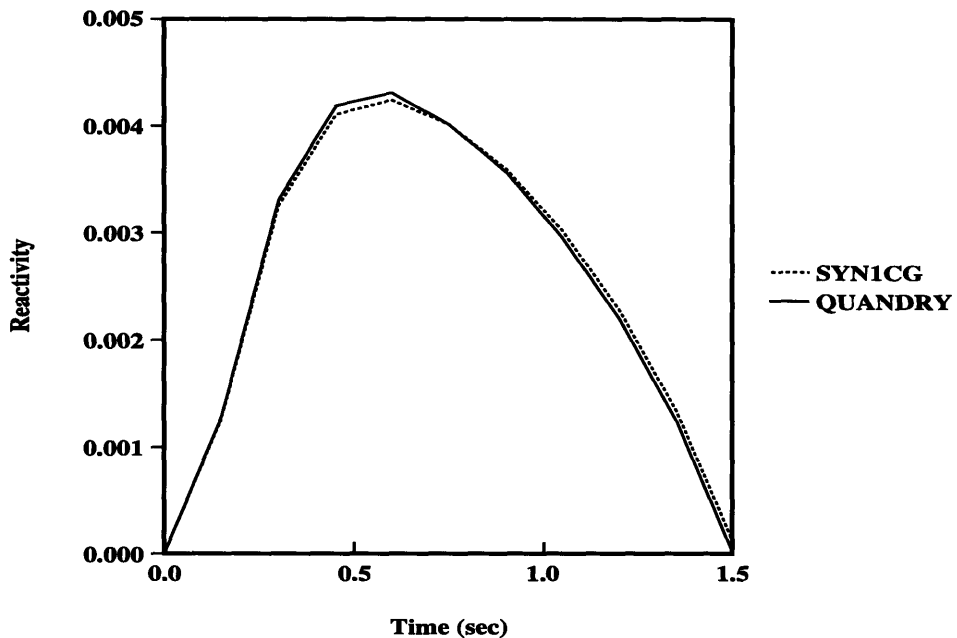


Figure 4-58: Total reactivity for transient case E-3CG

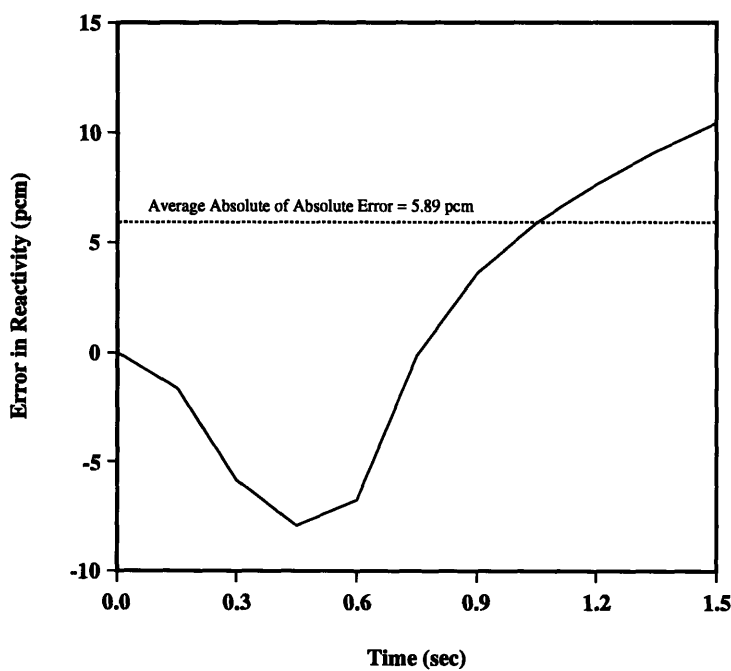


Figure 4-59: Absolute error in total reactivity for transient case E-3CG

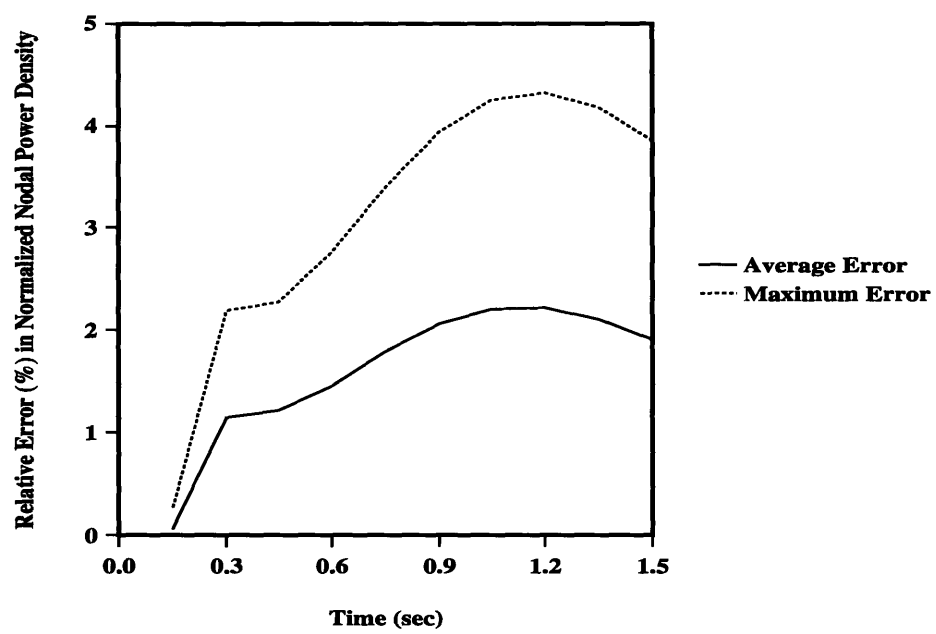


Figure 4-60: Relative error in nodal power density for transient case E-3CG

## **4.4 Comparison of the Nodal Synthesis Models**

It is interesting to make a comparison of the general nodal synthesis model and the collapsed-group nodal synthesis model. Specifically, their relative accuracy and the computing efficiency should be examined.

### **4.4.1 Accuracy**

Given the right choice of bracketing states, both the general synthesis and the collapsed-group synthesis models can generate the steady-state or the transient results which are in excellent agreement with the reference solutions. To compare the accuracy of the models, we select two sets of transient cases; cases E-2G and E-2, and cases E-3CG and E-3. Figures 4-61 and 4-62 show the comparison of the reactor power and the reactivity for cases E-2CG and E-2, and Figures 4-63 and 4-64 compare the reactor power and the reactivity for cases E-3CG and E-3, respectively.

The comparison shows that although both models are accurate, the general synthesis model is superior to the collapsed-group synthesis model. This result is expected on theoretical grounds, since the collapsed-group synthesis model is developed from the general synthesis model by allowing the mixing coefficients to be group independent and thereby causing the group-fluxes to be synthesized using the same mixing coefficient for each group.

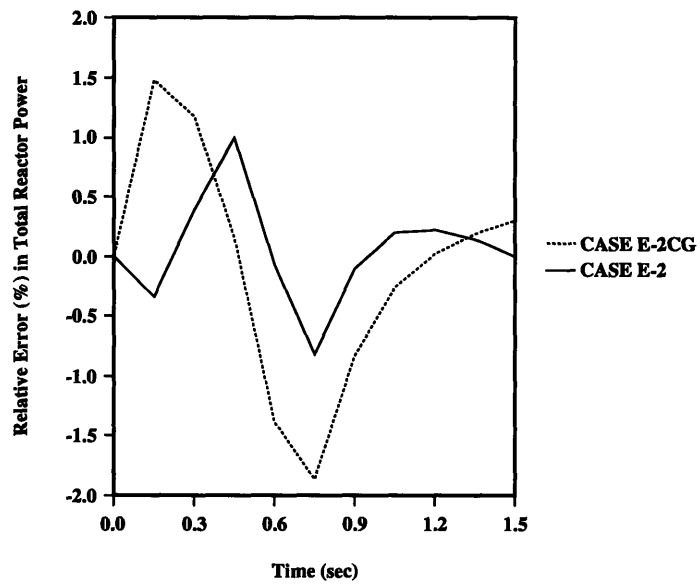


Figure 4-61: Comparison of error in reactor power for cases E-2CG and E-2

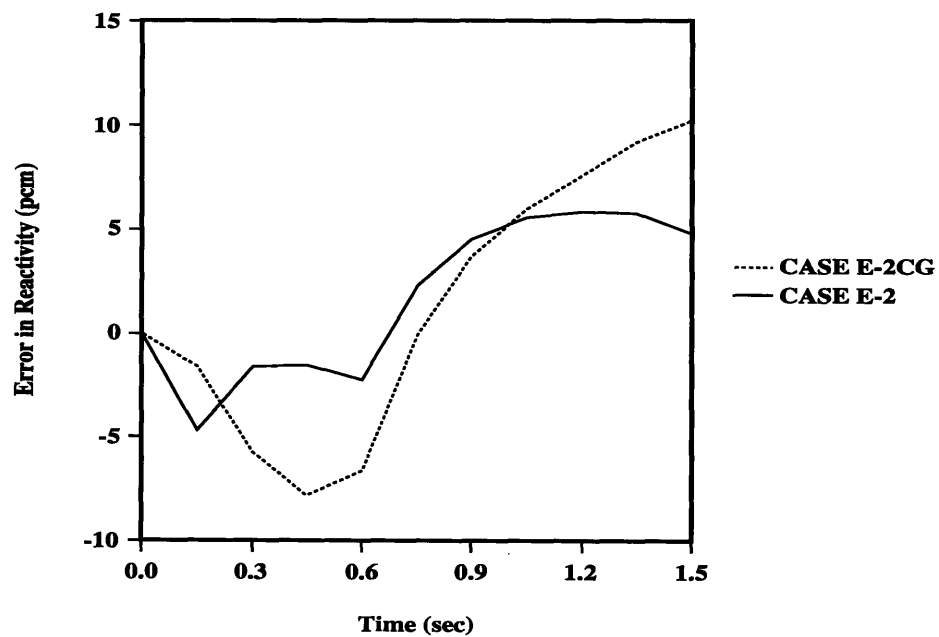


Figure 4-62: Comparison of error in reactivity for cases E-2CG and E-2

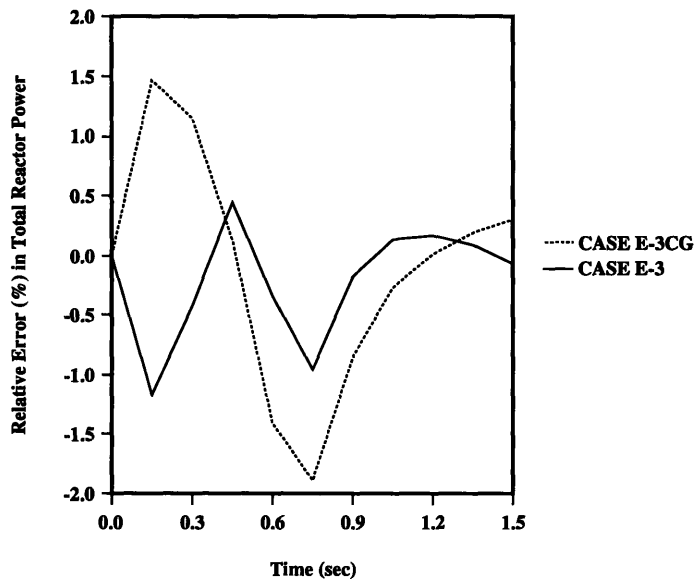


Figure 4-63: Comparison of error in reactor power for cases E-3CG and E-3

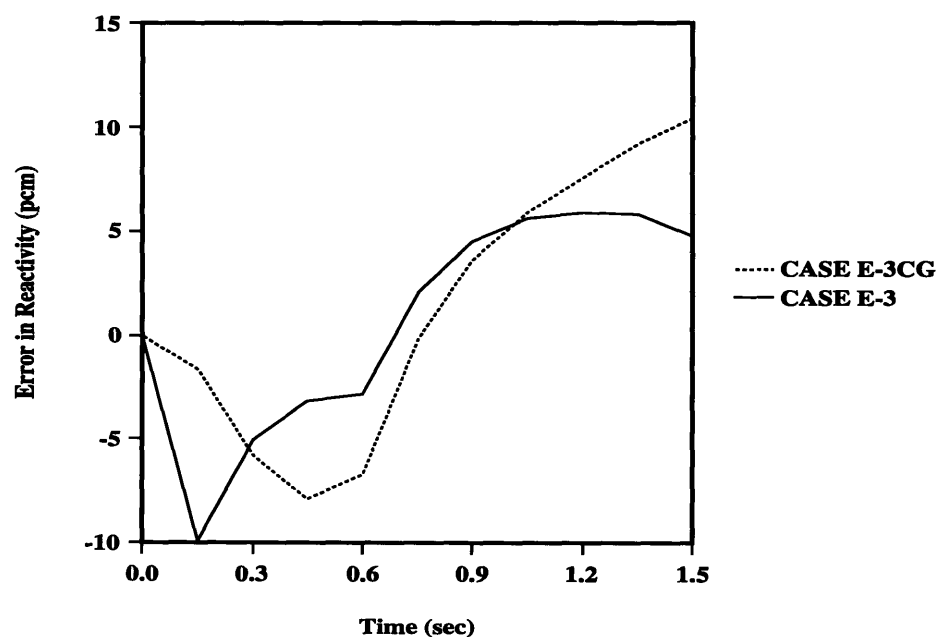


Figure 4-64: Comparison of error in reactivity for cases E-3CG and E-3

#### 4.4.2 Computing Efficiency

The computing efficiency for the synthesis models is plotted on Figure 4-65. This quantity is defined as the ratio of the total CPU time for the transient-synthesis computation to the total CPU time for the transient-reference computation. The larger the value of this relative computing efficiency, the more the CPU time spent for synthesis calculations. As seen in the plot, as the number of bracketing states increases, the CPU time for synthesis calculations increases. For the general synthesis model, the computing time increases rapidly reaching nearly twice the CPU time for the reference model for 3 bracketing states. For the collapsed-group synthesis model, the increase of the computing time is not as abrupt as that for the general synthesis model. However, as the number of bracketing states increases, the computing time approaches that for the reference model, and even for 2 or 3 bracketing states, the savings of the computing time is not encouraging for practical applications. For two and three dimensional problems, the disparity is expected to get much worse.

It is interesting to identify the essential factor in causing this deficiency in synthesis calculations. Studies show that over a half of the total CPU time is spent computing the loss and production matrices for a transient problem. This is demonstrated on Figure 4-66. For the general synthesis model, as the number of bracketing states increases, the fraction of the matrix computing time increases sharply. The increase for the collapsed-group synthesis model is much more moderate. Nevertheless, about 60% of the total computing time is spent calculating the matrices. If a nodal point synthesis method is ever to have practical applications, schemes must be found to speed up the matrix computations.

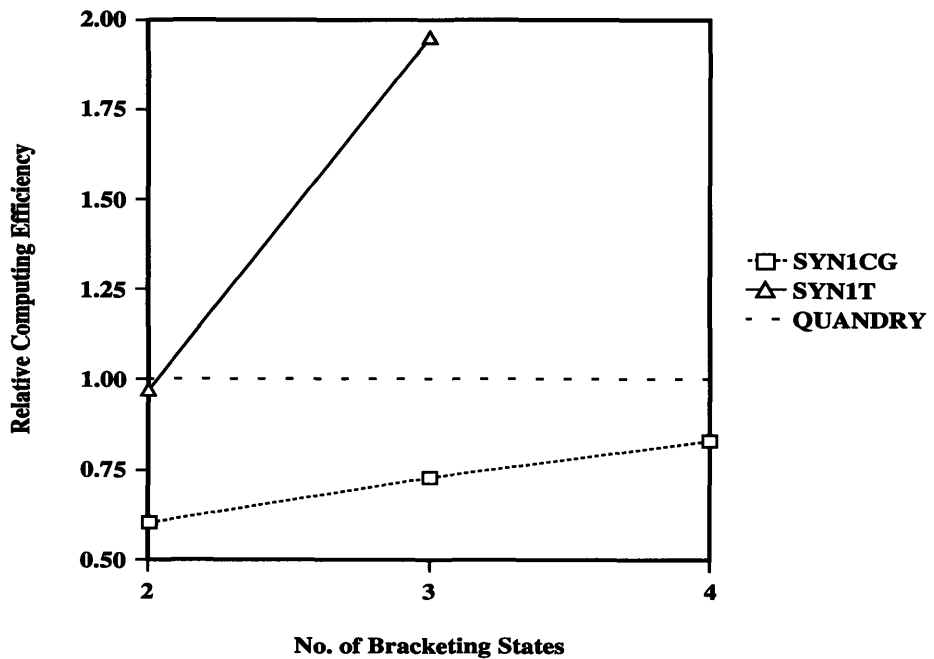


Figure 4-65: Computing efficiency for nodal synthesis models

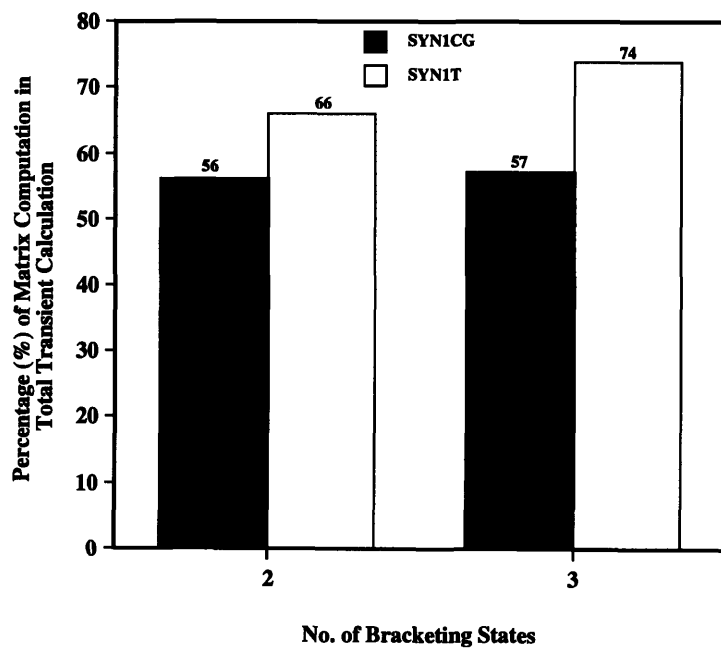


Figure 4-66: Percentage of matrix computing time in total CPU time for a transient calculation

## 4.5 Summary

One-dimensional steady-state and transient problems have been used to test the general nodal synthesis and the collapsed-group nodal synthesis models. With the right choice of bracketing states and proper treatment to the discontinuity factors, both models can reproduce the reference solutions. The average error in total reactor power is less than 1%, and the maximum error is less than 2%. The nodal power distribution is accurate to within 2% for the average error and within 4% for the maximum error. The total reactivity is correct to within 10 pcm. On the other hand, the computing efficiency for the general nodal synthesis model is worse than that for the reference model, whereas the computing speed for the collapsed-group nodal synthesis model is only slightly faster than that for the reference model. For both synthesis models, this computational deficiency is due to the large portion of the overall computation spent on the calculation of the loss and production matrices. If there are to be practical applications, this computing deficiency must be removed. Unless methods for doing so are discovered, there seems no point in pursuing the scheme.

For the remainder of the thesis, we shall concentrate on another application of the point synthesis idea, namely the experimental or instrumented nodal synthesis model. Chapter 5 gives a brief review of the theory of the experimental nodal synthesis model and discusses the application of this synthesis model to the MITR-II transient studies.

## **Chapter 5**

# **Review of the Experimental Nodal Synthesis Model and Application to MITR-II Transient Studies**

### **5.1 Introduction**

This Chapter briefly reviews the idea of the experimental nodal synthesis model [J-1]. The detailed description of the model is not given and only the governing equations and the solution method are highlighted. Additional information is given in Jacqmin's thesis [J-1]. In addition, an overview of the application of this synthesis model to the transient studies for the MIT Research Reactor (MITR-II) is provided.

## 5.2 Review of the Experimental Nodal Synthesis Model

### 5.2.1 Governing Equations

The basis of the experimental nodal synthesis model is to expand the time-dependent, three-dimensional neutron flux,  $\phi_{gn}(t)$ , in energy-group g and node n, into a linear combination of a set of K, precomputed, static expansion functions,  $\psi_{gn}^k$ :

$$\phi_{gn}(t) \approx \widehat{\phi}_{gn}(t) \equiv \sum_{k=1}^K \psi_{gn}^k T^k(t) \quad (5.1)$$

$$g = 1, 2, \dots, G; n = 1, 2, \dots, N.$$

These static expansion functions,  $\psi^k$ , are chosen in such a way as to closely bracket the reactor conditions expected throughout the transient.

The time-dependent mixing coefficients,  $T^k(t)$ , in Equation (5.1) are group-independent and can be inferred directly from local, counting rates,  $C^j(t)$ , provided by a set of J in-core neutron-detectors distributed throughout the reactor core. Specifically:

$$C^j(t) \equiv \sum_{g=1}^G \sum_{n=1}^N \Sigma_{gn}^j \phi_{gn}(t) V_n \approx \sum_{k=1}^K a_{jk} T^k(t) \quad (5.2)$$

$$j = 1, 2, \dots, J,$$

where,

$$a_{jk} \equiv \sum_{g=1}^G \sum_{n=1}^N \Sigma_{gn}^j \phi_{gn}(t) V_n. \quad (5.3)$$

Note that in Equation (5.2),  $\Sigma_{gn}^j$  is the node-n homogenized, group-g activation cross section of the j-th counter and is zero except for the node containing counter j.  $V_n$  is the volume of node n.

Equation (5.2) can be rewritten in matrix form as:

$$\mathbf{A} \mathbf{T}(t) \approx \mathbf{C}(t), \quad (5.4)$$

where  $\mathbf{A} \equiv \{a_{jk}\}$  is a J-by-K matrix. Usually,  $J > K$  and Equation (5.4) is an overdetermined system of linear algebraic equations.

Once the mixing coefficients,  $T^k(t)$ , are computed, the instantaneous group-fluxes can be reconstructed according to Equation (5.1). In addition, the point-kinetics parameters (including the amplitude function, the prompt neutron lifetime and the effective delayed-neutron fractions) can be computed, given a pre-selected weight function. Then, these estimates can be used to infer a value for reactivity by simple inversion of the point-kinetics equations.

### 5.2.2 Solution Method

Solving Equation (5.4) involves the inversion of matrix  $\mathbf{A}$ . However, the computation is complicated by the fact that  $\mathbf{A}$  is not necessarily a square matrix and is likely to be ill-conditioned.

The SVD technique as described in Chapter 2 is applied in the experimental nodal synthesis method. The SVD method decomposes the matrix  $\mathbf{A}$  and gives the least-squares solution to  $\mathbf{A} \mathbf{T} = \mathbf{C}$ . Moreover, the condition number can be used to detect the singularity of the problem and to serve as a criterion to eliminate ill-conditioned modes.

In Jacqmin's thesis, the SVD scheme was successfully tested with numerical problems. The results were in good agreement with reference solutions and the solution method was computationally very efficient.

### **5.3 Application of the Experimental Nodal Synthesis Model to MITR-II Transient Studies**

The success of the application of the experimental nodal synthesis method to numerical problems has stimulated the setup of a research project [M-2] at MIT. The project is to perform experimental tests to evaluate the experimental synthesis method with actual reactor-generated signals under steady-state and transient conditions. The results of the experiments are needed to determine if this synthesis method can provide an accurate evaluation of reactivity and local power density under actual operating conditions. The project has been underway since October, 1991. One fission-chamber detector has been installed and several steady-state low-power experiments have been conducted at the MIT Research Reactor (MITR-II) [S-5] to measure the thermal neutron flux. Unfortunately, because of damage to some experimental equipment, the transient experiments have not yet been performed. Moreover, the failure to normalizing the detecting system before making the measurements made the static results unreliable.

In this thesis, an approach is devised to determine the few-group homogenized cross sections and discontinuity factors for triangular-z nodes using the Monte-Carlo code MCNP [B-2]. These nodal parameters are needed for the a three-dimensional, triangular-z, nodal diffusion code, QUARTZ, developed by DeLorey [D-1], to reproduce reference solutions generated from the MCNP code. The procedure is validated by a simple test problem.

## **5.4 Summary**

In this chapter, the basis of the experimental nodal synthesis method has been highlighted and the application of the method to transient studies for the MIT Research Reactor (MITR-II) has been addressed. As a first step of the method, an approach to determine the few-group nodal parameters for the QUARTZ code must be set up and validated. Chapter 6 will describe the details of this approach and Chapter 7 will check the validity of the approach with a demonstration problem.

## **Chapter 6**

# **Determination of Few-Group Nodal Parameters for the Experimental Nodal Synthesis Model**

### **6.1 Introduction**

This Chapter describes an approach which can be taken to generate the two-group nodal parameters for the application of the experimental nodal synthesis method to the transient studies for the MIT Research Reactor (MITR-II). A direct, brute-force method, which applies the MCNP Monte-Carlo code [B-2], can be used to determine the nodal parameters. The task is too overwhelming to be done by a single person and therefore has been divided between that author and Tari [T-2]. A detailed method for determining nodal parameters for MITR-II will be outlined in the present thesis. Numerical results will be reported by Tari in a subsequent thesis.

Section 6.2 briefly describes MITR-II, Section 6.3 highlights the MCNP code, Section 6.4 briefly reviews the QUARTZ code [D-1], Section 6.5 describes the MITR-II MCNP models and the methods to be used to compute the nodal parameters, and finally, Section 6.6 discusses the consistency problem found in obtaining the nodal parameters.

## 6.2 Description of MITR-II

The Massachusetts Institute of Technology Reactor II (MITR-II) is a heavy-water reflected, light-water cooled and moderated research nuclear reactor, which functions as a center of research and education for many MIT departments and local-area universities and as a supplier of radioisotopes for medical and industrial research in the greater Boston area. This reactor uses highly enriched  $UAl_x$  plate-type fuels and is designed to operate at power levels up to 5  $MW_t$ . The MITR-II achieved its first criticality in August 1975 and has been in full power operation since March 1976. A pictorial cutway of the MITR-II reactor, its adjacent blanket test facility, the medical therapy beam line, as well as the medical room below the reactor is shown in Figure 6-1. Figure 6-2 provides a closer view of the vertical cross-section of the MITR-II.

The MITR fuel elements are specially designed and fabricated for use in a highly compact core. The fuel element is rhombic in shape and consists of 15 straight and finned fuel plates containing uranium enriched to approximately 93% U-235, Al-6061 cladding, and structural material. The reactor core includes 27 fuel element positions and is divided into 4 regions separated by the absorber spider which contains the fixed radial and hexagonal absorber plates. The four regions, as divided by the core structure, consists of one central and three outer regions. The core configuration is given on Figure 6-3.

The fuel elements are grouped into three rings designated A, B, and C. The inner ring, ring A, has 3 elements, ring B has 9 elements, and the outer ring, ring C, has 15 elements. Normally, two of the A-ring elements and/or one of the B-ring elements can be replaced by in-core sample irradiation facilities or dummy elements. These elements form a hexagonal right prism shaped core.

The reactor is controlled by using 6 Boron-stainless steel shim/safety blades and a cadmium fine-control regulating rod. The shim blades are arranged symmetrically with respect to the core, while the regulating rod is located in one of the six small circular water vent holes at the corner of the core.

The complete description of the MITR-II is too tedious and voluminous to be included in this section. A detailed description can be found in the reference [M-3].

VIEW OF M.I.T. RESEARCH REACTOR, MITR-II, SHOWING MAJOR COMPONENTS AND EXPERIMENTAL FACILITIES

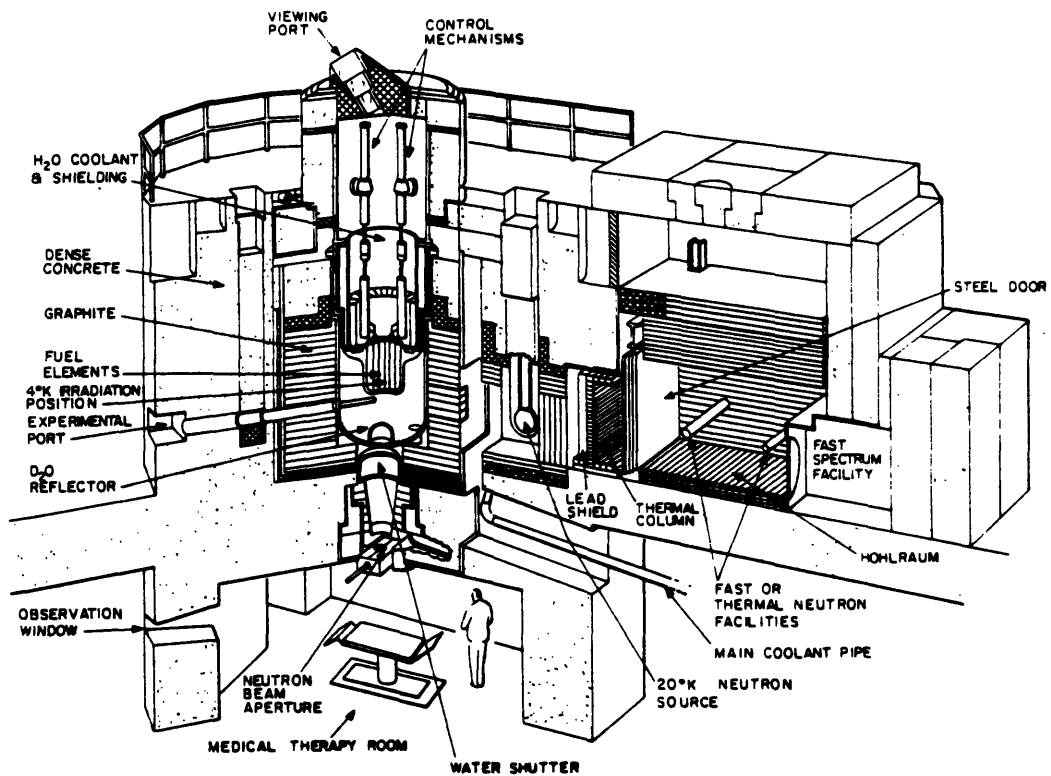


Figure 6-1: Artist's view of the MITR-II reactor facility [M-3]

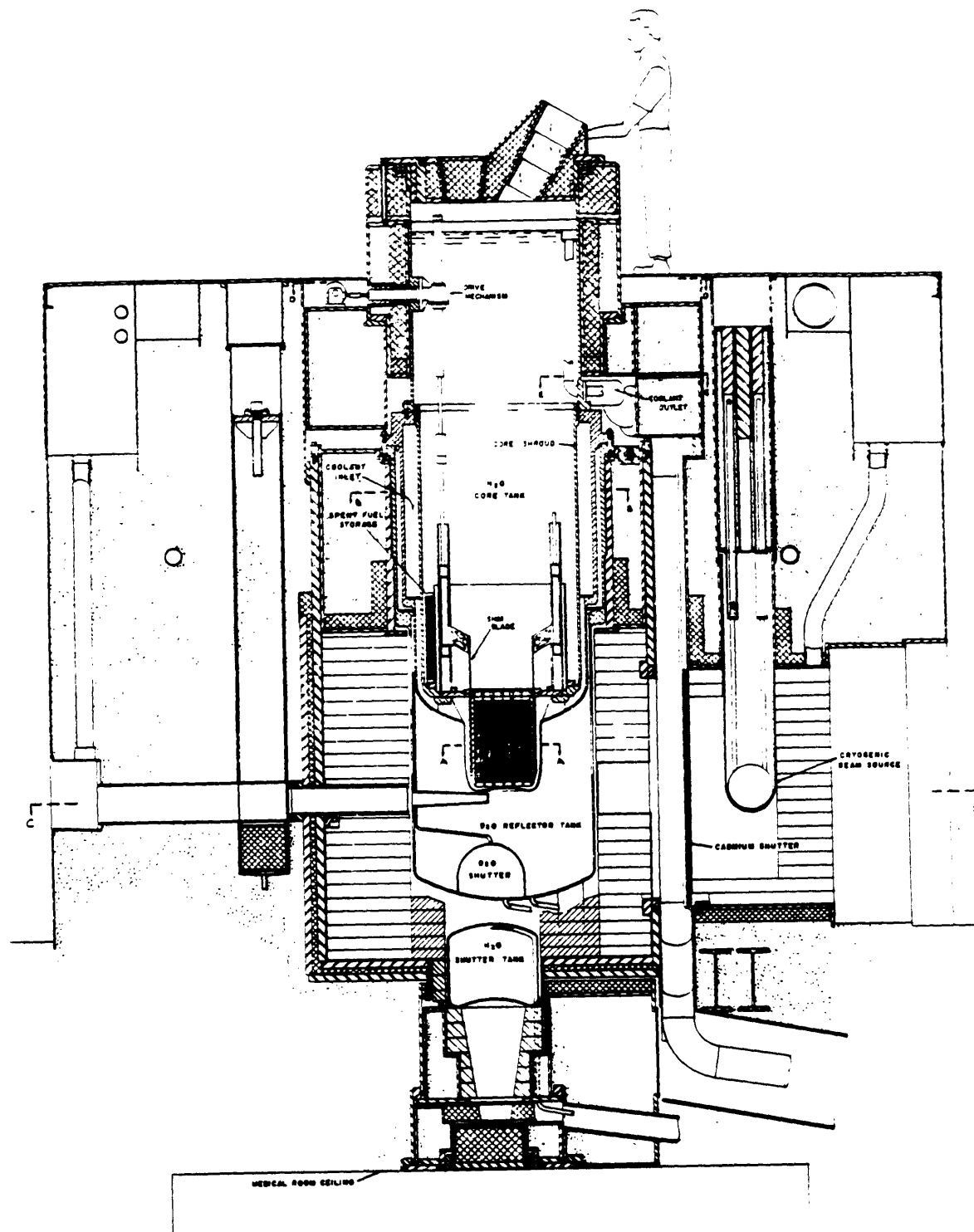
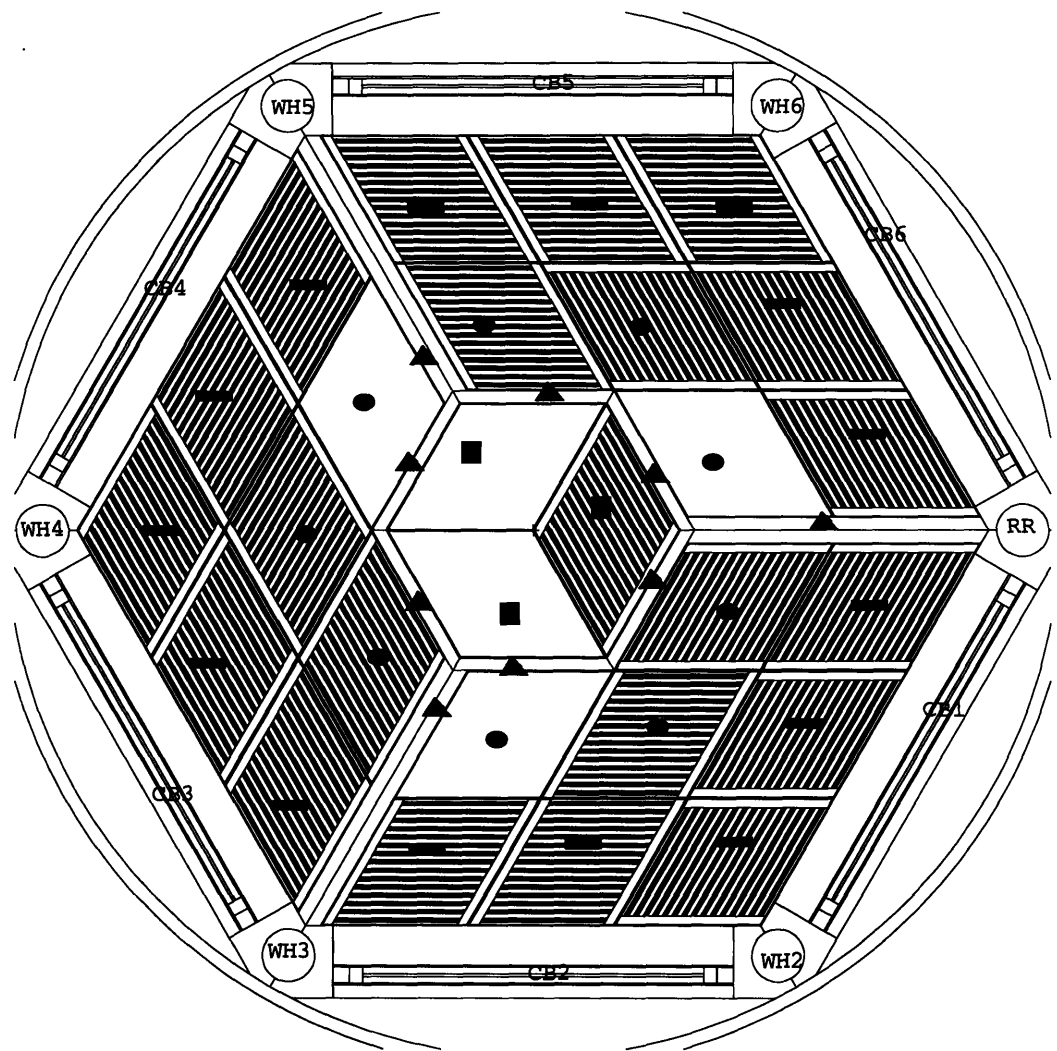


Figure 6-2: Vertical cross-section of the MITR-II [M-3]



- A Ring
- B Ring
- C Ring
- ▲ Absorber Plate
- RR : Regulating Rod
- CB : Control Blade
- WH: Water Hole

**Figure 6-3: MITR-II core configuration**

### **6.3 Description of the MCNP Monte-Carlo Code**

MCNP is a general-purpose, continuous-energy, generalized-geometry, time-dependent<sup>1</sup>, coupled neutron/photon Monte Carlo code that can be used for neutron, photon, or coupled neutron/photon transport <sup>2</sup>. It includes the capability to calculate eigenvalues for critical systems. MCNP is used throughout the world for many applications. At MIT, MCNP has already been used in studies of radiation science and technology, and for design and analysis of nuclear reactors.

The code treats an arbitrary three-dimensional configuration of materials in geometric cells bounded by first- and second-degree surfaces and some special fourth-degree surfaces. A unique repeated structure capability has been introduced into MCNP version 3B [B-3], making it possible to describe only once some cells and surfaces of any structure that appears more than once.

One of the most significant features of MCNP is its use of continuous-energy data. For neutrons, all reactions given by a particular cross-section evaluation (such as ENDF/B-V) are accounted for. Thermal neutrons are described by both the free gas and  $S(\alpha, \beta)$  models. For photons, the code takes account of incoherent and coherent scattering, the possibility of fluorescent emission after photoelectric absorption, and absorption in pair production with local emission of annihilation radiation.

Other standard features that make MCNP versatile and easy to use include a powerful general source, a geometry plotter, a very rich collection of variance reduction techniques, an elaborate tally structure and user interface that make possible calculating almost anything conceivable, and an extensive collection of cross-section data.

One significant drawback to MCNP and to all the Monte Carlo codes is the amount of computer time required to perform the calculations. Other shortcomings of MCNP are the lack of depletion and transient analysis capabilities.

---

<sup>1</sup>Actually, MCNP provides only a snapshot in time of any requested quantities.

<sup>2</sup>A fully coupled continuous-energy electron transport capability has been introduced in MCNP4 [B-4].

## **6.4 Description of the QUARTZ Nodal Code**

QUARTZ is a quadratic polynomial nodal code for triangular-z geometry developed by DeLorey [D-1] for his thesis. The code solves the static (forward or adjoint) and transient nodal equations for triangular-z geometry. For the solution of static problems, a corrected, three-dimensional, mesh-centered finite difference model was developed. To improve upon the spatial treatment, a higher order expression for the surface-averaged current was derived by assuming that the transverse-averaged flux can be represented by a quadratic polynomial within the triangular-z node. A non-linear iteration scheme along with other acceleration procedures is used to solve the quadratic equations.

The transient nodal equations are cast into fully implicit form, and the delayed neutron precursor equations are treated using a direct integration procedure. The resulting equations are solved using the improved quasi-static method.

The WIGL thermal-hydraulic model [V-1] is used for the temperature calculations and a quadratic, two-dimensional, cross-section interpolation procedure is implemented to take account of the thermal-hydraulic feedback response.

A flux and volume weighting scheme, which is similar to that used by Gehin [G-3], is incorporated to take account of the control-rod cusping effect for transient and no-feedback problems [D-2].

QUARTZ has been tested by various static and transient problems and shows promise for application to MITR-II, where the unique geometry is well suited for triangular-z nodal meshes.

## **6.5 Determination of Few-Group Nodal Parameters for QUARTZ**

### **6.5.1 MITR-II MCNP Models**

Various analytical and experimental methods are currently used to support the research of the MITR-II. CITATION [F-1], a multi-dimensional, mesh-centered finite-difference, diffusion-theory code, is currently a central tool for the reactor physics and fuel management program. A three-dimensional ( $r - \theta - z$ ), three energy group, CITATION model is routinely used with in-house codes [B-5] for depletion calculations. CITATION is also used to calculate power peakings and to estimate the reactivity impact of experiments. However, the CITATION calculations are not always reliable and the cross-sections used are obsolete.

On the other hand, the MCNP Monte-Carlo code [B-2, B-3, B-4] has been used to set up a detailed and accurate reactor physics model for the MITR-II [R-1, R-2]. The model has also been validated against experimental data. The excellent agreement between the MCNP predictions and the experimentally determined values has provided confidence in using the model.

For this thesis, MCNP models derived from Redmond's full core model for the MITR-II core number 2 [R-2] were developed. Core number 2 consisted of 22 fuel elements and 5 dummy elements. This core went critical with the control blades and regulating rod withdrawn to a position of 21.082 cm above full insertion. Figure 6-4 shows a cross sectional view of the fuel loading in core number 2 as it was originally modeled in MCNP, and Figure 6-5 provides an axial view of the model.

For our MCNP models, various modifications were made to the Redmond's full core model by the author and Tari [T-2]. A few of these changes include the deletion of the beam port and medical room, modification to the graphite reflector, simplification of a portion of the upper core tank, and segmentation and triangulation of MCNP cells. In addition, nine fission-chamber detectors were added into water holes number<sup>3</sup> 2, 4, and 6, with three chambers for each water hole, as suggested by Selby [S-5]. Details of the modification/simplification made for our MCNP model are illustrated on Figures 6-6, 6-7, and 6-8. Because of the editing restrictions of MCNP, three MCNP models were developed to tally

---

<sup>3</sup>The water holes are numbered clockwise, starting from the hole that contains the regulating rod.

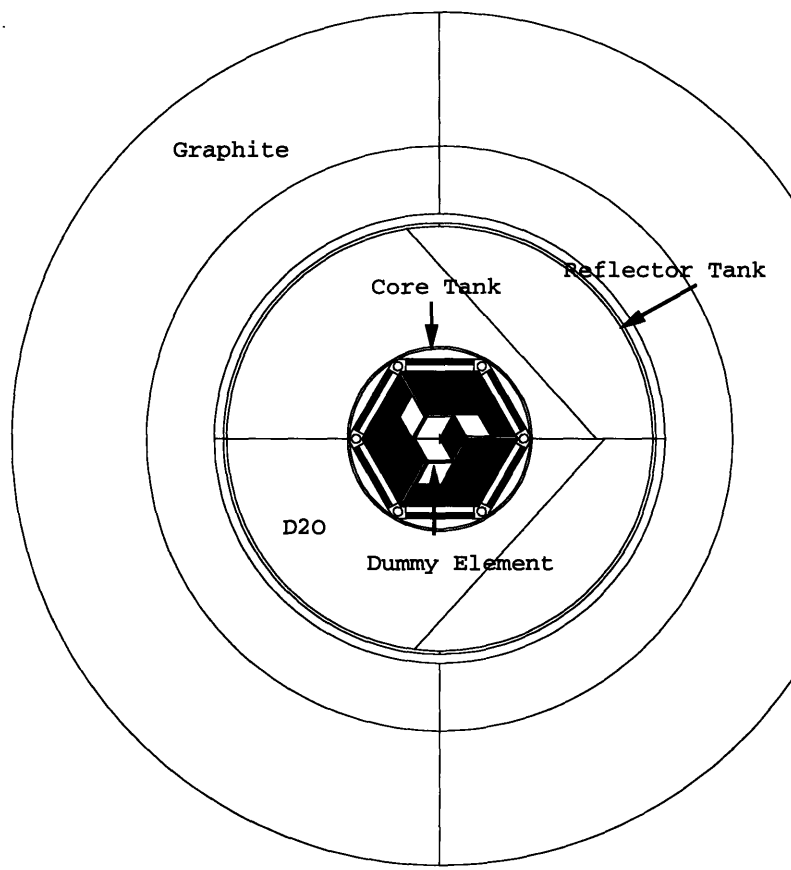
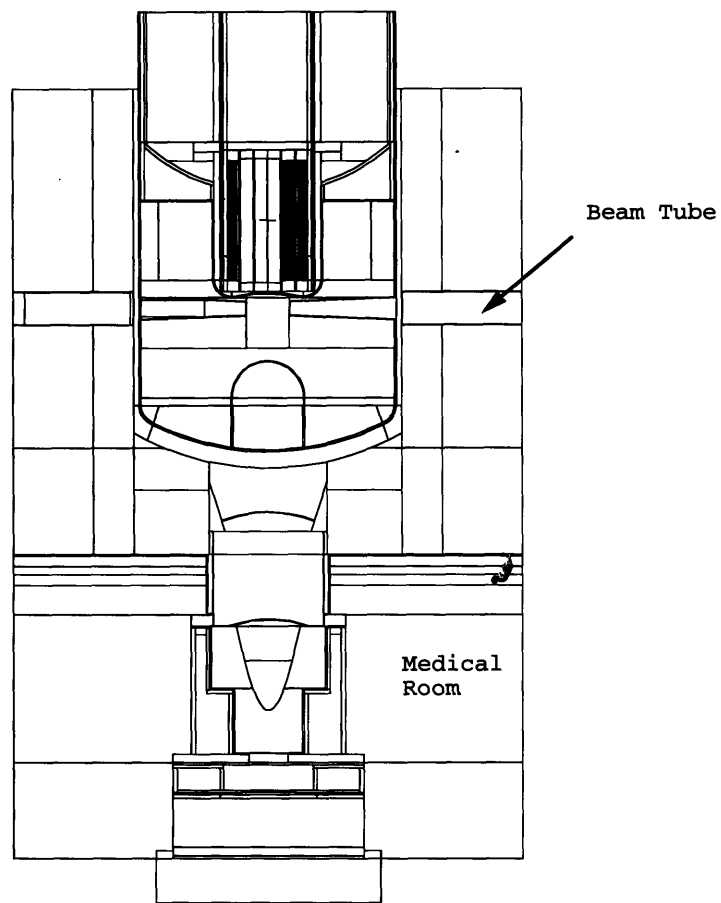


Figure 6-4: Cross-sectional view of MCNP model for MITR-II core number 2 (showing x-y plane at z=0)



**Figure 6-5:** Vertical view of MCNP model for MITR-II core number 2 (showing y-z plane at  $x=0$ )

the two-group reaction rates, cell-averaged fluxes, surface-fluxes, and surface-currents for the triangular-z model to be used for QUARTZ. The triangular-z model, for which homogenized group constants and discontinuity factors must be found, consists of 16 axial layers with 600 triangular nodes for each layer. The cells below the top of active fuel and above the bottom of active fuel are segmented to 12 axial layers, and the compositions below the bottom of active fuel are divided into 4 axial layers. The reaction rates and cell-averaged fluxes will be used by Tari [T-2] to construct the homogenized two-group cross-sections for the triangular nodes. The surface currents and surface fluxes were used by the author to construct the leakage rates and the CMFD (coarse-mesh finite-difference) discontinuity factors. Figure 6-9 shows a three-dimensional plot of the triangular-z nodal mesh boxes, and Figure 6-10 shows a two-dimensional slice of the meshes.

The in-core MCNP model tallies the nodal parameters for the nodes inside the core hexagon (the hexagonal area including 22 fuel elements, 5 dummy elements, spiders, and absorber plates). The out-of-core MCNP model tallies the nodal parameters for the nodes outside of the core hexagon (including six control blades, nine detectors, regulating rod, water holes, core tank,  $D_2O$  reflector, and graphite reflector). Finally, the supplement MCNP model tallies the nodal parameters for all the nodes that constitute the 4 axial layers below the bottom of the active fuel. Figure 6-11 shows a cross sectional view of the in-core model, and Figure 6-12 provides an axial view of the model. Figure 6-13 shows a cross sectional view of the out-of-core model, and Figure 6-14 provides an axial view. Finally, Figure 6-15 shows a cross sectional view of the supplement-model, and Figure 6-16 provides an axial view of the model. For simplicity, nodal parameters are computed for two types of triangular nodes. Graphite, some portion of the reflector tank, and some portion of the  $D_2O$  inside the reflector tank are separated into three rings of large triangular nodes<sup>4</sup>, for which the two-group node-averaged cross-sections are obtained. The core hexagon, the control-blade ring (the hexagonal ring of triangular nodes which include the control blades, water holes, detectors, and regulating rod), and the  $D_2O$  immediately surrounding the control-blade ring are separated into 4 rings of small triangular nodes for calculating the cross-sections. The discontinuity factors are computed for only those nodes that fall within

---

<sup>4</sup>As seen in Figure 6-13, there are only two rings of large nodes. However, the cross-sections data for those small triangular nodes that fall within the third large-node ring are averaged to get the homogenized cross-sections for the large nodes of that ring. Each large node is exactly 4 times the size of a small node.

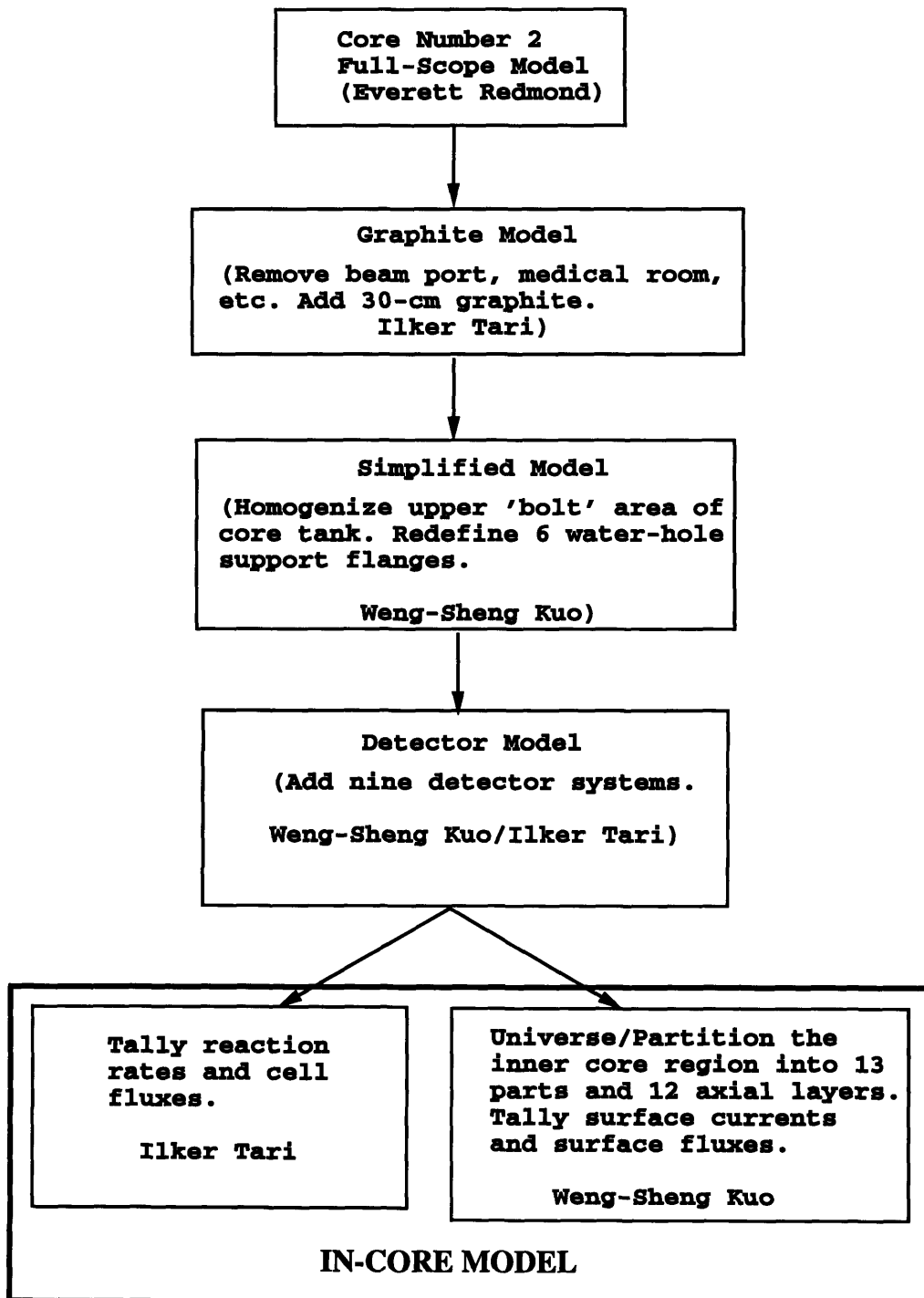


Figure 6-6: Steps in the development of the MCNP in-core model for MITR-II

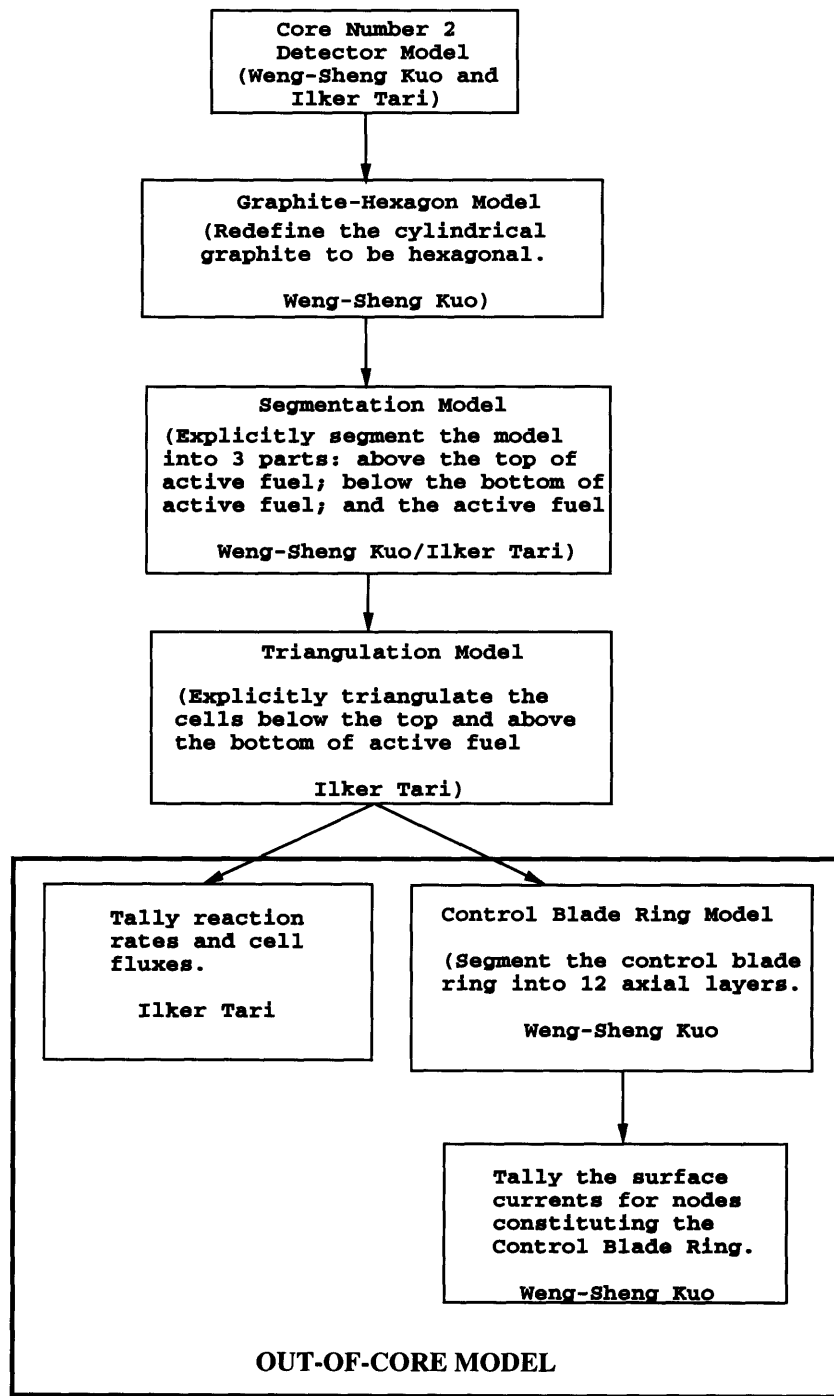


Figure 6-7: Steps in the development of the MCNP out-of-core model for MITR-II

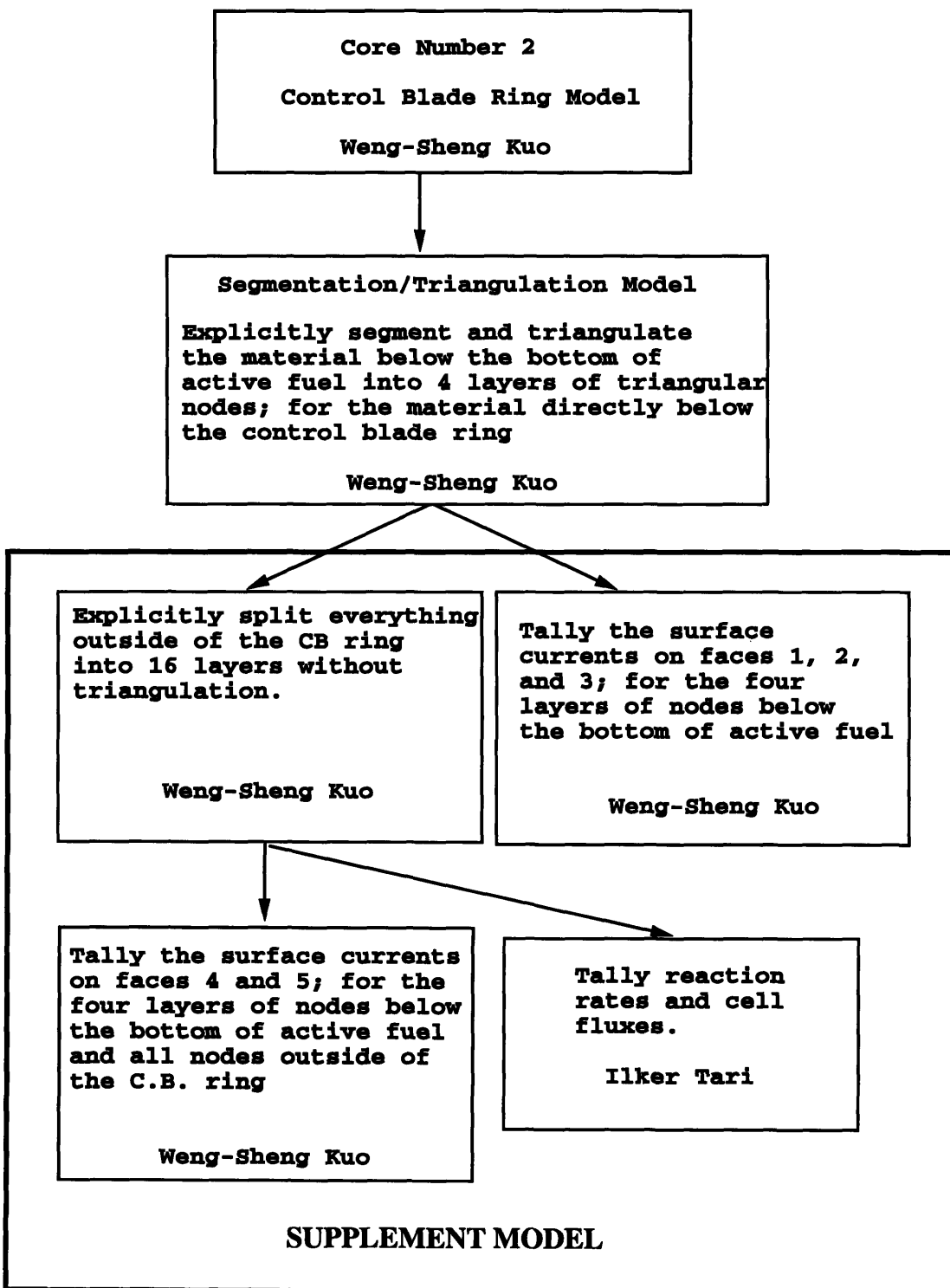


Figure 6-8: Steps in the development of the MCNP supplement model for MITR-II

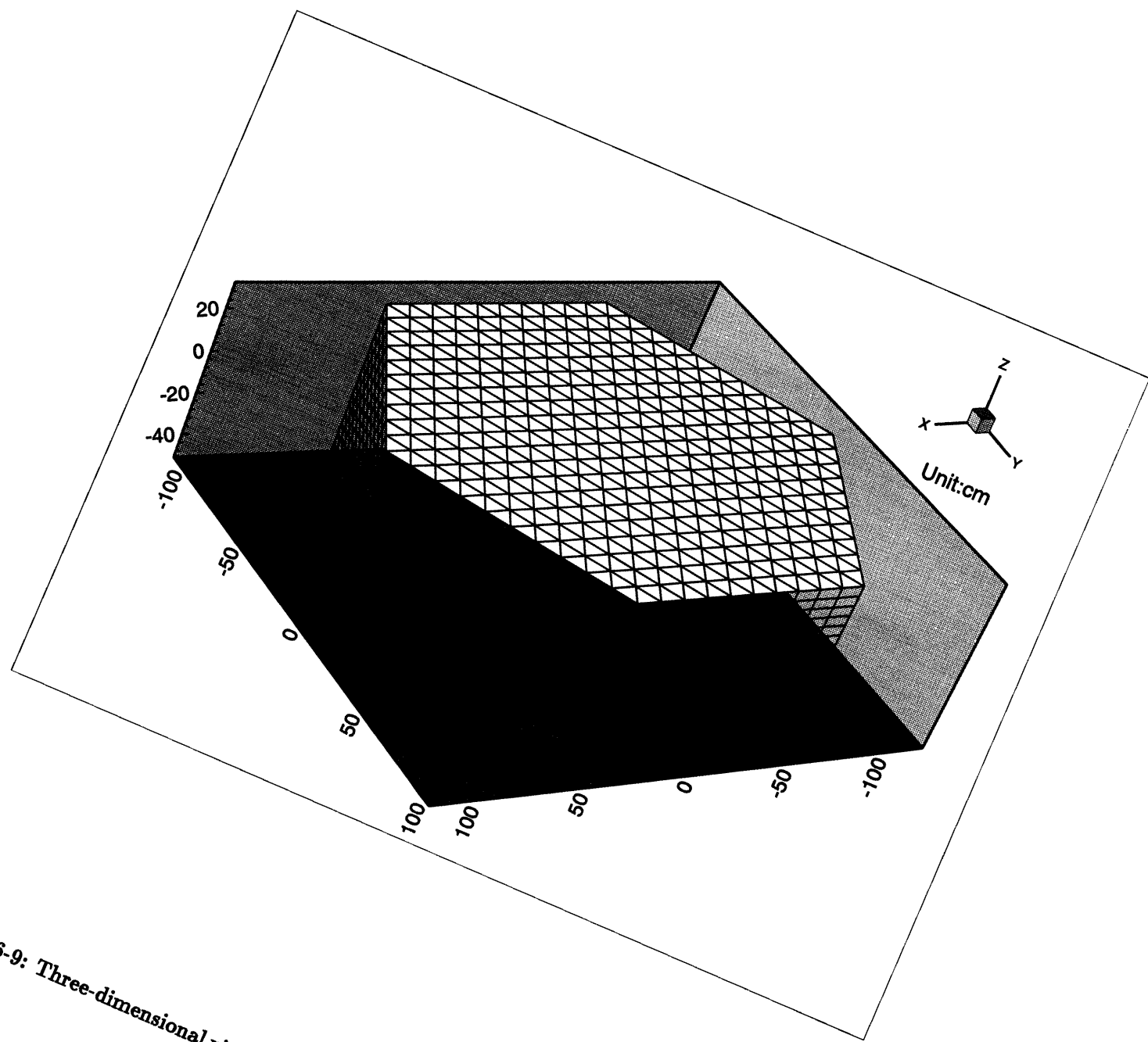


Figure 6-9: Three-dimensional view of the QUARTZ triangular-z geometry model for MITR.  
II  
146

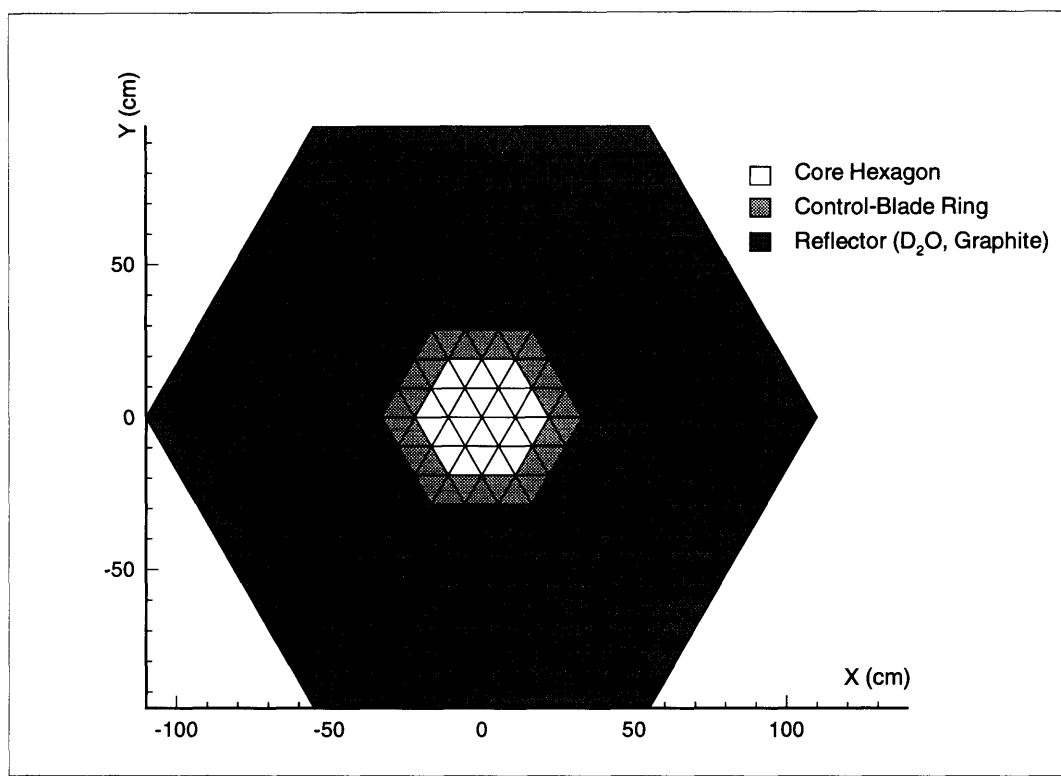


Figure 6-10: Two-dimensional slice of a 3-D QUARTZ triangular-z mesh layout for MITR-II (showing the x-y plane at  $z=0$ )

the core hexagon and the control-blade ring and are located between the top and bottom of active fuel. In addition, the annular-shaped graphite in the in-core model was replaced by the hexagon-shaped graphite in the out-of-core and the supplement models. In the supplement model, two different geometric models were set up to tally the surface currents on various faces of a triangular node, as shown in Figure 6-16. All the MCNP models were run on a SUN/SPARC machine.

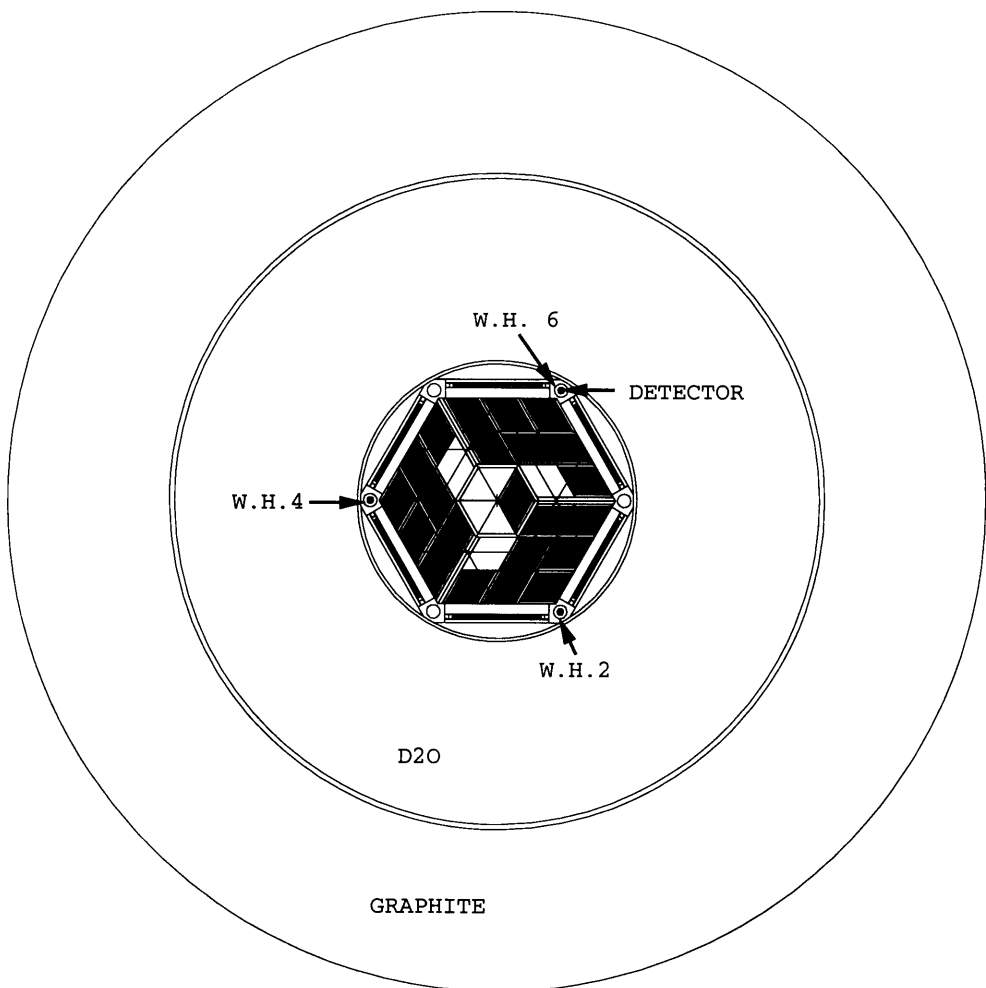


Figure 6-11: Cross-sectional view of MCNP in-core model (showing x-y plane at  $z=0$ )

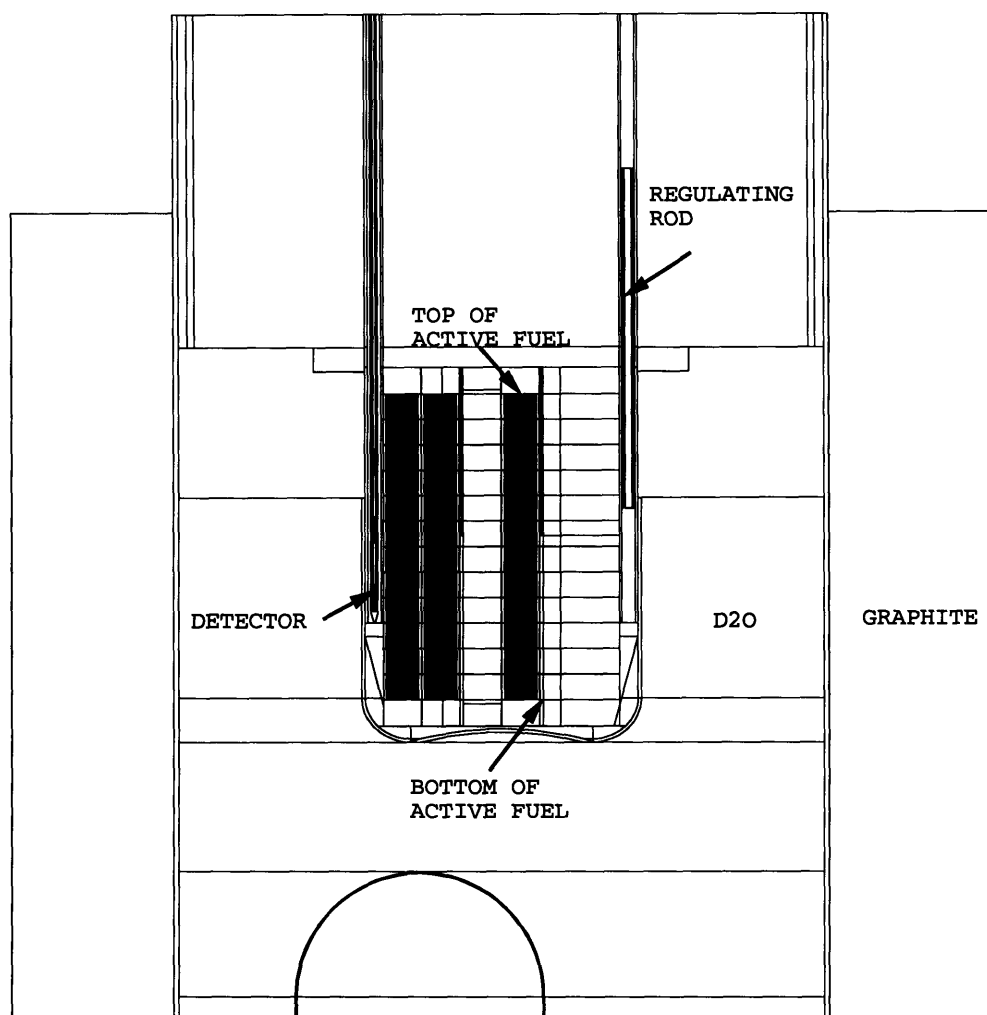


Figure 6-12: Vertical view of MCNP in-core model (showing x-z plane at y=0)

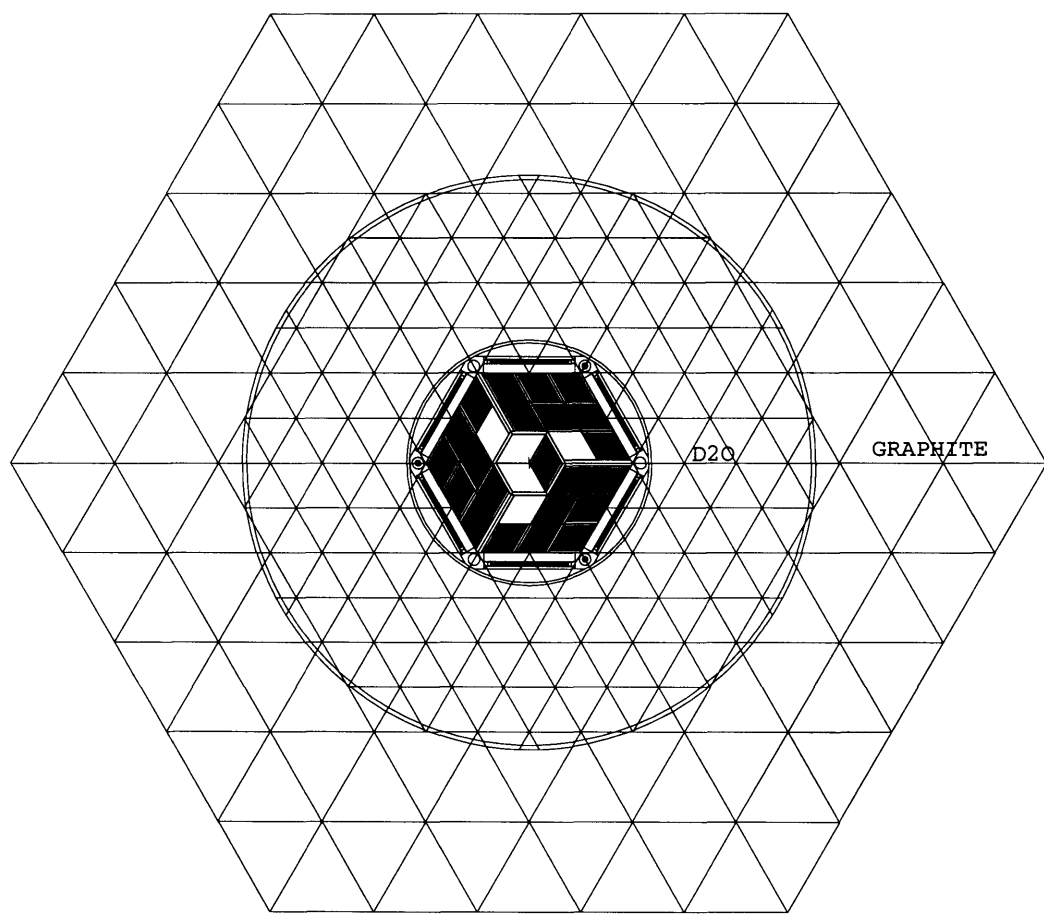


Figure 6-13: Cross-sectional view of MCNP out-of-core model (showing x-y plane at  $z=0$ )

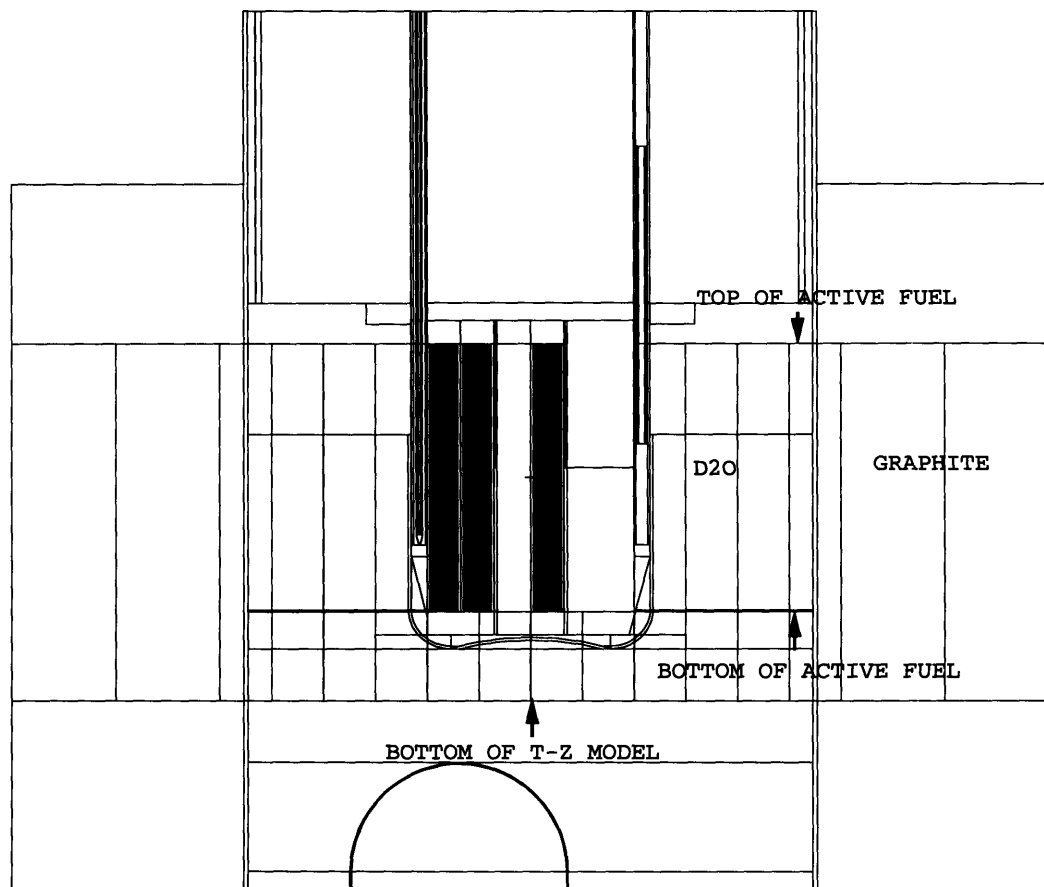
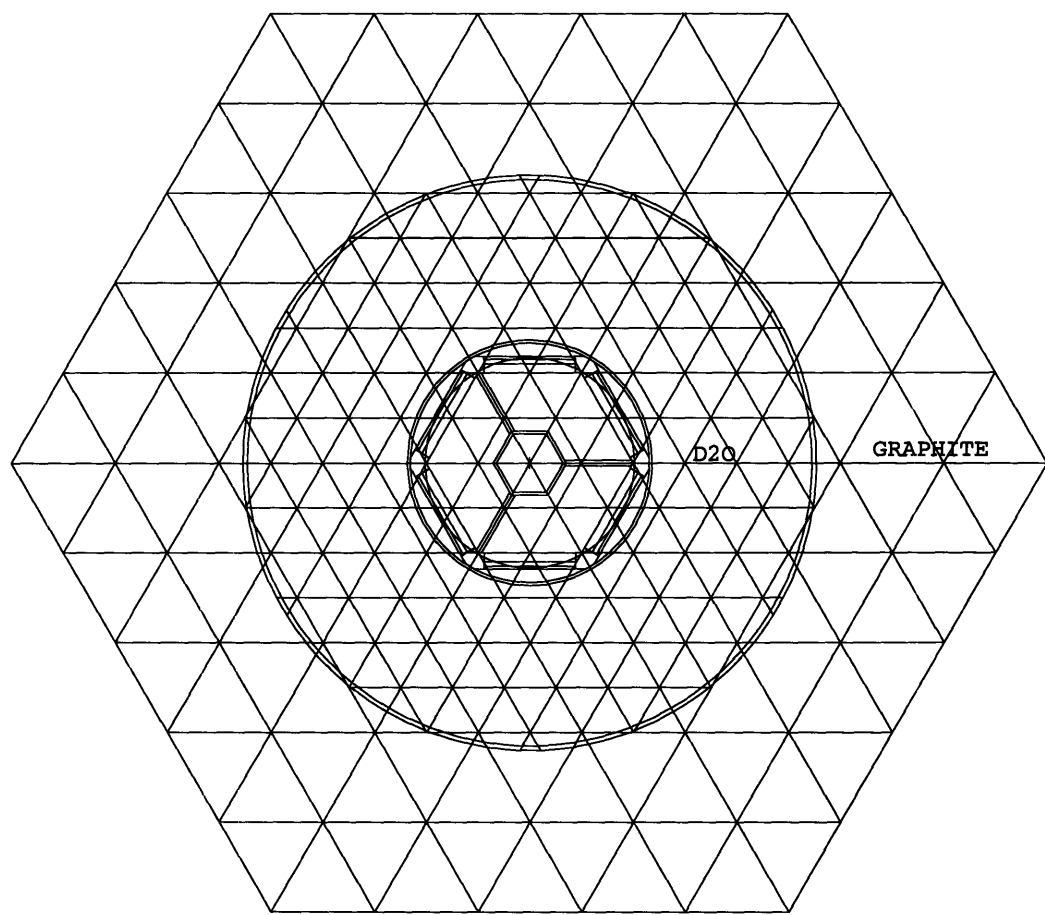
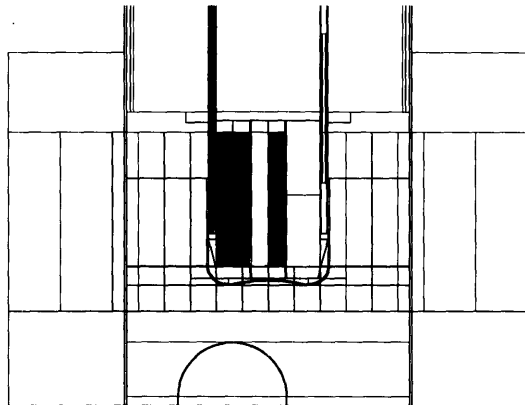


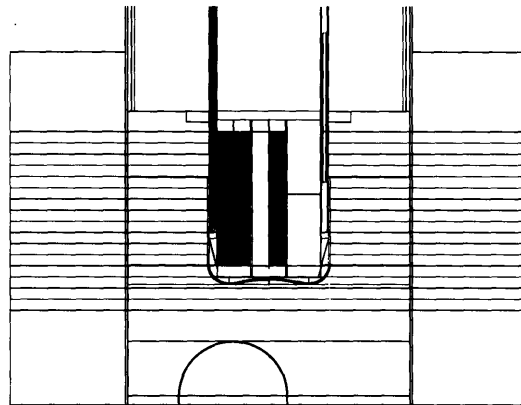
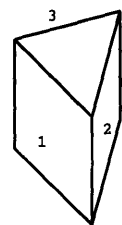
Figure 6-14: Vertical view of MCNP out-of-core model (showing x-z plane at  $y=0$ )



**Figure 6-15:** Cross-sectional view of MCNP supplement model (showing x-y plane at  $z=-28.5$ ; 0.1 cm below the bottom of active fuel)



(a) This model is used for tallying surface fluxes and surface currents for faces 1, 2, and 3, as shown below.



(b) This model is used for tallying surface fluxes and surface currents for faces 4 and 5, as shown below.

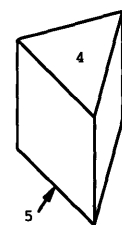


Figure 6-16: Vertical view of MCNP supplement model (showing x-z plane at y=0)

### 6.5.2 Homogenized Cross Sections

The homogenized two-group macroscopic cross sections for a triangular-z node can be computed by the following equation as used by Tari [T-2]:

$$\Sigma_g^j = \frac{\sum_i R_g^i V^{(i,j)}}{\sum_i \phi_g^{(i,j)} V^{(i,j)}}, \quad (6.1)$$

where,

$\Sigma_g^j$  = homogenized cross section for energy group g and triangular-z node j,

$R_g^i$  = MCNP reaction rate per unit volume for cell i,

$V^{(i,j)}$  = volume of the portion of cell i that is in triangular-z node j,

$\phi_g^{(i,j)}$  = MCNP flux density for energy group g and for the portion of cell i in node j.

Note that a triangular-z node-j may contain several cells (i), and in this equation, the reaction rates and fluxes are assumed to be uniform in each cell i.

The homogenized cross sections computed include the total cross sections ( $\Sigma_t$ ), absorption cross sections ( $\Sigma_a$ ), fission cross sections ( $\Sigma_f$ ), and fission neutron production cross sections ( $\nu\Sigma_f$ ). The edited MCNP absorption cross sections do not include the fission cross sections nor the ( $n,2n$ ) reaction cross sections, and the scattering cross sections can not be directly tallied. Two simple methods can be used to reduce the scattering cross sections:

1. Scattering cross sections can be computed from the principle of thermal neutron balance:

In two-group neutron balance equations, the thermal-group formula is as follow:

$$\nabla \cdot \underline{J}_2 + \Sigma_{a2} \phi_2 + \Sigma_{f2} \phi_2 = \Sigma_{21} \phi_1. \quad (6.2)$$

From this equation, the scattering cross section,  $\Sigma_{21}$ , can be easily found as

$$\Sigma_{21}^j = \frac{\int_{V_j} [\nabla \cdot \underline{J}_2 + \Sigma_{a2} \phi_2 + \Sigma_{f2} \phi_2] dV}{\int_{V_j} \phi_1 dV}. \quad (6.3)$$

One can obtain another scattering cross section from the fast-neutron balance equa-

tion, and because of statistical errors and the neglect of n-2n and upscattering event, these two scattering cross sections may not be the same. Since the neglected (n,2n) reaction can occur only in the fast group, it is believed that using the thermal neutron balance will give a better scattering-removal cross section.

2. An artificial method can be used to obtain a unique value of the scattering cross section, by writing the leakage rate from  $V^j$  as proportional to the nodal flux: The two-group neutron balance equations then become

$$\Gamma_1\phi_1 + \Sigma_{a1}\phi_1 + \Sigma_{f1}\phi_1 + \Sigma_{21}\phi_1 = \frac{1}{\lambda}(\nu\Sigma_{f1}\phi_1 + \nu\Sigma_{f2}\phi_2), \quad (6.4)$$

$$\Gamma_2\phi_2 + \Sigma_{a2}\phi_2 + \Sigma_{f2}\phi_2 = \Sigma_{21}\phi_1, \quad (6.5)$$

where  $\int_{V^j} \nabla \cdot \underline{J}_g dV = \Gamma_g \phi_g V^j$  so that  $\Gamma_g$  can be determined, and  $\lambda$  is the critical eigenvalue.

Combining these two equations and solving for  $\Sigma_{21}$ , we obtain

$$\Sigma_{21} = \frac{AB}{C - B}, \quad (6.6)$$

where,

$$A = \Gamma_1 + \Sigma_{a1} + \Sigma_{f1} - \frac{1}{\lambda}\nu\Sigma_{f1},$$

$$B = \Gamma_2 + \Sigma_{a2} + \Sigma_{f2},$$

$$C = \frac{1}{\lambda}\nu\Sigma_{f2}.$$

Since A, B, and C can be edited from the Monte Carlo results, a unique value of  $\Sigma_{21}$  can be found.

### 6.5.3 CMFD Discontinuity Factors

In MCNP, the net currents are tallied on each of five faces of a triangular-z node as shown on Figure 6-17. The directions of the net currents are represented as the arrows on the figure.

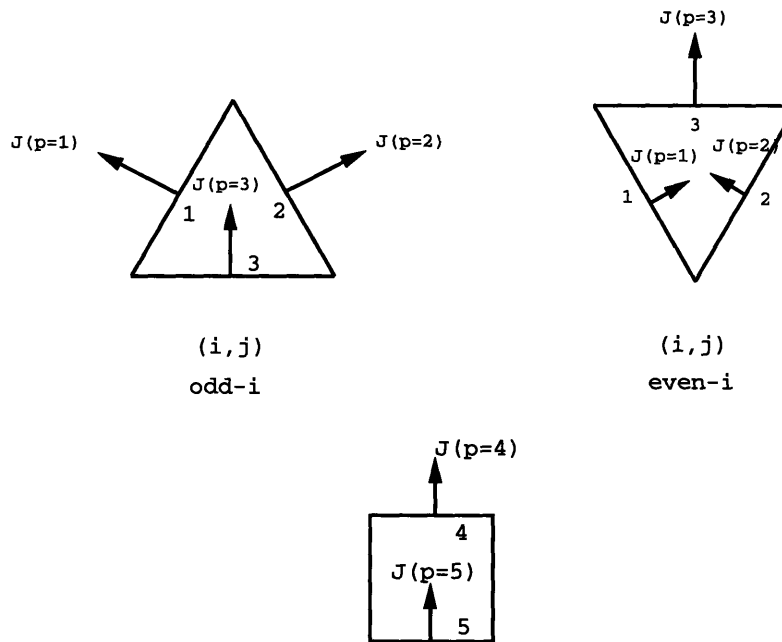


Figure 6-17: MCNP net current on triangular-z nodal faces

According to DeLorey's thesis [D-1], the CMFD discontinuity factors on these five faces can be computed according to the following equations:

$$f_g^{i,j,k}(p) = \frac{\overline{\phi}_g^{i,j,k}(p)}{\overline{\phi}_g^{i,j,k} + \frac{\overline{J}_g^{i,j,k}(p)X_c}{2D_g^{i,j,k}}}, \quad (6.7)$$

(on p=3,4,5 for odd-i nodes, and on p=1,2,4,5 for even-i nodes)

$$f_g^{i,j,k}(p) = \frac{\overline{\phi}_g^{i,j,k}(p)}{\overline{\phi}_g^{i,j,k} - \frac{\overline{J}_g^{i,j,k}(p)X_c}{2D_g^{i,j,k}}}, \quad (6.8)$$

(on p=1,2 for odd-i nodes, and on p=3 for even-i nodes)

where,

- $f_g^{i,j,k}(p)$  = group-g CMFD discontinuity factor on face p and for node (i,j,k),  
 $\bar{\phi}_g^{i,j,k}(p)$  = group-g surface flux on face p and for node (i,j,k),  
 $\overline{\phi}_g^{i,j,k}$  = group-g nodal flux for node (i,j,k),  
 $\bar{J}_g^{i,j,k}(p)$  = group-g net current density on face p and for node (i,j,k),  
 $D_g^{i,j,k}$  = group-g diffusion coefficient for node (i,j,k),  
 $X_c$  = node center-to-center distance.

The diffusion coefficients,  $D_g$ , are arbitrarily set to the inverse of three times the total cross sections. This procedure introduces no error since the discontinuity factors are defined so that reference results will be reproduced for any values of the  $D_g^{i,j,k}$ 's.

#### 6.5.4 Albedo Values

The constants specifying the albedo boundary condition can be obtained by using the MCNP net surface currents and surface fluxes on the boundary faces. Two constants,  $\alpha_g$ , and  $\beta_g$  are related to each other via:

$$\alpha_g \underline{n} \cdot \underline{J}_g = \beta_g \bar{\phi}_g, \quad (6.9)$$

where  $\underline{n}$  is an outward normal to the boundary face.

The form of the nodal equations is such that only the ratios of these two factors are used. Therefore, we can arbitrarily set a value of one constant and find the other one from this equation.

## 6.6 Self-Consistency Tests of the Nodal Parameters

Determination of the nodal parameters from the MCNP output is extremely complicated, particularly for the fuel-region, where homogenized parameters for triangles must be determined from values for the fuel plates making up a rhombic fuel element. Thus it is important to have some tests of the validity of the few-group nodal parameters edited from MCNP. There are two tests which provide a clear indication of the correctness of the few-group parameters:

1. They should be such that, within statistical errors, they yield a few-group nodal solution that obeys neutron balance for each group in each node.
2. The full core eigenvalue and flux distributions should agree (within statistics) with those edited from the Monte Carlo results.

Since the scattering removal cross sections are computed by invoking neutron balance, one might expect that balance to be automatic. However, if the discontinuity factors are incorrect, this will not be the case.

A first cut at determining two-group parameters for MITR-II by the author and Tari has resulted in a set that fails these tests. Reducing to a one-group model (thereby doing away with the negative removal cross section problem) did not alleviate the difficulty.

In doing these checks, two severe problems were encountered:

1. Negative fast-to-thermal group scattering cross sections were found. This phenomenon may be resulted from the statistical fluctuation of the net currents or the absorption cross sections, or from the failure to include up-scattering and n-2n cross sections in two-group neutron balance equations. Replacing the negative values by small positive values led to a nodal solution that failed the two tests.
2. Negative CMFD discontinuity factors were found. The negative CMFD discontinuity factors will result in loss of the diagonal dominance of the matrices used in QUARTZ, which can cause the problem of divergence. One way was found to avoid the negative discontinuity factors, namely to increase arbitrarily the diffusion coefficients so that the factors that cause a match with the reference leakages will be positive.

## **6.7 Summary**

In this Chapter, a procedure for determining the few-group nodal parameters by Monte Carlo methods was described, and the detailed application to MITR-II was outlined. Several MCNP models had to be set up to obtain all the necessary data for deriving the nodal cross sections and CMFD discontinuity factors. However a first attempt to obtain numerical results for MITR-II has not been successful.

To demonstrate that, if the few group parameters are edited correctly from MCNP results, the nodal solution will match that edited from the reference, a much simpler test problem has been set up and analyzed. Results will be described in Chapter 7.

## **Chapter 7**

# **Demonstration of the MCNP-QUARTZ Procedure with a Test Problem**

### **7.1 Introduction**

This Chapter applies the MCNP-QUARTZ computation procedure to a simplified test problem. The demonstration serves as a preliminary validation for the procedure used to prepare nodal parameters for application of the experimental nodal synthesis method to transient analysis of the MITR-II. Section 7.2 describes the demonstration problem; Section 7.3 describes the computation of the two-group nodal parameters for the test problem, and Section 7.4 presents results and discusses the errors.

### **7.2 Description of the Test Problem**

A simplified test problem was devised to demonstrate the MCNP-QUARTZ procedure. The test problem consists of a single layer of 54 triangular-z nodes with three different homogeneous materials: fuel/water mixture,  $D_2O$  reflector, and Al-dummy element. Figure 7-1 shows the configuration of this test problem. The materials are purposely arranged to form an asymmetric configuration. (Note that three assemblies at the bottom of the figure contain fuel rather than  $D_2O$ .) An MCNP model was set up for this problem, and for easy processing the MCNP output, three MCNP cases were run to obtain the nodal fluxes, cross

sections, surface fluxes, and surface currents. For this MCNP model, zero-current boundary conditions were applied to the top and bottom faces and zero incoming current boundary conditions were imposed on the radial faces. Each MCNP case was run using 1000 neutron cycles with 3000 histories per cycle. All the jobs were run on a SUN/SPARC machine. Appendix D collects the input data for these three cases.

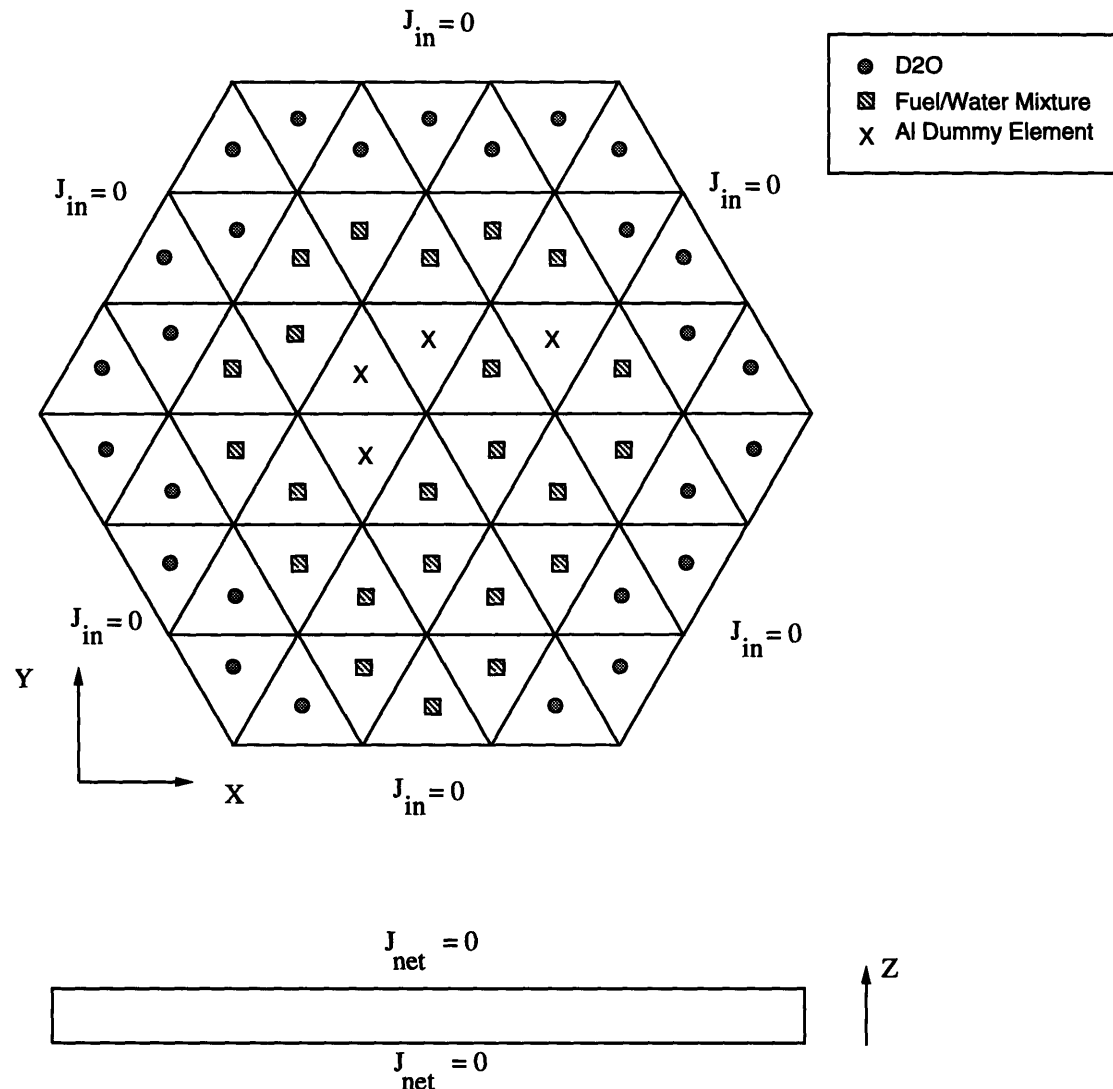


Figure 7-1: Configuration of a demonstration problem for MCNP-QUARTZ computation procedure

### 7.3 Determination of Two-Group Nodal Parameters

The two-group nodal parameters were computed according to the procedures described in Chapter 6. All the statistical errors were recorded along with the derived nodal parameters. CMFD discontinuity factors were computed for three radial faces of a node. The cell fluxes, homogenized cross sections (excluding the scattering cross sections), surface fluxes, surface currents, and CMFD discontinuity factors are all listed in Appendix E.

Three sets of group-1 to group-2 scattering cross sections ( $\Sigma_{21}$ 's) were computed using three different methods:

- Set A:  $\Sigma_{21}$ 's for the fuel and non-fuel region computed from thermal neutron balance.
- Set B:  $\Sigma_{21}$ 's for the fuel region computed from thermal neutron balance;  $\Sigma_{21}$ 's for the non-fuel region computed from fast-neutron balance.
- Set C:  $\Sigma_{21}$ 's for the fuel and non-fuel region computed from the approximate method described by Equation (6.6) in Section 6.5.2.<sup>1</sup>

These three sets of  $\Sigma_{21}$ 's were used, along with other nodal parameters, as QUARTZ input for reproducing the reference MCNP results. Appendix F lists the three sets.

---

<sup>1</sup>For non-fuel region, Equation (6.6) reduces to a form exactly the same as that derived from fast neutron balance.

## 7.4 Results and Analysis

Three QUARTZ cases were set up and tested as listed in Table 7.1. The cases differ in their use of group-to-group scattering cross sections. All three cases were run for the CMFD mode using discontinuity factors that results to match the reference leakages. The computed critical eigenvalues ( $k_{\text{eff}}$ 's) are listed in Table 7.2. As shown in the table, all the  $k_{\text{eff}}$ 's agree with the reference solution within 0.2%.

Table 7.1: QUARTZ test cases for demonstration problem

Case	Scattering Cross Sections Used
A	Set A <sup>a</sup>
B	Set B <sup>b</sup>
C	Set C <sup>c</sup>

<sup>a</sup>All the  $\Sigma_{21}$ 's computed from thermal-neutron balance principle.

<sup>b</sup> $\Sigma_{21}$ 's for the fuel regions computed from thermal-neutron balance; those for the non-fuel regions calculated from fast-neutron balance.

<sup>c</sup>All the  $\Sigma_{21}$ 's computed using the approximate method described in Section 6.5.2

Table 7.2:  $K_{\text{eff}}$  for QUARTZ test cases

Case	$K_{\text{eff}}$	Relative Error (%) <sup>a</sup>
A	1.32969	-0.126
B	1.32933	-0.153
C	1.33118	-0.014

<sup>a</sup>The reference  $K_{\text{eff}}$  from MCNP is 1.33137.

The relative flux errors as compared to the reference MCNP fluxes are shown on Figure 7-2 for case A, on Figure 7-3 for case B, and on Figure 7-4 for case C. For comparison, the statistical uncertainties of the reference MCNP fluxes are plotted on Figure 7-5.

Examination shows that the results of case A and case B are almost the same. The average errors for both cases are around 2% for each energy group. In comparing with the MCNP statistical errors, the errors in the thermal group are within 3 standard deviations except for the two fuel nodes on the lower boundary face. The fast-flux distribution shows a large fluctuation with some errors much higher than 1 standard deviation. Case C, on the

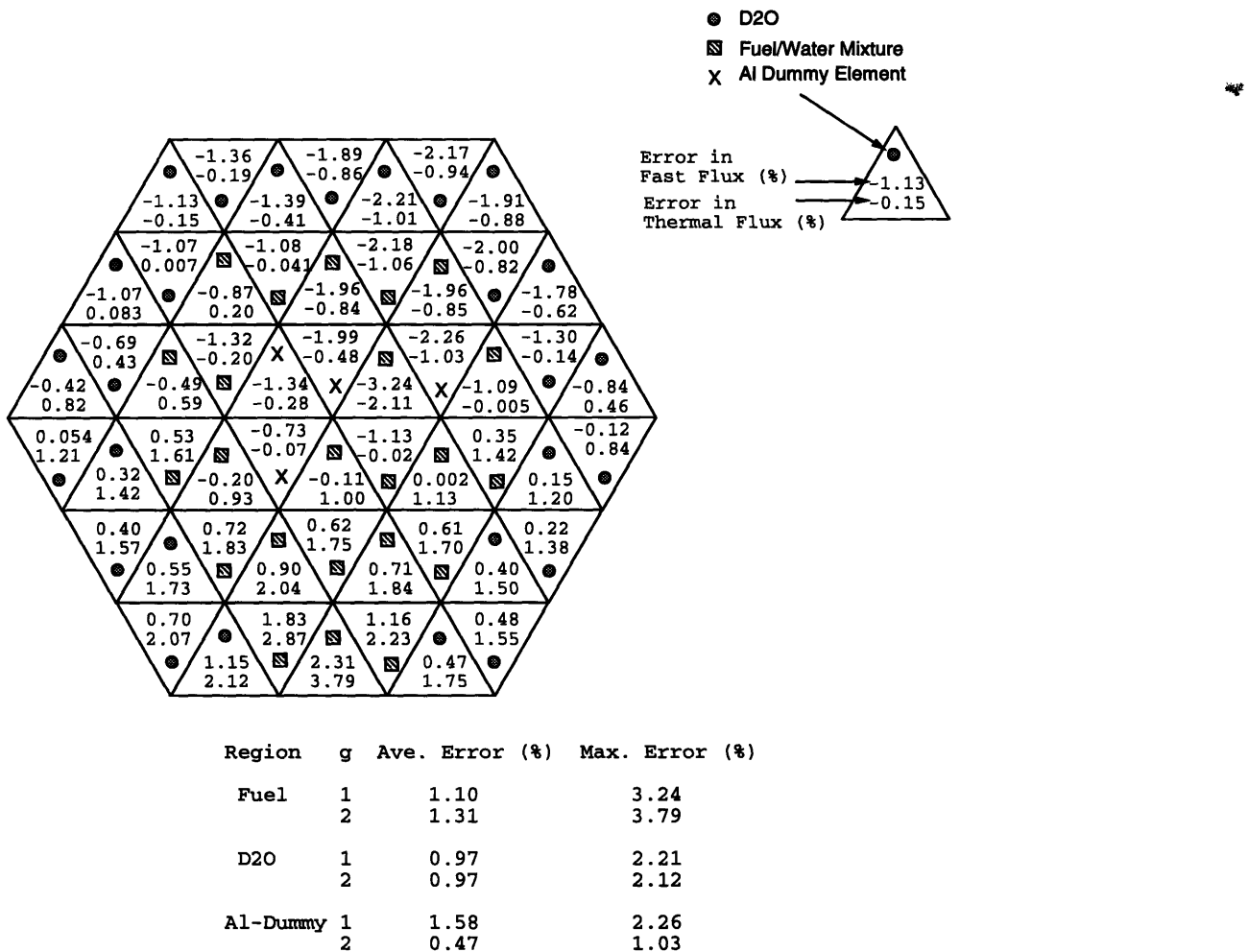


Figure 7-2: Relative error in group-flux for test case A

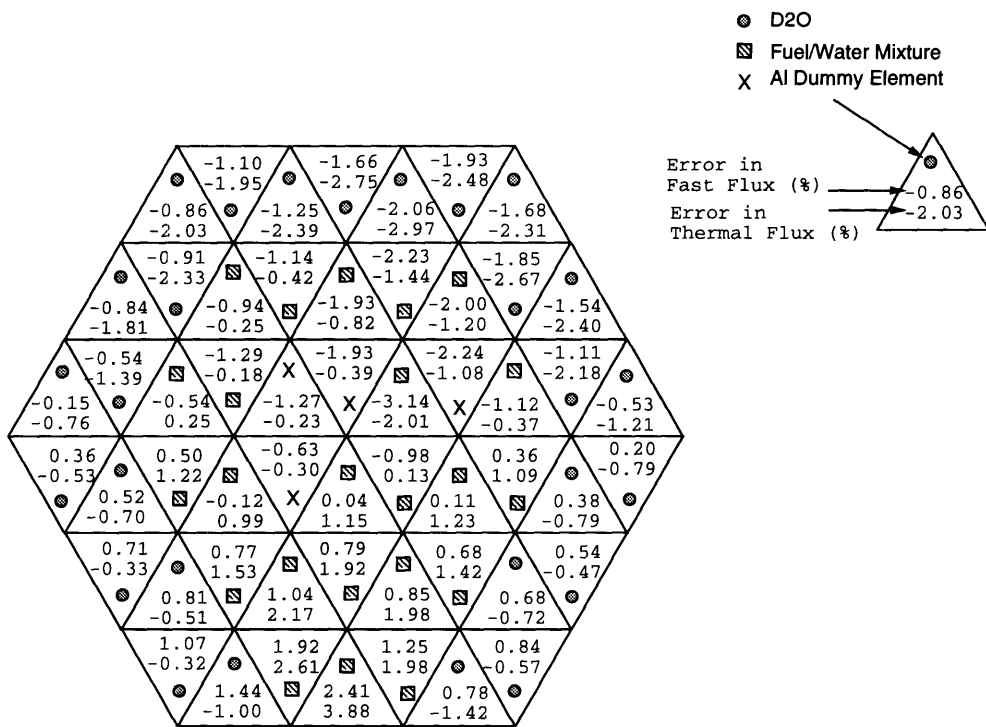
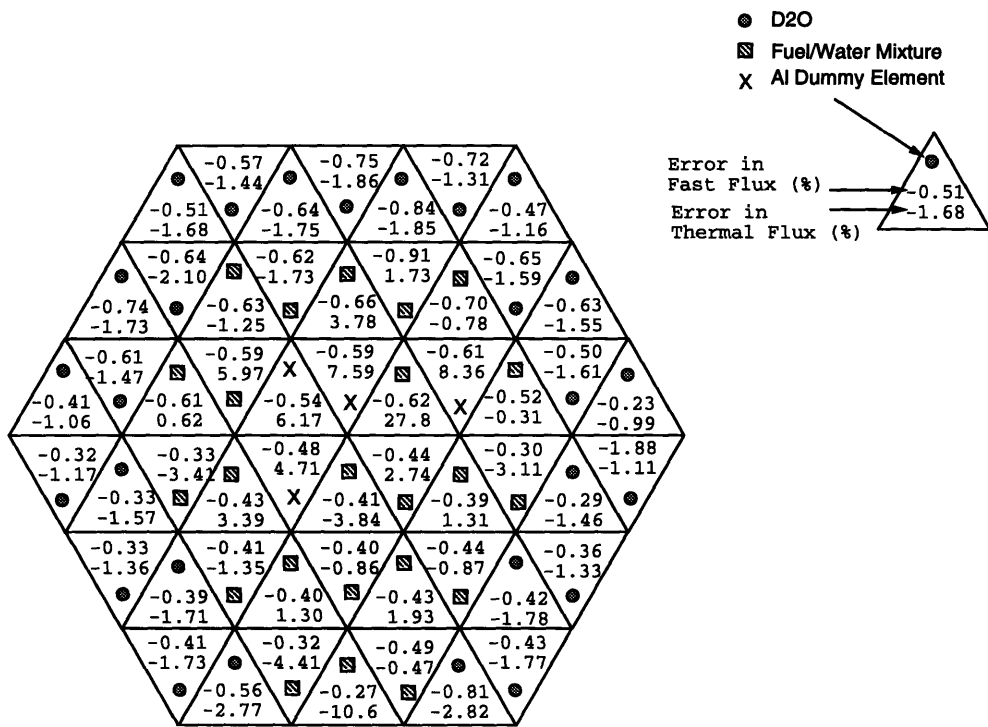


Figure 7-3: Relative error in group-flux for test case B



Region	g	Ave. Error (%)	Max. Error (%)
Fuel	1	0.49	0.91
	2	3.63	27.83
D <sub>2</sub> O	1	0.51	0.85
	2	1.62	2.82
Al-Dummy	1	0.56	0.61
	2	6.71	8.36

Figure 7-4: Relative error in group-flux for test case C

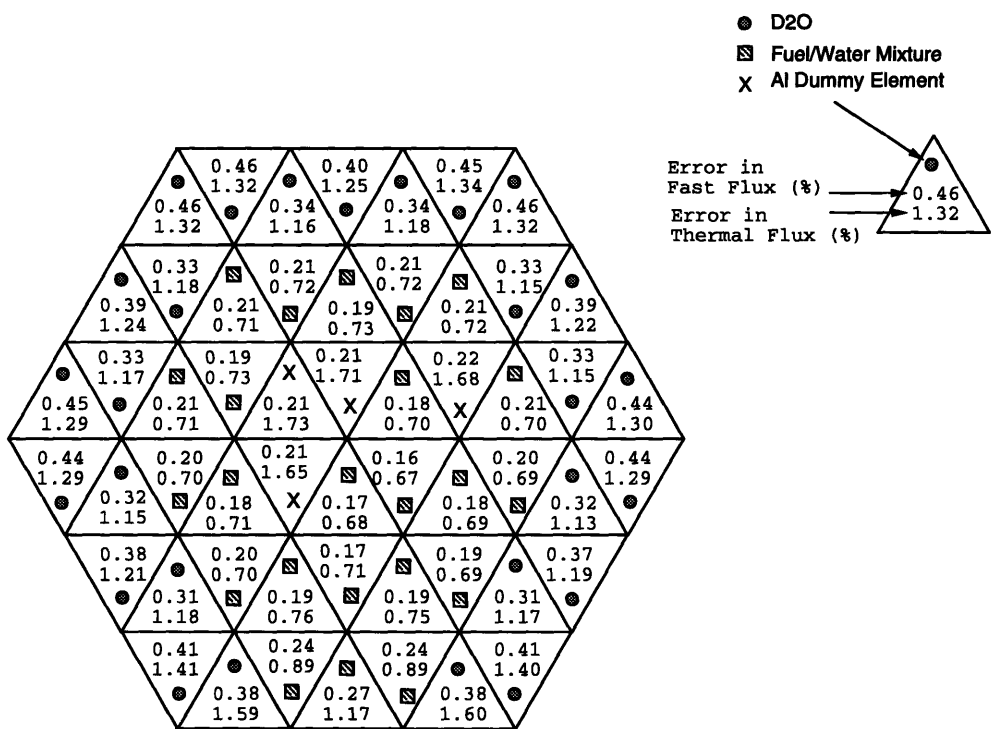


Figure 7-5: Statistical uncertainty in reference MCNP group-flux

other hand, reduces the fast-flux errors but increase the thermal-flux error. All the errors in fast energy group are less than 3 standard deviations with a few exceptions. Large errors in thermal group occur at the nodes close to the center part of the model where Al-dummy elements are located, and at two fuel nodes on the lower boundary face.

It is believed that this incomplete match within the statistical errors of the reference results is due to two factors. The two-group neutron balance equations are overdetermined because there is only one unknown, the scattering-removal cross section, but two equations to be satisfied. Thus, the computed  $\Sigma_{21}$  cross sections may be incorrect. The  $\Sigma_{21}$  found from one of the two neutron balance principles may cause the other equation to lose its balance. The approximate method based on making the leakage rates directly proportional to the nodal fluxes yields only one scattering cross section. However, the procedure becomes ambiguous if the  $\nu\Sigma_{fg}$  are zero, and the computed value of  $\Sigma_{21}$  may be wrong for the thermal group. Unfortunately, at this time, there is no systematic way to find values of the  $\Sigma_{21}$  directly from MCNP tallies.

The imposition of boundary conditions is another factor contributing to error. In QUARTZ, only one boundary condition can be imposed for all the peripheral faces. Accordingly, for our demonstration problem, average boundary condition constants were computed and imposed on all six radial boundary faces. As shown in the configuration map, Figure 7-1, there are three fuel nodes located on the lower side of the hexagonal reactor, while all the other five boundaries of the hexagon are next to a  $D_2O$  reflector. Specifying a single average boundary condition for all six faces will distort the leakage from those three boundary fuel nodes. Figure 7-6 shows the differences between the boundary surface flux to net current ratios and the average of those ratios for each boundary node. Most differences are within 2%. However the fuel node at the lower boundary has a 7.8% difference in the thermal group.

This demonstration problem appears to validate the MCNP-QUARTZ computational procedure. However, a completely unambiguous validation must await an MCNP edit yielding group-to-group scattering cross sections and an extension of QUARTZ permitting different albedo boundary conditions on every external surfaces.

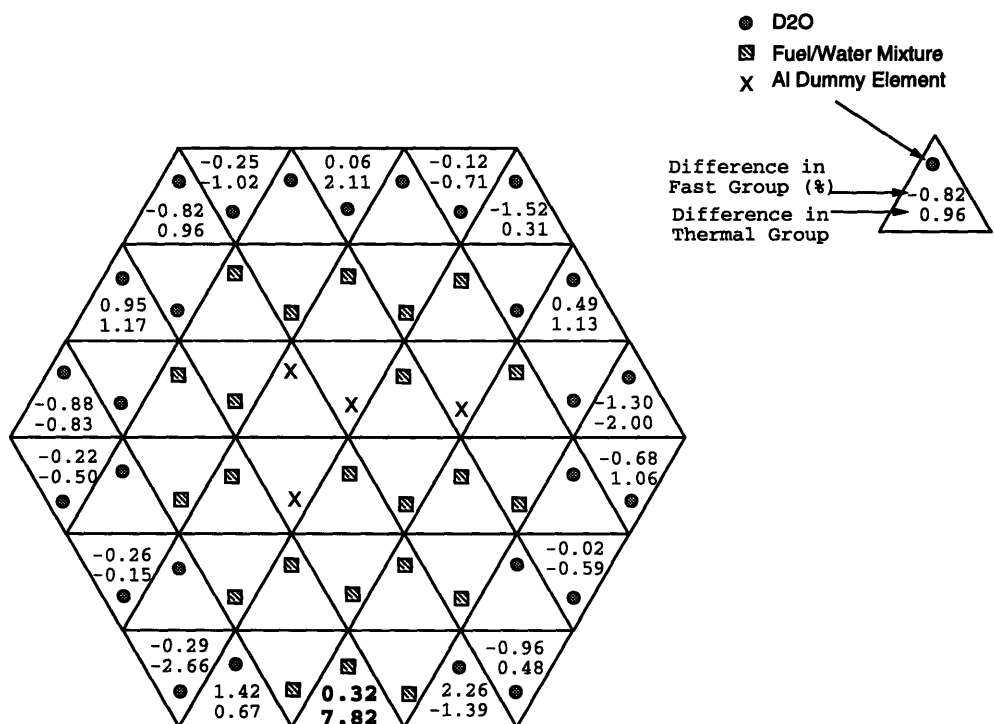


**Figure 7-6: Relative differences between the local boundary condition constants and the average constants**

## **7.5 Summary**

In this Chapter, the MCNP-QUARTZ procedure has been tested by analyzing a simplified problem involving an asymmetric arrangement of three homogeneous materials. The tests have shown that the unique and accurate determination of the group-to-group scattering cross sections is a key factor for the success of this procedure. An accurate treatment of the boundary conditions appears also to be necessary.

## **Chapter 8**

# **Summary, Conclusions, and Recommendations**

### **8.1 Summary**

In this thesis, theoretical and experimental nodal synthesis models have been evaluated. To examine the theoretical nodal synthesis model, a general nodal synthesis procedure and a collapsed-group nodal synthesis scheme were derived from the coarse-mesh finite difference (CMFD) equations corrected by the CMFD discontinuity factors. Two one-dimensional computer codes were constructed and a simple method was devised to update the CMFD discontinuity factors. Several steady-state and transient test cases were run to demonstrate the accuracy and efficiency of the models.

For the experimental nodal synthesis model, emphasis was on the validation of the MCNP-QUARTZ procedure. A detailed procedure was worked out for finding homogenized few-group cross sections and CMFD discontinuity factors for the QUARTZ triangular-z nodes comprising the MITR-II model. Hidden difficulties in determining the deterministic nodal parameters from the statistical results were brought to light, and ways of resolving these difficulties were suggested and tested. Finally, the computational procedure was tested by application to a simple reactor model composed of three homogeneous materials. The importance of finding an unambiguous and accurate method for determining the group-to-group scattering cross sections was demonstrated.

## **8.2 Conclusions**

### **8.2.1 Theoretical Nodal Synthesis Models**

The accuracy of the theoretical nodal synthesis models has been validated against reference results. Numerical tests have shown that the success of the nodal synthesis models relies on the careful choice of bracketing states for generating static expansion functions and proper treatment of the CMFD (Coarse Mesh Finite Difference) discontinuity factors. Physical insights to problems of interest may be a good guide, while intuition may not always work. In addition, updating the CMFD discontinuity factors rather than their ratios by pure synthesis or weighted-average schemes appeared to be the best approach for reproducing reference solutions.

On the other hand, the efficiency of the calculations was found to be inferior to that of the space-dependent, nodal kinetics model. The major reason for this inefficiency was found to be the extensive computing time spent on calculating the elements of iteration matrix. If there are to be practical applications, the efficiency of the nodal synthesis models has to be improved.

### **8.2.2 Experimental Nodal Synthesis Model**

Good statistical behavior and the determination of accurate group-to-group scattering cross sections are two key factors in finding nodal parameters from statistical data such that deterministic nodal models can reproduce reference solutions from statistical models. Once a set of accurate and self-consistent nodal parameters is obtained and the MCNP-QUARTZ procedure is validated completely, the experimental nodal synthesis model can be evaluated properly.

### **8.3 Recommendations for Future Work**

Several recommendations are made for future work:

1. The efficiency of the theoretical nodal synthesis models needs to be improved. A straightforward, brute-force method would be to vectorize or parallelize the synthesis codes. The idea is based on the fact that computing the matrix elements is an independent task. For example, if a system of equations involves a four by four matrix, then using 16 parallel cpu's will reduce the computing time for calculating the matrix elements by a factor of 16.
2. Other systematic ways should be devised to update the CMFD discontinuity factors, and other kinds of nodal synthesis methods should be tested.
3. For the experimental nodal synthesis model, it is important to develop a method to find a set of self-consistent and accurate scattering cross sections from the statistical data. One possible way might be to adjust the thermal cut-off energy arbitrarily until the group-to-group scattering cross sections computed from the fast and thermal equations were consistent.

# References

- [B-1] Brooks, K.W., *Application of the Point Synthesis Method to the Analytic Nodal, Two Group, Multidimensional Neutron Diffusion Equation*, M.S. Thesis, Department of Nuclear Engineering, Massachusetts Institute of Technology, Cambridge, MA (1989).
- [B-2] Briesmeister, J.F., Ed., *MCNP — A General Monte Carlo Code for Neutron and Photon Transport, Version 3A*, LA-7396-M, Rev. 2, Los Alamos National Laboratory (1991).
- [B-3] Briesmeister, J.F., *MCNP3B Newsletter*, Los Alamos National Laboratory (July 18, 1988, revised April 1991)
- [B-4] Briesmeister, J.F., *MCNP4 Newsletter*, Los Alamos National Laboratory (April 4 1991)
- [B-5] Bernard, J.A., Jr., *MITR-II Fuel Management, Core Depletion, and Analysis: Codes Developed for the Diffusion Theory Program CITATION*, N.E./M.S. Thesis, Department of Nuclear Engineering, Massachusetts Institute of Technology, Cambridge, MA (1979).
- [D-1] DeLorey, T.F., *A Transient, Quadratic Nodal Method for Triangular-Z Geometry*, Ph.D. Thesis, Department of Nuclear Engineering, Massachusetts Institute of Technology, Cambridge, MA (1993).
- [D-2] DeLorey, T.F., *Personal Communication*, Department of Nuclear Engineering, Massachusetts Institute of Technology, Cambridge, MA (1993)
- [F-1] Fowler, T.B., Vondy, D.R., and Cunningham G.W., *Nuclear Reactor Core Analysis Code: CITATION*, ORNL-TM-2496, Rev. 2, Oak Ridge National Laboratory (1971).

- [G-1] Gehin, J.C., *A Nodal Method for the Solution of the Static, Few-Group Diffusion Equations in Hexagonal Geometry*, M.S. Thesis, Department of Nuclear Engineering, Massachusetts Institute of Technology, Cambridge, MA (1990).
- [G-2] Golub, G.H., and Van Loan, C.F., *Matrix Computations*, John Hopkins University Press, Baltimore, MD (1989).
- [G-3] Gehin, J.C., *A Quasi-Static Polynomial Nodal Method for Nuclear Reactor Analysis*, Ph.D. Thesis, Department of Nuclear Engineering, Massachusetts Institute of Technology, Cambridge, MA (1992).
- [H-1] Henry, A.F., *Derivation of Nodal Equations Having the Finite-Difference Form*, Course Notes, 22.313, Department of Nuclear Engineering, Massachusetts Institute of Technology, Cambridge, MA (Fall 1989).
- [H-2] Henry, A.F., *Nuclear Reactor Analysis*, MIT Press, Cambridge, MA (1982).
- [H-3] Hansen, K., *Personal Communication*, Department of Nuclear Engineering, Massachusetts Institute of Technology, Cambridge, MA (1992).
- [J-1] Jacqmin, R.P., *A Semi-Experimental Nodal Synthesis Method for the On-Line Reconstruction of Three-Dimensional Neutron Flux-Shapes and Reactivity*, Ph.D. Thesis, Department of Nuclear Engineering, Massachusetts Institute of Technology, Cambridge, MA (1991).
- [K-1] Kaplan, S., *Synthesis Methods in Reactor Analysis*, Advances in Nuclear Science and Technology, P.R. Greebler, Ed., Vol. III, Academic Press, New York, NY (1966).
- [L-1] Lee, K.J., *Application of the Point Synthesis Method to Multidimensional Reactor Transient Analysis*, Ph.D. Thesis, Department of Nuclear Engineering, Massachusetts Institute of Technology, Cambridge, MA (1992).
- [M-1] Moler, C.B., and Stewart, G.W., *An Algorithm for Generalized Matrix Eigenvalue Problems*, SIAM J. Numer. Anal., **10**, pp. 241-256 (1973).
- [M-2] MIT Nuclear Reactor Laboratory and MIT Department of Nuclear Engineering, *Experimental Evaluation of an Instrumented Synthesis Method for the Real-Time*

*Estimation of Reactivity*, Proposal Submitted to the United States Department of Energy (1991).

- [M-3] MIT Reactor Staff, *Facility Description Manual for the MITR-II*, Massachusetts Institute of Technology, Cambridge, MA (1979).
- [P-1] Press, W.H., Flannery, B.P., Teukolsky, S.A., and Vetterling, W.T., *Numerical Recipes in FORTRAN*, Cambridge University Press, New York, NY (1992).
- [R-1] Redmond, E.L., II, Yanch, J.C., and Harling, O.K., *Monte Carlo Simulation of the MIT Research Reactor*, Department of Nuclear Engineering, Massachusetts Institute of Technology, Cambridge, MA (1993).
- [R-2] Redmond, E.L., II, *Monte Carlo Modeling of the MITR-II*, Report from Term Project, Course 22.39, Department of Nuclear Engineering, Massachusetts Institute of Technology, Cambridge, MA (1990).
- [S-1] Smith, K.S., *An Analytical Nodal Method for Solving the Two Group, Multidimensional, Static and Transient Neutron Diffusion Equations*, NE and SM Thesis, Department of Nuclear Engineering, Massachusetts Institute of Technology, Cambridge, MA (1979).
- [S-2] Smith, K.S., *QPANDA : An Advanced Nodal Method for LWR Analyses*, Trans. Am. Nucl. Soc., **50**, 532 (1985).
- [S-3] Stacey, W.M., Jr., *Space-Time Nuclear Reactor Kinetics*, Academic Press, New York, NY (1969).
- [S-4] Strang, G., *Linear Algebra and Its Applications*, Harcourt Brace Jovanovich, Orlando, FL (1988).
- [S-5] Selby, L.C., *Experimental Evaluation of an Instrumented Synthesis Method for the Real-Time Estimation of Reactivity*, N.E./M.S. Thesis, Department of Nuclear Engineering, Massachusetts Institute of Technology, Cambridge, MA (1993).
- [T-1] Tarantino, F.A., *The Development of Cross Sections from Bilinear Variational Theory for Use in Few-Group Transient Analysis*, Ph.D. Thesis, Department of Nuclear Engineering, Massachusetts Institute of Technology, Cambridge, MA (1990).

- [T-2] Tari, I., N.E. Thesis (To be Finished), Department of Nuclear Engineering, Massachusetts Institute of Technology, Cambridge, MA (1993).
- [T-3] Tari, I., *Personal Communication*, Department of Nuclear Engineering, Massachusetts Institute of Technology, Cambridge, MA (1993).
- [V-1] Vota, A.V., Curlee, N.J., Jr., and Henry, A.F., *WIGL3 — A Program for the Steady-State and Transient Solution of the One-Dimensional, Two-Group, Space-Time Diffusion Equations Accounting for Temperature, Xenon, and Control Feedback*, WAPD-TM-788 (1969).
- [Y-1] Yasinsky, J.B., *Numerical Studies of Combined Space-Time Synthesis*, Nucl. Sci. & Eng., **34**, 158 (1968).
- [Z-1] Zerkle, M.L., *Development of a Polynomial Nodal Methods with Flux and Current Discontinuity Factors*, Ph.D. Thesis, Department of Nuclear Engineering, Massachusetts Institute of Technology, Cambridge, MA (1992).

## Appendix A

# CMFD-DF3: A Program to Extract CMFD Discontinuity Factors from the QUANDRY Restart File

### A.1 Introduction

This program is used to extract CMFD discontinuity factors from the QUANDRY restart file. The program reads in the surface currents, surface fluxes, and diffusion coefficients kept in the QUANDRY restart file, computes the CMFD discontinuity factors and writes them to a specific file which is ready to use in synthesis programs SYN1T or SYN1CG.

The structure of QUANDRY restart file is provided in Table A.1, and the flow diagram of CMFD-DF3 is shown in Figure A-1. The CMFD discontinuity factors are computed as

$$f_{gl}^{(-)} = \frac{\bar{\phi}_{gl}^{(-)}}{\bar{\phi}_{gl}} + \frac{h_l}{2\bar{D}_{gl}} \bar{J}_{gl}^{(-)} \quad (\text{A.1})$$

$$f_{gl}^{(+)} = \frac{\bar{\phi}_{gl}^{(+)}}{\bar{\phi}_{gl}} - \frac{h_l}{2\bar{D}_{gl}} \bar{J}_{gl}^{(+)} \quad (\text{A.2})$$

where,

- $f_{gl}^{(u)}$  = discontinuity factor on the left-hand face ( $u=-$ ),  
 or right-hand face ( $u=+$ ) of node  $l$ ,  
 $\bar{\phi}_{gl}^{(u)}$  = surface flux on the left-hand face ( $u=-$ ),  
 or right hand-face ( $u=+$ ) of node  $l$ ,  
 $\bar{J}_{gl}^{(u)}$  = surface current on the left-hand face ( $u=-$ ),  
 or right-hand face ( $u=+$ ) of node  $l$ ,  
 $\bar{\bar{\phi}}_{gl}$  = volume-averaged flux in node  $l$ ,  
 $\bar{D}_{gl}$  = diffusion coefficient of node  $l$ ,  
 $h_l$  = node height in the axial direction.

Table A.1: Structure of the QUANDRY restart file

Record	Content
1	Neutron multiplication factor ( $k_{\text{eff}}$ )
2	Nodal cross sections
3	Nodal fluxes
4	Nodal surface currents
5	Nodal surface fluxes

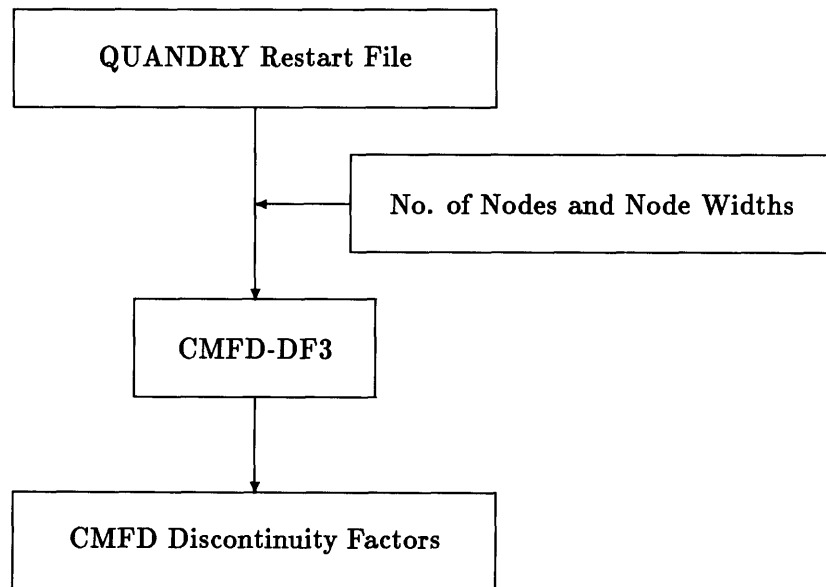


Figure A-1: Flow diagram of CMFD-DF3

## A.2 Program Listing of CMFD-DF3

**WIN=10**

```

OPEN(UNIT=NIN,FILE='CMFD-DF.INP',STATUS='OLD')
READ(NIN,1)FNAME
1 FORMAT(A32)
READ(NIN,1)DFNAME
READ(NIN,*)NX,NY,NZ,NXYZ
READ(NIN,*)(HX(I),I=1,NX)
READ(NIN,*)(HY(J),J=1,NY)
READ(NIN,*)(HZ(K),K=1,NZ)
READ(NIN,*)IDIF
IF (IDIF .GT. 0) READ(NIN,1)DIFFIL
C
PRINT 500,FNAME,DFNAME,NX,NY,NZ,NXYZ
500 FORMAT(//9X,'QUANDRY RESTART FILE NAME:',A32,/,
+         9X,'DISCONTINUITY-FACTOR FILE NAME:',A32,/,
+         9X,'NX =',I6,/,
+         9X,'NY =',I6,/,
+         9X,'NZ =',I6,/,
+         9X,'TOTAL # OF NODES =',I6)
C
PRINT 501,(HX(I),I=1,NX)
501 FORMAT(//9X,'NODE WIDTH (X-DIRECTED')/,
+ 6(1X,1PE12.5))
PRINT 502,(HY(J),J=1,NY)
502 FORMAT(//9X,'NODE WIDTH (Y-DIRECTED')/,
+ 6(1X,1PE12.5))
PRINT 503,(HZ(K),K=1,NZ)
503 FORMAT(//9X,'NODE WIDTH (Z-DIRECTED')/,
+ 6(1X,1PE12.5))
C
IF (IDIF .GT. 0) PRINT 504,DIFFIL
504 FORMAT(//9X,'DIFFUSION-COEFFICIENT FILE NAME:',A32)
C
OPEN(UNIT=NSCR,FILE=FNAME,STATUS='OLD',
+ FORM='UNFORMATTED')
REWIND NSCR
READ(NSCR)XKEFF
READ(NSCR)((XS(I,J),I=1,14),J=1,NXYZ)
READ(NSCR)((FLUX(I,J),I=1,2),J=1,NXYZ)
READ(NSCR)((CUR(I,J),I=1,12),J=1,NXYZ)
READ(NSCR)((PHI(I,J),I=1,12),J=1,NXYZ)
C
PRINT 510,XKEFF
510 FORMAT(/9X,'REFERENCE K-EFFECTIVE = ',F11.7)
PRINT 2
2 FORMAT(//9X,'CROSS SECTIONS BY NODE',//)
CALL PRINTB(XS,NX,NY,NZ,NX,NY,NZ,14)
C
PRINT 3

```

```

3   FORMAT(//9X,'NODE-AVERAGED FLUXES BY NODE',//)
CALL PRINTB(FLUX,NX,NY,NZ,NX,NY,NZ,2)

C
PRINT 4
4   FORMAT(//9X,'SURFACE CURRENTS BY NODE',//)
CALL PRINTB(CUR,NX,NY,NZ,NX,NY,NZ,12)

C
PRINT 5
5   FORMAT(//9X,'SURFACE FLUXES BY NODE',//)
CALL PRINTB(PHI,NX,NY,NZ,NX,NY,NZ,12)

C
DO 10 N=1,NXYZ
DX(1,N)=XS(1,N)
DX(2,N)=XS(6,N)
DY(1,N)=XS(11,N)
DY(2,N)=XS(12,N)
DZ(1,N)=XS(13,N)
DZ(2,N)=XS(14,N)

10 CONTINUE

C
DO 15 N=1,NXYZ
IP=0
DO 20 L=1,11,2
IP=IP+1
SURFC(1,IP,N)=CUR(L,N)
SURFF(1,IP,N)=PHI(L,N)

20 CONTINUE
IP=0
DO 25 L=2,12,2
IP=IP+1
SURFC(2,IP,N)=CUR(L,N)
SURFF(2,IP,N)=PHI(L,N)

25 CONTINUE
15 CONTINUE

C
DO 30 K=1,NZ
HK=HZ(K)
DO 30 J=1,NY
HJ=HY(J)
DO 30 I=1,NX
HI=HX(I)
N=(K-1)*NX*NY+(J-1)*NX+I
DO 30 IG=1,2
IF (DX(IG,N).NE.0.0 .AND. DY(IG,N).NE.0.0 .AND.
+ DZ(IG,N).NE.0.0) THEN
DENOM1=FLUX(IG,N)+HI/(2.0*DX(IG,N))*SURFC(IG,1,N)
DFAC(IG,1,N)=SURFF(IG,1,N)/DENOM1
DENOM2=FLUX(IG,N)-HI/(2.0*DX(IG,N))*SURFC(IG,2,N)

```

```

DFAC(IG,2,N)=SURFF(IG,2,N)/DENOM2
DENOM3=FLUX(IG,N)+HJ/(2.0*DY(IG,N))*SURFC(IG,3,N)
DFAC(IG,3,N)=SURFF(IG,3,N)/DENOM3
DENOM4=FLUX(IG,N)-HJ/(2.0*DY(IG,N))*SURFC(IG,4,N)
DFAC(IG,4,N)=SURFF(IG,4,N)/DENOM4
DENOM5=FLUX(IG,N)+HK/(2.0*DZ(IG,N))*SURFC(IG,5,N)
DFAC(IG,5,N)=SURFF(IG,5,N)/DENOM5
DENOM6=FLUX(IG,N)-HK/(2.0*DZ(IG,N))*SURFC(IG,6,N)
DFAC(IG,6,N)=SURFF(IG,6,N)/DENOM6
ENDIF
30 CONTINUE
C
DO 40 N=1,NXYZ
  I=0
DO 40 IP=1,6
DO 40 IG=1,2
  I=I+1
  DF(I,N)=DFAC(IG,IP,N)
40 CONTINUE
C
OPEN(UNIT=60,FILE=DFNAME,STATUS='NEW',FORM='UNFORMATTED')
WRITE(60)NXYZ
WRITE(60)((DF(I,N),I=1,12),N=1,NXYZ)
C
IF (IDIF .GT. 0) THEN
  OPEN(UNIT=70,FILE=DIFFIL,STATUS='NEW',
+      FORM='UNFORMATTED')
  WRITE(70)NXYZ
  WRITE(70)((XS(I,J),I=1,14),J=1,NXYZ)
  CLOSE(UNIT=70)
ENDIF
C
PRINT 6
6 FORMAT(//9X,'CMFD DISCONTINUITY FACTORS BY NODE',//)
CALL PRINTB(DF,NX,NY,NZ,NX,NY,NZ,12)
C
CLOSE(UNIT=NIN)
CLOSE(UNIT=NSCR)
CLOSE(UNIT=60)
C
STOP
END
SUBROUTINE PRINTB (A,NX,NY,NZ,N1,N2,N3,II)
C
DIMENSION A(II,N1,N2,N3)
C
C      MULTI-PURPOSE PRINTER
C      FIRST THREE ARGUMENTS ARE EDIT BOUNDS

```

```

C      SECOND THREE ARGUMENTS ARE ARRAY DIMENSIONS
C      LAST ARGUMENT IS THE NUMBER OF 'THINGS' PRINTED PER NODE
C
DO 300 K=1,NZ
PRINT 1000,K
1000 FORMAT (//,8X,'PLANE # ',I3)
IF (NZ.EQ.1) GO TO 50
IF (K.EQ.1 .AND. IDIM.NE.2) PRINT 1100
IF (K.EQ.NZ .AND. IDIM.NE.2) PRINT 1200
50 CONTINUE
NEND=0
c   NNOW=(NX-.5)/11.+1
NNOW=(NX-.5)/ 6.+1
DO 100 I=1,NNOW
c   NEND=NEND+11
NEND=NEND+6
c   NSTART=NEND-10
NSTART=NEND-5
NEND=MIN0(NEND,NX)
DO 200 J=1,NY
PRINT 500
NROW=NY-J+1
PRINT 2000,NROW,(A(1,L,NY-J+1,K),L=NSTART,NEND)
IF (II.EQ.1) GO TO 200
DO 99 M=2,II
PRINT 3000,(A(M,L,NY-J+1,K),L=NSTART,NEND)
99 CONTINUE
200 CONTINUE
PRINT 4000,(L,L=NSTART,NEND)
100 CONTINUE
300 CONTINUE
C
500 FORMAT (' ',2X)
1100 FORMAT (8X,'BOTTOM')
1200 FORMAT (8X,' TOP ')
c2000 FORMAT (6X,' Y =',I3,1X,(1P11E11.4))
2000 FORMAT (6X,' Y =',I3,1X,(1P6E11.4))
c3000 FORMAT (14X,(1P11E11.4))
3000 FORMAT (14X,(1P6E11.4))
c4000 FORMAT (/,5X,'          X = ',I3,10(8X,I3))
4000 FORMAT (/,5X,'          X = ',I3,5(8X,I3))
RETURN
END

```

## **Appendix B**

# **ZFXBC: A Program to Extract Zero-Flux Boundary Correction Factors from the QUANDRY Restart File**

### **B.1 Introduction**

This program is used to extract zero-flux boundary correction factors from the QUANDRY restart file. The program reads in the surface currents, surface fluxes, and diffusion coefficients kept in the QUANDRY restart file, computes the zero-flux boundary correction factors, and writes them to a specific file which is ready to use in synthesis programs SYN1T or SYN1CG. The flow diagram of ZFXBC is shown in Figure B-1.

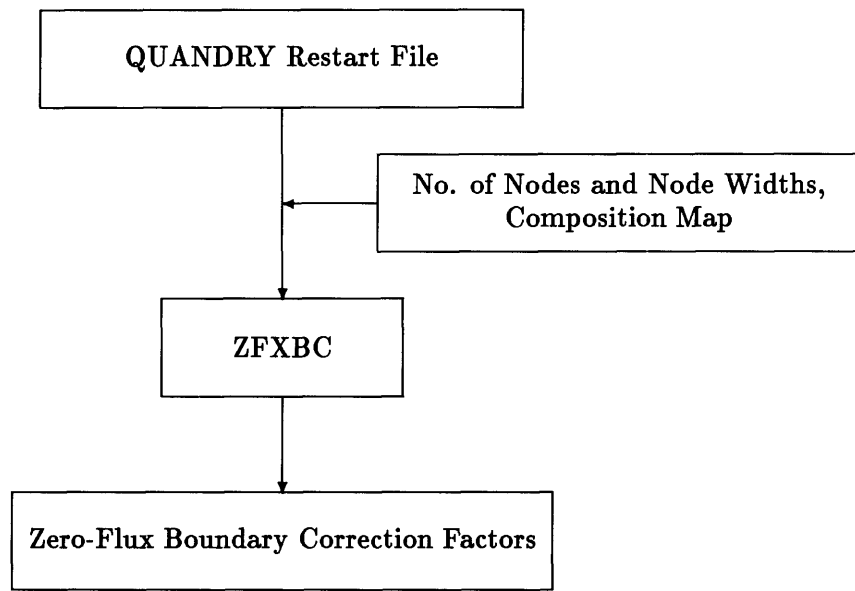


Figure B-1: Flow diagram of ZFXBC

## B.2 Program listing of ZFXBC

```
COMMON MAP(20,20,25),MAPCMP(20,20,25),NX,NY,NZ,NX2,NY2,NZ2,
+ NX,NYY,NZZ,IDLIM,ISTRTX(20),IENDX(20),ISTRTRY(20),IENDY(20),
+ ISX(20),IEX(20),ISY(20),IEY(20),IBCXL,IBCXU,IBCYL,IBCYU,
+ IBCZL,IBCZU,NXYZ,HX(20),HY(20),HZ(25)
COMMON XS(14,5000),FLUX(2,5000),CUR(12,5000),SURFC(2,6,5000),
+ DX(2,5000),DY(2,5000),DZ(2,5000)
DIMENSION IASSGN(100),ICUTX(100),ICUTY(100),IROW(100)
CHARACTER*32 FNAME1,FNAME2

C
C THIS PROGRAM IS USED TO EDIT OUT ZERO FLUX BOUNDARY CONDITION CORRECTION
C FACTOR, GOF (I.E. GAMMA OVER F) FROM QUANDRY RESTART FILE.
C
NIN=10
NOUT=11
NSCR=20
NBCC=21
C IDIM=3
OPEN(UNIT=NIN,FILE='ZFXBCC.INP',STATUS='OLD')
OPEN(UNIT=NOUT,FILE='ZFXBCC.OUT',STATUS='NEW')
C
READ(NIN,*)IDLIM,NX,NY,NZ
READ(NIN,*)(HX(I),I=1,NX)
READ(NIN,*)(HY(J),J=1,NY)
READ(NIN,*)(HZ(K),K=1,NZ)
READ(NIN,*)IBCXL,IBCXU,IBCYL,IBCYU,IBCZL,IBCZU
READ(NIN,1)FNAME1
READ(NIN,1)FNAME2
1 FORMAT(A32)
C
C OPEN RESTART FILE
C
OPEN(UNIT=NSCR,FILE=FNAME1,STATUS='OLD',
+ FORM='UNFORMATTED')
C
C OPEN ZERO-FLUX BOUNDARY CORRECTION-FACTOR FILE
C
OPEN(UNIT=NBCC,FILE=FNAME2,STATUS='NEW',
+ FORM='UNFORMATTED')
C
NX1=NX+1
NY1=NY+1
NZ1=NZ+1
NX2=NX+2
NY2=NY+2
NZ2=NZ+2
```

```

KPLANE=IDIM-1
ISET=1
IF (IDIM .EQ. 2) ISET=0
NXYZ=NX*NY*NZ
C
      WRITE(NOUT,1000)IDIM,NX,NY,NZ,NXYZ
1000 FORMAT(//9X,'PROBLEM DIMENSION          = ',I6,/
+           9X,'NO. OF NODES IN X-DIRECTION = ',I6,/
+           9X,'NO. OF NODES IN Y-DIRECTION = ',I6,/
+           9X,'NO. OF NODES IN Z-DIRECTION = ',I6,/
+           9X,'TOTAL NO. OF NODES       = ',I6)
      WRITE(NOUT,90)(HX(I),I=1,NX)
      WRITE(NOUT,91)(HY(J),J=1,NY)
      WRITE(NOUT,92)(HZ(K),K=1,NZ)
90   FORMAT(//9X,'NODE WIDTH (X-DIRECTED)',/, 
+        (9X,6(1PE12.5)))
91   FORMAT(//9X,'NODE WIDTH (Y-DIRECTED)',/, 
+        (9X,6(1PE12.5)))
92   FORMAT(//9X,'NODE WIDTH (Z-DIRECTED)',/, 
+        (9X,6(1PE12.5)))
      WRITE(NOUT,1001)IBCXL,IBCXU,IBCYL,IBCYU,IBCZL,IBCZU
1001 FORMAT(//9X,'BOUNDARY CONDITIONS X-LOWER = ',I6,' (0-ZERO FLUX)', 
+           /9X,'          X-UPPER = ',I6,' (1-ZERO CURRENT)' 
+           ,/,9X,'          Y-LOWER = ',I6,' (2-ALBEDO)', 
+           /9X,'          Y-UPPER = ',I6, 
+           /9X,'          Z-LOWER = ',I6, 
+           /9X,'          Z-UPPER = ',I6)
      WRITE(NOUT,1002)FNAME1,FNAME2
1002 FORMAT(//9X,'QUANDRY RESTART FILE NAME:          ',A32,/, 
+           9X,'FILE NAME FOR ZERO-FLUX BOUNDARY CORRECTORS:',A32)
C
C
C      READ COMPOSITION MAP
C      READ THE NUMBER OF UNIQUE PLANES
C
      READ (NIN,7000) NUNQPL
C
C      # OF NODES PER COMP X DIRECTION
C
      READ (NIN,7000) NCUTX,(ICUTX(I),I=1,NCUTX)
C
C      # OF NODES PER COMP Y DIRECTION
C
      READ (NIN,7000) NCUTY,(ICUTY(I),I=1,NCUTY)
C
C      SPLIT UP MESH AND ASSIGN PLANES
C
      DO 900 KKK=1,NUNQPL

```

```

READ (NIN,7000) NPLANE,(IASSGN(I),I=1,NPLANE)
KSET=IASSGN(1)
NXNOW=NCUTX+2
NTOTY=0
J=0
123 J=J+1
IF (J.GT.NY2) GO TO 501
READ (NIN,7000) (IROW(I),I=1,NXNOW)
IROW(NX2)=IROW(NXNOW)
NN=NXNOW-2
NXTOT=0
C
DO 200 II=1,NN
ICOMP=IROW(NXNOW-II)
IC=ICUTX(NCUTX-II+1)
DO 100 IICUT=1,IC
IROW(NX2-NXTOT-IICUT)=ICOMP
100 CONTINUE
NXTOT=NXTOT+IC
200 CONTINUE
C
J=J-1
IF (J.EQ.0 .OR. J.EQ.(NY2-1)) ICY=1
C
DO 400 JJ=1,ICY
J= J + 1
DO 300 I=1,NX2
MAP(I,NY2-J+1,KSET)=IROW(I)
300 CONTINUE
400 CONTINUE
C
NTOTY=NTOTY+1
IF (NTOTY.GT.NCUTY) GO TO 500
ICY=ICUTY(NCUTY-NTOTY+1)
500 GO TO 123
501 CONTINUE
IF (NPLANE.EQ.1) GO TO 900
C
DO 800 KK=2,NPLANE
K2=IASSGN(KK)
DO 700 J2=1,NY2
DO 600 I2=1,NX2
MAP(I2,J2,K2)=MAP(I2,J2,KSET)
600 CONTINUE
700 CONTINUE
800 CONTINUE
C
900 CONTINUE

```

```

C
7000 FORMAT (6X,11I6)
  NCARD=NCARD+1
C      PRINT 8000
  WRITE(NOUT,8000)
C
  CALL PRINTC(MAP,NX2,NY2,NZ2,20,20,25,1,IDIM)
  8000 FORMAT (/,9X,'REACTOR COMPOSITION MAP ')
C
C
C DO GEOMETRY PROCESSING
C
  CALL GEOM
C
C
C SET REACTOR ORIENTED COMP. MAP FOR LATER USE
C
  DO 3200 K=KPLANE,NZ1
  DO 3100 J=2,NY1
    IS=ISTRX(J)+1
    IE=IENDX(J)-1
    DO 3000 I=IS,IE
      MAPCMP(I-1,J-1,K-ISET)=MAP(I,J,K)
  3000 CONTINUE
  3100 CONTINUE
  3200 CONTINUE
C
  CALL PRINTC(MAPCMP,NX,NY,NZ,20,20,25,1,IDIM)
C
C
C READ XS, NODE-AVERAGED FLUX, SURFACE CURRENTS FROM RESTART FILE
C
  CALL READAT
C
C
C EDIT ZERO FLUX BC CORRECTION FACTORS, GOF
C
  CALL ZFXBCC
C
  CLOSE(UNIT=NIN)
  CLOSE(UNIT=NOUT)
  CLOSE(UNIT=NSCR)
  CLOSE(UNIT=NBCC)
C
  STOP
  END
C-----

```

SUBROUTINE PRINTC (A,NX,NY,NZ,N1,N2,N3,II,IDL)

```

INTEGER A
DIMENSION A(II,N1,N2,N3)
DATA NOUT/11/

C
C      MULTI-PURPOSE PRINTER FOR INTEGER MAPS
C      FIRST THREE ARGUMENTS ARE EDIT BOUNDS
C      SECOND THREE ARGUMENTS ARE ARRAY DIMENSIONS
C      LAST ARGUMENT IS THE NUMBER OF 'THINGS' PRINTED PER NODE
C

DO 300 K=1,NZ
C     IF (K.EQ.1) PRINT 1000,K
C     IF (K.NE.1) PRINT 1001,K
C     IF (K.EQ.1) WRITE(NOUT,1000)K
C     IF (K.NE.1) WRITE(NOUT,1001)K
C
1000 FORMAT (    /4X,'PLANE # ',I3)
1001 FORMAT (    /4X,'PLANE # ',I3)
     IF (NZ.EQ.1) GO TO 50
C     IF (K.EQ.1 .AND. IDIM.NE.2) PRINT 1100
C     IF (K.EQ.NZ .AND. IDIM.NE.2) PRINT 1200
C     IF (K.EQ.1 .AND. IDIM.NE.2) WRITE(NOUT,1100)
C     IF (K.EQ.NZ .AND. IDIM.NE.2) WRITE(NOUT,1200)

50 CONTINUE
NEND=0
NNOW=(NX-.5)/30.+1
DO 100 I=1,NNOW
NEND=NEND+30
NSTART=NEND-29
NEND=MIN0(NEND,NX)
DO 200 J=1,NY
NROW=NY-J+1
C     PRINT 2000,NROW,(A(1,L,NY-J+1,K),L=NSTART,NEND)
C     WRITE(NOUT,2000)NROW,(A(1,L,NY-J+1,K),L=NSTART,NEND)
     IF (II.EQ.1) GO TO 200
     DO 99 M=2,II
C     PRINT 3000,(A(M,L,NY-J+1,K),L=NSTART,NEND)
C     WRITE(NOUT,3000)(A(M,L,NY-J+1,K),L=NSTART,NEND)
99 CONTINUE
200 CONTINUE
C     PRINT 4000,(L,L=NSTART,NEND)
C     WRITE(NOUT,4000)(L,L=NSTART,NEND)
100 CONTINUE
300 CONTINUE
1100 FORMAT (4X,'BOTTOM   ')
1200 FORMAT (4X,' TOP'  )
2000 FORMAT (2X,'Y=',I3,1X,(31I4))
3000 FORMAT (08X,(31I4))

```

```

4000 FORMAT (1X,'      X = ',I3,31(1X,I3))
      RETURN
      END
C-----
C----- SUBROUTINE GEOM
C
COMMON MAP(20,20,25),MAPCMP(20,20,25),NX,NY,NZ,NX2,NY2,NZ2,
+ NX,NYY,NZZ,IDLIM,ISTRRTX(20),IENDX(20),ISTRRTY(20),IENDY(20),
+ ISX(20),IEX(20),ISY(20),IEY(20),IBCXL,IBCXL,IBCYL,IBCYL,
+ IBCZL,IBCZU,NXYZ,HX(20),HY(20),HZ(25)
C
C      DETERMINE THE STARTING AND ENDING POINTS FOR EACH ROW AND COLUM
C      TO ELIMINATE THE NEED TO SWEEP EMPTY NODES IN A JAGGED REACTOR
C
C      ALBEDO ORIENTED          REACTOR ORIENTED
C
C      ISTRRTX                  ISX
C      ISTRRTY                  ISY
C      IENDX                     IEY
C      IENDY                     IEY
C
C      DATA NOUT/11/
C
KPLANE=IDLIM-1
NX1=NX+1
NY1=NY+1
DO 400 J=2,NY1
DO 100 I=1,NX2
IF (MAP(I,J,KPLANE).LE.0) GO TO 100
C
C      ALBEDO ORIENTED
C
ISTRRTX(J)=I-1
C
C      REACTOR ORIENTED
C
ISX(J-1)=I-1
GO TO 200
100 CONTINUE
200 DO 300 I=1,NX2
IF (MAP(NX2-I+1,J,KPLANE).LE.0) GO TO 300
IENDX(J)=NX2-I+2
IEX(J-1)=NX2-I
GO TO 400
300 CONTINUE
400 CONTINUE
DO 800 I=2,NX1
DO 500 J=1,NY2

```

```

IF (MAP(I,J,KPLANE).LE.0) GO TO 500
ISTRTY(I)=J-1
ISY(I-1)=J-1
GO TO 600
500 CONTINUE
600 DO 700 J=1,NY2
    IF (MAP(I,NY2-J+1,KPLANE).LE.0) GO TO 700
    IENDY(I)=NY2-J+2
    IEY(I-1)=NY2-J
    GO TO 800
700 CONTINUE
800 CONTINUE
C     IF (JPRINT.LT.4) RETURN
C     PRINT 2000
     WRITE(NOUT,2000)
2000 FORMAT (1H1,T20,'ALBEDO ORIENTED',/ ,T20,'ROW #',T30,'ISTART X',T40,
     X 'IEND X',//)
     DO 900 J=1,NY2
C     PRINT 2100,J,ISTRTX(J),IENDX(J)
     WRITE(NOUT,2100)J,ISTRTX(J),IENDX(J)
900 CONTINUE
C     PRINT 2200
     WRITE(NOUT,2200)
2200 FORMAT (//20X,'COL #',T30,'ISTART Y',T40,'IEND Y'//)
2100 FORMAT (20X,I3,T33,I3,T43,I3)
     DO 1000 I=1,NX2
C     PRINT 2100,I,ISTRTY(I),IENDY(I)
     WRITE(11,2100)I,ISTRTY(I),IENDY(I)
1000 CONTINUE
C     PRINT 2300
     WRITE(NOUT,2300)
2300 FORMAT (1H1,T20,'REACTOR ORIENTED',/ ,T20,'ROW #',T30,'ISTRX X',
     X T40,'IEND X',//)
     DO 1200 J=1,NY
C     PRINT 2100,J,ISX(J),IEX(J)
     WRITE(NOUT,2100)J,ISX(J),IEX(J)
1200 CONTINUE
C     PRINT 2200
     WRITE(NOUT,2200)
     DO 1300 I=1,NX
C     PRINT 2100,I,ISY(I),IEY(I)
     WRITE(NOUT,2100)I,ISY(I),IEY(I)
1300 CONTINUE
     RETURN
     END
C-----
SUBROUTINE ZFBCC
COMMON MAP(20,20,25),MAPCMP(20,20,25),NX,NY,NZ,NX2,NY2,NZ2,

```

```

+ NXX,NYY,NZZ,NDIM,ISTRTRX(20),IENDX(20),ISTRTRY(20),IENDY(20),
+ ISI(20),IEX(20),ISY(20),IEY(20),IBCXL,IBCXU,IBCYL,IBCYU,
+ IBCZL,IBCZU,NXYZ,HX(20),HY(20),HZ(25)
COMMON XS(14,5000),FLUX(2,5000),CUR(12,5000),SURFC(2,6,5000),
+ DX(2,5000),DY(2,5000),DZ(2,5000)

C
COMMON/ZFXBCF/GOF(12,5000)

C
C GOF - GAMMA OVER F
C      (=FLUX/CUR-H/(2D) FOR RHS; =-(FLUX/CUR+H/(2D)) FOR LHS)
C
C      DATA NOUT/11/,NBCC/21/
C
C      NXBC=0
C      NYBC=0
C      NZBC=0
C
C      SWEEP THROUGH X-DIRECTION
C
DO 100 K=1,NZ
  HK=HZ(K)
DO 100 J=1,NY
  HJ=HY(J)
DO 100 I=1,NX
  HI=HX(I)
  N=(K-1)*NX*NY+(J-1)*NX+I
C
C      X - LOWER  (FACE 1, OR X-)
C
IF (I .EQ. ISX(J)) THEN
  JJ=J+1
  KK=K+1
  II=ISTRTRX(JJ)
  IF (MAP(II,JJ,KK) .EQ. 0 .AND. IBCXL .EQ. 0) THEN
    WRITE(NOUT,900)
    WRITE(NOUT,1000)I,J,K,MAPCMP(I,J,K),II,JJ,KK,
+      MAP(II,JJ,KK),N
    NXBC=NXBC+1
    GOF(1,N)=-(FLUX(1,N)/CUR(1,N)+HI/(2.0*DX(1,N)))
    GOF(2,N)=-(FLUX(2,N)/CUR(2,N)+HI/(2.0*DX(2,N)))
  ENDIF
ENDIF
C
C      X - UPPER  (FACE 2, OR X+)
C
IF (I .EQ. IEX(J)) THEN
  JJ=J+1
  KK=K+1

```

```

II=IEENDX(JJ)
IF (MAP(II,JJ,KK) .EQ. 0 .AND. IBCXU .EQ. 0) THEN
    WRITE(NOUT,910)
    WRITE(NOUT,1010)I,J,K,MAPCMP(I,J,K),II,JJ,KK,
+        MAP(II,JJ,KK),N
    NXBC=NXBC+1
    GOF(3,N)=FLUX(1,N)/CUR(3,N)-HI/(2.0*DX(1,N))
    GOF(4,N)=FLUX(2,N)/CUR(4,N)-HI/(2.0*DX(2,N))
ENDIF
ENDIF
100 CONTINUE
WRITE(NOUT,1015)NXBC
C
900 FORMAT(/9X,'X-LOWER BOUNDARY INFORMATION')
1000 FORMAT(/9X,'REACTOR-ORIENTED COORDINATES:      I,J,K = ',3I4,/,
+         9X,'COMPOSITION NUMBER                      = ',I4,/,
+         9X,'LHS ALBEDO-ORIENTED COORDINATES: II,JJ,KK = ',3I4,/,
+         9X,'LHS BOUNDARY CONDITION NUMBER           = ',I4,/,
+         9X,'NODE NUMBER IS = ',I4)
910 FORMAT(/9X,'X-UPPER BOUNDARY INFORMATION')
1010 FORMAT(/9X,'REACTOR-ORIENTED COORDINATES:      I,J,K = ',3I4,/,
+         9X,'COMPOSITION NUMBER                      = ',I4,/,
+         9X,'RHS ALBEDO-ORIENTED COORDINATES: II,JJ,KK = ',3I4,/,
+         9X,'RHS BOUNDARY CONDITION NUMBER           = ',I4,/,
+         9X,'NODE NUMBER IS = ',I4)
1015 FORMAT(/9X,'TOTAL # OF X-DIRECTED BOUNDARY CONDITION = ',I4)
C
C SWEEP THROUGH Y-DIRECTION
C
DO 200 K=1,NZ
    HK=HZ(K)
DO 200 I=1,NX
    HI=HX(I)
DO 200 J=1,NY
    HJ=HY(J)
    N=(K-1)*NX*NY+(J-1)*NX+I
C
C     Y - LOWER (FACE 3, OR Y-)
C
IF (J .EQ. ISY(I)) THEN
    II=I+1
    KK=K+1
    JJ=ISTRTRY(II)
    IF (MAP(II,JJ,KK) .EQ. 0 .AND. IBCYL .EQ. 0) THEN
        WRITE(NOUT,920)
        WRITE(NOUT,1000)I,J,K,MAPCMP(I,J,K),II,JJ,KK,
+            MAP(II,JJ,KK),N
        NYBC=NYBC+1

```

```

        GOF(5,N)=-(FLUX(1,N)/CUR(5,N)+HJ/(2.0*DY(1,N)))
        GOF(6,N)=-(FLUX(2,N)/CUR(6,N)+HJ/(2.0*DY(2,N)))
    ENDIF
ENDIF

C
C      Y - UPPER (FACE 4, OR Y+)
C
IF (J .EQ. IEY(I)) THEN
    II=I+1
    KK=K+1
    JJ=IENDY(II)
    IF (MAP(II,JJ,KK) .EQ. 0 .AND. IBCYU .EQ. 0) THEN
        WRITE(NOUT,930)
        WRITE(NOUT,1010)I,J,K,MAPCMP(I,J,K),II,JJ,KK,
+
        MAP(II,JJ,KK),N
        NYBC=NYBC+1
        GOF(7,N)=FLUX(1,N)/CUR(7,N)-HJ/(2.0*DY(1,N))
        GOF(8,N)=FLUX(2,N)/CUR(8,N)-HJ/(2.0*DY(2,N))
    ENDIF
ENDIF
200 CONTINUE
WRITE(NOUT,1025)NYBC
C
920 FORMAT(/9X,'Y-LOWER BOUNDARY INFORMATION')
930 FORMAT(/9X,'Y-UPPER BOUNDARY INFORMATION')
1025 FORMAT(/9X,'TOTAL # OF Y-DIRECTED BOUNDARY CONDITION = ',I4)
C
C BOTTOM & TOP PLANES
C
DO 300 J=1,NY
C DO 300 I=ISX(J),IEX(J)
DO 300 I=1,NX
    N1=(J-1)*NX+I
    N2=(NZ-1)*NX*NY+(J-1)*NX+I
    IF (I .LT. ISX(J) .OR. I .GT. IEY(J)) GO TO 300
    II=I+1
    JJ=J+1
C
C      Z - LOWER (FACE 5, OR Z-)
C
    IF (MAP(II,JJ,1) .EQ. 0 .AND. IBCZL .EQ. 0) THEN
        WRITE(NOUT,940)
        KK = 1
        K = 2
        WRITE(NOUT,1000)I,J,K,MAPCMP(I,J,K),II,JJ,KK,
+
        MAP(II,JJ,KK),N1
        NZBC=NZBC+1
        HK=HZ(1)

```

```

      GOF(9,N1)=-(FLUX(1,N1)/CUR(9,N1)+HK/(2.0*DZ(1,N1)))
      GOF(10,N1)=-(FLUX(2,N1)/CUR(10,N1)+HK/(2.0*DZ(2,N1)))
      ENDIF
C
C      Z - UPPER (FACE 6, OR Z+)
C
      IF (MAP(II,JJ,NZ2) .EQ. 0 .AND. IBCZU .EQ. 0) THEN
      WRITE(NOUT,950)
      KK=NZ2
      K=NZ
      WRITE(NOUT,1010)I,J,K,MAPCMP(I,J,K),II,JJ,KK,
+      MAP(II,JJ,KK),N2
      NZBC=NZBC+1
      HK=HZ(NZ)
      GOF(11,N2)=FLUX(1,N2)/CUR(11,N2)-HK/(2.0*DZ(1,N2))
      GOF(12,N2)=FLUX(2,N2)/CUR(12,N2)-HK/(2.0*DZ(2,N2))
      ENDIF
300  CONTINUE
      WRITE(NOUT,1030)NZBC
C
      940 FORMAT(/9X,'Z-LOWER BOUNDARY INFORMATION')
      950 FORMAT(/9X,'Z-UPPER BOUNDARY INFORMATION')
C
      1030 FORMAT(/9X,'TOTAL # OF Z-DIRECTED BOUNDARY CONDITION = ',I4)
C
      WRITE(NOUT,1040)
      1040 FORMAT(//9X,'ZERO-FLUX BOUNDARY CORRECTORS BY NODE',//)
      CALL PRINTB(GOF,NX,NY,NZ,NX,NY,NZ,12,IDIM)
C
      WRITE(NBCC)NXYZ
      WRITE(NBCC)((GOF(I,N),I=1,12),N=1,NXYZ)
C
      RETURN
      END
C-----
      SUBROUTINE READAT
      COMMON MAP(20,20,25),MAPCMP(20,20,25),NX,NY,NZ,NX2,NY2,NZ2,
+ NX2,NY2,NZ2,IDLIM,ISTRTRX(20),IENDX(20),ISTRRTY(20),IENDY(20),
+ ISX(20),IEX(20),ISY(20),IEY(20),IBCXL,IBCXU,IBCYL,IBCYU,
+ IBCZL,IBCZU,NXYZ,HX(20),HY(20),HZ(25)
      COMMON XS(14,5000),FLUX(2,5000),CUR(12,5000),SURFC(2,6,5000),
+ DX(2,5000),DY(2,5000),DZ(2,5000)
      DATA NSCR/20/,NOUT/11/
C
      REWIND NSCR
      READ(NSCR)XKEFF
      READ(NSCR)((XS(I,J),I=1,14),J=1,NXYZ)
      READ(NSCR)((FLUX(I,J),I=1,2),J=1,NXYZ)

```

```

READ(NSCR)((CUR(I,J),I=1,12),J=1,NXYZ)
C
      WRITE(NOUT,510)XKEFF
 510 FORMAT(//9X,'REFERENCE K-EFFECTIVE = ',F11.7)
C
      WRITE(NOUT,2)
 2  FORMAT(//9X,'CROSS SECTIONS BY NODE',//)
      CALL PRINTB(XS,NX,NY,NZ,NX,NY,NZ,14,IDIM)
C
      WRITE(NOUT,3)
 3  FORMAT(//9X,'NODE-AVERAGED FLUXES BY NODE',//)
      CALL PRINTB(FLUX,NX,NY,NZ,NX,NY,NZ,2,IDIM)
C
      WRITE(NOUT,4)
 4  FORMAT(//9X,'SURFACE CURRENTS BY NODE',//)
      CALL PRINTB(CUR,NX,NY,NZ,NX,NY,NZ,12,IDIM)
C
      DO 10 N=1,NXYZ
          DX(1,N)=XS(1,N)
          DX(2,N)=XS(6,N)
          DY(1,N)=XS(11,N)
          DY(2,N)=XS(12,N)
          DZ(1,N)=XS(13,N)
          DZ(2,N)=XS(14,N)
 10   CONTINUE
C
      DO 15 N=1,NXYZ
          IP=0
          DO 20 L=1,11,2
              IP=IP+1
              SURFC(1,IP,N)=CUR(L,N)
 20   CONTINUE
          IP=0
          DO 25 L=2,12,2
              IP=IP+1
              SURFC(2,IP,N)=CUR(L,N)
 25   CONTINUE
 15   CONTINUE
C
      RETURN
      END
C-----  

      SUBROUTINE PRINTB (A,NX,NY,NZ,N1,N2,N3,II,IDIM)
C
      DIMENSION A(II,N1,N2,N3)
      DATA NOUT/11/
C
      MULTI-PURPOSE PRINTER

```

```

C      FIRST THREE ARGUMENTS ARE EDIT BOUNDS
C      SECOND THREE ARGUMENTS ARE ARRAY DIMENSIONS
C      LAST ARGUMENT IS THE NUMBER OF 'THINGS' PRINTED PER NODE
C
C      DO 300 K=1,NZ
C      PRINT 1000,K
C      WRITE(NOUT,1000)K
1000 FORMAT (//,8X,'PLANE # ',I3)
      IF (NZ.EQ.1) GO TO 50
C      IF (K.EQ.1 .AND. IDIM.NE.2) PRINT 1100
C      IF (K.EQ.NZ .AND. IDIM.NE.2) PRINT 1200
      IF (K.EQ.1 .AND. IDIM.NE.2) WRITE(NOUT,1100)
      IF (K.EQ.NZ .AND. IDIM.NE.2) WRITE(NOUT,1200)
50 CONTINUE
      NEND=0
c      NNOW=(NX-.5)/11.+1
      NNOW=(NX-.5)/ 6.+1
      DO 100 I=1,NNOW
c      NEND=NEND+11
      NEND=NEND+6
c      NSTART=NEND-10
      NSTART=NEND-5
      NEND=MIN0(NEND,NX)
      DO 200 J=1,NY
C      PRINT 500
      WRITE(NOUT,500)
      NROW=NY-J+1
C      PRINT 2000,NROW,(A(1,L,NY-J+1,K),L=NSTART,NEND)
      WRITE(NOUT,2000)NROW,(A(1,L,NY-J+1,K),L=NSTART,NEND)
      IF (II.EQ.1) GO TO 200
      DO 99 M=2,II
C      PRINT 3000,(A(M,L,NY-J+1,K),L=NSTART,NEND)
      WRITE(NOUT,3000)(A(M,L,NY-J+1,K),L=NSTART,NEND)
99 CONTINUE
200 CONTINUE
C      PRINT 4000,(L,L=NSTART,NEND)
      WRITE(NOUT,4000)(L,L=NSTART,NEND)
100 CONTINUE
300 CONTINUE
C
      500 FORMAT (' ',2X)
      1100 FORMAT (8X,'BOTTOM')
      1200 FORMAT (8X,' TOP ')
c2000 FORMAT (6X,' Y =',I3,1X,(1P11E11.4))
      2000 FORMAT (6X,' Y =',I3,1X,(1P6E11.4))
c3000 FORMAT (14X,(1P11E11.4))
      3000 FORMAT (14X,(1P6E11.4))
c4000 FORMAT (/,5X,'      X = ',I3,10(8X,I3))

```

```
4000 FORMAT (/,5X,'          X = ',I3,5(8X,I3))
RETURN
END
```

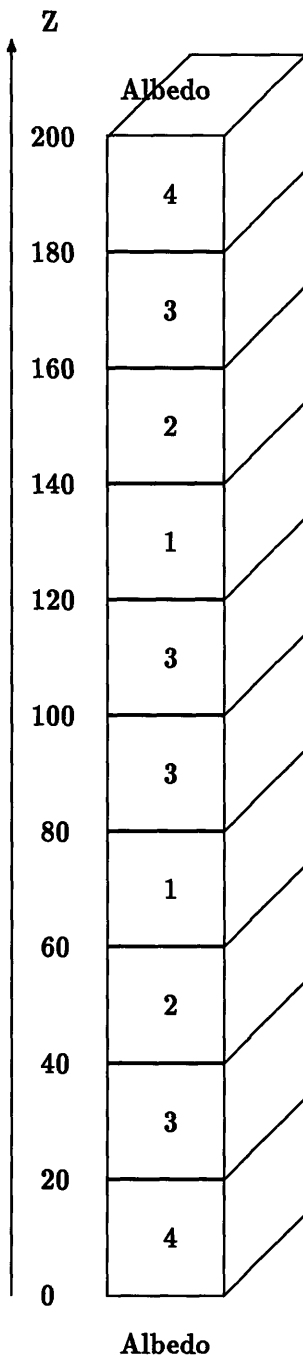
## **Appendix C**

# **Test Problem Specifications for the Theoretical Nodal Synthesis Models**

- C.1 Steady-State Variable Inlet Coolant Temperature Problem**
- C.2 Steady-State Variable Rod-Position Problem 1 – Fully-Rodded Case**
- C.3 Steady-State Variable Rod-Position Problem 2 – Partially-Rodded Case**
- C.4 Transient Variable Inlet Coolant Temperature Problem**

## C.1 Steady-State Variable Inlet Coolant Temperature Problem

Geometry:



**Material Properties:**

Composition	Group, g	$D_g \text{ (cm)}$	$\Sigma_g \text{ (cm}^{-1}\text{)}$	$\nu\Sigma_{fg} \text{ (cm}^{-1}\text{)}$	$\Sigma_{21} \text{ (cm}^{-1}\text{)}$
1	1	1.36480	0.026132	0.005550	0.017245
	2	0.48260	0.130772	0.185823	
2	1	1.36030	0.025603	0.006267	0.015942
	2	0.47760	0.169403	0.229195	
3	1	1.35720	0.025151	0.006894	0.014752
	2	0.47400	0.206951	0.268552	
4	1	1.39330	0.021484	0.000000	0.017943
	2	0.36590	0.068149	0.000000	

**Boundary Condition:**

Group, g	$\alpha_g$	$\beta_g$
1	1.00	0.25
2	1.00	0.25

**WIGL Thermal-Hydraulic Parameters:**

$$\begin{aligned}
 C_c &= 5.43 \times 10^7 \text{ erg/g/K} \\
 W_r &= 8.0166 \times 10^4 \text{ g/s} \\
 h_0 &= 3.293 \times 10^7 \text{ erg/cm}^2/\text{s/K} \\
 A_h &= 3.097 \text{ cm}^{-1} \\
 V_c/(V_c + V_f) &= 0.542 \\
 r &= 0.026 \\
 \text{Pressure} &= 1.551 \times 10^7 \text{ Pa}
 \end{aligned}$$

**Macroscopic Cross Section Derivatives:**

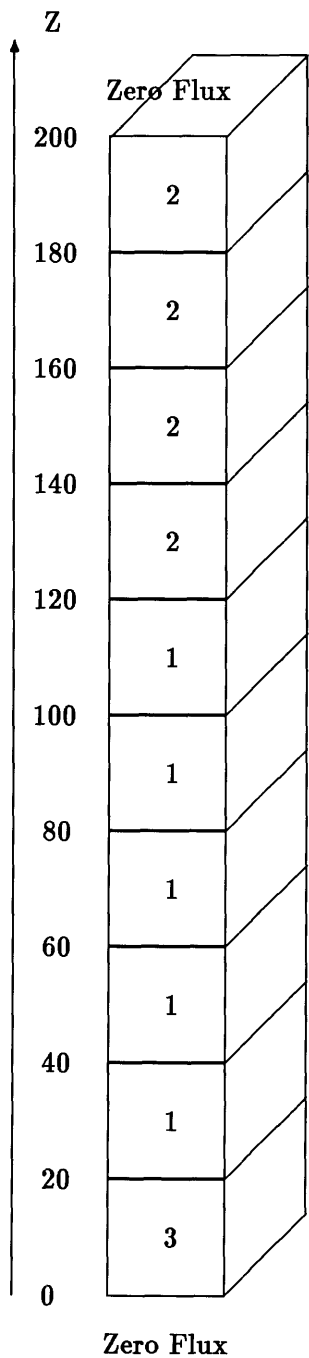
Parameter, $\Sigma$	$\frac{\partial \Sigma}{\partial \rho_c}$	$\frac{\partial \Sigma}{\partial T_c}$	$\frac{\partial \Sigma}{\partial T_f}$
$D_1^{-1}$	+0.41	$-8.0 \times 10^{-5}$	$-6.6 \times 10^{-6}$
$D_2^{-1}$	+2.70	$-1.3 \times 10^{-3}$	$-2.6 \times 10^{-6}$
$\Sigma_{c1}$	$+2.83 \times 10^{-3}$	$+3.0 \times 10^{-6}$	$+3.3 \times 10^{-7}$
$\Sigma_{c2}$	$+1.40 \times 10^{-2}$	$-8.2 \times 10^{-6}$	$-3.8 \times 10^{-7}$
$\nu \Sigma_{f1}$	+0.0	+0.0	+0.0
$\nu \Sigma_{f2}^\dagger$	$+4.250 \times 10^{-2}$	$-2.075 \times 10^{-5}$	$-2.500 \times 10^{-6}$
$\Sigma_{f1}$	+0.0	+0.0	+0.0
$\Sigma_{f2}^\dagger$	$+1.7 \times 10^{-2}$	$-8.3 \times 10^{-6}$	$-1.0 \times 10^{-6}$
$\Sigma_{21}$	$+2.4 \times 10^{-2}$	$-1.5 \times 10^{-6}$	$-8.5 \times 10^{-8}$

†Zero for reflector materials (composition 4)

$$\begin{aligned}
 \rho_0 &= 0.7961 \text{ g/cm}^3 \\
 \bar{T}_{f0} &= 533 \text{ K} \\
 \bar{T}_{c0} &= 533 \text{ K}
 \end{aligned}$$

## C.2 Steady-State Variable Rod-Position Problem 1 – Fully-Rodded Case

Geometry:



**Material Properties:**

Composition	Group, g	$D_g$ (cm)	$\Sigma_g$ (cm $^{-1}$ )	$\nu\Sigma_{fg}$ (cm $^{-1}$ )	$\Sigma_{21}$ (cm $^{-1}$ )
1	1	1.42390	0.027960	0.006478	0.017560
	2	0.35630	0.087660	0.112700	
2	1	1.42390	0.028510 <sup>a</sup>	0.006478	0.017560
	2	0.35630	0.091460 <sup>b</sup>	0.112700	
3	1	1.63420	0.030260	0.000000	0.027600
	2	0.35060	0.099260	0.000000	

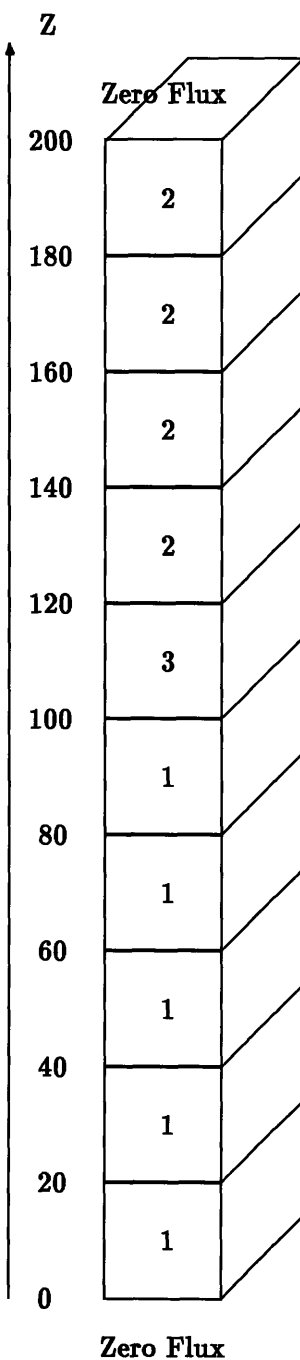
<sup>a</sup> $\Sigma_{a1}$  increases by 5.29% as compared with composition 1.

<sup>b</sup> $\Sigma_{a2}$  increases by 4.33% as compared with composition 1.

**Reactor Power: 15 MW<sub>t</sub>**

### C.3 Steady-State Variable Rod-Position Problem 2 – Partially-Rodded Case

Geometry:



**Material Properties:**

Composition	Group, g	$D_g$ (cm)	$\Sigma_g$ (cm $^{-1}$ )	$\nu\Sigma_{fg}$ (cm $^{-1}$ )	$\Sigma_{21}$ (cm $^{-1}$ )
1	1	1.5130	0.03323	0.006012	0.02113
	2	0.3950	0.16840	0.218600	
2	1	1.4630	0.03422 <sup>a</sup>	0.004633	0.02129
	2	0.3772	0.19210 <sup>b</sup>	0.170700	
3 <sup>c</sup>	1	—	—	—	—
	2	—	—	—	

<sup>a</sup> $\Sigma_{a1}$  increases by 6.86% as compared with composition 1.

<sup>b</sup> $\Sigma_{a2}$  increases by 14.1% as compared with composition 1.

<sup>c</sup>Partially-rodded node.

**WIGL Thermal-Hydraulic Parameters:**

$$C_c = 5.43 \times 10^7 \text{ erg/g/K}$$

$$W_r = 8.0166 \times 10^4 \text{ g/s}$$

$$h_0 = 3.293 \times 10^7 \text{ erg/cm}^2/\text{s/K}$$

$$A_h = 3.097 \text{ cm}^{-1}$$

$$V_c/(V_c + V_f) = 0.542$$

$$r = 0.026$$

$$\text{Pressure} = 1.551 \times 10^7 \text{ Pa}$$

Macroscopic Cross Section Derivatives:

Parameter, $\Sigma$	$\frac{\partial \Sigma}{\partial \rho_c}$	$\frac{\partial \Sigma}{\partial \bar{T}_c}$	$\frac{\partial \Sigma}{\partial \bar{T}_f}$
$D_1^{-1}$	+0.41	$-8.0 \times 10^{-5}$	$-6.6 \times 10^{-6}$
$D_2^{-1}$	+2.70	$-1.3 \times 10^{-3}$	$-2.6 \times 10^{-6}$
$\Sigma_{c1}$	$+2.83 \times 10^{-3}$	$+3.0 \times 10^{-6}$	$+3.3 \times 10^{-7}$
$\Sigma_{c2}$	$+1.40 \times 10^{-2}$	$-8.2 \times 10^{-6}$	$-3.8 \times 10^{-7}$
$\nu \Sigma_{f1}$	+0.0	+0.0	+0.0
$\nu \Sigma_{f2}$	$+4.250 \times 10^{-2}$	$-2.075 \times 10^{-5}$	$-2.500 \times 10^{-6}$
$\Sigma_{f1}$	+0.0	+0.0	+0.0
$\Sigma_{f2}$	$+1.7 \times 10^{-2}$	$-8.3 \times 10^{-6}$	$-1.0 \times 10^{-6}$
$\Sigma_{21}$	$+2.4 \times 10^{-2}$	$-1.5 \times 10^{-6}$	$-8.5 \times 10^{-8}$

$$\rho_0 = 0.7961 \text{ g/cm}^3$$

$$\bar{T}_{f0} = 533 \text{ K}$$

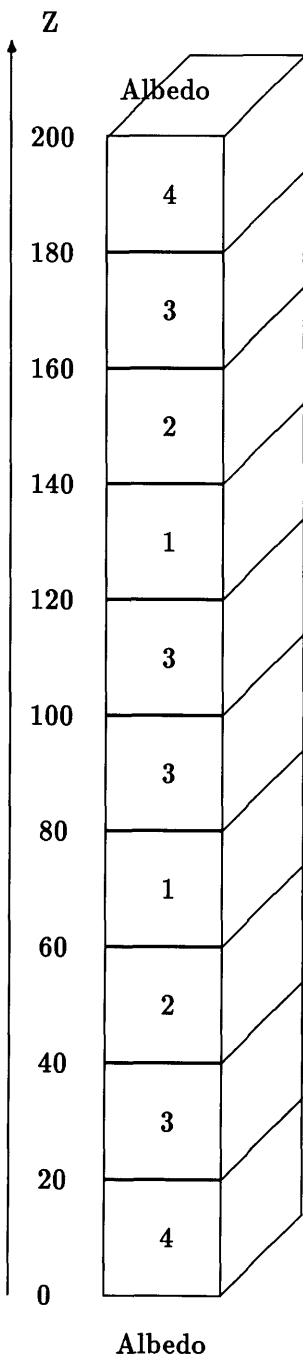
$$\bar{T}_{c0} = 533 \text{ K}$$

$$\text{Reactor Power} = 10 \text{ MW}_t$$

$$\text{Inlet Coolant Temperature} = 555 \text{ K}$$

## C.4 Transient Variable Inlet Coolant Temperature Problem

Geometry:



**Material Properties:**

Composition	Group, g	$D_g$ (cm)	$\Sigma_g$ (cm $^{-1}$ )	$\nu \Sigma_{fg}$ (cm $^{-1}$ )	$\Sigma_{21}$ (cm $^{-1}$ )
1	1	1.36480	0.026132	0.005550	0.017245
	2	0.48260	0.130772	0.185823	
2	1	1.36030	0.025603	0.006267	0.015942
	2	0.47760	0.169403	0.229195	
3	1	1.35720	0.025151	0.006894	0.014752
	2	0.47400	0.206951	0.268552	
4	1	1.39330	0.021484	0.000000	0.017943
	2	0.36590	0.068149	0.000000	

**Boundary Condition:**

Group, g	$\alpha_g$	$\beta_g$
1	1.00	0.25
2	1.00	0.25

**WIGL Thermal-Hydraulic Parameters:**

$$\begin{aligned}
 C_c &= 5.43 \times 10^7 \text{ erg/g/K} \\
 W_r &= 8.0166 \times 10^4 \text{ g/s} \\
 h_0 &= 3.293 \times 10^7 \text{ erg/cm}^2/\text{s/K} \\
 A_h &= 3.097 \text{ cm}^{-1} \\
 V_c/(V_c + V_f) &= 0.542 \\
 r &= 0.026 \\
 \text{Pressure} &= 1.551 \times 10^7 \text{ Pa}
 \end{aligned}$$

**Macroscopic Cross Section Derivatives:**

Parameter, $\Sigma$	$\frac{\partial \Sigma}{\partial \rho_c}$	$\frac{\partial \Sigma}{\partial T_c}$	$\frac{\partial \Sigma}{\partial T_f}$
$D_1^{-1}$	+0.41	$-8.0 \times 10^{-5}$	$-6.6 \times 10^{-6}$
$D_2^{-1}$	+2.70	$-1.3 \times 10^{-3}$	$-2.6 \times 10^{-6}$
$\Sigma_{c1}$	$+2.83 \times 10^{-3}$	$+3.0 \times 10^{-6}$	$+3.3 \times 10^{-7}$
$\Sigma_{c2}$	$+1.40 \times 10^{-2}$	$-8.2 \times 10^{-6}$	$-3.8 \times 10^{-7}$
$\nu\Sigma_{f1}$	+0.0	+0.0	+0.0
$\nu\Sigma_{f2}^\dagger$	$+4.250 \times 10^{-2}$	$-2.075 \times 10^{-5}$	$-2.500 \times 10^{-6}$
$\Sigma_{f1}$	+0.0	+0.0	+0.0
$\Sigma_{f2}^\dagger$	$+1.7 \times 10^{-2}$	$-8.3 \times 10^{-6}$	$-1.0 \times 10^{-6}$
$\Sigma_{21}$	$+2.4 \times 10^{-2}$	$-1.5 \times 10^{-6}$	$-8.5 \times 10^{-8}$

†Zero for reflector materials (composition 4)

**Initial Condition:**

Reactor Power = 10 MW<sub>t</sub>

Inlet Coolant Temperature = 555 K

**Transient Condition:**

Forcing Function :  $T_{in}(t) = 555 - 38.836 t + 20.8 t^2$  K

Transient Period : [0.0,1.5]

**Miscellaneous Parameters:**

Time Step Size = 0.01 sec

No. of Time Steps = 150

$\theta$  = 1.0

$\theta_d$  = 1.0

No. of Precursor Families = 1

$\beta$  = 0.0075

$\lambda$  = 0.08 sec<sup>-1</sup>

$v_1$  =  $1.0 \times 10^7$  cm/sec

$v_2$  =  $2.0 \times 10^5$  cm/sec

## **Appendix D**

# **MCNP Input Data for the Test Problem**

- D.1 Input Data for Tallying Cell Fluxes and Cross Sections**
- D.2 Input Data for Tallying Surface Fluxes**
- D.3 Input Data for Tallying Surface Currents**

## D.1 Input Data for Tallying Cell Fluxes and Cross Sections

2-D Simplified, Homogenized, 3-Ring Core (D20, Fuel, Dummy)

00001	1	-1.10445	525	-5011	-750	-80	85	\$ (1,1)
00002	1	-1.10445	-5010	750	625	-80	85	\$ (2,1)
00003	1	-1.10445	525	-625	-5002	-80	85	\$ (3,1)
00004	1	-1.10445	-5010	5002	5001	-80	85	\$ (4,1)
00005	1	-1.10445	525	-5001	-725	-80	85	\$ (5,1)
00006	1	-1.10445	-5010	725	650	-80	85	\$ (6,1)
00007	1	-1.10445	525	-650	-5012	-80	85	\$ (7,1)
00008	1	-1.10445	5000	-5011	-5102	-80	85	\$ (1,2)
00009	1	-1.10445	-525	5102	625	-80	85	\$ (2,2)
00010	3	0.0667252	5000	-625	-750	-80	85	\$ (3,2)
00011	3	0.0667252	-525	750	5001	-80	85	\$ (4,2)
00012	3	0.0667252	5000	-5001	-5002	-80	85	\$ (5,2)
00013	3	0.0667252	-525	5002	650	-80	85	\$ (6,2)
00014	3	0.0667252	5000	-650	-725	-80	85	\$ (7,2)
00015	1	-1.10445	-525	725	5101	-80	85	\$ (8,2)
00016	1	-1.10445	5000	-5101	-5012	-80	85	\$ (9,2)
00017	1	-1.10445	550	-5011	-775	-80	85	\$ (1,3)
00018	1	-1.10445	-5000	775	625	-80	85	\$ (2,3)
00019	3	0.0667252	550	-625	-5102	-80	85	\$ (3,3)
00020	3	0.0667252	-5000	5102	5001	-80	85	\$ (4,3)
00021	2	-2.7	550	-5001	-750	-80	85	\$ (5,3)
00022	2	-2.7	-5000	750	650	-80	85	\$ (6,3)
00023	3	0.0667252	550	-650	-5002	-80	85	\$ (7,3)
00024	2	-2.7	-5000	5002	5101	-80	85	\$ (8,3)
00025	3	0.0667252	550	-5101	-725	-80	85	\$ (9,3)
00026	1	-1.10445	-5000	725	675	-80	85	\$ (10,3)
00027	1	-1.10445	550	-675	-5012	-80	85	\$ (11,3)
00028	1	-1.10445	-550	5112	625	-80	85	\$ (2,4)
00029	1	-1.10445	5100	-625	-775	-80	85	\$ (3,4)
00030	3	0.0667252	-550	775	5001	-80	85	\$ (4,4)
00031	3	0.0667252	5100	-5001	-5102	-80	85	\$ (5,4)
00032	2	-2.7	-550	5102	650	-80	85	\$ (6,4)
00033	3	0.0667252	5100	-650	-750	-80	85	\$ (7,4)
00034	3	0.0667252	-550	750	5101	-80	85	\$ (8,4)
00035	3	0.0667252	5100	-5101	-5002	-80	85	\$ (9,4)
00036	3	0.0667252	-550	5002	675	-80	85	\$ (10,4)
00037	1	-1.10445	5100	-675	-725	-80	85	\$ (11,4)
00038	1	-1.10445	-550	725	5111	-80	85	\$ (12,4)
00039	1	-1.10445	-5100	5112	5001	-80	85	\$ (4,5)
00040	1	-1.10445	575	-5001	-775	-80	85	\$ (5,5)
00041	3	0.0667252	-5100	775	650	-80	85	\$ (6,5)
00042	3	0.0667252	575	-650	-5102	-80	85	\$ (7,5)
00043	3	0.0667252	-5100	5102	5101	-80	85	\$ (8,5)
00044	3	0.0667252	575	-5101	-750	-80	85	\$ (9,5)

00045	3	0.0667252	-5100	750	675	-80	85	\$ (10,5)
00046	1	-1.10445	575	-675	-5002	-80	85	\$ (11,5)
00047	1	-1.10445	-5100	5002	5111	-80	85	\$ (12,5)
00048	1	-1.10445	-575	5112	650	-80	85	\$ (6,6)
00049	1	-1.10445	5110	-650	-775	-80	85	\$ (7,6)
00050	3	0.0667252	-575	775	5101	-80	85	\$ (8,6)
00051	3	0.0667252	5110	-5101	-5102	-80	85	\$ (9,6)
00052	3	0.0667252	-575	5102	675	-80	85	\$ (10,6)
00053	1	-1.10445	5110	-675	-750	-80	85	\$ (11,6)
00054	1	-1.10445	-575	750	5111	-80	85	\$ (12,6)
c								
c	99998	0	(5010:5011:5012:-5112:-5110:-5111:80:-85)	-9999				
99998	0	5010:5011:5012:-5112:-5110:-5111:80:-85						
c	99999	0	9999					
c								
*80	pz	2.5						
*85	pz	-2.5						
c								
5010	py	28.575						
525	py	19.05						
5000	py	9.525						
550	py	0.0						
5100	py	-9.525						
575	py	-19.05						
5110	py	-28.575						
c								
5011	1	py	28.575					
625	1	py	19.05					
5001	1	py	9.525					
650	1	py	0.0					
5101	1	py	-9.525					
675	1	py	-19.05					
5111	1	py	-28.575					
c								
5012	2	py	28.575					
725	2	py	19.05					
5002	2	py	9.525					
750	2	py	0.0					
5102	2	py	-9.525					
775	2	py	-19.05					
5112	2	py	-28.575					
c								
c	9999	so	250.0					
c								
c								

```

c      Triangular transformations
c
*tr1   0  0  0  60 30 90 150 60 90  90 90 0
*tr2   0  0  0  60 150 90 30 60 90  90 90 0
c
c      Material 1 - D2O reflector total conc = -1.10445 gm/cc
c
m1    1001.50c 1.6671-3 1002.55c 6.6502-1 8016.50c 3.3332-1
c
c
c      Material 2 - Al total conc = -2.7 gm/cc
c
m2    13027.50c 1.0
c
c
c      Material 3 - Fuel/Water mixture total conc = 0.0667252 atoms/cc
c
m3    92238.50c 0.0042776 92235.50c 0.0583758
      13027.50c 0.1088325 1001.50c 0.5516012
      8016.50c 0.2769129
c
mode n
imp:n 1.0 53r 0.0
c
print 10 60 50 40 110 170 90
prdmp 2j 1 1
c
phys:n 20.0 0
c
c      void
c      sdef sur=9999 nrm=-1
c      nps 5000000
c
kcode 3000 1.0 0 1000
ksrc  5.0 4.5 0.0
c
c ****
c
c      TALLY INFORMATION
c
e0    0.625e-6 20.0
c
c      CELL FLUX
f004:n 1 2 3 4 5 6 7 8 9 10 11 12 13 14 15 16 17 18 19 20 21 22 23 24 25
      26 27 28 29 30 31 32 33 34 35 36 37 38 39 40 41 42 43 44 45 46 47
      48 49 50 51 52 53 54
fq04  f s e
c

```

```
c      REACTION RATE FOR D20
f014:n 1 2 3 4 5 6 7 8 9 15 16 17 18 26 27 28 29 37 38 39 40 46 47 48 49
      53 54
fm14  -1.0 1  (1)  (-2)  (2)  (16)
fq14  e s m
fc14      SIGT, SIGABS, SIGES, SIG(n,2n) for D20
c
c      REACTION RATE FOR AL DUMMY ELEMENT
f024:n 21 22 24 32
fm24  -1.0 2  (1)  (-2)  (2)  (16)
fq24  e s m
fc24      SIGT, SIGABS, SIGES, SIG(n,2n) for AL
c
c      REACTION RATE FOR FUEL/WATER MIXTURE
f034:n 10 11 12 13 14 19 20 23 25 30 31 33 34 35 36 41 42 43 44 45 50 51 52
fm34  -1.0 3  (1)  (-2)  (2)  (16)  (-6)  (-6 -7)
fq34  e s m
fc34      SIGT, SIGABS, SIGES, SIG(n,2n), SIGF,  NU*SIGF  for FUEL/WATER
c
c
c      END
```

## D.2 Input Data for Tallying Surface Fluxes

2-D Simplified, Homogenized, 3-Ring Core (D20, Fuel, Dummy)

00001	1	-1.10445	525	-5011	-750	-80	85	\$ (1,1)
00002	1	-1.10445	-5010	750	625	-80	85	\$ (2,1)
00003	1	-1.10445	525	-625	-5002	-80	85	\$ (3,1)
00004	1	-1.10445	-5010	5002	5001	-80	85	\$ (4,1)
00005	1	-1.10445	525	-5001	-725	-80	85	\$ (5,1)
00006	1	-1.10445	-5010	725	650	-80	85	\$ (6,1)
00007	1	-1.10445	525	-650	-5012	-80	85	\$ (7,1)
00008	1	-1.10445	5000	-5011	-5102	-80	85	\$ (1,2)
00009	1	-1.10445	-525	5102	625	-80	85	\$ (2,2)
00010	3	0.0667252	5000	-625	-750	-80	85	\$ (3,2)
00011	3	0.0667252	-525	750	5001	-80	85	\$ (4,2)
00012	3	0.0667252	5000	-5001	-5002	-80	85	\$ (5,2)
00013	3	0.0667252	-525	5002	650	-80	85	\$ (6,2)
00014	3	0.0667252	5000	-650	-725	-80	85	\$ (7,2)
00015	1	-1.10445	-525	725	5101	-80	85	\$ (8,2)
00016	1	-1.10445	5000	-5101	-5012	-80	85	\$ (9,2)
00017	1	-1.10445	550	-5011	-775	-80	85	\$ (1,3)
00018	1	-1.10445	-5000	775	625	-80	85	\$ (2,3)
00019	3	0.0667252	550	-625	-5102	-80	85	\$ (3,3)
00020	3	0.0667252	-5000	5102	5001	-80	85	\$ (4,3)
00021	2	-2.7	550	-5001	-750	-80	85	\$ (5,3)
00022	2	-2.7	-5000	750	650	-80	85	\$ (6,3)
00023	3	0.0667252	550	-650	-5002	-80	85	\$ (7,3)
00024	2	-2.7	-5000	5002	5101	-80	85	\$ (8,3)
00025	3	0.0667252	550	-5101	-725	-80	85	\$ (9,3)
00026	1	-1.10445	-5000	725	675	-80	85	\$ (10,3)
00027	1	-1.10445	550	-675	-5012	-80	85	\$ (11,3)
00028	1	-1.10445	-550	5112	625	-80	85	\$ (2,4)
00029	1	-1.10445	5100	-625	-775	-80	85	\$ (3,4)
00030	3	0.0667252	-550	775	5001	-80	85	\$ (4,4)
00031	3	0.0667252	5100	-5001	-5102	-80	85	\$ (5,4)
00032	2	-2.7	-550	5102	650	-80	85	\$ (6,4)
00033	3	0.0667252	5100	-650	-750	-80	85	\$ (7,4)
00034	3	0.0667252	-550	750	5101	-80	85	\$ (8,4)
00035	3	0.0667252	5100	-5101	-5002	-80	85	\$ (9,4)
00036	3	0.0667252	-550	5002	675	-80	85	\$ (10,4)
00037	1	-1.10445	5100	-675	-725	-80	85	\$ (11,4)
00038	1	-1.10445	-550	725	5111	-80	85	\$ (12,4)
00039	1	-1.10445	-5100	5112	5001	-80	85	\$ (4,5)
00040	1	-1.10445	575	-5001	-775	-80	85	\$ (5,5)
00041	3	0.0667252	-5100	775	650	-80	85	\$ (6,5)
00042	3	0.0667252	575	-650	-5102	-80	85	\$ (7,5)
00043	3	0.0667252	-5100	5102	5101	-80	85	\$ (8,5)
00044	3	0.0667252	575	-5101	-750	-80	85	\$ (9,5)

00045	3	0.0667252	-5100	750	675	-80	85	\$ (10,5)
00046	1	-1.10445	575	-675	-5002	-80	85	\$ (11,5)
00047	1	-1.10445	-5100	5002	5111	-80	85	\$ (12,5)
00048	1	-1.10445	-575	5112	650	-80	85	\$ (6,6)
00049	1	-1.10445	5110	-650	-775	-80	85	\$ (7,6)
00050	3	0.0667252	-575	775	5101	-80	85	\$ (8,6)
00051	3	0.0667252	5110	-5101	-5102	-80	85	\$ (9,6)
00052	3	0.0667252	-575	5102	675	-80	85	\$ (10,6)
00053	1	-1.10445	5110	-675	-750	-80	85	\$ (11,6)
00054	1	-1.10445	-575	750	5111	-80	85	\$ (12,6)
c								
c	99998	0	(5010:5011:5012:-5112:-5110:-5111:80:-85)	-9999				
99998	0	5010:5011:5012:-5112:-5110:-5111:80:-85						
c	99999	0	9999					
c								
*80	pz	2.5						
*85	pz	-2.5						
c								
5010	py	28.575						
525	py	19.05						
5000	py	9.525						
550	py	0.0						
5100	py	-9.525						
575	py	-19.05						
5110	py	-28.575						
c								
5011	1	py	28.575					
625	1	py	19.05					
5001	1	py	9.525					
650	1	py	0.0					
5101	1	py	-9.525					
675	1	py	-19.05					
5111	1	py	-28.575					
c								
5012	2	py	28.575					
725	2	py	19.05					
5002	2	py	9.525					
750	2	py	0.0					
5102	2	py	-9.525					
775	2	py	-19.05					
5112	2	py	-28.575					
c								
c	9999	so	250.0					
c								
c								

```

c      Triangular transformations
c
*tr1   0  0  0  60 30 90 150 60 90  90 90 0
*tr2   0  0  0  60 150 90 30 60 90  90 90 0
c
c      Material 1 - D20 reflector total conc = -1.10445 gm/cc
c
m1    1001.50c 1.6671-3 1002.55c 6.6502-1 8016.50c 3.3332-1
c
c
c      Material 2 - Al total conc = -2.7 gm/cc
c
m2    13027.50c 1.0
c
c
c      Material 3 - Fuel/Water mixture total conc = 0.0667252 atoms/cc
c
m3    92238.50c 0.0042776 92235.50c 0.0583758
      13027.50c 0.1088325 1001.50c 0.5516012
      8016.50c 0.2769129
c
mode n
imp:n 1.0 53r 0.0
c
print 10 60 50 40 110 170 90
prdmp 2j 1 1
c
phys:n 20.0 0
c
c      void
c      sdef sur=9999 nrm=-1
c      nps 5000000
c
kcode 3000 1.0 0 1000
ksrc  5.0 4.5 0.0
c
c ****
c
c      TALLY INFORMATION
c
e0    0.625e-6 20.0
c
c      SURFACE FLUX TALLY
c      Surfaces 1: 5011, 625, 5001, 650, 5101, 675, 5111
c      Surfaces 2: 5012, 725, 5002, 750, 5102, 775, 5112
c      Surfaces 3: 5010, 525, 5000, 550, 5100, 575, 5110
c
c

```

c           Surfaces 1: 5011, 625, 5001, 650, 5101, 675, 5111  
c  
f002:n 5011  
fs002 525 5000  
c  
c  
f012:n 625  
fs012 525 5000 550  
c  
c  
f022:n 5001  
fs022 525 5000 550 5100  
c  
c  
f032:n 650  
fs032 525 5000 550 5100 575  
c  
c  
f042:n 5101  
fs042 5000 550 5100 575  
c  
c  
f052:n 675  
fs052 550 5100 575  
c  
c  
f062:n 5111  
fs062 5100 575  
c  
c  
c           Surfaces 2: 5012, 725, 5002, 750, 5102, 775, 5112  
c  
f072:n 5012  
fs072 525 5000  
c  
c  
f082:n 725  
fs082 525 5000 550  
c  
c  
f092:n 5002  
fs092 525 5000 550 5100  
c  
c  
f102:n 750  
fs102 525 5000 550 5100 575  
c  
c

```
f112:n 5102
fs112 5000 550 5100 575
c
c
f122:n 775
fs122 550 5100 575
c
c
f132:n 5112
fs132 5100 575
c
c
c      Surfaces 3: 5010, 525, 5000, 550, 5100, 575, 5110
c
f142:n 5010
fs142 625 5001
c
c
f152:n 525
fs152 625 5001 650
c
c
f162:n 5000
fs162 625 5001 650 5101
c
c
f172:n 550
fs172 625 5001 650 5101 675
c
c
f182:n 5100
fs182 5001 650 5101 675
c
c
f192:n 575
fs192 650 5101 675
c
c
f202:n 5110
fs202 5101 675
c
c
c      END
```

### D.3 Input Data for Tallying Surface Currents

2-D Simplified, Homogenized, 3-Ring Core (D20, Fuel, Dummy)

00001	1	-1.10445	525	-5011	-750	-80	85	\$ (1,1)
00002	1	-1.10445	-5010	750	625	-80	85	\$ (2,1)
00003	1	-1.10445	525	-625	-5002	-80	85	\$ (3,1)
00004	1	-1.10445	-5010	5002	5001	-80	85	\$ (4,1)
00005	1	-1.10445	525	-5001	-725	-80	85	\$ (5,1)
00006	1	-1.10445	-5010	725	650	-80	85	\$ (6,1)
00007	1	-1.10445	525	-650	-5012	-80	85	\$ (7,1)
00008	1	-1.10445	5000	-5011	-5102	-80	85	\$ (1,2)
00009	1	-1.10445	-525	5102	625	-80	85	\$ (2,2)
00010	3	0.0667252	5000	-625	-750	-80	85	\$ (3,2)
00011	3	0.0667252	-525	750	5001	-80	85	\$ (4,2)
00012	3	0.0667252	5000	-5001	-5002	-80	85	\$ (5,2)
00013	3	0.0667252	-525	5002	650	-80	85	\$ (6,2)
00014	3	0.0667252	5000	-650	-725	-80	85	\$ (7,2)
00015	1	-1.10445	-525	725	5101	-80	85	\$ (8,2)
00016	1	-1.10445	5000	-5101	-5012	-80	85	\$ (9,2)
00017	1	-1.10445	550	-5011	-775	-80	85	\$ (1,3)
00018	1	-1.10445	-5000	775	625	-80	85	\$ (2,3)
00019	3	0.0667252	550	-625	-5102	-80	85	\$ (3,3)
00020	3	0.0667252	-5000	5102	5001	-80	85	\$ (4,3)
00021	2	-2.7	550	-5001	-750	-80	85	\$ (5,3)
00022	2	-2.7	-5000	750	650	-80	85	\$ (6,3)
00023	3	0.0667252	550	-650	-5002	-80	85	\$ (7,3)
00024	2	-2.7	-5000	5002	5101	-80	85	\$ (8,3)
00025	3	0.0667252	550	-5101	-725	-80	85	\$ (9,3)
00026	1	-1.10445	-5000	725	675	-80	85	\$ (10,3)
00027	1	-1.10445	550	-675	-5012	-80	85	\$ (11,3)
00028	1	-1.10445	-550	5112	625	-80	85	\$ (2,4)
00029	1	-1.10445	5100	-625	-775	-80	85	\$ (3,4)
00030	3	0.0667252	-550	775	5001	-80	85	\$ (4,4)
00031	3	0.0667252	5100	-5001	-5102	-80	85	\$ (5,4)
00032	2	-2.7	-550	5102	650	-80	85	\$ (6,4)
00033	3	0.0667252	5100	-650	-750	-80	85	\$ (7,4)
00034	3	0.0667252	-550	750	5101	-80	85	\$ (8,4)
00035	3	0.0667252	5100	-5101	-5002	-80	85	\$ (9,4)
00036	3	0.0667252	-550	5002	675	-80	85	\$ (10,4)
00037	1	-1.10445	5100	-675	-725	-80	85	\$ (11,4)
00038	1	-1.10445	-550	725	5111	-80	85	\$ (12,4)
00039	1	-1.10445	-5100	5112	5001	-80	85	\$ (4,5)
00040	1	-1.10445	575	-5001	-775	-80	85	\$ (5,5)
00041	3	0.0667252	-5100	775	650	-80	85	\$ (6,5)
00042	3	0.0667252	575	-650	-5102	-80	85	\$ (7,5)
00043	3	0.0667252	-5100	5102	5101	-80	85	\$ (8,5)
00044	3	0.0667252	575	-5101	-750	-80	85	\$ (9,5)

00045	3	0.0667252	-5100	750	675	-80	85	\$ (10,5)	
00046	1	-1.10445	575	-675	-5002	-80	85	\$ (11,5)	
00047	1	-1.10445	-5100	5002	5111	-80	85	\$ (12,5)	
00048	1	-1.10445	-575	5112	650	-80	85	\$ (6,6)	
00049	1	-1.10445	5110	-650	-775	-80	85	\$ (7,6)	
00050	3	0.0667252	-575	775	5101	-80	85	\$ (8,6)	
00051	3	0.0667252	5110	-5101	-5102	-80	85	\$ (9,6)	
00052	3	0.0667252	-575	5102	675	-80	85	\$ (10,6)	
00053	1	-1.10445	5110	-675	-750	-80	85	\$ (11,6)	
00054	1	-1.10445	-575	750	5111	-80	85	\$ (12,6)	
c									
c	99998	0	(5010:5011:5012:-5112:-5110:-5111:80:-85)						-9999
99998	0	5010:5011:5012:-5112:-5110:-5111:80:-85							
c	99999	0	9999						
c									
*80	pz	2.5							
*85	pz	-2.5							
c									
5010	py	28.575							
525	py	19.05							
5000	py	9.525							
550	py	0.0							
5100	py	-9.525							
575	py	-19.05							
5110	py	-28.575							
c									
5011	1	py	28.575						
625	1	py	19.05						
5001	1	py	9.525						
650	1	py	0.0						
5101	1	py	-9.525						
675	1	py	-19.05						
5111	1	py	-28.575						
c									
5012	2	py	28.575						
725	2	py	19.05						
5002	2	py	9.525						
750	2	py	0.0						
5102	2	py	-9.525						
775	2	py	-19.05						
5112	2	py	-28.575						
c									
c	9999	so	250.0						
c									
c									

```

c      Triangular transformations
c
*tr1   0  0  0  60 30 90 150 60 90  90 90 0
*tr2   0  0  0  60 150 90 30 60 90  90 90 0
c
c      Material 1 - D2O reflector total conc = -1.10445 gm/cc
c
m1    1001.50c 1.6671-3 1002.55c 6.6502-1 8016.50c 3.3332-1
c
c
c      Material 2 - Al total conc = -2.7 gm/cc
c
m2    13027.50c 1.0
c
c
c      Material 3 - Fuel/Water mixture total conc = 0.0667252 atoms/cc
c
m3    92238.50c 0.0042776 92235.50c 0.0583758
      13027.50c 0.1088325 1001.50c 0.5516012
      8016.50c 0.2769129
c
mode n
imp:n 1.0 53r 0.0
c
print 10 60 50 40 110 170 90
prdmp 2j 1 1
c
phys:n 20.0 0
c
c      void
c      sdef sur=9999 nrm=-1
c      nps 5000000
c
kcode 3000 1.0 0 1000
ksrc 5.0 4.5 0.0
c
c ****
c      TALLY INFORMATION
c
e0    0.625e-6 20.0
c
c
c      SURFACE CURRENT TALLY
c      Surfaces 1: 5011, 625, 5001, 650, 5101, 675, 5111
c      Surfaces 2: 5012, 725, 5002, 750, 5102, 775, 5112
c      Surfaces 3: 5010, 525, 5000, 550, 5100, 575, 5110
c

```

```
c0      0 1 t
cm0    -1 1
c
c
c      Surfaces 1: 5011, 625, 5001, 650, 5101, 675, 5111
c
f001:n 5011
fs001  525 5000
c
c
f011:n 625
fs011  525 5000 550
c
c
f021:n 5001
fs021  525 5000 550 5100
c
c
f031:n 650
fs031  525 5000 550 5100 575
c
c
f041:n 5101
fs041  5000 550 5100 575
c
c
f051:n 675
fs051  550 5100 575
c
c
f061:n 5111
fs061  5100 575
c
c
c      Surfaces 2: 5012, 725, 5002, 750, 5102, 775, 5112
c
f071:n 5012
fs071  525 5000
c
c
f081:n 725
fs081  525 5000 550
c
c
f091:n 5002
fs091  525 5000 550 5100
c
c
```

**f101:n 750**  
**fs101 525 5000 550 5100 575**  
c  
c  
**f111:n 5102**  
**fs111 5000 550 5100 575**  
c  
c  
**f121:n 775**  
**fs121 550 5100 575**  
c  
c  
**f131:n 5112**  
**fs131 5100 575**  
c  
c  
c       **Surfaces 3: 5010, 525, 5000, 550, 5100, 575, 5110**  
c  
**f141:n 5010**  
**fs141 625 5001**  
c  
c  
**f151:n 525**  
**fs151 625 5001 650**  
c  
c  
**f161:n 5000**  
**fs161 625 5001 650 5101**  
c  
c  
**f171:n 550**  
**fs171 625 5001 650 5101 675**  
c  
c  
**f181:n 5100**  
**fs181 5001 650 5101 675**  
c  
c  
**f191:n 575**  
**fs191 650 5101 675**  
c  
c  
**f201:n 5110**  
**fs201 5101 675**  
c  
c  
c       **END**

## **Appendix E**

# **Cross Sections, Fluxes, Currents, and CMFD Discontinuity Factors for the Test Problem**

- E.1 Nodal Fluxes**
- E.2 Two-Group Cross Sections**
- E.3 Surface Fluxes**
- E.4 Surface Currents**
- E.5 CMFD Discontinuity Factors**

## E.1 Nodal Fluxes

The cell fluxes along with the statistical errors as edited from the MCNP output are listed below.

I	J	NODE	G	FLUX	STAT ERR(%)
1	1	1			
		1	8.35384E-04	4.60000E-01	
		2	1.07177E-04	1.32000E+00	
2	1	2			
		1	8.30042E-04	4.60000E-01	
		2	1.03208E-04	1.32000E+00	
3	1	3			
		1	1.69450E-03	3.40000E-01	
		2	1.31418E-04	1.16000E+00	
4	1	4			
		1	1.09784E-03	4.00000E-01	
		2	1.16045E-04	1.25000E+00	
5	1	5			
		1	1.69788E-03	3.40000E-01	
		2	1.28429E-04	1.18000E+00	
6	1	6			
		1	8.33302E-04	4.50000E-01	
		2	1.01962E-04	1.34000E+00	
7	1	7			
		1	8.38597E-04	4.60000E-01	
		2	1.06696E-04	1.32000E+00	
1	2	8			
		1	1.12342E-03	3.90000E-01	
		2	1.16920E-04	1.24000E+00	
2	2	9			
		1	1.71066E-03	3.30000E-01	
		2	1.35828E-04	1.18000E+00	
3	2	10			
		1	2.92772E-03	2.10000E-01	
		2	3.49515E-05	7.10000E-01	
4	2	11			
		1	2.91417E-03	2.10000E-01	
		2	3.48306E-05	7.20000E-01	
5	2	12			
		1	3.42177E-03	1.90000E-01	
		2	3.33427E-05	7.30000E-01	
6	2	13			
		1	2.90794E-03	2.10000E-01	
		2	3.50531E-05	7.20000E-01	
7	2	14			
		1	2.89971E-03	2.10000E-01	

			2	3.55813E-05	7.20000E-01
8	2	15	1	1.71059E-03	3.30000E-01
			2	1.34792E-04	1.15000E+00
9	2	16	1	1.12092E-03	3.90000E-01
			2	1.19919E-04	1.22000E+00
1	3	17	1	8.68057E-04	4.50000E-01
			2	1.08187E-04	1.29000E+00
2	3	18	1	1.74620E-03	3.30000E-01
			2	1.33209E-04	1.17000E+00
3	3	19	1	2.99721E-03	2.10000E-01
			2	3.56412E-05	7.10000E-01
4	3	20	1	3.45870E-03	1.90000E-01
			2	3.40817E-05	7.30000E-01
5	3	21	1	3.72081E-03	2.10000E-01
			2	3.54788E-05	1.73000E+00
6	3	22	1	3.75005E-03	2.10000E-01
			2	3.60649E-05	1.71000E+00
7	3	23	1	4.03735E-03	1.80000E-01
			2	3.70955E-05	7.00000E-01
8	3	24	1	3.33100E-03	2.20000E-01
			2	3.73182E-05	1.68000E+00
9	3	25	1	3.03765E-03	2.10000E-01
			2	3.71882E-05	7.00000E-01
10	3	26	1	1.77168E-03	3.30000E-01
			2	1.37296E-04	1.15000E+00
11	3	27	1	8.84971E-04	4.40000E-01
			2	1.09125E-04	1.30000E+00
2	4	28	1	8.85625E-04	4.40000E-01
			2	1.10370E-04	1.29000E+00
3	4	29	1	1.82482E-03	3.20000E-01
			2	1.40882E-04	1.15000E+00
4	4	30	1	3.08040E-03	2.00000E-01

			2	3.69104E-05	7.00000E-01
5	4	31	1	3.66364E-03	1.80000E-01
			2	3.50936E-05	7.10000E-01
6	4	32	1	3.91588E-03	2.10000E-01
			2	3.57514E-05	1.65000E+00
7	4	33	1	4.31126E-03	1.70000E-01
			2	3.85684E-05	6.80000E-01
8	4	34	1	4.31095E-03	1.60000E-01
			2	3.89425E-05	6.70000E-01
9	4	35	1	3.84889E-03	1.80000E-01
			2	3.63904E-05	6.90000E-01
10	4	36	1	3.17598E-03	2.00000E-01
			2	3.77378E-05	6.90000E-01
11	4	37	1	1.87371E-03	3.20000E-01
			2	1.41804E-04	1.13000E+00
12	4	38	1	9.03231E-04	4.40000E-01
			2	1.10226E-04	1.29000E+00
4	5	39	1	1.21410E-03	3.80000E-01
			2	1.22938E-04	1.21000E+00
5	5	40	1	1.92316E-03	3.10000E-01
			2	1.30523E-04	1.18000E+00
6	5	41	1	3.26636E-03	2.00000E-01
			2	3.69456E-05	7.00000E-01
7	5	42	1	3.32011E-03	1.90000E-01
			2	3.11042E-05	7.60000E-01
8	5	43	1	3.91460E-03	1.70000E-01
			2	3.55701E-05	7.10000E-01
9	5	44	1	3.38199E-03	1.90000E-01
			2	3.15926E-05	7.50000E-01
10	5	45	1	3.38908E-03	1.90000E-01
			2	3.82390E-05	6.90000E-01
11	5	46	1	1.99935E-03	3.10000E-01

			2	1.31464E-04	1.17000E+00
12	5	47	1	1.25638E-03	3.70000E-01
			2	1.25892E-04	1.19000E+00
6	6	48	1	1.01226E-03	4.10000E-01
			2	8.91980E-05	1.41000E+00
7	6	49	1	1.11956E-03	3.80000E-01
			2	5.74775E-05	1.59000E+00
8	6	50	1	2.18571E-03	2.40000E-01
			2	2.26692E-05	8.90000E-01
9	6	51	1	1.53710E-03	2.70000E-01
			2	1.31801E-05	1.17000E+00
10	6	52	1	2.20538E-03	2.40000E-01
			2	2.26776E-05	8.90000E-01
11	6	53	1	1.14484E-03	3.80000E-01
			2	5.92624E-05	1.60000E+00
12	6	54	1	1.04317E-03	4.10000E-01
			2	9.03164E-05	1.40000E+00

## E.2 Two-Group Cross Sections

A list of two-group nodal cross sections edited from the MCNP output is shown below followed by a list of the statistical errors for the nodal cross sections.

### [CROSS SECTION LIST]

I	J	NODE	G	DIFF	ABSORPTION	ELSC	SCATT	FISSION	NU*FISSION	(N,2N)
1	1	1								
			1	1.01100E+00	6.72236E-05	3.29537E-01	0.00000E+00	0.00000E+00	0.00000E+00	0.00000E+00
2	1	2								
			1	1.01148E+00	6.86738E-05	3.29375E-01	0.00000E+00	0.00000E+00	0.00000E+00	0.00000E+00
3	1	3								
			1	1.02913E+00	8.20378E-05	3.23690E-01	0.00000E+00	0.00000E+00	0.00000E+00	0.00000E+00
4	1	4								
			1	1.01559E+00	7.14615E-05	3.28037E-01	0.00000E+00	0.00000E+00	0.00000E+00	0.00000E+00
5	1	5								
			1	1.02905E+00	8.17997E-05	3.23720E-01	0.00000E+00	0.00000E+00	0.00000E+00	0.00000E+00
6	1	6								
			1	1.01140E+00	6.65456E-05	3.29406E-01	0.00000E+00	0.00000E+00	0.00000E+00	0.00000E+00
7	1	7								
			1	1.00985E+00	6.65829E-05	3.29915E-01	0.00000E+00	0.00000E+00	0.00000E+00	0.00000E+00
1	2	8								
			1	1.01563E+00	7.16399E-05	3.28022E-01	0.00000E+00	0.00000E+00	0.00000E+00	0.00000E+00
2	2	9								
			1	1.02895E+00	8.04152E-05	3.23753E-01	0.00000E+00	0.00000E+00	0.00000E+00	0.00000E+00
3	2	10								
			1	6.25677E-01	9.91317E-03	4.97244E-01	2.10290E-02	5.17744E-02	1.58919E-05	
4	2	11								
			1	6.25932E-01	9.83367E-03	4.97205E-01	2.09334E-02	5.15399E-02	1.57840E-05	
5	2	12								
			1	6.38453E-01	9.28455E-03	4.88303E-01	1.98534E-02	4.89098E-02	1.53032E-05	
6	2	13								
			1	6.25836E-01	9.86932E-03	4.97249E-01	2.09357E-02	5.15461E-02	1.57812E-05	
7	2	14								
			1	6.18264E-01	1.01191E-02	5.03268E-01	2.12864E-02	5.23832E-02	1.49002E-05	
8	2	15								
			1	1.02564E+00	7.71634E-05	3.24805E-01	0.00000E+00	0.00000E+00	0.00000E+00	
9	2	16								
			1	1.01227E+00	6.76289E-05	3.29119E-01	0.00000E+00	0.00000E+00	0.00000E+00	
1	3	17								
			1	1.01206E+00	6.89766E-05	3.29188E-01	0.00000E+00	0.00000E+00	0.00000E+00	
2	3	18								
			1	1.02949E+00	8.16023E-05	3.23580E-01	0.00000E+00	0.00000E+00	0.00000E+00	
3	3	19								
			1	6.25623E-01	9.88016E-03	4.97459E-01	2.08939E-02	5.14438E-02	1.57059E-05	
			2	1.75491E-01	1.48385E-01	9.66957E-01	7.84095E-01	1.91061E+00	0.00000E+00	

4	3	20
	1	6.37306E-01
	2	1.82050E-01
5	3	21
	1	2.03483E+00
	2	3.84908E+00
6	3	22
	1	2.00557E+00
	2	3.85043E+00
7	3	23
	1	6.44449E-01
	2	1.82014E-01
8	3	24
	1	2.00156E+00
	2	3.83879E+00
9	3	25
	1	6.21616E-01
	2	1.75802E-01
10	3	26
	1	1.02692E+00
	2	8.60294E-01
11	3	27
	1	1.01187E+00
	2	8.53793E-01
2	4	28
	1	1.01163E+00
	2	8.53572E-01
3	4	29
	1	1.02896E+00
	2	8.58979E-01
4	4	30
	1	6.26082E-01
	2	1.75361E-01
5	4	31
	1	6.42751E-01
	2	1.81306E-01
6	4	32
	1	2.00101E+00
	2	3.85295E+00
7	4	33
	1	6.51191E-01
	2	1.81845E-01
8	4	34
	1	6.54295E-01
	2	1.81639E-01
9	4	35
	1	6.51059E-01
	2	1.81727E-01
10	4	36
	1	6.29319E-01
	2	1.75698E-01
11	4	37
	1	1.03040E+00
	2	8.60067E-01
12	4	38
	1	1.01223E+00
	2	8.56341E-01
4	5	39
	1	1.01570E+00
	2	8.58623E-01
5	5	40
	1	1.03252E+00
	2	8.63043E-01
6	5	41
	1	6.31283E-01
	2	1.76367E-01
7	5	42
	1	6.52164E-01
	2	8.93293E-03
	1	9.34634E-03
	2	1.39175E-01
	1	9.58124E-01
	2	7.33705E-01
	1	1.99992E-02
	2	1.78782E+00
	1	4.92636E-02
	2	0.00000E+00
	1	1.49797E-05
	2	0.00000E+00
	1	2.03334E-04
	2	5.14254E-03
	1	1.57352E-01
	2	8.14582E-02
	0.00000E+00	0.00000E+00
	1	0.00000E+00
	2	0.00000E+00
	1	2.35718E-04
	2	5.12130E-03
	1	1.59518E-01
	2	8.14490E-02
	0.00000E+00	0.00000E+00
	1	4.84293E-01
	2	9.58070E-01
	1	1.93124E-02
	2	7.33849E-01
	1	4.75901E-02
	2	1.78817E+00
	1	1.47435E-05
	2	0.00000E+00
	1	2.53635E-04
	2	5.34618E-03
	1	1.59522E-01
	2	8.14886E-02
	0.00000E+00	0.00000E+00
	1	5.00489E-01
	2	9.66834E-01
	1	2.11796E-02
	2	7.81613E-01
	1	5.21301E-02
	2	1.90456E+00
	1	1.54123E-05
	2	0.00000E+00
	1	3.24397E-01
	2	6.04348E-05
	1	0.00000E+00
	2	3.87404E-01
	0.00000E+00	0.00000E+00
	1	3.29247E-01
	2	6.33065E-05
	1	0.00000E+00
	2	3.90351E-01
	0.00000E+00	0.00000E+00
	1	6.84358E-05
	2	6.34863E-05
	1	3.29327E-01
	2	3.90452E-01
	0.00000E+00	0.00000E+00
	1	7.96966E-05
	2	6.07634E-05
	1	3.23751E-01
	2	3.87997E-01
	0.00000E+00	0.00000E+00
	1	9.86054E-03
	2	1.48350E-01
	1	4.97062E-01
	2	9.67229E-01
	1	2.09115E-02
	2	7.85261E-01
	1	5.14888E-02
	2	1.91344E+00
	1	1.58153E-05
	2	0.00000E+00
	1	9.18663E-03
	2	1.40335E-01
	1	4.85029E-01
	2	9.58967E-01
	1	1.96753E-02
	2	7.39215E-01
	1	4.84848E-02
	2	1.80124E+00
	1	1.53823E-05
	2	0.00000E+00
	1	2.40683E-04
	2	5.07200E-03
	1	1.59712E-01
	2	8.14418E-02
	0.00000E+00	0.00000E+00
	1	4.78712E-01
	2	9.58541E-01
	1	1.94262E-02
	2	7.35919E-01
	1	4.79058E-02
	2	1.79321E+00
	1	1.71985E-05
	2	0.00000E+00
	1	3.23293E-01
	2	6.04915E-05
	1	0.00000E+00
	2	3.87506E-01
	0.00000E+00	0.00000E+00
	1	6.98072E-05
	2	1.39794E-01
	1	3.29130E-01
	2	8.89190E-01
	0.00000E+00	0.00000E+00
	1	2.07818E-02
	2	9.66689E-01
	1	5.11817E-02
	2	7.82687E-01
	1	1.90717E+00
	2	0.00000E+00
	1	8.41053E-05
	2	1.47824E-01
	1	3.28007E-01
	2	9.58139E-01
	0.00000E+00	0.00000E+00
	1	4.79155E-01
	2	7.35135E-01
	1	1.91017E-02
	2	1.79130E+00
	1	4.70985E-02
	2	1.79130E+00
	1	1.62237E-05
	2	0.00000E+00
	1	8.83607E-03
	2	1.39789E-01
	1	4.79155E-01
	2	9.58139E-01
	1	1.91017E-02
	2	7.35135E-01
	1	4.70985E-02
	2	1.79130E+00
	1	1.67121E-05
	2	0.00000E+00
	1	9.00914E-03
	2	1.81727E-01
	1	4.78712E-01
	2	9.58541E-01
	1	1.94262E-02
	2	7.35919E-01
	1	4.79058E-02
	2	1.79321E+00
	1	1.71985E-05
	2	0.00000E+00
	1	9.78400E-03
	2	1.47824E-01
	1	4.94484E-01
	2	9.66689E-01
	1	2.07818E-02
	2	7.82687E-01
	1	5.11817E-02
	2	1.90717E+00
	1	1.63569E-05
	2	0.00000E+00
	1	8.41053E-05
	2	1.47824E-01
	1	3.23293E-01
	2	9.58139E-01
	0.00000E+00	0.00000E+00
	1	6.98072E-05
	2	1.39794E-01
	1	3.29130E-01
	2	8.89190E-01
	0.00000E+00	0.00000E+00
	1	2.07818E-02
	2	9.66689E-01
	1	5.11817E-02
	2	1.90717E+00
	1	1.63569E-05
	2	0.00000E+00
	1	8.41053E-05
	2	1.47824E-01
	1	3.23293E-01
	2	9.58139E-01
	0.00000E+00	0.00000E+00
	1	6.98072E-05
	2	1.39794E-01
	1	3.29130E-01
	2	8.89190E-01
	0.00000E+00	0.00000E+00
	1	2.07818E-02
	2	9.66689E-01
	1	5.11817E-02
	2	1.90717E+00
	1	1.63569E-05
	2	0.00000E+00
	1	8.41053E-05
	2	1.47824E-01
	1	3.23293E-01
	2	9.58139E-01
	0.00000E+00	0.00000E+00
	1	6.98072E-05
	2	1.39794E-01
	1	3.29130E-01
	2	8.89190E-01
	0.00000E+00	0.00000E+00
	1	2.07818E-02
	2	9.66689E-01
	1	5.11817E-02
	2	1.90717E+00
	1	1.63569E-05
	2	0.00000E+00
	1	8.41053E-05
	2	1.47824E-01
	1	3.23293E-01
	2	9.58139E-01
	0.00000E+00	0.00000E+00
	1	6.98072E-05
	2	1.39794E-01
	1	3.29130E-01
	2	8.89190E-01
	0.00000E+00	0.00000E+00
	1	2.07818E-02
	2	9.66689E-01
	1	5.11817E-02
	2	1.90717E+00
	1	1.63569E-05
	2	0.00000E+00
	1	8.41053E-05
	2	1.47824E-01
	1	3.23293E-01
	2	9.58139E-01
	0.00000E+00	0.00000E+00
	1	6.98072E-05
	2	1.39794E-01
	1	3.29130E-01
	2	8.89190E-01
	0.00000E+00	0.00000E+00
	1	2.07818E-02
	2	9.66689E-01
	1	5.11817E-02
	2	1.90717E+00
	1	1.63569E-05
	2	0.00000E+00
	1	8.41053E-05
	2	1.47824E-01
	1	3.23293E-01
	2	9.58139E-01
	0.00000E+00	0.00000E+00
	1	6.98072E-05
	2	1.39794E-01
	1	3.29130E-01
	2	8.89190E-01
	0.00000E+00	0.00000E+00
	1	2.07818E-02
	2	9.66689E-01
	1	5.11817E-02
	2	1.90717E+00
	1	1.63569E-05
	2	0.00000E+00
	1	8.41053E-05
	2	1.47824E-01
	1	3.23293E-01
	2	9.58139E-01
	0.00000E+00	0.00000E+00
	1	6.98072E-05
	2	1.39794E-01
	1	3.29130E-01
	2	8.89190E-01
	0.00000E+00	0.00000E+00
	1	2.07818E-02
	2	9.66689E-01
	1	5.11817E-02
	2	1.90717E+00
	1	1.63569E-05
	2	0.00000E+00
	1	8.41053E-05
	2	1.47824E-01
	1	3.23293E-01
	2	9.58139E-01
	0.00000E+00	0.00000E+00
	1	6.98072E-05
	2	1.39794E-01
	1	3.29130E-01
	2	8.89190E-01
	0.00000E+00	0.00000E+00
	1	2.07818E-02
	2	9.66689E-01
	1	5.11817E-02
	2	1.90717E+00
	1	1.63569E-05
	2	0.00000E+00
	1	8.41053E-05
	2	1.47824E-01
	1	3.23293E-01
	2	9.58139E-01
	0.00000E+00	0.00000E+00
	1	6.98072E-05
	2	1.39794E-01
	1	3.29130E-01
	2	8.89190E-01
	0.00000E+00	0.00000E+00
	1	2.07818E-02
	2	9.66689E-01
	1	5.11817E-02</td

			2	1.81594E-01	1.40037E-01	9.58607E-01	7.36949E-01	1.79573E+00	0.00000E+00
8	5	43	1	6.57168E-01	8.73701E-03	4.74646E-01	1.89499E-02	4.67514E-02	1.74114E-05
			2	1.82471E-01	1.38918E-01	9.57394E-01	7.30467E-01	1.77993E+00	0.00000E+00
9	5	44	1	6.53521E-01	8.89890E-03	4.77051E-01	1.92422E-02	4.74626E-02	1.75619E-05
			2	1.81984E-01	1.39335E-01	9.58148E-01	7.34181E-01	1.78898E+00	0.00000E+00
10	5	45	1	6.34260E-01	9.59240E-03	4.90894E-01	2.03851E-02	5.02240E-02	1.66954E-05
			2	1.76505E-01	1.46646E-01	9.65786E-01	7.76092E-01	1.89110E+00	0.00000E+00
11	5	46	1	1.03222E+00	8.49201E-05	3.22714E-01	0.00000E+00	0.00000E+00	0.00000E+00
			2	8.62567E-01	5.91264E-05	3.86384E-01	0.00000E+00	0.00000E+00	0.00000E+00
12	5	47	1	1.01746E+00	7.32225E-05	3.27423E-01	0.00000E+00	0.00000E+00	0.00000E+00
			2	8.58121E-01	6.13798E-05	3.88384E-01	0.00000E+00	0.00000E+00	0.00000E+00
6	6	48	1	1.02081E+00	7.70594E-05	3.26346E-01	0.00000E+00	0.00000E+00	0.00000E+00
			2	8.59962E-01	6.06549E-05	3.87554E-01	0.00000E+00	0.00000E+00	0.00000E+00
7	6	49	1	1.04471E+00	9.96445E-05	3.18813E-01	0.00000E+00	0.00000E+00	0.00000E+00
			2	8.67508E-01	5.72073E-05	3.84185E-01	0.00000E+00	0.00000E+00	0.00000E+00
8	6	50	1	6.43431E-01	9.22263E-03	4.84282E-01	1.97804E-02	4.87672E-02	1.81525E-05
			2	1.77545E-01	1.45298E-01	9.64308E-01	7.67848E-01	1.87101E+00	0.00000E+00
9	6	51	1	6.89799E-01	8.41800E-03	4.65768E-01	1.84294E-02	4.55152E-02	1.98155E-05
			2	1.81114E-01	1.40577E-01	9.59492E-01	7.40386E-01	1.80410E+00	0.00000E+00
10	6	52	1	6.43499E-01	9.24965E-03	4.84170E-01	1.98079E-02	4.88356E-02	1.84208E-05
			2	1.78662E-01	1.43573E-01	9.63021E-01	7.59132E-01	1.84977E+00	0.00000E+00
11	6	53	1	1.04645E+00	1.00795E-04	3.18275E-01	0.00000E+00	0.00000E+00	0.00000E+00
			2	8.64850E-01	5.79573E-05	3.85366E-01	0.00000E+00	0.00000E+00	0.00000E+00
12	6	54	1	1.02122E+00	7.58497E-05	3.28210E-01	0.00000E+00	0.00000E+00	0.00000E+00
			2	8.61508E-01	6.00371E-05	3.86859E-01	0.00000E+00	0.00000E+00	0.00000E+00

[STATISTICAL ERROR (%) LIST]

I	J	MODE	G	DIFF	ABSORPTION	ELSC	SCATT	FISSION	NU*FISSION	(N,2N)
1	1	1		1	6.50538E-01	2.34555E+00	6.50538E-01	4.60000E-01	4.60000E-01	4.60000E-01
				2	1.88809E+00	2.04353E+00	1.88809E+00	1.32000E+00	1.32000E+00	1.32000E+00
2	1	2		1	6.57647E-01	2.39460E+00	6.57647E-01	4.60000E-01	4.60000E-01	4.60000E-01
				2	1.88809E+00	2.03590E+00	1.88809E+00	1.32000E+00	1.32000E+00	1.32000E+00
3	1	3		1	4.80833E-01	1.53805E+00	4.80833E-01	3.40000E-01	3.40000E-01	3.40000E-01
				2	1.65469E+00	1.79513E+00	1.65469E+00	1.16000E+00	1.16000E+00	1.16000E+00
4	1	4		1	5.72800E-01	2.04941E+00	5.72800E-01	4.00000E-01	4.00000E-01	4.00000E-01
				2	1.78197E+00	1.92961E+00	1.78197E+00	1.25000E+00	1.25000E+00	1.25000E+00
5	1	5		1	4.80833E-01	1.55756E+00	4.80833E-01	3.40000E-01	3.40000E-01	3.40000E-01
				2	1.69012E+00	1.83861E+00	1.69012E+00	1.18000E+00	1.18000E+00	1.18000E+00
6	1	6		1	6.43506E-01	2.39270E+00	6.43506E-01	4.50000E-01	4.50000E-01	4.50000E-01
				2	1.90924E+00	2.04893E+00	1.90924E+00	1.34000E+00	1.34000E+00	1.34000E+00
7	1	7		1	6.57647E-01	2.41423E+00	6.57647E-01	4.60000E-01	4.60000E-01	4.60000E-01
				2	1.88096E+00	2.03590E+00	1.88096E+00	1.32000E+00	1.32000E+00	1.32000E+00
1	2	8		1	5.58659E-01	1.98862E+00	5.58659E-01	3.90000E-01	3.90000E-01	3.90000E-01
				2	1.76782E+00	1.91552E+00	1.76782E+00	1.24000E+00	1.24000E+00	1.24000E+00
2	2	9								

			1	4.73814E-01	1.49683E+00	4.73814E-01	3.30000E-01	3.30000E-01	3.30000E-01
			2	1.68297E+00	1.83096E+00	1.68297E+00	1.18000E+00	1.18000E+00	1.18000E+00
3	2	10	1	3.11448E-01	4.34166E-01	3.11448E-01	3.66197E-01	3.66197E-01	1.68315E+00
			2	9.97046E-01	1.01833E+00	1.00409E+00	1.01833E+00	1.01833E+00	7.10000E-01
4	2	11	1	3.11448E-01	4.34166E-01	3.11448E-01	3.66197E-01	3.66197E-01	1.67323E+00
			2	1.01119E+00	1.02533E+00	1.01119E+00	1.02533E+00	1.02533E+00	7.20000E-01
5	2	12	1	2.83196E-01	4.07063E-01	2.83196E-01	3.38378E-01	3.30151E-01	1.62117E+00
			2	1.02533E+00	1.04661E+00	1.02533E+00	1.04661E+00	1.04661E+00	7.30000E-01
6	2	13	1	3.11448E-01	4.34166E-01	3.11448E-01	3.66197E-01	3.66197E-01	1.68315E+00
			2	1.01119E+00	1.03247E+00	1.01119E+00	1.02533E+00	1.02533E+00	7.20000E-01
7	2	14	1	3.11448E-01	4.34166E-01	3.11448E-01	3.66197E-01	3.66197E-01	1.72285E+00
			2	1.00419E+00	1.02533E+00	1.01119E+00	1.02533E+00	1.02533E+00	7.20000E-01
8	2	15	1	4.73814E-01	1.57496E+00	4.73814E-01	3.30000E-01	3.30000E-01	3.30000E-01
			2	1.64770E+00	1.78869E+00	1.64770E+00	1.15000E+00	1.15000E+00	1.15000E+00
9	2	16	1	5.58659E-01	2.05730E+00	5.58659E-01	3.90000E-01	3.90000E-01	3.90000E-01
			2	1.73954E+00	1.87971E+00	1.73954E+00	1.22000E+00	1.22000E+00	1.22000E+00
1	3	17	1	6.36396E-01	2.28475E+00	6.36396E-01	4.50000E-01	4.50000E-01	4.50000E-01
			2	1.84567E+00	1.97841E+00	1.84567E+00	1.29000E+00	1.29000E+00	1.29000E+00
2	3	18	1	4.73814E-01	1.50659E+00	4.73814E-01	3.30000E-01	3.30000E-01	3.30000E-01
			2	1.67598E+00	1.81687E+00	1.67598E+00	1.17000E+00	1.17000E+00	1.17000E+00
3	3	19	1	3.11448E-01	4.34166E-01	3.11448E-01	3.66197E-01	3.58050E-01	1.70300E+00
			2	9.97046E-01	1.01833E+00	9.97046E-01	1.01833E+00	1.01833E+00	7.10000E-01
4	3	20	1	2.83196E-01	3.98246E-01	2.83196E-01	3.30151E-01	3.30151E-01	1.60131E+00
			2	1.02533E+00	1.04661E+00	1.02533E+00	1.04661E+00	1.04661E+00	7.30000E-01
5	3	21	1	3.18904E-01	5.51543E-01	3.18904E-01	2.10000E-01	2.10000E-01	5.52504E+01
			2	2.44659E+00	2.62179E+00	2.44659E+00	1.73000E+00	1.73000E+00	1.73000E+00
6	3	22	1	3.11448E-01	5.42310E-01	3.18904E-01	2.10000E-01	2.10000E-01	4.99304E+01
			2	2.41831E+00	2.56363E+00	2.41831E+00	1.71000E+00	1.71000E+00	1.71000E+00
7	3	23	1	2.61725E-01	3.75899E-01	2.61725E-01	3.16228E-01	3.08058E-01	1.48098E+00
			2	9.82904E-01	1.00419E+00	9.82904E-01	1.00419E+00	1.00419E+00	7.00000E-01
8	3	24	1	3.25576E-01	5.73847E-01	3.33017E-01	2.20000E-01	2.20000E-01	7.28803E+01
			2	2.37588E+00	2.57389E+00	2.37588E+00	1.68000E+00	1.68000E+00	1.68000E+00
9	3	25	1	3.04138E-01	4.25441E-01	3.04138E-01	3.58050E-01	3.58050E-01	1.70300E+00
			2	9.75910E-01	9.97046E-01	9.82904E-01	9.97046E-01	9.97046E-01	7.00000E-01
10	3	26	1	4.73814E-01	1.52611E+00	4.73814E-01	3.30000E-01	3.30000E-01	3.30000E-01
			2	1.64055E+00	1.78104E+00	1.64055E+00	1.15000E+00	1.15000E+00	1.15000E+00
11	3	27	1	6.29365E-01	2.35153E+00	6.29365E-01	4.40000E-01	4.40000E-01	4.40000E-01
			2	1.85267E+00	1.98494E+00	1.85267E+00	1.30000E+00	1.30000E+00	1.30000E+00
2	4	28	1	6.29365E-01	2.31225E+00	6.29365E-01	4.40000E-01	4.40000E-01	4.40000E-01
			2	1.83853E+00	1.98600E+00	1.83853E+00	1.29000E+00	1.29000E+00	1.29000E+00
3	4	29	1	4.59674E-01	1.48489E+00	4.59674E-01	3.20000E-01	3.20000E-01	3.20000E-01
			2	1.64770E+00	1.79636E+00	1.64770E+00	1.15000E+00	1.15000E+00	1.15000E+00
4	4	30	1	2.97321E-01	4.20595E-01	2.97321E-01	3.52278E-01	3.52278E-01	1.67200E+00
			2	9.82904E-01	1.00419E+00	9.82904E-01	1.00419E+00	1.00419E+00	7.00000E-01
5	4	31	1	2.69072E-01	3.93573E-01	2.69072E-01	3.24500E-01	3.16228E-01	1.52069E+00
			2	1.00409E+00	1.02552E+00	1.00409E+00	1.02552E+00	1.02552E+00	7.10000E-01

6	4	32
	1	3.11448E-01
	2	5.33104E-01
	1	2.33345E+00
	2	2.46402E+00
7	4	33
	1	2.47588E-01
	2	3.62353E-01
	1	9.54620E-01
	2	9.75910E-01
8	4	34
	1	2.40832E-01
	2	3.57771E-01
	1	9.47523E-01
	2	9.68969E-01
9	4	35
	1	2.61725E-01
	2	3.84708E-01
	1	9.75807E-01
	2	9.97246E-01
10	4	36
	1	2.97321E-01
	2	4.20595E-01
	1	9.68762E-01
	2	9.90050E-01
11	4	37
	1	4.59674E-01
	2	1.44586E+00
	1	1.61227E+00
	2	4.59674E-01
12	4	38
	1	6.29365E-01
	2	2.20436E+00
	1	1.83853E+00
	2	6.29365E-01
4	5	39
	1	5.44518E-01
	2	1.96705E+00
	1	1.87323E+00
	2	5.44518E-01
5	5	40
	1	4.45533E-01
	2	1.42415E+00
	1	1.89012E+00
	2	4.45533E-01
6	5	41
	1	2.97321E-01
	2	4.11825E-01
	1	9.82904E-01
	2	1.00419E+00
7	5	42
	1	2.83196E-01
	2	4.15933E-01
	1	1.06775E+00
	2	2.83196E-01
8	5	43
	1	2.54951E-01
	2	3.80132E-01
	1	9.97046E-01
	2	2.54951E-01
9	5	44
	1	2.83196E-01
	2	4.07063E-01
	1	1.05361E+00
	2	2.83196E-01
10	5	45
	1	2.83196E-01
	2	4.07063E-01
	1	9.68762E-01
	2	2.83196E-01
11	5	46
	1	4.45533E-01
	2	1.40464E+00
	1	1.66883E+00
	2	4.45533E-01
12	5	47
	1	5.30377E-01
	2	1.86703E+00
	1	1.69712E+00
	2	5.30377E-01
6	6	48
	1	5.86941E-01
	2	2.05139E+00
	1	2.18563E+00
	2	5.86941E-01
7	6	49
	1	5.51725E-01
	2	1.66397E+00
	1	2.26991E+00
	2	5.51725E-01
8	6	50
	1	3.61248E-01
	2	5.10000E-01
	1	1.25160E+00
	2	3.61248E-01
9	6	51
	1	4.11096E-01
	2	6.12699E-01
	1	1.64757E+00
	2	4.11096E-01
10	6	52
	1	3.53836E-01
	2	5.10000E-01
	1	1.25160E+00
	2	3.53836E-01
11	6	53
	1	5.44518E-01
	2	1.65424E+00
	1	2.28405E+00
	2	5.44518E-01
12	6	54
	1	5.86941E-01
	2	1.98285E+00
	1	5.86941E-01
	2	4.10000E-01
	1	4.10000E-01
	2	4.10000E-01

2 1.99409E+00 2.17154E+00 1.99409E+00 1.40000E+00 1.40000E+00 1.40000E+00

### E.3 Surface Fluxes

I	J	NODE	FACE	FAST FLUX	FAST FLUX ERROR	THERMAL FLUX	THERMAL FLUX ERROR
1	1	1	1	2.99367E-04	2.24525E-06	4.04622E-05	8.94215E-07
			2	9.54644E-04	6.49158E-06	1.02677E-04	2.05354E-06
			3	1.24902E-03	7.24432E-06	1.20716E-04	2.16082E-06
			4	0.00000E+00	0.00000E+00	0.00000E+00	0.00000E+00
			5	0.00000E+00	0.00000E+00	0.00000E+00	0.00000E+00
2	1	2	1	9.54644E-04	6.49158E-06	1.02677E-04	2.05354E-06
			2	1.24436E-03	7.21729E-06	1.21923E-04	2.24338E-06
			3	2.99990E-04	2.27992E-06	4.00029E-05	8.16059E-07
			4	0.00000E+00	0.00000E+00	0.00000E+00	0.00000E+00
			5	0.00000E+00	0.00000E+00	0.00000E+00	0.00000E+00
3	1	3	1	1.24436E-03	7.21729E-06	1.21923E-04	2.24338E-06
			2	1.45389E-03	7.85101E-06	1.24516E-04	2.29109E-06
			3	2.49748E-03	1.02397E-05	8.77618E-05	1.52706E-06
			4	0.00000E+00	0.00000E+00	0.00000E+00	0.00000E+00
			5	0.00000E+00	0.00000E+00	0.00000E+00	0.00000E+00
4	1	4	1	1.45389E-03	7.85101E-06	1.24516E-04	2.29109E-06
			2	1.45765E-03	7.87131E-06	1.24927E-04	2.28616E-06
			3	4.09711E-04	2.66312E-06	4.93458E-05	9.72112E-07
			4	0.00000E+00	0.00000E+00	0.00000E+00	0.00000E+00
			5	0.00000E+00	0.00000E+00	0.00000E+00	0.00000E+00
5	1	5	1	1.45765E-03	7.87131E-06	1.24927E-04	2.28616E-06
			2	1.24670E-03	7.23086E-06	1.22029E-04	2.20872E-06
			3	2.49078E-03	1.02122E-05	8.95098E-05	1.59327E-06
			4	0.00000E+00	0.00000E+00	0.00000E+00	0.00000E+00
			5	0.00000E+00	0.00000E+00	0.00000E+00	0.00000E+00
6	1	6	1	1.24670E-03	7.23086E-06	1.22029E-04	2.20872E-06
			2	9.67315E-04	6.57774E-06	1.12746E-04	2.17600E-06
			3	2.96286E-04	2.28140E-06	4.05314E-05	8.43053E-07
			4	0.00000E+00	0.00000E+00	0.00000E+00	0.00000E+00
			5	0.00000E+00	0.00000E+00	0.00000E+00	0.00000E+00
7	1	7	1	9.67315E-04	6.57774E-06	1.12746E-04	2.17600E-06
			2	2.96396E-04	2.19333E-06	4.22155E-05	9.03412E-07
			3	1.24192E-03	7.20314E-06	1.27442E-04	2.30670E-06
			4	0.00000E+00	0.00000E+00	0.00000E+00	0.00000E+00
			5	0.00000E+00	0.00000E+00	0.00000E+00	0.00000E+00
1	2	8					

			1	4.18132E-04	2.71786E-06	5.00849E-05	9.56622E-07
			2	1.45915E-03	7.87941E-06	1.21222E-04	2.14563E-06
			3	1.49097E-03	8.05124E-06	1.26120E-04	2.23232E-06
			4	0.00000E+00	0.00000E+00	0.00000E+00	0.00000E+00
			5	0.00000E+00	0.00000E+00	0.00000E+00	0.00000E+00
2	2	9	1	1.45915E-03	7.87941E-06	1.21222E-04	2.14563E-06
			2	2.51789E-03	1.03233E-05	9.19402E-05	1.61815E-06
			3	1.24902E-03	7.24432E-06	1.20716E-04	2.16082E-06
			4	0.00000E+00	0.00000E+00	0.00000E+00	0.00000E+00
			5	0.00000E+00	0.00000E+00	0.00000E+00	0.00000E+00
3	2	10	1	2.51789E-03	1.03233E-05	9.19402E-05	1.61815E-06
			2	2.95806E-03	1.03532E-05	3.47321E-05	8.99561E-07
			3	3.26329E-03	1.07689E-05	3.44675E-05	8.54794E-07
			4	0.00000E+00	0.00000E+00	0.00000E+00	0.00000E+00
			5	0.00000E+00	0.00000E+00	0.00000E+00	0.00000E+00
4	2	11	1	2.95806E-03	1.03532E-05	3.47321E-05	8.99561E-07
			2	3.20911E-03	1.05901E-05	3.41410E-05	8.39869E-07
			3	2.49748E-03	1.02397E-05	8.77618E-05	1.52706E-06
			4	0.00000E+00	0.00000E+00	0.00000E+00	0.00000E+00
			5	0.00000E+00	0.00000E+00	0.00000E+00	0.00000E+00
5	2	12	1	3.20911E-03	1.05901E-05	3.41410E-05	8.39869E-07
			2	3.21868E-03	1.09435E-05	3.43505E-05	8.45022E-07
			3	3.70529E-03	1.14864E-05	3.44204E-05	8.60510E-07
			4	0.00000E+00	0.00000E+00	0.00000E+00	0.00000E+00
			5	0.00000E+00	0.00000E+00	0.00000E+00	0.00000E+00
6	2	13	1	3.21868E-03	1.09435E-05	3.43505E-05	8.45022E-07
			2	2.94672E-03	1.03135E-05	3.39034E-05	9.01830E-07
			3	2.49078E-03	1.02122E-05	8.95098E-05	1.59327E-06
			4	0.00000E+00	0.00000E+00	0.00000E+00	0.00000E+00
			5	0.00000E+00	0.00000E+00	0.00000E+00	0.00000E+00
7	2	14	1	2.94672E-03	1.03135E-05	3.39034E-05	9.01830E-07
			2	2.50302E-03	1.02624E-05	9.19495E-05	1.57234E-06
			3	3.21227E-03	1.09217E-05	3.74616E-05	1.01146E-06
			4	0.00000E+00	0.00000E+00	0.00000E+00	0.00000E+00
			5	0.00000E+00	0.00000E+00	0.00000E+00	0.00000E+00
8	2	15	1	2.50302E-03	1.02624E-05	9.19495E-05	1.57234E-06
			2	1.47322E-03	7.95539E-06	1.22614E-04	2.17027E-06
			3	1.24192E-03	7.20314E-06	1.27442E-04	2.30670E-06
			4	0.00000E+00	0.00000E+00	0.00000E+00	0.00000E+00
			5	0.00000E+00	0.00000E+00	0.00000E+00	0.00000E+00
9	2	16					

			1	1.47322E-03	7.95539E-06	1.22614E-04	2.17027E-06
			2	4.10961E-04	2.67125E-06	5.03658E-05	9.87170E-07
			3	1.47894E-03	7.98628E-06	1.29600E-04	2.30688E-06
			4	0.00000E+00	0.00000E+00	0.00000E+00	0.00000E+00
			5	0.00000E+00	0.00000E+00	0.00000E+00	0.00000E+00
1	3	17	1	3.09393E-04	2.28951E-06	4.14318E-05	8.53495E-07
			2	1.29394E-03	7.37546E-06	1.31438E-04	2.36588E-06
			3	1.00844E-03	6.65570E-06	1.08504E-04	2.10498E-06
			4	0.00000E+00	0.00000E+00	0.00000E+00	0.00000E+00
			5	0.00000E+00	0.00000E+00	0.00000E+00	0.00000E+00
2	3	18	1	1.29394E-03	7.37546E-06	1.31438E-04	2.36588E-06
			2	2.57570E-03	1.03028E-05	9.47654E-05	1.61101E-06
			3	1.49097E-03	8.05124E-06	1.26120E-04	2.23232E-06
			4	0.00000E+00	0.00000E+00	0.00000E+00	0.00000E+00
			5	0.00000E+00	0.00000E+00	0.00000E+00	0.00000E+00
3	3	19	1	2.57570E-03	1.03028E-05	9.47654E-05	1.61101E-06
			2	3.28985E-03	1.08565E-05	3.57527E-05	9.11694E-07
			3	3.04998E-03	1.03699E-05	3.47580E-05	8.68950E-07
			4	0.00000E+00	0.00000E+00	0.00000E+00	0.00000E+00
			5	0.00000E+00	0.00000E+00	0.00000E+00	0.00000E+00
4	3	20	1	3.28985E-03	1.08565E-05	3.57527E-05	9.11694E-07
			2	3.74189E-03	1.15999E-05	3.56307E-05	8.83641E-07
			3	3.26329E-03	1.07689E-05	3.44675E-05	8.54794E-07
			4	0.00000E+00	0.00000E+00	0.00000E+00	0.00000E+00
			5	0.00000E+00	0.00000E+00	0.00000E+00	0.00000E+00
5	3	21	1	3.74189E-03	1.15999E-05	3.56307E-05	8.83641E-07
			2	3.77380E-03	1.16988E-05	3.63691E-05	9.31049E-07
			3	3.83194E-03	1.18790E-05	3.57187E-05	9.07255E-07
			4	0.00000E+00	0.00000E+00	0.00000E+00	0.00000E+00
			5	0.00000E+00	0.00000E+00	0.00000E+00	0.00000E+00
6	3	22	1	3.77380E-03	1.16988E-05	3.63691E-05	9.31049E-07
			2	3.96572E-03	1.18972E-05	3.62081E-05	9.05203E-07
			3	3.70529E-03	1.14864E-05	3.44204E-05	8.60510E-07
			4	0.00000E+00	0.00000E+00	0.00000E+00	0.00000E+00
			5	0.00000E+00	0.00000E+00	0.00000E+00	0.00000E+00
7	3	23	1	3.96572E-03	1.18972E-05	3.62081E-05	9.05203E-07
			2	3.73256E-03	1.15709E-05	3.61727E-05	8.97083E-07
			3	4.20241E-03	1.21870E-05	3.79968E-05	9.04324E-07
			4	0.00000E+00	0.00000E+00	0.00000E+00	0.00000E+00
			5	0.00000E+00	0.00000E+00	0.00000E+00	0.00000E+00
8	3	24					

			1	3.73256E-03	1.15709E-05	3.61727E-05	8.97083E-07
			2	3.28090E-03	1.08270E-05	3.78069E-05	9.64076E-07
			3	3.21227E-03	1.09217E-05	3.74616E-05	1.01146E-06
			4	0.00000E+00	0.00000E+00	0.00000E+00	0.00000E+00
			5	0.00000E+00	0.00000E+00	0.00000E+00	0.00000E+00
9	3	25	1	3.28090E-03	1.08270E-05	3.78069E-05	9.64076E-07
			2	2.57865E-03	1.03146E-05	9.54931E-05	1.60428E-06
			3	3.13644E-03	1.06639E-05	3.49621E-05	9.05518E-07
			4	0.00000E+00	0.00000E+00	0.00000E+00	0.00000E+00
			5	0.00000E+00	0.00000E+00	0.00000E+00	0.00000E+00
10	3	26	1	2.57865E-03	1.03146E-05	9.54931E-05	1.60428E-06
			2	1.30414E-03	7.43360E-06	1.31791E-04	2.35906E-06
			3	1.47894E-03	7.98628E-06	1.29600E-04	2.30688E-06
			4	0.00000E+00	0.00000E+00	0.00000E+00	0.00000E+00
			5	0.00000E+00	0.00000E+00	0.00000E+00	0.00000E+00
11	3	27	1	1.30414E-03	7.43360E-06	1.31791E-04	2.35906E-06
			2	3.14089E-04	2.26144E-06	4.21163E-05	8.33903E-07
			3	1.02057E-03	6.73576E-06	1.20286E-04	2.24935E-06
			4	0.00000E+00	0.00000E+00	0.00000E+00	0.00000E+00
			5	0.00000E+00	0.00000E+00	0.00000E+00	0.00000E+00
2	4	28	1	3.18026E-04	2.35339E-06	4.22761E-05	8.24384E-07
			2	1.32220E-03	7.40432E-06	1.32373E-04	2.35624E-06
			3	1.00844E-03	6.65570E-06	1.08504E-04	2.10498E-06
			4	0.00000E+00	0.00000E+00	0.00000E+00	0.00000E+00
			5	0.00000E+00	0.00000E+00	0.00000E+00	0.00000E+00
3	4	29	1	1.32220E-03	7.40432E-06	1.32373E-04	2.35624E-06
			2	2.66718E-03	1.06687E-05	9.61146E-05	1.61473E-06
			3	1.57036E-03	8.16587E-06	1.27763E-04	2.23585E-06
			4	0.00000E+00	0.00000E+00	0.00000E+00	0.00000E+00
			5	0.00000E+00	0.00000E+00	0.00000E+00	0.00000E+00
4	4	30	1	2.66718E-03	1.06687E-05	9.61146E-05	1.61473E-06
			2	3.40882E-03	1.09082E-05	3.69901E-05	9.39548E-07
			3	3.04998E-03	1.03699E-05	3.47580E-05	8.68950E-07
			4	0.00000E+00	0.00000E+00	0.00000E+00	0.00000E+00
			5	0.00000E+00	0.00000E+00	0.00000E+00	0.00000E+00
5	4	31	1	3.40882E-03	1.09082E-05	3.69901E-05	9.39548E-07
			2	3.89911E-03	1.16973E-05	3.72134E-05	9.78712E-07
			3	3.53365E-03	1.13077E-05	3.59356E-05	9.27139E-07
			4	0.00000E+00	0.00000E+00	0.00000E+00	0.00000E+00
			5	0.00000E+00	0.00000E+00	0.00000E+00	0.00000E+00
6	4	32					

			1	3.89911E-03	1.16973E-05	3.72134E-05	9.78712E-07
			2	4.14069E-03	1.20080E-05	3.53382E-05	8.76387E-07
			3	3.83194E-03	1.18790E-05	3.57187E-05	9.07255E-07
			4	0.00000E+00	0.00000E+00	0.00000E+00	0.00000E+00
			5	0.00000E+00	0.00000E+00	0.00000E+00	0.00000E+00
7	4	33	1	4.14069E-03	1.20080E-05	3.53382E-05	8.76387E-07
			2	4.37817E-03	1.22589E-05	4.02416E-05	1.00604E-06
			3	4.21473E-03	1.22227E-05	3.79360E-05	9.10464E-07
			4	0.00000E+00	0.00000E+00	0.00000E+00	0.00000E+00
			5	0.00000E+00	0.00000E+00	0.00000E+00	0.00000E+00
8	4	34	1	4.37817E-03	1.22589E-05	4.02416E-05	1.00604E-06
			2	4.13169E-03	1.19819E-05	3.69304E-05	8.75251E-07
			3	4.20241E-03	1.21870E-05	3.79968E-05	9.04324E-07
			4	0.00000E+00	0.00000E+00	0.00000E+00	0.00000E+00
			5	0.00000E+00	0.00000E+00	0.00000E+00	0.00000E+00
9	4	35	1	4.13169E-03	1.19819E-05	3.69304E-05	8.75251E-07
			2	3.54039E-03	1.13292E-05	3.65725E-05	9.03341E-07
			3	3.66785E-03	1.13703E-05	3.75999E-05	8.79838E-07
			4	0.00000E+00	0.00000E+00	0.00000E+00	0.00000E+00
			5	0.00000E+00	0.00000E+00	0.00000E+00	0.00000E+00
10	4	36	1	3.54039E-03	1.13292E-05	3.65725E-05	9.03341E-07
			2	2.73233E-03	1.06561E-05	9.87783E-05	1.60021E-06
			3	3.13644E-03	1.06639E-05	3.49621E-05	9.05518E-07
			4	0.00000E+00	0.00000E+00	0.00000E+00	0.00000E+00
			5	0.00000E+00	0.00000E+00	0.00000E+00	0.00000E+00
11	4	37	1	2.73233E-03	1.06561E-05	9.87783E-05	1.60021E-06
			2	1.34842E-03	7.41631E-06	1.38794E-04	2.47053E-06
			3	1.63199E-03	8.48635E-06	1.38334E-04	2.36551E-06
			4	0.00000E+00	0.00000E+00	0.00000E+00	0.00000E+00
			5	0.00000E+00	0.00000E+00	0.00000E+00	0.00000E+00
12	4	38	1	1.34842E-03	7.41631E-06	1.38794E-04	2.47053E-06
			2	3.22180E-04	2.31970E-06	4.40267E-05	8.80534E-07
			3	1.02057E-03	6.73576E-06	1.20286E-04	2.24935E-06
			4	0.00000E+00	0.00000E+00	0.00000E+00	0.00000E+00
			5	0.00000E+00	0.00000E+00	0.00000E+00	0.00000E+00
4	5	39	1	4.43271E-04	2.70395E-06	4.95365E-05	9.16425E-07
			2	1.59903E-03	8.15505E-06	1.28226E-04	2.34654E-06
			3	1.57036E-03	8.16587E-06	1.27763E-04	2.23585E-06
			4	0.00000E+00	0.00000E+00	0.00000E+00	0.00000E+00
			5	0.00000E+00	0.00000E+00	0.00000E+00	0.00000E+00
5	5	40					

			1	1.59903E-03	8.15505E-06	1.28226E-04	2.34654E-06
			2	2.76927E-03	1.05232E-05	8.70752E-05	1.49769E-06
			3	1.44940E-03	7.82676E-06	1.07002E-04	1.99024E-06
			4	0.00000E+00	0.00000E+00	0.00000E+00	0.00000E+00
			5	0.00000E+00	0.00000E+00	0.00000E+00	0.00000E+00
6	5	41	1	2.76927E-03	1.05232E-05	8.70752E-05	1.49769E-06
			2	3.34887E-03	1.10513E-05	3.56300E-05	9.40632E-07
			3	3.53365E-03	1.13077E-05	3.59356E-05	9.27139E-07
			4	0.00000E+00	0.00000E+00	0.00000E+00	0.00000E+00
			5	0.00000E+00	0.00000E+00	0.00000E+00	0.00000E+00
7	5	42	1	3.34887E-03	1.10513E-05	3.56300E-05	9.40632E-07
			2	3.65045E-03	1.13164E-05	3.23391E-05	8.27881E-07
			3	2.76721E-03	9.96196E-06	2.76798E-05	7.58426E-07
			4	0.00000E+00	0.00000E+00	0.00000E+00	0.00000E+00
			5	0.00000E+00	0.00000E+00	0.00000E+00	0.00000E+00
8	5	43	1	3.65045E-03	1.13164E-05	3.23391E-05	8.27881E-07
			2	3.71823E-03	1.15265E-05	3.38172E-05	8.35285E-07
			3	4.21473E-03	1.22227E-05	3.79360E-05	9.10464E-07
			4	0.00000E+00	0.00000E+00	0.00000E+00	0.00000E+00
			5	0.00000E+00	0.00000E+00	0.00000E+00	0.00000E+00
9	5	44	1	3.71823E-03	1.15265E-05	3.38172E-05	8.35285E-07
			2	3.43843E-03	1.10030E-05	3.46389E-05	8.69436E-07
			3	2.83952E-03	9.93832E-06	2.87344E-05	7.78702E-07
			4	0.00000E+00	0.00000E+00	0.00000E+00	0.00000E+00
			5	0.00000E+00	0.00000E+00	0.00000E+00	0.00000E+00
10	5	45	1	3.43843E-03	1.10030E-05	3.46389E-05	8.69436E-07
			2	2.89333E-03	1.09947E-05	9.30591E-05	1.58200E-06
			3	3.66785E-03	1.13703E-05	3.75999E-05	8.79838E-07
			4	0.00000E+00	0.00000E+00	0.00000E+00	0.00000E+00
			5	0.00000E+00	0.00000E+00	0.00000E+00	0.00000E+00
11	5	46	1	2.89333E-03	1.09947E-05	9.30591E-05	1.58200E-06
			2	1.66086E-03	8.30430E-06	1.33412E-04	2.37473E-06
			3	1.48643E-03	7.72944E-06	1.12936E-04	2.12320E-06
			4	0.00000E+00	0.00000E+00	0.00000E+00	0.00000E+00
			5	0.00000E+00	0.00000E+00	0.00000E+00	0.00000E+00
12	5	47	1	1.66086E-03	8.30430E-06	1.33412E-04	2.37473E-06
			2	4.64910E-04	2.83595E-06	5.21648E-05	9.18100E-07
			3	1.63199E-03	8.48635E-06	1.38334E-04	2.36551E-06
			4	0.00000E+00	0.00000E+00	0.00000E+00	0.00000E+00
			5	0.00000E+00	0.00000E+00	0.00000E+00	0.00000E+00
6	6	48					

			1	3.61048E-04	2.49123E-06	3.38603E-05	7.41541E-07
			2	1.19167E-03	7.15002E-06	7.78747E-05	1.76776E-06
			3	1.44940E-03	7.82676E-06	1.07002E-04	1.99024E-06
			4	0.00000E+00	0.00000E+00	0.00000E+00	0.00000E+00
			5	0.00000E+00	0.00000E+00	0.00000E+00	0.00000E+00
7	6	49	1	1.19167E-03	7.15002E-06	7.78747E-05	1.76776E-06
			2	1.71312E-03	8.22298E-06	4.41508E-05	1.12143E-06
			3	4.26177E-04	2.68491E-06	1.98191E-05	5.98537E-07
			4	0.00000E+00	0.00000E+00	0.00000E+00	0.00000E+00
			5	0.00000E+00	0.00000E+00	0.00000E+00	0.00000E+00
8	6	50	1	1.71312E-03	8.22298E-06	4.41508E-05	1.12143E-06
			2	1.87547E-03	8.25207E-06	1.70029E-05	6.92018E-07
			3	2.76721E-03	9.96196E-06	2.76798E-05	7.58426E-07
			4	0.00000E+00	0.00000E+00	0.00000E+00	0.00000E+00
			5	0.00000E+00	0.00000E+00	0.00000E+00	0.00000E+00
9	6	51	1	1.87547E-03	8.25207E-06	1.70029E-05	6.92018E-07
			2	1.90786E-03	8.39458E-06	1.69106E-05	5.93562E-07
			3	6.33853E-04	3.29604E-06	3.73255E-06	2.69117E-07
			4	0.00000E+00	0.00000E+00	0.00000E+00	0.00000E+00
			5	0.00000E+00	0.00000E+00	0.00000E+00	0.00000E+00
10	6	52	1	1.90786E-03	8.39458E-06	1.69106E-05	5.93562E-07
			2	1.74769E-03	8.21414E-06	4.44153E-05	1.10594E-06
			3	2.83952E-03	9.93832E-06	2.87344E-05	7.78702E-07
			4	0.00000E+00	0.00000E+00	0.00000E+00	0.00000E+00
			5	0.00000E+00	0.00000E+00	0.00000E+00	0.00000E+00
11	6	53	1	1.74769E-03	8.21414E-06	4.44153E-05	1.10594E-06
			2	1.21841E-03	7.31046E-06	7.76849E-05	1.73237E-06
			3	4.37865E-04	2.80234E-06	2.03333E-05	5.95766E-07
			4	0.00000E+00	0.00000E+00	0.00000E+00	0.00000E+00
			5	0.00000E+00	0.00000E+00	0.00000E+00	0.00000E+00
12	6	54	1	1.21841E-03	7.31046E-06	7.76849E-05	1.73237E-06
			2	3.72613E-04	2.49651E-06	3.67305E-05	7.93379E-07
			3	1.48643E-03	7.72944E-06	1.12936E-04	2.12320E-06
			4	0.00000E+00	0.00000E+00	0.00000E+00	0.00000E+00
			5	0.00000E+00	0.00000E+00	0.00000E+00	0.00000E+00

## E.4 Surface Currents

I	J	NODE	FACE	FAST CURRENT	ERROR	THERMAL CURRENT	ERROR
1	1	1	1	9.93988E-03	5.56633E-05	1.23551E-03	1.87798E-05
			2	7.88216E-05	5.91398E-05	-7.39455E-06	-7.39455E-06
			3	1.10847E-02	7.09421E-05	1.59081E-04	1.98851E-05
			4	0.00000E+00	0.00000E+00	0.00000E+00	0.00000E+00
			5	0.00000E+00	0.00000E+00	0.00000E+00	0.00000E+00
2	1	2	1	7.88216E-05	5.91398E-05	-7.39455E-06	-7.39455E-06
			2	1.09122E-02	7.09293E-05	1.63326E-04	1.97788E-05
			3	9.90340E-03	5.54590E-05	1.24599E-03	1.88144E-05
			4	0.00000E+00	0.00000E+00	0.00000E+00	0.00000E+00
			5	0.00000E+00	0.00000E+00	0.00000E+00	0.00000E+00
3	1	3	1	1.09122E-02	7.09293E-05	1.63326E-04	1.97788E-05
			2	7.37048E-03	7.44418E-05	1.03367E-04	2.00119E-05
			3	1.99525E-02	9.57720E-05	-1.40319E-03	-2.27317E-05
			4	0.00000E+00	0.00000E+00	0.00000E+00	0.00000E+00
			5	0.00000E+00	0.00000E+00	0.00000E+00	0.00000E+00
4	1	4	1	7.37048E-03	7.44418E-05	1.03367E-04	2.00119E-05
			2	7.42753E-03	7.50180E-05	6.81038E-05	2.00702E-05
			3	1.34836E-02	6.47213E-05	1.48981E-03	2.05594E-05
			4	0.00000E+00	0.00000E+00	0.00000E+00	0.00000E+00
			5	0.00000E+00	0.00000E+00	0.00000E+00	0.00000E+00
5	1	5	1	7.42753E-03	7.50180E-05	6.81038E-05	2.00702E-05
			2	1.09652E-02	7.01773E-05	1.43112E-04	1.99355E-05
			3	2.00484E-02	9.42275E-05	-1.44617E-03	-2.27049E-05
			4	0.00000E+00	0.00000E+00	0.00000E+00	0.00000E+00
			5	0.00000E+00	0.00000E+00	0.00000E+00	0.00000E+00
6	1	6	1	1.09652E-02	7.01773E-05	1.43112E-04	1.99355E-05
			2	-7.45540E-05	-5.91213E-05	-7.85407E-06	-7.85407E-06
			3	9.76801E-03	5.47009E-05	1.25852E-03	1.88778E-05
			4	0.00000E+00	0.00000E+00	0.00000E+00	0.00000E+00
			5	0.00000E+00	0.00000E+00	0.00000E+00	0.00000E+00
7	1	7	1	-7.45540E-05	-5.91213E-05	-7.85407E-06	-7.85407E-06
			2	9.91143E-03	5.55040E-05	1.29737E-03	1.92011E-05
			3	1.09461E-02	7.00550E-05	1.82830E-04	2.03124E-05
			4	0.00000E+00	0.00000E+00	0.00000E+00	0.00000E+00
			5	0.00000E+00	0.00000E+00	0.00000E+00	0.00000E+00
1	2	8					

			1	1.36396E-02	6.54701E-05	1.52627E-03	2.07573E-05
			2	-7.25600E-03	-7.47368E-05	-9.43469E-05	-2.00487E-05
			3	7.70114E-03	7.54712E-05	1.13024E-04	2.04234E-05
			4	0.00000E+00	0.00000E+00	0.00000E+00	0.00000E+00
			5	0.00000E+00	0.00000E+00	0.00000E+00	0.00000E+00
2	2	9	1	-7.25600E-03	-7.47368E-05	-9.43469E-05	-2.00487E-05
			2	2.00017E-02	9.60082E-05	-1.41955E-03	-2.29967E-05
			3	1.10847E-02	7.09421E-05	1.59081E-04	1.98851E-05
			4	0.00000E+00	0.00000E+00	0.00000E+00	0.00000E+00
			5	0.00000E+00	0.00000E+00	0.00000E+00	0.00000E+00
3	2	10	1	2.00017E-02	9.60082E-05	-1.41955E-03	-2.29967E-05
			2	-1.73902E-05	-1.73902E-05	2.42452E-06	2.42452E-06
			3	7.96140E-03	1.27382E-04	-5.24363E-06	-5.24363E-06
			4	0.00000E+00	0.00000E+00	0.00000E+00	0.00000E+00
			5	0.00000E+00	0.00000E+00	0.00000E+00	0.00000E+00
4	2	11	1	-1.73902E-05	-1.73902E-05	2.42452E-06	2.42452E-06
			2	8.07707E-03	1.26810E-04	-1.83207E-05	-1.44037E-05
			3	1.99525E-02	9.57720E-05	-1.40319E-03	-2.27317E-05
			4	0.00000E+00	0.00000E+00	0.00000E+00	0.00000E+00
			5	0.00000E+00	0.00000E+00	0.00000E+00	0.00000E+00
5	2	12	1	8.07707E-03	1.26810E-04	-1.83207E-05	-1.44037E-05
			2	8.37234E-03	1.26422E-04	-9.75118E-06	-9.75118E-06
			3	5.37240E-03	1.33236E-04	1.36392E-05	1.33705E-05
			4	0.00000E+00	0.00000E+00	0.00000E+00	0.00000E+00
			5	0.00000E+00	0.00000E+00	0.00000E+00	0.00000E+00
6	2	13	1	8.37234E-03	1.26422E-04	-9.75118E-06	-9.75118E-06
			2	-5.45836E-04	-1.20193E-04	-1.02729E-05	-1.02729E-05
			3	2.00484E-02	9.42275E-05	-1.44617E-03	-2.27049E-05
			4	0.00000E+00	0.00000E+00	0.00000E+00	0.00000E+00
			5	0.00000E+00	0.00000E+00	0.00000E+00	0.00000E+00
7	2	14	1	-5.45836E-04	-1.20193E-04	-1.02729E-05	-1.02729E-05
			2	1.97129E-02	9.46219E-05	-1.45430E-03	-2.29779E-05
			3	7.06008E-03	1.24257E-04	1.22587E-05	1.22587E-05
			4	0.00000E+00	0.00000E+00	0.00000E+00	0.00000E+00
			5	0.00000E+00	0.00000E+00	0.00000E+00	0.00000E+00
8	2	15	1	1.97129E-02	9.46219E-05	-1.45430E-03	-2.29779E-05
			2	-7.06035E-03	-7.48397E-05	-7.17281E-05	-2.03923E-05
			3	1.09461E-02	7.00550E-05	1.82830E-04	2.03124E-05
			4	0.00000E+00	0.00000E+00	0.00000E+00	0.00000E+00
			5	0.00000E+00	0.00000E+00	0.00000E+00	0.00000E+00
9	2	16					

			1	-7.06035E-03	-7.48397E-05	-7.17281E-05	-2.03923E-05
			2	1.34663E-02	6.46382E-05	1.53533E-03	2.08805E-05
			3	7.73053E-03	7.49861E-05	1.37408E-04	2.02677E-05
			4	0.00000E+00	0.00000E+00	0.00000E+00	0.00000E+00
			5	0.00000E+00	0.00000E+00	0.00000E+00	0.00000E+00
1	3	17	1	1.02788E-02	5.65334E-05	1.28801E-03	1.91913E-05
			2	-1.12650E-02	-7.20960E-05	-1.37206E-04	-2.04849E-05
			3	1.75700E-04	6.03529E-05	-1.13829E-05	-1.13829E-05
			4	0.00000E+00	0.00000E+00	0.00000E+00	0.00000E+00
			5	0.00000E+00	0.00000E+00	0.00000E+00	0.00000E+00
2	3	18	1	-1.12650E-02	-7.20960E-05	-1.37206E-04	-2.04849E-05
			2	2.06968E-02	9.72750E-05	-1.47698E-03	-2.31886E-05
			3	7.70114E-03	7.54712E-05	1.13024E-04	2.04234E-05
			4	0.00000E+00	0.00000E+00	0.00000E+00	0.00000E+00
			5	0.00000E+00	0.00000E+00	0.00000E+00	0.00000E+00
3	3	19	1	2.06968E-02	9.72750E-05	-1.47698E-03	-2.31886E-05
			2	-7.54386E-03	-1.28246E-04	3.26520E-05	1.42852E-05
			3	8.20269E-04	1.24025E-04	-1.06282E-05	-1.06282E-05
			4	0.00000E+00	0.00000E+00	0.00000E+00	0.00000E+00
			5	0.00000E+00	0.00000E+00	0.00000E+00	0.00000E+00
4	3	20	1	-7.54386E-03	-1.28246E-04	3.26520E-05	1.42852E-05
			2	4.10360E-03	1.32546E-04	-2.01779E-07	-2.01779E-07
			3	7.96140E-03	1.27382E-04	-5.24363E-06	-5.24363E-06
			4	0.00000E+00	0.00000E+00	0.00000E+00	0.00000E+00
			5	0.00000E+00	0.00000E+00	0.00000E+00	0.00000E+00
5	3	21	1	4.10360E-03	1.32546E-04	-2.01779E-07	-2.01779E-07
			2	-4.89590E-04	-1.32091E-04	-1.29067E-05	-1.26963E-05
			3	3.89086E-03	1.33067E-04	-1.17834E-05	-1.17834E-05
			4	0.00000E+00	0.00000E+00	0.00000E+00	0.00000E+00
			5	0.00000E+00	0.00000E+00	0.00000E+00	0.00000E+00
6	3	22	1	-4.89590E-04	-1.32091E-04	-1.29067E-05	-1.26963E-05
			2	6.13244E-03	1.36140E-04	3.64497E-05	1.34827E-05
			3	5.37240E-03	1.33236E-04	1.36392E-05	1.33705E-05
			4	0.00000E+00	0.00000E+00	0.00000E+00	0.00000E+00
			5	0.00000E+00	0.00000E+00	0.00000E+00	0.00000E+00
7	3	23	1	6.13244E-03	1.36140E-04	3.64497E-05	1.34827E-05
			2	1.28312E-02	1.32161E-04	2.41547E-05	1.38914E-05
			3	5.30949E-03	1.45480E-04	-1.21863E-05	-1.21863E-05
			4	0.00000E+00	0.00000E+00	0.00000E+00	0.00000E+00
			5	0.00000E+00	0.00000E+00	0.00000E+00	0.00000E+00
8	3	24					

			1	1.28312E-02	1.32161E-04	2.41547E-05	1.38914E-05
			2	-5.50395E-03	-1.24940E-04	-5.10263E-06	-5.10263E-06
			3	7.06008E-03	1.24257E-04	1.22587E-05	1.22587E-05
			4	0.00000E+00	0.00000E+00	0.00000E+00	0.00000E+00
			5	0.00000E+00	0.00000E+00	0.00000E+00	0.00000E+00
9	3	25	1	-5.50395E-03	-1.24940E-04	-5.10263E-06	-5.10263E-06
			2	2.07063E-02	9.73196E-05	-1.48351E-03	-2.32911E-05
			3	2.58182E-03	1.23927E-04	-1.65660E-06	-1.65660E-06
			4	0.00000E+00	0.00000E+00	0.00000E+00	0.00000E+00
			5	0.00000E+00	0.00000E+00	0.00000E+00	0.00000E+00
10	3	26	1	2.07063E-02	9.73196E-05	-1.48351E-03	-2.32911E-05
			2	-1.12253E-02	-7.18419E-05	-1.35803E-04	-2.05334E-05
			3	7.73053E-03	7.49861E-05	1.37408E-04	2.02677E-05
			4	0.00000E+00	0.00000E+00	0.00000E+00	0.00000E+00
			5	0.00000E+00	0.00000E+00	0.00000E+00	0.00000E+00
11	3	27	1	-1.12253E-02	-7.18419E-05	-1.35803E-04	-2.05334E-05
			2	1.04789E-02	5.65861E-05	1.32493E-03	1.93440E-05
			3	4.21712E-04	6.09374E-05	1.95642E-05	1.93060E-05
			4	0.00000E+00	0.00000E+00	0.00000E+00	0.00000E+00
			5	0.00000E+00	0.00000E+00	0.00000E+00	0.00000E+00
2	4	28	1	-1.04962E-02	-5.66795E-05	-1.30988E-03	-1.92552E-05
			2	1.18356E-02	7.21972E-05	1.31480E-04	2.04977E-05
			3	1.75700E-04	6.03529E-05	-1.13829E-05	-1.13829E-05
			4	0.00000E+00	0.00000E+00	0.00000E+00	0.00000E+00
			5	0.00000E+00	0.00000E+00	0.00000E+00	0.00000E+00
3	4	29	1	1.18356E-02	7.21972E-05	1.31480E-04	2.04977E-05
			2	-2.08464E-02	-9.79781E-05	1.52374E-03	2.34656E-05
			3	-7.26966E-03	-7.70584E-05	-9.15263E-05	-2.05568E-05
			4	0.00000E+00	0.00000E+00	0.00000E+00	0.00000E+00
			5	0.00000E+00	0.00000E+00	0.00000E+00	0.00000E+00
4	4	30	1	-2.08464E-02	-9.79781E-05	1.52374E-03	2.34656E-05
			2	9.21505E-03	1.30854E-04	-3.15297E-05	-1.47338E-05
			3	8.20269E-04	1.24025E-04	-1.06282E-05	-1.06282E-05
			4	0.00000E+00	0.00000E+00	0.00000E+00	0.00000E+00
			5	0.00000E+00	0.00000E+00	0.00000E+00	0.00000E+00
5	4	31	1	9.21505E-03	1.30854E-04	-3.15297E-05	-1.47338E-05
			2	-3.95182E-03	-1.35943E-04	-2.18438E-05	-1.34077E-05
			3	-6.55977E-03	-1.32507E-04	4.59805E-05	1.46172E-05
			4	0.00000E+00	0.00000E+00	0.00000E+00	0.00000E+00
			5	0.00000E+00	0.00000E+00	0.00000E+00	0.00000E+00
6	4	32					

			1	-3.95182E-03	-1.35943E-04	-2.18438E-05	-1.34077E-05
			2	8.12651E-03	1.39776E-04	1.62687E-05	1.34379E-05
			3	3.89086E-03	1.33067E-04	-1.17834E-05	-1.17834E-05
			4	0.00000E+00	0.00000E+00	0.00000E+00	0.00000E+00
			5	0.00000E+00	0.00000E+00	0.00000E+00	0.00000E+00
7	4	33	1	8.12651E-03	1.39776E-04	1.62687E-05	1.34379E-05
			2	-4.97668E-04	-1.49002E-04	1.32280E-05	1.32280E-05
			3	-5.24179E-03	-1.45722E-04	-3.23399E-05	-1.48861E-05
			4	0.00000E+00	0.00000E+00	0.00000E+00	0.00000E+00
			5	0.00000E+00	0.00000E+00	0.00000E+00	0.00000E+00
8	4	34	1	-4.97668E-04	-1.49002E-04	1.32280E-05	1.32280E-05
			2	-7.51939E-03	-1.45124E-04	-1.08046E-05	-1.08046E-05
			3	5.30949E-03	1.45480E-04	-1.21863E-05	-1.21863E-05
			4	0.00000E+00	0.00000E+00	0.00000E+00	0.00000E+00
			5	0.00000E+00	0.00000E+00	0.00000E+00	0.00000E+00
9	4	35	1	-7.51939E-03	-1.45124E-04	-1.08046E-05	-1.08046E-05
			2	1.16119E-02	1.33537E-04	-4.46054E-05	-1.47287E-05
			3	-7.98063E-03	-1.36469E-04	1.26780E-05	1.26780E-05
			4	0.00000E+00	0.00000E+00	0.00000E+00	0.00000E+00
			5	0.00000E+00	0.00000E+00	0.00000E+00	0.00000E+00
10	4	36	1	1.16119E-02	1.33537E-04	-4.46054E-05	-1.47287E-05
			2	-2.17712E-02	-1.00148E-04	1.54630E-03	2.38130E-05
			3	2.58182E-03	1.23927E-04	-1.65660E-06	-1.65660E-06
			4	0.00000E+00	0.00000E+00	0.00000E+00	0.00000E+00
			5	0.00000E+00	0.00000E+00	0.00000E+00	0.00000E+00
11	4	37	1	-2.17712E-02	-1.00148E-04	1.54630E-03	2.38130E-05
			2	1.23124E-02	7.38744E-05	1.52495E-04	2.10138E-05
			3	-7.60952E-03	-7.91390E-05	-1.52600E-04	-2.09367E-05
			4	0.00000E+00	0.00000E+00	0.00000E+00	0.00000E+00
			5	0.00000E+00	0.00000E+00	0.00000E+00	0.00000E+00
12	4	38	1	1.23124E-02	7.38744E-05	1.52495E-04	2.10138E-05
			2	-1.06817E-02	-5.76812E-05	-1.34308E-03	-1.96090E-05
			3	4.21712E-04	6.09374E-05	1.95642E-05	1.93060E-05
			4	0.00000E+00	0.00000E+00	0.00000E+00	0.00000E+00
			5	0.00000E+00	0.00000E+00	0.00000E+00	0.00000E+00
4	5	39	1	-1.46356E-02	-6.73238E-05	-1.52949E-03	-2.08011E-05
			2	8.78050E-03	7.81464E-05	2.23661E-05	2.02212E-05
			3	-7.26966E-03	-7.70584E-05	-9.15263E-05	-2.05568E-05
			4	0.00000E+00	0.00000E+00	0.00000E+00	0.00000E+00
			5	0.00000E+00	0.00000E+00	0.00000E+00	0.00000E+00
5	5	40					

			1	8.78050E-03	7.81464E-05	2.23661E-05	2.02212E-05
			2	-2.18260E-02	-1.00400E-04	1.36598E-03	2.24021E-05
			3	-1.13140E-02	-7.58038E-05	-3.44190E-04	-1.87239E-05
			4	0.00000E+00	0.00000E+00	0.00000E+00	0.00000E+00
			5	0.00000E+00	0.00000E+00	0.00000E+00	0.00000E+00
6	5	41	1	-2.18260E-02	-1.00400E-04	1.36598E-03	2.24021E-05
			2	2.64430E-03	1.29835E-04	-4.57057E-05	-1.43516E-05
			3	-6.55977E-03	-1.32507E-04	4.59805E-05	1.46172E-05
			4	0.00000E+00	0.00000E+00	0.00000E+00	0.00000E+00
			5	0.00000E+00	0.00000E+00	0.00000E+00	0.00000E+00
7	5	42	1	2.64430E-03	1.29835E-04	-4.57057E-05	-1.43516E-05
			2	-8.86758E-03	-1.36561E-04	-3.06226E-05	-1.38506E-05
			3	-1.67148E-02	-1.18675E-04	-4.53243E-06	-4.53243E-06
			4	0.00000E+00	0.00000E+00	0.00000E+00	0.00000E+00
			5	0.00000E+00	0.00000E+00	0.00000E+00	0.00000E+00
8	5	43	1	-8.86758E-03	-1.36561E-04	-3.06226E-05	-1.38506E-05
			2	-8.25309E-03	-1.37001E-04	-2.63173E-05	-1.39034E-05
			3	-5.24179E-03	-1.45722E-04	-3.23399E-05	-1.48861E-05
			4	0.00000E+00	0.00000E+00	0.00000E+00	0.00000E+00
			5	0.00000E+00	0.00000E+00	0.00000E+00	0.00000E+00
9	5	44	1	-8.25309E-03	-1.37001E-04	-2.63173E-05	-1.39034E-05
			2	1.72607E-03	1.31699E-04	-5.23911E-05	-1.43237E-05
			3	-1.71887E-02	-1.20321E-04	-9.71888E-06	-9.71888E-06
			4	0.00000E+00	0.00000E+00	0.00000E+00	0.00000E+00
			5	0.00000E+00	0.00000E+00	0.00000E+00	0.00000E+00
10	5	45	1	1.72607E-03	1.31699E-04	-5.23911E-05	-1.43237E-05
			2	-2.28350E-02	-1.02757E-04	1.42174E-03	2.27478E-05
			3	-7.98063E-03	-1.36469E-04	1.26780E-05	1.26780E-05
			4	0.00000E+00	0.00000E+00	0.00000E+00	0.00000E+00
			5	0.00000E+00	0.00000E+00	0.00000E+00	0.00000E+00
11	5	46	1	-2.28350E-02	-1.02757E-04	1.42174E-03	2.27478E-05
			2	9.13791E-03	8.04136E-05	3.10713E-05	2.06562E-05
			3	-1.18862E-02	-7.72603E-05	-3.60954E-04	-1.93832E-05
			4	0.00000E+00	0.00000E+00	0.00000E+00	0.00000E+00
			5	0.00000E+00	0.00000E+00	0.00000E+00	0.00000E+00
12	5	47	1	9.13791E-03	8.04136E-05	3.10713E-05	2.06562E-05
			2	-1.53127E-02	-6.89071E-05	-1.61775E-03	-2.13543E-05
			3	-7.60952E-03	-7.91390E-05	-1.52600E-04	-2.09367E-05
			4	0.00000E+00	0.00000E+00	0.00000E+00	0.00000E+00
			5	0.00000E+00	0.00000E+00	0.00000E+00	0.00000E+00
6	6	48					

			1	-1.19239E-02	-6.08119E-05	-1.07237E-03	-1.73724E-05
			2	1.66625E-03	6.66500E-05	-3.33747E-04	-1.60532E-05
			3	-1.13140E-02	-7.58038E-05	-3.44190E-04	-1.87239E-05
			4	0.00000E+00	0.00000E+00	0.00000E+00	0.00000E+00
			5	0.00000E+00	0.00000E+00	0.00000E+00	0.00000E+00
7	6	49	1	1.66625E-03	6.66500E-05	-3.33747E-04	-1.60532E-05
			2	-1.63581E-02	-8.34263E-05	5.85884E-04	1.54087E-05
			3	-1.38371E-02	-6.50344E-05	-6.06902E-04	-1.28663E-05
			4	0.00000E+00	0.00000E+00	0.00000E+00	0.00000E+00
			5	0.00000E+00	0.00000E+00	0.00000E+00	0.00000E+00
8	6	50	1	-1.63581E-02	-8.34263E-05	5.85884E-04	1.54087E-05
			2	-8.01241E-03	-9.77514E-05	-3.42790E-05	-9.87235E-06
			3	-1.67148E-02	-1.18675E-04	-4.53243E-06	-4.53243E-06
			4	0.00000E+00	0.00000E+00	0.00000E+00	0.00000E+00
			5	0.00000E+00	0.00000E+00	0.00000E+00	0.00000E+00
9	6	51	1	-8.01241E-03	-9.77514E-05	-3.42790E-05	-9.87235E-06
			2	-8.42323E-03	-9.85518E-05	-4.32033E-05	-1.00102E-05
			3	-2.08062E-02	-7.90636E-05	-1.06723E-04	-5.12270E-06
			4	0.00000E+00	0.00000E+00	0.00000E+00	0.00000E+00
			5	0.00000E+00	0.00000E+00	0.00000E+00	0.00000E+00
10	6	52	1	-8.42323E-03	-9.85518E-05	-4.32033E-05	-1.00102E-05
			2	-1.65693E-02	-8.45034E-05	5.71098E-04	1.56481E-05
			3	-1.71887E-02	-1.20321E-04	-9.71888E-06	-9.71888E-06
			4	0.00000E+00	0.00000E+00	0.00000E+00	0.00000E+00
			5	0.00000E+00	0.00000E+00	0.00000E+00	0.00000E+00
11	6	53	1	-1.65693E-02	-8.45034E-05	5.71098E-04	1.56481E-05
			2	1.61487E-03	6.75016E-05	-3.45782E-04	-1.63209E-05
			3	-1.41000E-02	-6.62700E-05	-6.35666E-04	-1.31583E-05
			4	0.00000E+00	0.00000E+00	0.00000E+00	0.00000E+00
			5	0.00000E+00	0.00000E+00	0.00000E+00	0.00000E+00
12	6	54	1	1.61487E-03	6.75016E-05	-3.45782E-04	-1.63209E-05
			2	-1.23892E-02	-6.19460E-05	-1.12694E-03	-1.78057E-05
			3	-1.18862E-02	-7.72603E-05	-3.60954E-04	-1.93832E-05
			4	0.00000E+00	0.00000E+00	0.00000E+00	0.00000E+00
			5	0.00000E+00	0.00000E+00	0.00000E+00	0.00000E+00

## E.5 CMFD Discontinuity Factors

I	J	NODE	FACE	FAST GROUP	THERMAL GROUP
1	1		1		
			1	1.11809E+00	1.70591E+00
			2	1.14895E+00	9.53569E-01
			3	8.50601E-01	1.02369E+00
			4	1.00000E+00	1.00000E+00
			5	1.00000E+00	1.00000E+00
2	1		2		
			1	1.14391E+00	9.99696E-01
			2	8.56462E-01	1.06719E+00
			3	1.13307E+00	2.10601E+00
			4	1.00000E+00	1.00000E+00
			5	1.00000E+00	1.00000E+00
3	1		3		
			1	1.14972E+00	1.01223E+00
			2	1.13496E+00	1.00032E+00
			3	8.87566E-01	2.36003E+00
			4	1.00000E+00	1.00000E+00
			5	1.00000E+00	1.00000E+00
4	1		4		
			1	9.58498E-01	1.01225E+00
			2	9.58926E-01	1.03559E+00
			3	1.23662E+00	3.14854E+00
			4	1.00000E+00	1.00000E+00
			5	1.00000E+00	1.00000E+00
5	1		5		
			1	1.13776E+00	1.00862E+00
			2	1.15150E+00	1.02694E+00
			3	8.82411E-01	2.85021E+00
			4	1.00000E+00	1.00000E+00
			5	1.00000E+00	1.00000E+00
6	1		6		
			1	8.54347E-01	1.09336E+00
			2	1.16678E+00	1.11154E+00
			3	1.07466E+00	2.36704E+00
			4	1.00000E+00	1.00000E+00
			5	1.00000E+00	1.00000E+00
7	1		7		
			1	1.14766E+00	1.05148E+00
			2	1.08992E+00	2.20683E+00
			3	8.48071E-01	1.07062E+00
			4	1.00000E+00	1.00000E+00
			5	1.00000E+00	1.00000E+00
1	2		8		
			1	1.20133E+00	3.53949E+00

			2	9.50030E-01	9.83364E-01
			3	9.55014E-01	1.01277E+00
			4	1.00000E+00	1.00000E+00
			5	1.00000E+00	1.00000E+00
2	2	9	1	1.11939E+00	9.36146E-01
			2	8.88782E-01	2.27156E+00
			3	1.14727E+00	9.64630E-01
			4	1.00000E+00	1.00000E+00
			5	1.00000E+00	1.00000E+00
3	2	10	1	2.32698E+00	1.82918E-01
			2	1.00981E+00	1.01696E+00
			3	8.91033E-01	1.03743E+00
			4	1.00000E+00	1.00000E+00
			5	1.00000E+00	1.00000E+00
4	2	11	1	1.01562E+00	9.74883E-01
			2	8.77001E-01	1.18491E+00
			3	2.32587E+00	1.77040E-01
			4	1.00000E+00	1.00000E+00
			5	1.00000E+00	1.00000E+00
5	2	12	1	1.19237E+00	8.72220E-01
			2	1.20791E+00	9.42925E-01
			3	9.48228E-01	9.13963E-01
			4	1.00000E+00	1.00000E+00
			5	1.00000E+00	1.00000E+00
6	2	13	1	8.74568E-01	1.07887E+00
			2	1.03119E+00	1.07061E+00
			3	2.35330E+00	1.74932E-01
			4	1.00000E+00	1.00000E+00
			5	1.00000E+00	1.00000E+00
7	2	14	1	9.98657E-01	8.70287E-01
			2	2.36386E+00	1.79097E-01
			3	9.02577E-01	9.45784E-01
			4	1.00000E+00	1.00000E+00
			5	1.00000E+00	1.00000E+00
8	2	15	1	8.87513E-01	2.47507E+00
			2	1.12190E+00	9.43357E-01
			3	1.13478E+00	1.04020E+00
			4	1.00000E+00	1.00000E+00
			5	1.00000E+00	1.00000E+00
9	2	16	1	9.66928E-01	9.82868E-01

			2	1.16463E+00	3.05498E+00
			3	9.46926E-01	1.00328E+00
			4	1.00000E+00	1.00000E+00
			5	1.00000E+00	1.00000E+00
1	3	17	1	1.09838E+00	1.94348E+00
			2	8.56521E-01	1.11919E+00
			3	1.14846E+00	1.01010E+00
			4	1.00000E+00	1.00000E+00
			5	1.00000E+00	1.00000E+00
2	3	18	1	1.16106E+00	1.05995E+00
			2	8.86064E-01	2.77724E+00
			3	1.13441E+00	1.00393E+00
			4	1.00000E+00	1.00000E+00
			5	1.00000E+00	1.00000E+00
3	3	19	1	2.36906E+00	1.81698E-01
			2	8.90740E-01	1.43591E+00
			3	9.92539E-01	1.08130E+00
			4	1.00000E+00	1.00000E+00
			5	1.00000E+00	1.00000E+00
4	3	20	1	1.18541E+00	8.04572E-01
			2	9.76879E-01	1.04742E+00
			3	1.19209E+00	9.64270E-01
			4	1.00000E+00	1.00000E+00
			5	1.00000E+00	1.00000E+00
5	3	21	1	1.03815E+00	1.00420E+00
			2	1.01047E+00	1.01953E+00
			3	1.00019E+00	1.01180E+00
			4	1.00000E+00	1.00000E+00
			5	1.00000E+00	1.00000E+00
6	3	22	1	1.01013E+00	1.01388E+00
			2	1.00997E+00	9.88983E-01
			3	1.03057E+00	9.59845E-01
			4	1.00000E+00	1.00000E+00
			5	1.00000E+00	1.00000E+00
7	3	23	1	1.13698E+00	1.41806E+00
			2	1.29252E+00	1.22896E+00
			3	9.31175E-01	1.14345E+00
			4	1.00000E+00	1.00000E+00
			5	1.00000E+00	1.00000E+00
8	3	24	1	1.00850E+00	9.59960E-01

			2	1.03425E+00	1.01518E+00
			3	1.02715E+00	1.00883E+00
			4	1.00000E+00	1.00000E+00
			5	1.00000E+00	1.00000E+00
9	3	25	1	9.24496E-01	9.72801E-01
			2	2.31379E+00	1.82104E-01
			3	9.56977E-01	9.54097E-01
			4	1.00000E+00	1.00000E+00
			5	1.00000E+00	1.00000E+00
10	3	26	1	8.78341E-01	2.53053E+00
			2	1.14340E+00	1.02815E+00
			3	1.10612E+00	1.01191E+00
			4	1.00000E+00	1.00000E+00
			5	1.00000E+00	1.00000E+00
11	3	27	1	8.54915E-01	1.11396E+00
			2	1.09413E+00	2.15640E+00
			3	1.12270E+00	1.08907E+00
			4	1.00000E+00	1.00000E+00
			5	1.00000E+00	1.00000E+00
2	4	28	1	1.10968E+00	1.94189E+00
			2	8.46968E-01	1.10992E+00
			3	1.15172E+00	9.76283E-01
			4	1.00000E+00	1.00000E+00
			5	1.00000E+00	1.00000E+00
3	4	29	1	1.13912E+00	1.00249E+00
			2	8.90689E-01	2.49869E+00
			3	1.10829E+00	9.48288E-01
			4	1.00000E+00	1.00000E+00
			5	1.00000E+00	1.00000E+00
4	4	30	1	2.30322E+00	1.78459E-01
			2	8.67345E-01	1.39429E+00
			3	1.01505E+00	8.60143E-01
			4	1.00000E+00	1.00000E+00
			5	1.00000E+00	1.00000E+00
5	4	31	1	1.20202E+00	8.19563E-01
			2	9.70263E-01	8.84990E-01
			3	1.14938E+00	7.22533E-01
			4	1.00000E+00	1.00000E+00
			5	1.00000E+00	1.00000E+00
6	4	32	1	1.02558E+00	1.05051E+00

			2	9.97672E-01	9.81748E-01
			3	1.00745E+00	9.94175E-01
			4	1.00000E+00	1.00000E+00
			5	1.00000E+00	1.00000E+00
7	4	33	1	1.15315E+00	1.05793E+00
			2	1.00523E+00	1.17088E+00
			3	1.09573E+00	1.34047E+00
			4	1.00000E+00	1.00000E+00
			5	1.00000E+00	1.00000E+00
8	4	34	1	1.02604E+00	9.32661E-01
			2	1.13276E+00	1.04005E+00
			3	1.09368E+00	8.87444E-01
			4	1.00000E+00	1.00000E+00
			5	1.00000E+00	1.00000E+00
9	4	35	1	9.14961E-01	9.27363E-01
			2	1.25583E+00	7.23325E-01
			3	1.16767E+00	9.30271E-01
			4	1.00000E+00	1.00000E+00
			5	1.00000E+00	1.00000E+00
10	4	36	1	8.34746E-01	1.58458E+00
			2	2.31820E+00	1.80960E-01
			3	1.06714E+00	9.13274E-01
			4	1.00000E+00	1.00000E+00
			5	1.00000E+00	1.00000E+00
11	4	37	1	8.83224E-01	2.59921E+00
			2	1.13904E+00	1.05493E+00
			3	1.12758E+00	1.05149E+00
			4	1.00000E+00	1.00000E+00
			5	1.00000E+00	1.00000E+00
12	4	38	1	8.39876E-01	1.15175E+00
			2	1.09595E+00	2.23773E+00
			3	1.16082E+00	1.10448E+00
			4	1.00000E+00	1.00000E+00
			5	1.00000E+00	1.00000E+00
4	5	39	1	1.15987E+00	2.46537E+00
			2	9.33355E-01	1.03041E+00
			3	9.64994E-01	9.89702E-01
			4	1.00000E+00	1.00000E+00
			5	1.00000E+00	1.00000E+00
5	5	40	1	1.11650E+00	9.93794E-01

			2	8.80924E-01	2.22454E+00
			3	1.12311E+00	9.95389E-01
			4	1.00000E+00	1.00000E+00
			5	1.00000E+00	1.00000E+00
6	5	41	1	2.18014E+00	1.79867E-01
			2	9.54584E-01	1.62076E+00
			3	9.13963E-01	1.64138E+00
			4	1.00000E+00	1.00000E+00
			5	1.00000E+00	1.00000E+00
7	5	42	1	1.08518E+00	7.80750E-01
			2	8.89238E-01	7.91845E-01
			3	1.50361E+00	9.33137E-01
			4	1.00000E+00	1.00000E+00
			5	1.00000E+00	1.00000E+00
8	5	43	1	1.16422E+00	1.24953E+00
			2	1.16576E+00	1.24131E+00
			3	9.63342E-01	8.28249E-01
			4	1.00000E+00	1.00000E+00
			5	1.00000E+00	1.00000E+00
9	5	44	1	9.04436E-01	8.46661E-01
			2	1.06469E+00	7.18443E-01
			3	1.52379E+00	1.00790E+00
			4	1.00000E+00	1.00000E+00
			5	1.00000E+00	1.00000E+00
10	5	45	1	9.69610E-01	1.64151E+00
			2	2.20786E+00	1.84901E-01
			3	8.91221E-01	1.10289E+00
			4	1.00000E+00	1.00000E+00
			5	1.00000E+00	1.00000E+00
11	5	46	1	8.83034E-01	2.56352E+00
			2	1.11599E+00	1.03113E+00
			3	1.11383E+00	1.05249E+00
			4	1.00000E+00	1.00000E+00
			5	1.00000E+00	1.00000E+00
12	5	47	1	9.35746E-01	1.04242E+00
			2	1.19985E+00	3.05978E+00
			3	9.66718E-01	1.01597E+00
			4	1.00000E+00	1.00000E+00
			5	1.00000E+00	1.00000E+00
6	6	48	1	1.06861E+00	1.96832E+00

			2	1.07697E+00	1.16594E+00
			3	8.77277E-01	9.52774E-01
			4	1.00000E+00	1.00000E+00
			5	1.00000E+00	1.00000E+00
7	6	49	1	1.15980E+00	9.77229E-01
			2	8.46580E-01	2.38842E+00
			3	1.20096E+00	1.15993E+00
			4	1.00000E+00	1.00000E+00
			5	1.00000E+00	1.00000E+00
8	6	50	1	2.38630E+00	2.07096E-01
			2	1.27865E+00	1.47567E+00
			3	7.50831E-01	1.14649E+00
			4	1.00000E+00	1.00000E+00
			5	1.00000E+00	1.00000E+00
9	6	51	1	8.41867E-01	7.05296E-01
			2	8.43006E-01	6.27426E-01
			3	-2.47267E+00	-1.79099E-01
			4	1.00000E+00	1.00000E+00
			5	1.00000E+00	1.00000E+00
10	6	52	1	1.31609E+00	1.94010E+00
			2	2.43148E+00	2.14329E-01
			3	7.57699E-01	1.11295E+00
			4	1.00000E+00	1.00000E+00
			5	1.00000E+00	1.00000E+00
11	6	53	1	8.48803E-01	2.10126E+00
			2	1.15408E+00	9.43398E-01
			3	1.19338E+00	1.20837E+00
			4	1.00000E+00	1.00000E+00
			5	1.00000E+00	1.00000E+00
12	6	54	1	1.07399E+00	1.15700E+00
			2	1.08715E+00	2.48294E+00
			3	8.66642E-01	9.86287E-01
			4	1.00000E+00	1.00000E+00
			5	1.00000E+00	1.00000E+00

## **Appendix F**

# **Scattering Cross Sections for the Test Problem**

**F.1** Introduction

**F.2** Set A

**F.3** Set B

**F.4** Set C

## F.1 Introduction

Three sets of scattering cross sections ( $\Sigma_{21}$ ) from the fast to thermal group are listed in this Appendix. These cross sections are computed with different methods:

- Set A:  $\Sigma_{21}$  for the fuel and non-fuel region are computed from thermal neutron balance.
- Set B:  $\Sigma_{21}$  for the fuel region are computed from thermal neutron balance. Scattering cross sections for the non-fuel region are computed from fast-neutron balance.
- Set C:  $\Sigma_{21}$  for the fuel and non-fuel region are computed from the approximate method<sup>1</sup> described by Equation (6.6) in Section 6.5.2.

The next three sections will list these scattering cross sections.

---

<sup>1</sup>For non-fuel region, Equation (6.6) reduces to a form exactly the same as derived from fast neutron balance.

## F.2 Set A

I	J	NODE	SCAT. XS (FAST-TO-THERMAL)
1	1	1	4.89423E-03
2	1	2	5.02215E-03
3	1	3	3.76744E-03
4	1	4	4.59165E-03
5	1	5	3.73170E-03
6	1	6	5.15446E-03
7	1	7	5.04684E-03
1	2	8	4.48904E-03
2	2	9	3.73894E-03
3	2	10	9.31769E-03
4	2	11	9.29237E-03
5	2	12	8.43098E-03
6	2	13	9.39882E-03
7	2	14	9.47062E-03
8	2	15	3.81912E-03
9	2	16	4.52408E-03
1	3	17	5.11976E-03
2	3	18	3.78129E-03
3	3	19	9.26212E-03
4	3	20	8.55966E-03
5	3	21	4.76756E-05
6	3	22	3.91686E-05
7	3	23	8.09270E-03
8	3	24	5.21078E-05
9	3	25	9.50702E-03
10	3	26	3.79066E-03
11	3	27	5.05390E-03
2	4	28	5.03931E-03
3	4	29	3.65955E-03
4	4	30	9.32405E-03
5	4	31	8.32156E-03
6	4	32	4.02532E-05
7	4	33	7.88181E-03
8	4	34	7.90633E-03
9	4	35	8.21213E-03
10	4	36	9.24921E-03
11	4	37	3.77732E-03
12	4	38	5.12326E-03
4	5	39	4.45811E-03
5	5	40	3.44376E-03
6	5	41	8.96508E-03
7	5	42	8.13341E-03
8	5	43	7.92368E-03
9	5	44	8.08199E-03

10	5	45	8.88280E-03
11	5	46	3.46769E-03
12	5	47	4.36440E-03
6	6	48	4.01091E-03
7	6	49	2.93266E-03
8	6	50	8.49922E-03
9	6	51	7.62659E-03
10	6	52	8.35160E-03
11	6	53	2.87451E-03
12	6	54	4.07450E-03

### F.3 Set B

I	J	NODE	SCAT. XS (FAST-TO-THERMAL)
1	1	1	4.80504E-03
2	1	2	4.93442E-03
3	1	3	3.68057E-03
4	1	4	4.49997E-03
5	1	5	3.64150E-03
6	1	6	5.07741E-03
7	1	7	4.98383E-03
1	2	8	4.40634E-03
2	2	9	3.62696E-03
3	2	10	9.31769E-03
4	2	11	9.29237E-03
5	2	12	8.43098E-03
6	2	13	9.39882E-03
7	2	14	9.47062E-03
8	2	15	3.73181E-03
9	2	16	4.44432E-03
1	3	17	5.04174E-03
2	3	18	3.70264E-03
3	3	19	9.26212E-03
4	3	20	8.55966E-03
5	3	21	5.07628E-05
6	3	22	3.96490E-05
7	3	23	8.09270E-03
8	3	24	5.26124E-05
9	3	25	9.50702E-03
10	3	26	3.69332E-03
11	3	27	4.96932E-03
2	4	28	4.94865E-03
3	4	29	3.56343E-03
4	4	30	9.32405E-03
5	4	31	8.32156E-03
6	4	32	3.60696E-05
7	4	33	7.88181E-03
8	4	34	7.90633E-03
9	4	35	8.21213E-03
10	4	36	9.24921E-03
11	4	37	3.68433E-03
12	4	38	5.04093E-03
4	5	39	4.37934E-03
5	5	40	3.35417E-03
6	5	41	8.96508E-03
7	5	42	8.13341E-03
8	5	43	7.92368E-03
9	5	44	8.08199E-03

10	5	45	8.88280E-03
11	5	46	3.37339E-03
12	5	47	4.28701E-03
6	6	48	3.90746E-03
7	6	49	2.81545E-03
8	6	50	8.49922E-03
9	6	51	7.62659E-03
10	6	52	8.35160E-03
11	6	53	2.74886E-03
12	6	54	3.99382E-03

#### F.4 Set C

I	J	NODE	SCAT. XS (FAST-TO-THERMAL)
1	1	1	4.80504E-03
2	1	2	4.93442E-03
3	1	3	3.68057E-03
4	1	4	4.49997E-03
5	1	5	3.64150E-03
6	1	6	5.07741E-03
7	1	7	4.98383E-03
1	2	8	4.40634E-03
2	2	9	3.62696E-03
3	2	10	9.16873E-03
4	2	11	9.08402E-03
5	2	12	8.71003E-03
6	2	13	9.61118E-03
7	2	14	9.35685E-03
8	2	15	3.73181E-03
9	2	16	4.44432E-03
1	3	17	5.04174E-03
2	3	18	3.70264E-03
3	3	19	9.31225E-03
4	3	20	9.03154E-03
5	3	21	5.07628E-05
6	3	22	3.96490E-05
7	3	23	1.03380E-02
8	3	24	5.26124E-05
9	3	25	9.43496E-03
10	3	26	3.69332E-03
11	3	27	4.96932E-03
2	4	28	4.94865E-03
3	4	29	3.56343E-03
4	4	30	8.89379E-03
5	4	31	8.55235E-03
6	4	32	3.60696E-05
7	4	33	7.51364E-03
8	4	34	8.05886E-03
9	4	35	8.04418E-03
10	4	36	8.85477E-03
11	4	37	3.68433E-03
12	4	38	5.04093E-03
4	5	39	4.37934E-03
5	5	40	3.35417E-03
6	5	41	8.78458E-03
7	5	42	8.18672E-03
8	5	43	7.79957E-03
9	5	44	8.18745E-03

10	5	45	8.75950E-03
11	5	46	3.37339E-03
12	5	47	4.28701E-03
6	6	48	3.90746E-03
7	6	49	2.81545E-03
8	6	50	8.03942E-03
9	6	51	6.71864E-03
10	6	52	8.28494E-03
11	6	53	2.74886E-03
12	6	54	3.99382E-03

## Appendix G

# QUARTZ Input Data for the Test Problem

```
QUARTZ 3 MATERIAL, 54 NODES, 2 GROUP, STEADY-STATE, NO FEEDBACK
C..geom..ng...iupg...nc...nr..irun..ih0..ithfdbk
    3      2      1      54      54      1      0      0
    12      6      1  10.99852262  5.0      0      0
    1      1     950      7   1.00E-6   1.00E-6   1.00E-4   1.00E+0   3
    1.0E-2     20   1.00E-3
    0.08     1.5     0.6
    1.00    200.00
C...cfuel.....ccool....rhof..frozro.....hzero.....u
    2.46E+06  5.43E+07  10.3  2.03252E+05  2.71E+07  2.2E+06
C...ah...vfracc..tinlet..ratioc..pressr....drhdtc
    2.59     0.559    533.0     0.0    1.53E+07  1.60E+07
C..tfref..tcref
    533.0    533.0
C..itmeth..itrtype..nprec..ntdom..nxsmod..icusp..iwt
    2      1      6      1      1      1      3
    0 0 0 0 0 0 0
    1 0 0 0 0 0 0 0 1
    0 0 0 0 0 0 0 0 10
C...Region Map
    1  2  3  4  5  6  7  0  0  0  0  0  0  0
    8  9 10 11 12 13 14 15 16  0  0  0  0  0
    17 18 19 20 21 22 23 24 25 26 27  0
    0 28 29 30 31 32 33 34 35 36 37 38
    0  0  0 39 40 41 42 43 44 45 46 47
    0  0  0  0 48 49 50 51 52 53 54
C...Composition of Regions
    1 2 3 4 5 6 7 8 9 10 11 12 13 14 15 16 17 18 19 20 21 22 23 24 25
    26 27 28 29 30 31 32 33 34 35 36 37 38 39 40 41 42 43 44 45 46 47
    48 49 50 51 52 53 54
C...Cross sections
[Composition 01]: Node (01,01), Non-fuel
    1.011000E+00    1.000000E+00    0.000000E+00    0.000000E+00    4.961454E-03
```

8.547060E-01	0.000000E+00	0.000000E+00	0.000000E+00	6.301030E-05
4.894230E-03				
0.000000E+00				
1.011000E+00	1.000000E+00	0.000000E+00	0.000000E+00	4.961454E-03
8.547060E-01	0.000000E+00	0.000000E+00	0.000000E+00	6.301030E-05
4.894230E-03				
0.000000E+00				
1.011000E+00	1.000000E+00	0.000000E+00	0.000000E+00	4.961454E-03
8.547060E-01	0.000000E+00	0.000000E+00	0.000000E+00	6.301030E-05
4.894230E-03				
0.000000E+00				
1.011000E+00	1.000000E+00	0.000000E+00	0.000000E+00	4.961454E-03
8.547060E-01	0.000000E+00	0.000000E+00	0.000000E+00	6.301030E-05
4.894230E-03				
0.000000E+00				
1.011000E+00	1.000000E+00	0.000000E+00	0.000000E+00	4.961454E-03
8.547060E-01	0.000000E+00	0.000000E+00	0.000000E+00	6.301030E-05
4.894230E-03				
0.000000E+00				
1.011000E+00	1.000000E+00	0.000000E+00	0.000000E+00	4.961454E-03
8.547060E-01	0.000000E+00	0.000000E+00	0.000000E+00	6.301030E-05
4.894230E-03				
0.000000E+00				
1.118089E+00	1.148952E+00	8.506014E-01	1.000000E+00	1.000000E+00
1.705911E+00	9.535692E-01	1.023686E+00	1.000000E+00	1.000000E+00
3.000000E+02	3.000000E+02	3.000000E+02	3.000000E+02	

#### C...Cross sections

[Composition 02]: Node (02,01), Non-fuel

1.011480E+00	1.000000E+00	0.000000E+00	0.000000E+00	5.090824E-03
8.542260E-01	0.000000E+00	0.000000E+00	0.000000E+00	6.312820E-05
5.022150E-03				
0.000000E+00				
1.011480E+00	1.000000E+00	0.000000E+00	0.000000E+00	5.090824E-03
8.542260E-01	0.000000E+00	0.000000E+00	0.000000E+00	6.312820E-05
5.022150E-03				
0.000000E+00				
1.011480E+00	1.000000E+00	0.000000E+00	0.000000E+00	5.090824E-03
8.542260E-01	0.000000E+00	0.000000E+00	0.000000E+00	6.312820E-05
5.022150E-03				
0.000000E+00				
1.011480E+00	1.000000E+00	0.000000E+00	0.000000E+00	5.090824E-03
8.542260E-01	0.000000E+00	0.000000E+00	0.000000E+00	6.312820E-05
5.022150E-03				
0.000000E+00				
1.011480E+00	1.000000E+00	0.000000E+00	0.000000E+00	5.090824E-03
8.542260E-01	0.000000E+00	0.000000E+00	0.000000E+00	6.312820E-05
5.022150E-03				
0.000000E+00				
1.011480E+00	1.000000E+00	0.000000E+00	0.000000E+00	5.090824E-03
8.542260E-01	0.000000E+00	0.000000E+00	0.000000E+00	6.312820E-05
5.022150E-03				
0.000000E+00				
1.143915E+00	8.564618E-01	1.133071E+00	1.000000E+00	1.000000E+00
9.996960E-01	1.067190E+00	2.106013E+00	1.000000E+00	1.000000E+00
3.000000E+02	3.000000E+02	3.000000E+02	3.000000E+02	

#### C...Cross sections

[Composition 03]: Node (03,01), Non-fuel

1.029130E+00	1.000000E+00	0.000000E+00	0.000000E+00	3.849478E-03
8.597270E-01	0.000000E+00	0.000000E+00	0.000000E+00	6.047470E-05
3.767440E-03				
0.000000E+00				
1.029130E+00	1.000000E+00	0.000000E+00	0.000000E+00	3.849478E-03

8.597270E-01	0.000000E+00	0.000000E+00	0.000000E+00	6.047470E-05
3.767440E-03				
0.000000E+00				
1.029130E+00	1.000000E+00	0.000000E+00	0.000000E+00	3.849478E-03
8.597270E-01	0.000000E+00	0.000000E+00	0.000000E+00	6.047470E-05
3.767440E-03				
0.000000E+00				
1.029130E+00	1.000000E+00	0.000000E+00	0.000000E+00	3.849478E-03
8.597270E-01	0.000000E+00	0.000000E+00	0.000000E+00	6.047470E-05
3.767440E-03				
0.000000E+00				
1.029130E+00	1.000000E+00	0.000000E+00	0.000000E+00	3.849478E-03
8.597270E-01	0.000000E+00	0.000000E+00	0.000000E+00	6.047470E-05
3.767440E-03				
0.000000E+00				
1.149719E+00	1.134956E+00	8.875664E-01	1.000000E+00	1.000000E+00
1.012231E+00	1.000318E+00	2.360034E+00	1.000000E+00	1.000000E+00
3.000000E+02	3.000000E+02	3.000000E+02	3.000000E+02	

#### C...Cross sections

##### [Composition 04]: Node (04,01), Non-fuel

1.015590E+00	1.000000E+00	0.000000E+00	0.000000E+00	4.663111E-03
8.569510E-01	0.000000E+00	0.000000E+00	0.000000E+00	6.189730E-05
4.591650E-03				
0.000000E+00				
1.015590E+00	1.000000E+00	0.000000E+00	0.000000E+00	4.663111E-03
8.569510E-01	0.000000E+00	0.000000E+00	0.000000E+00	6.189730E-05
4.591650E-03				
0.000000E+00				
1.015590E+00	1.000000E+00	0.000000E+00	0.000000E+00	4.663111E-03
8.569510E-01	0.000000E+00	0.000000E+00	0.000000E+00	6.189730E-05
4.591650E-03				
0.000000E+00				
1.015590E+00	1.000000E+00	0.000000E+00	0.000000E+00	4.663111E-03
8.569510E-01	0.000000E+00	0.000000E+00	0.000000E+00	6.189730E-05
4.591650E-03				
0.000000E+00				
1.015590E+00	1.000000E+00	0.000000E+00	0.000000E+00	4.663111E-03
8.569510E-01	0.000000E+00	0.000000E+00	0.000000E+00	6.189730E-05
4.591650E-03				
0.000000E+00				
9.584976E-01	9.589261E-01	1.236624E+00	1.000000E+00	1.000000E+00
1.012250E+00	1.035593E+00	3.148536E+00	1.000000E+00	1.000000E+00
3.000000E+02	3.000000E+02	3.000000E+02	3.000000E+02	

#### C...Cross sections

##### [Composition 05]: Node (05,01), Non-fuel

1.029050E+00	1.000000E+00	0.000000E+00	0.000000E+00	3.813500E-03
8.605530E-01	0.000000E+00	0.000000E+00	0.000000E+00	6.014400E-05
3.731700E-03				
0.000000E+00				
1.029050E+00	1.000000E+00	0.000000E+00	0.000000E+00	3.813500E-03
8.605530E-01	0.000000E+00	0.000000E+00	0.000000E+00	6.014400E-05
3.731700E-03				
0.000000E+00				
1.029050E+00	1.000000E+00	0.000000E+00	0.000000E+00	3.813500E-03

8.605530E-01	0.000000E+00	0.000000E+00	0.000000E+00	6.014400E-05
3.731700E-03				
0.000000E+00				
1.029050E+00	1.000000E+00	0.000000E+00	0.000000E+00	3.813500E-03
8.605530E-01	0.000000E+00	0.000000E+00	0.000000E+00	6.014400E-05
3.731700E-03				
0.000000E+00				
1.029050E+00	1.000000E+00	0.000000E+00	0.000000E+00	3.813500E-03
8.605530E-01	0.000000E+00	0.000000E+00	0.000000E+00	6.014400E-05
3.731700E-03				
0.000000E+00				
1.137761E+00	1.151499E+00	8.824108E-01	1.000000E+00	1.000000E+00
1.008615E+00	1.026942E+00	2.850214E+00	1.000000E+00	1.000000E+00
3.000000E+02	3.000000E+02	3.000000E+02	3.000000E+02	

#### C...Cross sections

[Composition 06]: Node (06,01), Non-fuel

1.011400E+00	1.000000E+00	0.000000E+00	0.000000E+00	5.221006E-03
8.564560E-01	0.000000E+00	0.000000E+00	0.000000E+00	6.238670E-05
5.154460E-03				
0.000000E+00				
1.011400E+00	1.000000E+00	0.000000E+00	0.000000E+00	5.221006E-03
8.564560E-01	0.000000E+00	0.000000E+00	0.000000E+00	6.238670E-05
5.154460E-03				
0.000000E+00				
1.011400E+00	1.000000E+00	0.000000E+00	0.000000E+00	5.221006E-03
8.564560E-01	0.000000E+00	0.000000E+00	0.000000E+00	6.238670E-05
5.154460E-03				
0.000000E+00				
1.011400E+00	1.000000E+00	0.000000E+00	0.000000E+00	5.221006E-03
8.564560E-01	0.000000E+00	0.000000E+00	0.000000E+00	6.238670E-05
5.154460E-03				
0.000000E+00				
1.011400E+00	1.000000E+00	0.000000E+00	0.000000E+00	5.221006E-03
8.564560E-01	0.000000E+00	0.000000E+00	0.000000E+00	6.238670E-05
5.154460E-03				
0.000000E+00				
1.011400E+00	1.000000E+00	0.000000E+00	0.000000E+00	5.221006E-03
8.564560E-01	0.000000E+00	0.000000E+00	0.000000E+00	6.238670E-05
5.154460E-03				
0.000000E+00				
8.543475E-01	1.166781E+00	1.074659E+00	1.000000E+00	1.000000E+00
1.093358E+00	1.111537E+00	2.367043E+00	1.000000E+00	1.000000E+00
3.000000E+02	3.000000E+02	3.000000E+02	3.000000E+02	

#### C...Cross sections

[Composition 07]: Node (07,01), Non-fuel

1.009850E+00	1.000000E+00	0.000000E+00	0.000000E+00	5.113423E-03
8.553920E-01	0.000000E+00	0.000000E+00	0.000000E+00	6.275500E-05
5.046840E-03				
0.000000E+00				
1.009850E+00	1.000000E+00	0.000000E+00	0.000000E+00	5.113423E-03
8.553920E-01	0.000000E+00	0.000000E+00	0.000000E+00	6.275500E-05
5.046840E-03				
0.000000E+00				
1.009850E+00	1.000000E+00	0.000000E+00	0.000000E+00	5.113423E-03
8.553920E-01	0.000000E+00	0.000000E+00	0.000000E+00	6.275500E-05
5.046840E-03				
0.000000E+00				
1.009850E+00	1.000000E+00	0.000000E+00	0.000000E+00	5.113423E-03

8.553920E-01	0.000000E+00	0.000000E+00	0.000000E+00	6.275500E-05
5.046840E-03				
0.000000E+00				
1.009850E+00	1.000000E+00	0.000000E+00	0.000000E+00	5.113423E-03
8.553920E-01	0.000000E+00	0.000000E+00	0.000000E+00	6.275500E-05
5.046840E-03				
0.000000E+00				
1.147659E+00	1.089924E+00	8.480709E-01	1.000000E+00	1.000000E+00
1.051479E+00	2.206827E+00	1.070616E+00	1.000000E+00	1.000000E+00
3.000000E+02	3.000000E+02	3.000000E+02	3.000000E+02	

### C...Cross sections

[Composition 08]: Node (01,02), Non-fuel

1.015630E+00	1.000000E+00	0.000000E+00	0.000000E+00	4.560680E-03
8.574440E-01	0.000000E+00	0.000000E+00	0.000000E+00	6.194700E-05
4.489040E-03				
0.000000E+00				
1.015630E+00	1.000000E+00	0.000000E+00	0.000000E+00	4.560680E-03
8.574440E-01	0.000000E+00	0.000000E+00	0.000000E+00	6.194700E-05
4.489040E-03				
0.000000E+00				
1.015630E+00	1.000000E+00	0.000000E+00	0.000000E+00	4.560680E-03
8.574440E-01	0.000000E+00	0.000000E+00	0.000000E+00	6.194700E-05
4.489040E-03				
0.000000E+00				
1.015630E+00	1.000000E+00	0.000000E+00	0.000000E+00	4.560680E-03
8.574440E-01	0.000000E+00	0.000000E+00	0.000000E+00	6.194700E-05
4.489040E-03				
0.000000E+00				
1.015630E+00	1.000000E+00	0.000000E+00	0.000000E+00	4.560680E-03
8.574440E-01	0.000000E+00	0.000000E+00	0.000000E+00	6.194700E-05
4.489040E-03				
0.000000E+00				
1.015630E+00	1.000000E+00	0.000000E+00	0.000000E+00	4.560680E-03
8.574440E-01	0.000000E+00	0.000000E+00	0.000000E+00	6.194700E-05
4.489040E-03				
0.000000E+00				
1.201334E+00	9.500303E-01	9.550136E-01	1.000000E+00	1.000000E+00
3.539485E+00	9.833642E-01	1.012765E+00	1.000000E+00	1.000000E+00
3.000000E+02	3.000000E+02	3.000000E+02	3.000000E+02	

### C...Cross sections

[Composition 09]: Node (02.02). Non-fuel

1.028950E+00	1.000000E+00	0.000000E+00	0.000000E+00	3.819355E-03
8.595140E-01	0.000000E+00	0.000000E+00	0.000000E+00	6.081510E-05
3.738940E-03				
0.000000E+00				
1.028950E+00	1.000000E+00	0.000000E+00	0.000000E+00	3.819355E-03
8.595140E-01	0.000000E+00	0.000000E+00	0.000000E+00	6.081510E-05
3.738940E-03				
0.000000E+00				
1.028950E+00	1.000000E+00	0.000000E+00	0.000000E+00	3.819355E-03
8.595140E-01	0.000000E+00	0.000000E+00	0.000000E+00	6.081510E-05
3.738940E-03				
0.000000E+00				
1.028950E+00	1.000000E+00	0.000000E+00	0.000000E+00	3.819355E-03
8.595140E-01	0.000000E+00	0.000000E+00	0.000000E+00	6.081510E-05
3.738940E-03				
0.000000E+00				
1.028950E+00	1.000000E+00	0.000000E+00	0.000000E+00	3.819355E-03

8.595140E-01	0.000000E+00	0.000000E+00	0.000000E+00	6.081510E-05
3.738940E-03				
0.000000E+00				
1.119391E+00	8.887817E-01	1.147268E+00	1.000000E+00	1.000000E+00
9.361455E-01	2.271564E+00	9.646302E-01	1.000000E+00	1.000000E+00
3.000000E+02	3.000000E+02	3.000000E+02	3.000000E+02	

C...Cross sections

[Composition 10]: Node (03,02), Fuel

6.256770E-01	1.000000E+00	2.102900E-02	5.177440E-02	4.025986E-02
1.752440E-01	0.000000E+00	7.861640E-01	1.915650E+00	9.347370E-01
9.317690E-03				
0.000000E+00				
6.256770E-01	1.000000E+00	2.102900E-02	5.177440E-02	4.025986E-02
1.752440E-01	0.000000E+00	7.861640E-01	1.915650E+00	9.347370E-01
9.317690E-03				
0.000000E+00				
6.256770E-01	1.000000E+00	2.102900E-02	5.177440E-02	4.025986E-02
1.752440E-01	0.000000E+00	7.861640E-01	1.915650E+00	9.347370E-01
9.317690E-03				
0.000000E+00				
6.256770E-01	1.000000E+00	2.102900E-02	5.177440E-02	4.025986E-02
1.752440E-01	0.000000E+00	7.861640E-01	1.915650E+00	9.347370E-01
9.317690E-03				
0.000000E+00				
6.256770E-01	1.000000E+00	2.102900E-02	5.177440E-02	4.025986E-02
1.752440E-01	0.000000E+00	7.861640E-01	1.915650E+00	9.347370E-01
9.317690E-03				
0.000000E+00				
2.326981E+00	1.009809E+00	8.910331E-01	1.000000E+00	1.000000E+00
1.829185E-01	1.016964E+00	1.037429E+00	1.000000E+00	1.000000E+00
3.000000E+02	3.000000E+02	3.000000E+02	3.000000E+02	

C...Cross sections

[Composition 11]: Node (04,02), Fuel

6.259320E-01	1.000000E+00	2.093340E-02	5.153990E-02	4.005944E-02
1.757770E-01	0.000000E+00	7.819390E-01	1.905350E+00	9.295430E-01
9.292370E-03				
0.000000E+00				
6.259320E-01	1.000000E+00	2.093340E-02	5.153990E-02	4.005944E-02
1.757770E-01	0.000000E+00	7.819390E-01	1.905350E+00	9.295430E-01
9.292370E-03				
0.000000E+00				
6.259320E-01	1.000000E+00	2.093340E-02	5.153990E-02	4.005944E-02
1.757770E-01	0.000000E+00	7.819390E-01	1.905350E+00	9.295430E-01
9.292370E-03				
0.000000E+00				
6.259320E-01	1.000000E+00	2.093340E-02	5.153990E-02	4.005944E-02
1.757770E-01	0.000000E+00	7.819390E-01	1.905350E+00	9.295430E-01
9.292370E-03				
0.000000E+00				
6.259320E-01	1.000000E+00	2.093340E-02	5.153990E-02	4.005944E-02
1.757770E-01	0.000000E+00	7.819390E-01	1.905350E+00	9.295430E-01
9.292370E-03				
0.000000E+00				
1.015620E+00	8.770008E-01	2.325874E+00	1.000000E+00	1.000000E+00

9.748828E-01	1.184914E+00	1.770402E-01	1.000000E+00	1.000000E+00
3.000000E+02	3.000000E+02	3.000000E+02	3.000000E+02	

C...Cross sections

[Composition 12]: Node (05,02), Fuel

6.384530E-01	1.000000E+00	1.985340E-02	4.890980E-02	3.756893E-02
1.823710E-01	0.000000E+00	7.311980E-01	1.781710E+00	8.700000E-01
8.430980E-03				
0.000000E+00				
6.384530E-01	1.000000E+00	1.985340E-02	4.890980E-02	3.756893E-02
1.823710E-01	0.000000E+00	7.311980E-01	1.781710E+00	8.700000E-01
8.430980E-03				
0.000000E+00				
6.384530E-01	1.000000E+00	1.985340E-02	4.890980E-02	3.756893E-02
1.823710E-01	0.000000E+00	7.311980E-01	1.781710E+00	8.700000E-01
8.430980E-03				
0.000000E+00				
6.384530E-01	1.000000E+00	1.985340E-02	4.890980E-02	3.756893E-02
1.823710E-01	0.000000E+00	7.311980E-01	1.781710E+00	8.700000E-01
8.430980E-03				
0.000000E+00				
1.192373E+00	1.207913E+00	9.482280E-01	1.000000E+00	1.000000E+00
8.722196E-01	9.429250E-01	9.139632E-01	1.000000E+00	1.000000E+00
3.000000E+02	3.000000E+02	3.000000E+02	3.000000E+02	

C...Cross sections

[Composition 13]: Node (06,02), Fuel

6.258360E-01	1.000000E+00	2.093570E-02	5.154610E-02	4.020384E-02
1.751770E-01	0.000000E+00	7.866550E-01	1.916850E+00	9.350540E-01
9.398820E-03				
0.000000E+00				
6.258360E-01	1.000000E+00	2.093570E-02	5.154610E-02	4.020384E-02
1.751770E-01	0.000000E+00	7.866550E-01	1.916850E+00	9.350540E-01
9.398820E-03				
0.000000E+00				
6.258360E-01	1.000000E+00	2.093570E-02	5.154610E-02	4.020384E-02
1.751770E-01	0.000000E+00	7.866550E-01	1.916850E+00	9.350540E-01
9.398820E-03				
0.000000E+00				
6.258360E-01	1.000000E+00	2.093570E-02	5.154610E-02	4.020384E-02
1.751770E-01	0.000000E+00	7.866550E-01	1.916850E+00	9.350540E-01
9.398820E-03				
0.000000E+00				
8.745675E-01	1.031192E+00	2.353296E+00	1.000000E+00	1.000000E+00
1.078871E+00	1.070611E+00	1.749320E-01	1.000000E+00	1.000000E+00
3.000000E+02	3.000000E+02	3.000000E+02	3.000000E+02	

C...Cross sections

[Composition 14]: Node (07,02), Fuel

6.182640E-01	1.000000E+00	2.128640E-02	5.238320E-02	4.087612E-02
1.757210E-01	0.000000E+00	7.823520E-01	1.906360E+00	9.302900E-01
9.470620E-03	0.000000E+00			
6.182640E-01	1.000000E+00	2.128640E-02	5.238320E-02	4.087612E-02
1.757210E-01	0.000000E+00	7.823520E-01	1.906360E+00	9.302900E-01
9.470620E-03	0.000000E+00			
6.182640E-01	1.000000E+00	2.128640E-02	5.238320E-02	4.087612E-02
1.757210E-01	0.000000E+00	7.823520E-01	1.906360E+00	9.302900E-01
9.470620E-03	0.000000E+00			
6.182640E-01	1.000000E+00	2.128640E-02	5.238320E-02	4.087612E-02
1.757210E-01	0.000000E+00	7.823520E-01	1.906360E+00	9.302900E-01
9.470620E-03	0.000000E+00			
6.182640E-01	1.000000E+00	2.128640E-02	5.238320E-02	4.087612E-02
1.757210E-01	0.000000E+00	7.823520E-01	1.906360E+00	9.302900E-01
9.470620E-03	0.000000E+00			
6.182640E-01	1.000000E+00	2.128640E-02	5.238320E-02	4.087612E-02
1.757210E-01	0.000000E+00	7.823520E-01	1.906360E+00	9.302900E-01
9.470620E-03	0.000000E+00			
6.182640E-01	1.000000E+00	2.128640E-02	5.238320E-02	4.087612E-02
1.757210E-01	0.000000E+00	7.823520E-01	1.906360E+00	9.302900E-01
9.470620E-03	0.000000E+00			
6.182640E-01	1.000000E+00	2.128640E-02	5.238320E-02	4.087612E-02
1.757210E-01	0.000000E+00	7.823520E-01	1.906360E+00	9.302900E-01
9.470620E-03	0.000000E+00			
9.986574E-01	2.363858E+00	9.025772E-01	1.000000E+00	1.000000E+00
8.702871E-01	1.790966E-01	9.457844E-01	1.000000E+00	1.000000E+00
3.000000E+02	3.000000E+02	3.000000E+02	3.000000E+02	

#### C...Cross sections

[Composition 15]: Node (08,02), Non-fuel

1.025640E+00	1.000000E+00	0.000000E+00	0.000000E+00	3.896283E-03
8.599190E-01	0.000000E+00	0.000000E+00	0.000000E+00	6.048710E-05
3.819120E-03	0.000000E+00			
1.025640E+00	1.000000E+00	0.000000E+00	0.000000E+00	3.896283E-03
8.599190E-01	0.000000E+00	0.000000E+00	0.000000E+00	6.048710E-05
3.819120E-03	0.000000E+00			
1.025640E+00	1.000000E+00	0.000000E+00	0.000000E+00	3.896283E-03
8.599190E-01	0.000000E+00	0.000000E+00	0.000000E+00	6.048710E-05
3.819120E-03	0.000000E+00			
1.025640E+00	1.000000E+00	0.000000E+00	0.000000E+00	3.896283E-03
8.599190E-01	0.000000E+00	0.000000E+00	0.000000E+00	6.048710E-05
3.819120E-03	0.000000E+00			
1.025640E+00	1.000000E+00	0.000000E+00	0.000000E+00	3.896283E-03
8.599190E-01	0.000000E+00	0.000000E+00	0.000000E+00	6.048710E-05
3.819120E-03	0.000000E+00			
1.025640E+00	1.000000E+00	0.000000E+00	0.000000E+00	3.896283E-03
8.599190E-01	0.000000E+00	0.000000E+00	0.000000E+00	6.048710E-05
3.819120E-03	0.000000E+00			
8.875130E-01	1.121897E+00	1.134779E+00	1.000000E+00	1.000000E+00
2.475074E+00	9.433575E-01	1.040200E+00	1.000000E+00	1.000000E+00
3.000000E+02	3.000000E+02	3.000000E+02	3.000000E+02	

#### C...Cross sections

[Composition 16]: Node (09,02), Non-fuel

1.012270E+00	1.000000E+00	0.000000E+00	0.000000E+00	4.591709E-03
8.570060E-01	0.000000E+00	0.000000E+00	0.000000E+00	6.195170E-05
4.524080E-03	0.000000E+00			

1.012270E+00	1.000000E+00	0.000000E+00	0.000000E+00	4.591709E-03
8.570060E-01	0.000000E+00	0.000000E+00	0.000000E+00	6.195170E-05
4.524080E-03				
0.000000E+00				
1.012270E+00	1.000000E+00	0.000000E+00	0.000000E+00	4.591709E-03
8.570060E-01	0.000000E+00	0.000000E+00	0.000000E+00	6.195170E-05
4.524080E-03				
0.000000E+00				
1.012270E+00	1.000000E+00	0.000000E+00	0.000000E+00	4.591709E-03
8.570060E-01	0.000000E+00	0.000000E+00	0.000000E+00	6.195170E-05
4.524080E-03				
0.000000E+00				
9.669282E-01	1.164635E+00	9.469263E-01	1.000000E+00	1.000000E+00
9.828683E-01	3.054981E+00	1.003283E+00	1.000000E+00	1.000000E+00
3.000000E+02	3.000000E+02	3.000000E+02	3.000000E+02	

#### C...Cross sections

[Composition 17]: Node (01,03), Non-fuel

1.012060E+00	1.000000E+00	0.000000E+00	0.000000E+00	5.188737E-03
8.560430E-01	0.000000E+00	0.000000E+00	0.000000E+00	6.254890E-05
5.119760E-03				
0.000000E+00				
1.012060E+00	1.000000E+00	0.000000E+00	0.000000E+00	5.188737E-03
8.560430E-01	0.000000E+00	0.000000E+00	0.000000E+00	6.254890E-05
5.119760E-03				
0.000000E+00				
1.012060E+00	1.000000E+00	0.000000E+00	0.000000E+00	5.188737E-03
8.560430E-01	0.000000E+00	0.000000E+00	0.000000E+00	6.254890E-05
5.119760E-03				
0.000000E+00				
1.012060E+00	1.000000E+00	0.000000E+00	0.000000E+00	5.188737E-03
8.560430E-01	0.000000E+00	0.000000E+00	0.000000E+00	6.254890E-05
5.119760E-03				
0.000000E+00				
1.012060E+00	1.000000E+00	0.000000E+00	0.000000E+00	5.188737E-03
8.560430E-01	0.000000E+00	0.000000E+00	0.000000E+00	6.254890E-05
5.119760E-03				
0.000000E+00				
1.098377E+00	8.565215E-01	1.148460E+00	1.000000E+00	1.000000E+00
1.943480E+00	1.119186E+00	1.010098E+00	1.000000E+00	1.000000E+00
3.000000E+02	3.000000E+02	3.000000E+02	3.000000E+02	

#### C...Cross sections

[Composition 18]: Node (02,03), Non-fuel

1.029490E+00	1.000000E+00	0.000000E+00	0.000000E+00	3.862892E-03
8.605930E-01	0.000000E+00	0.000000E+00	0.000000E+00	6.031070E-05
3.781290E-03				
0.000000E+00				
1.029490E+00	1.000000E+00	0.000000E+00	0.000000E+00	3.862892E-03
8.605930E-01	0.000000E+00	0.000000E+00	0.000000E+00	6.031070E-05
3.781290E-03				
0.000000E+00				

1.029490E+00	1.000000E+00	0.000000E+00	0.000000E+00	3.862892E-03
8.605930E-01	0.000000E+00	0.000000E+00	0.000000E+00	6.031070E-05
3.781290E-03				
0.000000E+00				
1.029490E+00	1.000000E+00	0.000000E+00	0.000000E+00	3.862892E-03
8.605930E-01	0.000000E+00	0.000000E+00	0.000000E+00	6.031070E-05
3.781290E-03				
0.000000E+00				
1.029490E+00	1.000000E+00	0.000000E+00	0.000000E+00	3.862892E-03
8.605930E-01	0.000000E+00	0.000000E+00	0.000000E+00	6.031070E-05
3.781290E-03				
0.000000E+00				
1.161062E+00	8.860638E-01	1.134412E+00	1.000000E+00	1.000000E+00
1.059948E+00	2.777243E+00	1.003928E+00	1.000000E+00	1.000000E+00
3.000000E+02	3.000000E+02	3.000000E+02	3.000000E+02	

#### C...Cross sections

##### [Composition 19]: Node (03,03), Fuel

6.256230E-01	1.000000E+00	2.089390E-02	5.144380E-02	4.003618E-02
1.754910E-01	0.000000E+00	7.840950E-01	1.910610E+00	9.324800E-01
9.262120E-03				
0.000000E+00				
6.256230E-01	1.000000E+00	2.089390E-02	5.144380E-02	4.003618E-02
1.754910E-01	0.000000E+00	7.840950E-01	1.910610E+00	9.324800E-01
9.262120E-03				
0.000000E+00				
6.256230E-01	1.000000E+00	2.089390E-02	5.144380E-02	4.003618E-02
1.754910E-01	0.000000E+00	7.840950E-01	1.910610E+00	9.324800E-01
9.262120E-03				
0.000000E+00				
6.256230E-01	1.000000E+00	2.089390E-02	5.144380E-02	4.003618E-02
1.754910E-01	0.000000E+00	7.840950E-01	1.910610E+00	9.324800E-01
9.262120E-03				
0.000000E+00				
6.256230E-01	1.000000E+00	2.089390E-02	5.144380E-02	4.003618E-02
1.754910E-01	0.000000E+00	7.840950E-01	1.910610E+00	9.324800E-01
9.262120E-03				
0.000000E+00				
2.369058E+00	8.907404E-01	9.925388E-01	1.000000E+00	1.000000E+00
1.816978E-01	1.435911E+00	1.081301E+00	1.000000E+00	1.000000E+00
3.000000E+02	3.000000E+02	3.000000E+02	3.000000E+02	

#### C...Cross sections

##### [Composition 20]: Node (04,03), Fuel

6.373060E-01	1.000000E+00	1.999920E-02	4.926360E-02	3.790520E-02
1.820500E-01	0.000000E+00	7.337050E-01	1.787820E+00	8.728800E-01
8.559660E-03				
0.000000E+00				
6.373060E-01	1.000000E+00	1.999920E-02	4.926360E-02	3.790520E-02
1.820500E-01	0.000000E+00	7.337050E-01	1.787820E+00	8.728800E-01
8.559660E-03				
0.000000E+00				
6.373060E-01	1.000000E+00	1.999920E-02	4.926360E-02	3.790520E-02
1.820500E-01	0.000000E+00	7.337050E-01	1.787820E+00	8.728800E-01
8.559660E-03				
0.000000E+00				

6.373060E-01	1.000000E+00	1.999920E-02	4.926360E-02	3.790520E-02
1.820500E-01	0.000000E+00	7.337050E-01	1.787820E+00	8.728800E-01
8.559660E-03				
0.000000E+00				
6.373060E-01	1.000000E+00	1.999920E-02	4.926360E-02	3.790520E-02
1.820500E-01	0.000000E+00	7.337050E-01	1.787820E+00	8.728800E-01
8.559660E-03				
0.000000E+00				
1.185410E+00	9.768788E-01	1.192088E+00	1.000000E+00	1.000000E+00
8.045723E-01	1.047416E+00	9.642700E-01	1.000000E+00	1.000000E+00
3.000000E+02	3.000000E+02	3.000000E+02	3.000000E+02	

#### C...Cross sections

##### [Composition 21]: Node (05,03), Non-fuel

2.034830E+00	1.000000E+00	0.000000E+00	0.000000E+00	2.810096E-04
3.849080E+00	0.000000E+00	0.000000E+00	0.000000E+00	5.142540E-03
4.767560E-05				
0.000000E+00				
2.034830E+00	1.000000E+00	0.000000E+00	0.000000E+00	2.810096E-04
3.849080E+00	0.000000E+00	0.000000E+00	0.000000E+00	5.142540E-03
4.767560E-05				
0.000000E+00				
2.034830E+00	1.000000E+00	0.000000E+00	0.000000E+00	2.810096E-04
3.849080E+00	0.000000E+00	0.000000E+00	0.000000E+00	5.142540E-03
4.767560E-05				
0.000000E+00				
2.034830E+00	1.000000E+00	0.000000E+00	0.000000E+00	2.810096E-04
3.849080E+00	0.000000E+00	0.000000E+00	0.000000E+00	5.142540E-03
4.767560E-05				
0.000000E+00				
2.034830E+00	1.000000E+00	0.000000E+00	0.000000E+00	2.810096E-04
3.849080E+00	0.000000E+00	0.000000E+00	0.000000E+00	5.142540E-03
4.767560E-05				
0.000000E+00				
1.038152E+00	1.010469E+00	1.000191E+00	1.000000E+00	1.000000E+00
1.004196E+00	1.019531E+00	1.011802E+00	1.000000E+00	1.000000E+00
3.000000E+02	3.000000E+02	3.000000E+02	3.000000E+02	

#### C...Cross sections

##### [Composition 22]: Node (06,03), Non-fuel

2.005570E+00	1.000000E+00	0.000000E+00	0.000000E+00	2.748866E-04
3.850430E+00	0.000000E+00	0.000000E+00	0.000000E+00	5.121300E-03
3.916860E-05				
0.000000E+00				
2.005570E+00	1.000000E+00	0.000000E+00	0.000000E+00	2.748866E-04
3.850430E+00	0.000000E+00	0.000000E+00	0.000000E+00	5.121300E-03
3.916860E-05				
0.000000E+00				
2.005570E+00	1.000000E+00	0.000000E+00	0.000000E+00	2.748866E-04
3.850430E+00	0.000000E+00	0.000000E+00	0.000000E+00	5.121300E-03
3.916860E-05				
0.000000E+00				
2.005570E+00	1.000000E+00	0.000000E+00	0.000000E+00	2.748866E-04
3.850430E+00	0.000000E+00	0.000000E+00	0.000000E+00	5.121300E-03
3.916860E-05				
0.000000E+00				

2.005570E+00	1.000000E+00	0.000000E+00	0.000000E+00	2.748866E-04
3.850430E+00	0.000000E+00	0.000000E+00	0.000000E+00	5.121300E-03
3.916860E-05				
0.000000E+00				
1.010130E+00	1.009966E+00	1.030566E+00	1.000000E+00	1.000000E+00
1.013875E+00	9.889832E-01	9.598447E-01	1.000000E+00	1.000000E+00
3.000000E+02	3.000000E+02	3.000000E+02	3.000000E+02	

#### C...Cross sections

##### [Composition 23]: Node (07,03), Fuel

6.444490E-01	1.000000E+00	1.931240E-02	4.759010E-02	3.635129E-02
1.820140E-01	0.000000E+00	7.338490E-01	1.788170E+00	8.732900E-01
8.092700E-03				
0.000000E+00				
6.444490E-01	1.000000E+00	1.931240E-02	4.759010E-02	3.635129E-02
1.820140E-01	0.000000E+00	7.338490E-01	1.788170E+00	8.732900E-01
8.092700E-03				
0.000000E+00				
6.444490E-01	1.000000E+00	1.931240E-02	4.759010E-02	3.635129E-02
1.820140E-01	0.000000E+00	7.338490E-01	1.788170E+00	8.732900E-01
8.092700E-03				
0.000000E+00				
6.444490E-01	1.000000E+00	1.931240E-02	4.759010E-02	3.635129E-02
1.820140E-01	0.000000E+00	7.338490E-01	1.788170E+00	8.732900E-01
8.092700E-03				
0.000000E+00				
6.444490E-01	1.000000E+00	1.931240E-02	4.759010E-02	3.635129E-02
1.820140E-01	0.000000E+00	7.338490E-01	1.788170E+00	8.732900E-01
8.092700E-03				
0.000000E+00				
6.444490E-01	1.000000E+00	1.931240E-02	4.759010E-02	3.635129E-02
1.820140E-01	0.000000E+00	7.338490E-01	1.788170E+00	8.732900E-01
8.092700E-03				
0.000000E+00				
1.136975E+00	1.292516E+00	9.311752E-01	1.000000E+00	1.000000E+00
1.418056E+00	1.228959E+00	1.143449E+00	1.000000E+00	1.000000E+00
3.000000E+02	3.000000E+02	3.000000E+02	3.000000E+02	

#### C...Cross sections

##### [Composition 24]: Node (08,03), Non-fuel

2.001560E+00	1.000000E+00	0.000000E+00	0.000000E+00	3.057428E-04
3.838790E+00	0.000000E+00	0.000000E+00	0.000000E+00	5.346180E-03
5.210780E-05				
0.000000E+00				
2.001560E+00	1.000000E+00	0.000000E+00	0.000000E+00	3.057428E-04
3.838790E+00	0.000000E+00	0.000000E+00	0.000000E+00	5.346180E-03
5.210780E-05				
0.000000E+00				
2.001560E+00	1.000000E+00	0.000000E+00	0.000000E+00	3.057428E-04
3.838790E+00	0.000000E+00	0.000000E+00	0.000000E+00	5.346180E-03
5.210780E-05				
0.000000E+00				
2.001560E+00	1.000000E+00	0.000000E+00	0.000000E+00	3.057428E-04
3.838790E+00	0.000000E+00	0.000000E+00	0.000000E+00	5.346180E-03
5.210780E-05				
0.000000E+00				
2.001560E+00	1.000000E+00	0.000000E+00	0.000000E+00	3.057428E-04
3.838790E+00	0.000000E+00	0.000000E+00	0.000000E+00	5.346180E-03
5.210780E-05				
0.000000E+00				

1.008496E+00	1.034254E+00	1.027153E+00	1.000000E+00	1.000000E+00
9.599595E-01	1.015183E+00	1.008827E+00	1.000000E+00	1.000000E+00
3.000000E+02	3.000000E+02	3.000000E+02	3.000000E+02	

C...Cross sections

[Composition 25]: Node (09,03), Fuel

6.216160E-01	1.000000E+00	2.117960E-02	5.213010E-02	4.074412E-02
1.758020E-01	0.000000E+00	7.816130E-01	1.904560E+00	9.292330E-01
9.507020E-03	0.000000E+00			
6.216160E-01	1.000000E+00	2.117960E-02	5.213010E-02	4.074412E-02
1.758020E-01	0.000000E+00	7.816130E-01	1.904560E+00	9.292330E-01
9.507020E-03	0.000000E+00			
6.216160E-01	1.000000E+00	2.117960E-02	5.213010E-02	4.074412E-02
1.758020E-01	0.000000E+00	7.816130E-01	1.904560E+00	9.292330E-01
9.507020E-03	0.000000E+00			
6.216160E-01	1.000000E+00	2.117960E-02	5.213010E-02	4.074412E-02
1.758020E-01	0.000000E+00	7.816130E-01	1.904560E+00	9.292330E-01
9.507020E-03	0.000000E+00			
6.216160E-01	1.000000E+00	2.117960E-02	5.213010E-02	4.074412E-02
1.758020E-01	0.000000E+00	7.816130E-01	1.904560E+00	9.292330E-01
9.507020E-03	0.000000E+00			
6.216160E-01	2.313788E+00	9.569767E-01	1.000000E+00	1.000000E+00
9.728013E-01	1.821043E-01	9.540974E-01	1.000000E+00	1.000000E+00
3.000000E+02	3.000000E+02	3.000000E+02	3.000000E+02	

C...Cross sections

[Composition 26]: Node (10,03), Non-fuel

1.026920E+00	1.000000E+00	0.000000E+00	0.000000E+00	3.869841E-03
8.602940E-01	0.000000E+00	0.000000E+00	0.000000E+00	6.043480E-05
3.790660E-03	0.000000E+00			
1.026920E+00	1.000000E+00	0.000000E+00	0.000000E+00	3.869841E-03
8.602940E-01	0.000000E+00	0.000000E+00	0.000000E+00	6.043480E-05
3.790660E-03	0.000000E+00			
1.026920E+00	1.000000E+00	0.000000E+00	0.000000E+00	3.869841E-03
8.602940E-01	0.000000E+00	0.000000E+00	0.000000E+00	6.043480E-05
3.790660E-03	0.000000E+00			
1.026920E+00	1.000000E+00	0.000000E+00	0.000000E+00	3.869841E-03
8.602940E-01	0.000000E+00	0.000000E+00	0.000000E+00	6.043480E-05
3.790660E-03	0.000000E+00			
1.026920E+00	1.000000E+00	0.000000E+00	0.000000E+00	3.869841E-03
8.602940E-01	0.000000E+00	0.000000E+00	0.000000E+00	6.043480E-05
3.790660E-03	0.000000E+00			
8.783406E-01	1.143404E+00	1.106115E+00	1.000000E+00	1.000000E+00
2.530528E+00	1.028154E+00	1.011912E+00	1.000000E+00	1.000000E+00
3.000000E+02	3.000000E+02	3.000000E+02	3.000000E+02	

C...Cross sections

[Composition 27]: Node (11,03), Non-fuel

1.011870E+00	1.000000E+00	0.000000E+00	0.000000E+00	5.124417E-03
8.537930E-01	0.000000E+00	0.000000E+00	0.000000E+00	6.330650E-05
5.053900E-03				
0.000000E+00				
1.011870E+00	1.000000E+00	0.000000E+00	0.000000E+00	5.124417E-03
8.537930E-01	0.000000E+00	0.000000E+00	0.000000E+00	6.330650E-05
5.053900E-03				
0.000000E+00				
1.011870E+00	1.000000E+00	0.000000E+00	0.000000E+00	5.124417E-03
8.537930E-01	0.000000E+00	0.000000E+00	0.000000E+00	6.330650E-05
5.053900E-03				
0.000000E+00				
1.011870E+00	1.000000E+00	0.000000E+00	0.000000E+00	5.124417E-03
8.537930E-01	0.000000E+00	0.000000E+00	0.000000E+00	6.330650E-05
5.053900E-03				
0.000000E+00				
1.011870E+00	1.000000E+00	0.000000E+00	0.000000E+00	5.124417E-03
8.537930E-01	0.000000E+00	0.000000E+00	0.000000E+00	6.330650E-05
5.053900E-03				
0.000000E+00				
1.011870E+00	1.000000E+00	0.000000E+00	0.000000E+00	5.124417E-03
8.537930E-01	0.000000E+00	0.000000E+00	0.000000E+00	6.330650E-05
5.053900E-03				
0.000000E+00				
8.549151E-01	1.094126E+00	1.122699E+00	1.000000E+00	1.000000E+00
1.113963E+00	2.156399E+00	1.089074E+00	1.000000E+00	1.000000E+00
3.000000E+02	3.000000E+02	3.000000E+02	3.000000E+02	

#### C...Cross sections

[Composition 28]: Node (02,04), Non-fuel

1.011630E+00	1.000000E+00	0.000000E+00	0.000000E+00	5.107746E-03
8.535720E-01	0.000000E+00	0.000000E+00	0.000000E+00	6.348630E-05
5.039310E-03				
0.000000E+00				
1.011630E+00	1.000000E+00	0.000000E+00	0.000000E+00	5.107746E-03
8.535720E-01	0.000000E+00	0.000000E+00	0.000000E+00	6.348630E-05
5.039310E-03				
0.000000E+00				
1.011630E+00	1.000000E+00	0.000000E+00	0.000000E+00	5.107746E-03
8.535720E-01	0.000000E+00	0.000000E+00	0.000000E+00	6.348630E-05
5.039310E-03				
0.000000E+00				
1.011630E+00	1.000000E+00	0.000000E+00	0.000000E+00	5.107746E-03
8.535720E-01	0.000000E+00	0.000000E+00	0.000000E+00	6.348630E-05
5.039310E-03				
0.000000E+00				
1.011630E+00	1.000000E+00	0.000000E+00	0.000000E+00	5.107746E-03
8.535720E-01	0.000000E+00	0.000000E+00	0.000000E+00	6.348630E-05
5.039310E-03				
0.000000E+00				
1.109676E+00	8.469681E-01	1.151716E+00	1.000000E+00	1.000000E+00
1.941889E+00	1.109923E+00	9.762828E-01	1.000000E+00	1.000000E+00
3.000000E+02	3.000000E+02	3.000000E+02	3.000000E+02	

#### C...Cross sections

[Composition 29]: Node (03,04), Non-fuel

1.028960E+00	1.000000E+00	0.000000E+00	0.000000E+00	3.739247E-03
8.589790E-01	0.000000E+00	0.000000E+00	0.000000E+00	6.076340E-05
3.659550E-03				

0.000000E+00				
1.028960E+00	1.000000E+00	0.000000E+00	0.000000E+00	3.739247E-03
8.589790E-01	0.000000E+00	0.000000E+00	0.000000E+00	6.076340E-05
3.659550E-03				
0.000000E+00				
1.028960E+00	1.000000E+00	0.000000E+00	0.000000E+00	3.739247E-03
8.589790E-01	0.000000E+00	0.000000E+00	0.000000E+00	6.076340E-05
3.659550E-03				
0.000000E+00				
1.028960E+00	1.000000E+00	0.000000E+00	0.000000E+00	3.739247E-03
8.589790E-01	0.000000E+00	0.000000E+00	0.000000E+00	6.076340E-05
3.659550E-03				
0.000000E+00				
1.028960E+00	1.000000E+00	0.000000E+00	0.000000E+00	3.739247E-03
8.589790E-01	0.000000E+00	0.000000E+00	0.000000E+00	6.076340E-05
3.659550E-03				
0.000000E+00				
1.139117E+00	8.906890E-01	1.108292E+00	1.000000E+00	1.000000E+00
1.002486E+00	2.498688E+00	9.482879E-01	1.000000E+00	1.000000E+00
3.000000E+02	3.000000E+02	3.000000E+02	3.000000E+02	

#### C...Cross sections

##### [Composition 30]: Node (04,04), Fuel

6.260820E-01	1.000000E+00	2.091150E-02	5.148880E-02	4.009609E-02
1.753610E-01	0.000000E+00	7.852610E-01	1.913440E+00	9.336110E-01
9.324050E-03				
0.000000E+00				
6.260820E-01	1.000000E+00	2.091150E-02	5.148880E-02	4.009609E-02
1.753610E-01	0.000000E+00	7.852610E-01	1.913440E+00	9.336110E-01
9.324050E-03				
0.000000E+00				
6.260820E-01	1.000000E+00	2.091150E-02	5.148880E-02	4.009609E-02
1.753610E-01	0.000000E+00	7.852610E-01	1.913440E+00	9.336110E-01
9.324050E-03				
0.000000E+00				
6.260820E-01	1.000000E+00	2.091150E-02	5.148880E-02	4.009609E-02
1.753610E-01	0.000000E+00	7.852610E-01	1.913440E+00	9.336110E-01
9.324050E-03				
0.000000E+00				
2.303225E+00	8.673448E-01	1.015050E+00	1.000000E+00	1.000000E+00
1.784595E-01	1.394290E+00	8.601426E-01	1.000000E+00	1.000000E+00
3.000000E+02	3.000000E+02	3.000000E+02	3.000000E+02	

#### C...Cross sections

##### [Composition 31]: Node (05,04), Fuel

6.427510E-01	1.000000E+00	1.967530E-02	4.848480E-02	3.718349E-02
1.813060E-01	0.000000E+00	7.392150E-01	1.801240E+00	8.795500E-01
8.321560E-03				
0.000000E+00				
6.427510E-01	1.000000E+00	1.967530E-02	4.848480E-02	3.718349E-02
1.813060E-01	0.000000E+00	7.392150E-01	1.801240E+00	8.795500E-01
8.321560E-03				

0.000000E+00				
6.427510E-01	1.000000E+00	1.967530E-02	4.848480E-02	3.718349E-02
1.813060E-01	0.000000E+00	7.392150E-01	1.801240E+00	8.795500E-01
8.321560E-03				
0.000000E+00				
6.427510E-01	1.000000E+00	1.967530E-02	4.848480E-02	3.718349E-02
1.813060E-01	0.000000E+00	7.392150E-01	1.801240E+00	8.795500E-01
8.321560E-03				
0.000000E+00				
6.427510E-01	1.000000E+00	1.967530E-02	4.848480E-02	3.718349E-02
1.813060E-01	0.000000E+00	7.392150E-01	1.801240E+00	8.795500E-01
8.321560E-03				
0.000000E+00				
1.202024E+00	9.702629E-01	1.149375E+00	1.000000E+00	1.000000E+00
8.195634E-01	8.849897E-01	7.225326E-01	1.000000E+00	1.000000E+00
3.000000E+02	3.000000E+02	3.000000E+02	3.000000E+02	
C...Cross sections				
[Composition 32]: Node (06,04), Non-fuel				
2.001010E+00	1.000000E+00	0.000000E+00	0.000000E+00	2.809362E-04
3.852950E+00	0.000000E+00	0.000000E+00	0.000000E+00	5.072000E-03
4.025320E-05				
0.000000E+00				
2.001010E+00	1.000000E+00	0.000000E+00	0.000000E+00	2.809362E-04
3.852950E+00	0.000000E+00	0.000000E+00	0.000000E+00	5.072000E-03
4.025320E-05				
0.000000E+00				
2.001010E+00	1.000000E+00	0.000000E+00	0.000000E+00	2.809362E-04
3.852950E+00	0.000000E+00	0.000000E+00	0.000000E+00	5.072000E-03
4.025320E-05				
0.000000E+00				
2.001010E+00	1.000000E+00	0.000000E+00	0.000000E+00	2.809362E-04
3.852950E+00	0.000000E+00	0.000000E+00	0.000000E+00	5.072000E-03
4.025320E-05				
0.000000E+00				
1.025580E+00	9.976717E-01	1.007446E+00	1.000000E+00	1.000000E+00
1.050511E+00	9.817480E-01	9.941753E-01	1.000000E+00	1.000000E+00
3.000000E+02	3.000000E+02	3.000000E+02	3.000000E+02	
C...Cross sections				
[Composition 33]: Node (07,04), Fuel				
6.511910E-01	1.000000E+00	1.910170E-02	4.709850E-02	3.581958E-02
1.818450E-01	0.000000E+00	7.351350E-01	1.791300E+00	8.749240E-01
7.881810E-03				
0.000000E+00				
6.511910E-01	1.000000E+00	1.910170E-02	4.709850E-02	3.581958E-02
1.818450E-01	0.000000E+00	7.351350E-01	1.791300E+00	8.749240E-01
7.881810E-03				
0.000000E+00				
6.511910E-01	1.000000E+00	1.910170E-02	4.709850E-02	3.581958E-02
1.818450E-01	0.000000E+00	7.351350E-01	1.791300E+00	8.749240E-01
7.881810E-03				

0.000000E+00				
6.511910E-01	1.000000E+00	1.910170E-02	4.709850E-02	3.581958E-02
1.818450E-01	0.000000E+00	7.351350E-01	1.791300E+00	8.749240E-01
7.881810E-03				
0.000000E+00				
6.511910E-01	1.000000E+00	1.910170E-02	4.709850E-02	3.581958E-02
1.818450E-01	0.000000E+00	7.351350E-01	1.791300E+00	8.749240E-01
7.881810E-03				
0.000000E+00				
1.153152E+00	1.005232E+00	1.095726E+00	1.000000E+00	1.000000E+00
1.057930E+00	1.170884E+00	1.340466E+00	1.000000E+00	1.000000E+00
3.000000E+02	3.000000E+02	3.000000E+02	3.000000E+02	
C...Cross sections				
[Composition 34]: Node (08,04), Fuel				
6.542950E-01	1.000000E+00	1.910270E-02	4.711300E-02	3.584618E-02
1.816390E-01	0.000000E+00	7.367190E-01	1.795160E+00	8.766660E-01
7.906330E-03				
0.000000E+00				
6.542950E-01	1.000000E+00	1.910270E-02	4.711300E-02	3.584618E-02
1.816390E-01	0.000000E+00	7.367190E-01	1.795160E+00	8.766660E-01
7.906330E-03				
0.000000E+00				
6.542950E-01	1.000000E+00	1.910270E-02	4.711300E-02	3.584618E-02
1.816390E-01	0.000000E+00	7.367190E-01	1.795160E+00	8.766660E-01
7.906330E-03				
0.000000E+00				
6.542950E-01	1.000000E+00	1.910270E-02	4.711300E-02	3.584618E-02
1.816390E-01	0.000000E+00	7.367190E-01	1.795160E+00	8.766660E-01
7.906330E-03				
0.000000E+00				
6.542950E-01	1.000000E+00	1.910270E-02	4.711300E-02	3.584618E-02
1.816390E-01	0.000000E+00	7.367190E-01	1.795160E+00	8.766660E-01
7.906330E-03				
0.000000E+00				
1.026045E+00	1.132765E+00	1.093683E+00	1.000000E+00	1.000000E+00
9.326606E-01	1.040053E+00	8.874442E-01	1.000000E+00	1.000000E+00
3.000000E+02	3.000000E+02	3.000000E+02	3.000000E+02	
C...Cross sections				
[Composition 35]: Node (09,04), Fuel				
6.510590E-01	1.000000E+00	1.942620E-02	4.790580E-02	3.664747E-02
1.817270E-01	0.000000E+00	7.359190E-01	1.793210E+00	8.757130E-01
8.212130E-03				
0.000000E+00				
6.510590E-01	1.000000E+00	1.942620E-02	4.790580E-02	3.664747E-02
1.817270E-01	0.000000E+00	7.359190E-01	1.793210E+00	8.757130E-01
8.212130E-03				
0.000000E+00				
6.510590E-01	1.000000E+00	1.942620E-02	4.790580E-02	3.664747E-02
1.817270E-01	0.000000E+00	7.359190E-01	1.793210E+00	8.757130E-01
8.212130E-03				
0.000000E+00				
6.510590E-01	1.000000E+00	1.942620E-02	4.790580E-02	3.664747E-02
1.817270E-01	0.000000E+00	7.359190E-01	1.793210E+00	8.757130E-01
8.212130E-03				

0.000000E+00				
6.510590E-01	1.000000E+00	1.942620E-02	4.790580E-02	3.664747E-02
1.817270E-01	0.000000E+00	7.359190E-01	1.793210E+00	8.757130E-01
8.212130E-03				
0.000000E+00				
9.149613E-01	1.255830E+00	1.167667E+00	1.000000E+00	1.000000E+00
9.273626E-01	7.233253E-01	9.302710E-01	1.000000E+00	1.000000E+00
3.000000E+02	3.000000E+02	3.000000E+02	3.000000E+02	
C...Cross sections				
[Composition 36]: Node (10,04), Fuel				
6.293190E-01	1.000000E+00	2.078180E-02	5.118170E-02	3.981501E-02
1.756980E-01	0.000000E+00	7.826870E-01	1.907170E+00	9.305110E-01
9.249210E-03				
0.000000E+00				
6.293190E-01	1.000000E+00	2.078180E-02	5.118170E-02	3.981501E-02
1.756980E-01	0.000000E+00	7.826870E-01	1.907170E+00	9.305110E-01
9.249210E-03				
0.000000E+00				
6.293190E-01	1.000000E+00	2.078180E-02	5.118170E-02	3.981501E-02
1.756980E-01	0.000000E+00	7.826870E-01	1.907170E+00	9.305110E-01
9.249210E-03				
0.000000E+00				
6.293190E-01	1.000000E+00	2.078180E-02	5.118170E-02	3.981501E-02
1.756980E-01	0.000000E+00	7.826870E-01	1.907170E+00	9.305110E-01
9.249210E-03				
0.000000E+00				
6.293190E-01	1.000000E+00	2.078180E-02	5.118170E-02	3.981501E-02
1.756980E-01	0.000000E+00	7.826870E-01	1.907170E+00	9.305110E-01
9.249210E-03				
0.000000E+00				
6.293190E-01	1.000000E+00	2.078180E-02	5.118170E-02	3.981501E-02
1.756980E-01	0.000000E+00	7.826870E-01	1.907170E+00	9.305110E-01
9.249210E-03				
0.000000E+00				
8.347458E-01	2.318195E+00	1.067136E+00	1.000000E+00	1.000000E+00
1.584577E+00	1.809598E-01	9.132739E-01	1.000000E+00	1.000000E+00
3.000000E+02	3.000000E+02	3.000000E+02	3.000000E+02	
C...Cross sections				
[Composition 37]: Node (11,04), Non-fuel				
1.030400E+00	1.000000E+00	0.000000E+00	0.000000E+00	3.861425E-03
8.600670E-01	0.000000E+00	0.000000E+00	0.000000E+00	6.049150E-05
3.777320E-03				
0.000000E+00				
1.030400E+00	1.000000E+00	0.000000E+00	0.000000E+00	3.861425E-03
8.600670E-01	0.000000E+00	0.000000E+00	0.000000E+00	6.049150E-05
3.777320E-03				
0.000000E+00				
1.030400E+00	1.000000E+00	0.000000E+00	0.000000E+00	3.861425E-03
8.600670E-01	0.000000E+00	0.000000E+00	0.000000E+00	6.049150E-05
3.777320E-03				
0.000000E+00				
1.030400E+00	1.000000E+00	0.000000E+00	0.000000E+00	3.861425E-03
8.600670E-01	0.000000E+00	0.000000E+00	0.000000E+00	6.049150E-05
3.777320E-03				
0.000000E+00				
1.030400E+00	1.000000E+00	0.000000E+00	0.000000E+00	3.861425E-03
8.600670E-01	0.000000E+00	0.000000E+00	0.000000E+00	6.049150E-05
3.777320E-03				
0.000000E+00				
1.030400E+00	1.000000E+00	0.000000E+00	0.000000E+00	3.861425E-03
8.600670E-01	0.000000E+00	0.000000E+00	0.000000E+00	6.049150E-05
3.777320E-03				

<b>0.000000E+00</b>				
<b>8.832241E-01</b>	<b>1.139036E+00</b>	<b>1.127582E+00</b>	<b>1.000000E+00</b>	<b>1.000000E+00</b>
<b>2.599211E+00</b>	<b>1.054928E+00</b>	<b>1.051488E+00</b>	<b>1.000000E+00</b>	<b>1.000000E+00</b>
<b>3.000000E+02</b>	<b>3.000000E+02</b>	<b>3.000000E+02</b>	<b>3.000000E+02</b>	

### C...Cross sections

### [Composition 38]: Node (12,04), Non-fuel

1.012230E+00	1.000000E+00	0.000000E+00	0.000000E+00	5.193067E-03
8.563410E-01	0.000000E+00	0.000000E+00	0.000000E+00	6.238190E-05
5.123260E-03				
0.000000E+00				
1.012230E+00	1.000000E+00	0.000000E+00	0.000000E+00	5.193067E-03
8.563410E-01	0.000000E+00	0.000000E+00	0.000000E+00	6.238190E-05
5.123260E-03				
0.000000E+00				
1.012230E+00	1.000000E+00	0.000000E+00	0.000000E+00	5.193067E-03
8.563410E-01	0.000000E+00	0.000000E+00	0.000000E+00	6.238190E-05
5.123260E-03				
0.000000E+00				
1.012230E+00	1.000000E+00	0.000000E+00	0.000000E+00	5.193067E-03
8.563410E-01	0.000000E+00	0.000000E+00	0.000000E+00	6.238190E-05
5.123260E-03				
0.000000E+00				
1.012230E+00	1.000000E+00	0.000000E+00	0.000000E+00	5.193067E-03
8.563410E-01	0.000000E+00	0.000000E+00	0.000000E+00	6.238190E-05
5.123260E-03				
0.000000E+00				
8.398760E-01	1.095948E+00	1.160824E+00	1.000000E+00	1.000000E+00
1.151748E+00	2.237727E+00	1.104484E+00	1.000000E+00	1.000000E+00
3.000000E+02	3.000000E+02	3.000000E+02	3.000000E+02	

### C...Cross sections

### [Composition 39]: Node (04,05), Non-fuel

1.015700E+00	1.000000E+00	0.000000E+00	0.000000E+00	4.527411E-03
8.586230E-01	0.000000E+00	0.000000E+00	0.000000E+00	6.130380E-05
4.458110E-03				
0.000000E+00				
1.015700E+00	1.000000E+00	0.000000E+00	0.000000E+00	4.527411E-03
8.586230E-01	0.000000E+00	0.000000E+00	0.000000E+00	6.130380E-05
4.458110E-03				
0.000000E+00				
1.015700E+00	1.000000E+00	0.000000E+00	0.000000E+00	4.527411E-03
8.586230E-01	0.000000E+00	0.000000E+00	0.000000E+00	6.130380E-05
4.458110E-03				
0.000000E+00				
1.015700E+00	1.000000E+00	0.000000E+00	0.000000E+00	4.527411E-03
8.586230E-01	0.000000E+00	0.000000E+00	0.000000E+00	6.130380E-05
4.458110E-03				
0.000000E+00				
1.015700E+00	1.000000E+00	0.000000E+00	0.000000E+00	4.527411E-03
8.586230E-01	0.000000E+00	0.000000E+00	0.000000E+00	6.130380E-05
4.458110E-03				
0.000000E+00				
1.015700E+00	1.000000E+00	0.000000E+00	0.000000E+00	4.527411E-03
8.586230E-01	0.000000E+00	0.000000E+00	0.000000E+00	6.130380E-05
4.458110E-03				
0.000000E+00				
1.015700E+00	1.000000E+00	0.000000E+00	0.000000E+00	4.527411E-03
8.586230E-01	0.000000E+00	0.000000E+00	0.000000E+00	6.130380E-05
4.458110E-03				
0.000000E+00				
1.159865E+00	9.333551E-01	9.649939E-01	1.000000E+00	1.000000E+00
2.465369E+00	1.030408E+00	9.897023E-01	1.000000E+00	1.000000E+00
3.000000E+02	3.000000E+02	3.000000E+02	3.000000E+02	

C...Cross sections

[Composition 40]: Node (05,05), Non-fuel

1.032520E+00	1.000000E+00	0.000000E+00	0.000000E+00	3.527290E-03
8.630430E-01	0.000000E+00	0.000000E+00	0.000000E+00	5.904410E-05
3.443760E-03				
0.000000E+00				
1.032520E+00	1.000000E+00	0.000000E+00	0.000000E+00	3.527290E-03
8.630430E-01	0.000000E+00	0.000000E+00	0.000000E+00	5.904410E-05
3.443760E-03				
0.000000E+00				
1.032520E+00	1.000000E+00	0.000000E+00	0.000000E+00	3.527290E-03
8.630430E-01	0.000000E+00	0.000000E+00	0.000000E+00	5.904410E-05
3.443760E-03				
0.000000E+00				
1.032520E+00	1.000000E+00	0.000000E+00	0.000000E+00	3.527290E-03
8.630430E-01	0.000000E+00	0.000000E+00	0.000000E+00	5.904410E-05
3.443760E-03				
0.000000E+00				
1.032520E+00	1.000000E+00	0.000000E+00	0.000000E+00	3.527290E-03
8.630430E-01	0.000000E+00	0.000000E+00	0.000000E+00	5.904410E-05
3.443760E-03				
0.000000E+00				
1.032520E+00	1.000000E+00	0.000000E+00	0.000000E+00	3.527290E-03
8.630430E-01	0.000000E+00	0.000000E+00	0.000000E+00	5.904410E-05
3.443760E-03				
0.000000E+00				
1.032520E+00	1.000000E+00	0.000000E+00	0.000000E+00	3.527290E-03
8.630430E-01	0.000000E+00	0.000000E+00	0.000000E+00	5.904410E-05
3.443760E-03				
0.000000E+00				
1.032520E+00	1.000000E+00	0.000000E+00	0.000000E+00	3.527290E-03
8.630430E-01	0.000000E+00	0.000000E+00	0.000000E+00	5.904410E-05
3.443760E-03				
0.000000E+00				
1.116497E+00	8.809243E-01	1.123114E+00	1.000000E+00	1.000000E+00
9.937938E-01	2.224542E+00	9.953887E-01	1.000000E+00	1.000000E+00
3.000000E+02	3.000000E+02	3.000000E+02	3.000000E+02	

C...Cross sections

[Composition 41]: Node (06,05), Fuel

6.312830E-01	1.000000E+00	2.053240E-02	5.057530E-02	3.917948E-02
1.763670E-01	0.000000E+00	7.772350E-01	1.893890E+00	9.242970E-01
8.965080E-03				
0.000000E+00				
6.312830E-01	1.000000E+00	2.053240E-02	5.057530E-02	3.917948E-02
1.763670E-01	0.000000E+00	7.772350E-01	1.893890E+00	9.242970E-01
8.965080E-03				
0.000000E+00				
6.312830E-01	1.000000E+00	2.053240E-02	5.057530E-02	3.917948E-02
1.763670E-01	0.000000E+00	7.772350E-01	1.893890E+00	9.242970E-01
8.965080E-03				
0.000000E+00				
6.312830E-01	1.000000E+00	2.053240E-02	5.057530E-02	3.917948E-02
1.763670E-01	0.000000E+00	7.772350E-01	1.893890E+00	9.242970E-01
8.965080E-03				
0.000000E+00				
6.312830E-01	1.000000E+00	2.053240E-02	5.057530E-02	3.917948E-02
1.763670E-01	0.000000E+00	7.772350E-01	1.893890E+00	9.242970E-01
8.965080E-03				
0.000000E+00				
2.180138E+00	9.545839E-01	9.139630E-01	1.000000E+00	1.000000E+00
1.798669E-01	1.620761E+00	1.641379E+00	1.000000E+00	1.000000E+00
3.000000E+02	3.000000E+02	3.000000E+02	3.000000E+02	

C...Cross sections

[Composition 42]: Node (07,05), Fuel

6.521640E-01	1.000000E+00	1.931450E-02	4.763760E-02	3.638084E-02
1.815940E-01	0.000000E+00	7.369490E-01	1.795730E+00	8.769860E-01

8.133410E-03				
0.000000E+00				
6.521640E-01	1.000000E+00	1.931450E-02	4.763760E-02	3.638084E-02
1.815940E-01	0.000000E+00	7.369490E-01	1.795730E+00	8.769860E-01
8.133410E-03				
0.000000E+00				
6.521640E-01	1.000000E+00	1.931450E-02	4.763760E-02	3.638084E-02
1.815940E-01	0.000000E+00	7.369490E-01	1.795730E+00	8.769860E-01
8.133410E-03				
0.000000E+00				
6.521640E-01	1.000000E+00	1.931450E-02	4.763760E-02	3.638084E-02
1.815940E-01	0.000000E+00	7.369490E-01	1.795730E+00	8.769860E-01
8.133410E-03				
0.000000E+00				
6.521640E-01	1.000000E+00	1.931450E-02	4.763760E-02	3.638084E-02
1.815940E-01	0.000000E+00	7.369490E-01	1.795730E+00	8.769860E-01
8.133410E-03				
0.000000E+00				
6.521640E-01	1.000000E+00	1.931450E-02	4.763760E-02	3.638084E-02
1.815940E-01	0.000000E+00	7.369490E-01	1.795730E+00	8.769860E-01
8.133410E-03				
0.000000E+00				
1.085176E+00	8.892384E-01	1.503611E+00	1.000000E+00	1.000000E+00
7.807497E-01	7.918451E-01	9.331366E-01	1.000000E+00	1.000000E+00
3.000000E+02	3.000000E+02	3.000000E+02	3.000000E+02	

#### C...Cross sections

[Composition 43]: Node (08,05), Fuel				
6.571680E-01	1.000000E+00	1.894990E-02	4.675140E-02	3.561059E-02
1.824710E-01	0.000000E+00	7.304670E-01	1.779930E+00	8.693850E-01
7.923680E-03				
0.000000E+00				
6.571680E-01	1.000000E+00	1.894990E-02	4.675140E-02	3.561059E-02
1.824710E-01	0.000000E+00	7.304670E-01	1.779930E+00	8.693850E-01
7.923680E-03				
0.000000E+00				
6.571680E-01	1.000000E+00	1.894990E-02	4.675140E-02	3.561059E-02
1.824710E-01	0.000000E+00	7.304670E-01	1.779930E+00	8.693850E-01
7.923680E-03				
0.000000E+00				
6.571680E-01	1.000000E+00	1.894990E-02	4.675140E-02	3.561059E-02
1.824710E-01	0.000000E+00	7.304670E-01	1.779930E+00	8.693850E-01
7.923680E-03				
0.000000E+00				
6.571680E-01	1.000000E+00	1.894990E-02	4.675140E-02	3.561059E-02
1.824710E-01	0.000000E+00	7.304670E-01	1.779930E+00	8.693850E-01
7.923680E-03				
0.000000E+00				
1.164216E+00	1.165761E+00	9.633418E-01	1.000000E+00	1.000000E+00
1.249535E+00	1.241311E+00	8.282489E-01	1.000000E+00	1.000000E+00
3.000000E+02	3.000000E+02	3.000000E+02	3.000000E+02	

#### C...Cross sections

[Composition 44]: Node (09,05), Fuel				
6.535210E-01	1.000000E+00	1.924220E-02	4.746260E-02	3.622309E-02
1.819840E-01	0.000000E+00	7.341810E-01	1.788980E+00	8.735160E-01
8.081990E-03				
0.000000E+00				
6.535210E-01	1.000000E+00	1.924220E-02	4.746260E-02	3.622309E-02
1.819840E-01	0.000000E+00	7.341810E-01	1.788980E+00	8.735160E-01

8.081990E-03				
0.000000E+00				
6.535210E-01	1.000000E+00	1.924220E-02	4.746260E-02	3.622309E-02
1.819840E-01	0.000000E+00	7.341810E-01	1.788980E+00	8.735160E-01
8.081990E-03				
0.000000E+00				
6.535210E-01	1.000000E+00	1.924220E-02	4.746260E-02	3.622309E-02
1.819840E-01	0.000000E+00	7.341810E-01	1.788980E+00	8.735160E-01
8.081990E-03				
0.000000E+00				
6.535210E-01	1.000000E+00	1.924220E-02	4.746260E-02	3.622309E-02
1.819840E-01	0.000000E+00	7.341810E-01	1.788980E+00	8.735160E-01
8.081990E-03				
0.000000E+00				
9.044355E-01	1.064694E+00	1.523788E+00	1.000000E+00	1.000000E+00
8.466609E-01	7.184429E-01	1.007897E+00	1.000000E+00	1.000000E+00
3.000000E+02	3.000000E+02	3.000000E+02	3.000000E+02	
C...Cross sections				
[Composition 45]: Node (10,05), Fuel				
6.342600E-01	1.000000E+00	2.038510E-02	5.022400E-02	3.886030E-02
1.765050E-01	0.000000E+00	7.760920E-01	1.891100E+00	9.227380E-01
8.882800E-03				
0.000000E+00				
6.342600E-01	1.000000E+00	2.038510E-02	5.022400E-02	3.886030E-02
1.765050E-01	0.000000E+00	7.760920E-01	1.891100E+00	9.227380E-01
8.882800E-03				
0.000000E+00				
6.342600E-01	1.000000E+00	2.038510E-02	5.022400E-02	3.886030E-02
1.765050E-01	0.000000E+00	7.760920E-01	1.891100E+00	9.227380E-01
8.882800E-03				
0.000000E+00				
6.342600E-01	1.000000E+00	2.038510E-02	5.022400E-02	3.886030E-02
1.765050E-01	0.000000E+00	7.760920E-01	1.891100E+00	9.227380E-01
8.882800E-03				
0.000000E+00				
6.342600E-01	1.000000E+00	2.038510E-02	5.022400E-02	3.886030E-02
1.765050E-01	0.000000E+00	7.760920E-01	1.891100E+00	9.227380E-01
8.882800E-03				
0.000000E+00				
9.696097E-01	2.207857E+00	8.912205E-01	1.000000E+00	1.000000E+00
1.641514E+00	1.849008E-01	1.102895E+00	1.000000E+00	1.000000E+00
3.000000E+02	3.000000E+02	3.000000E+02	3.000000E+02	
C...Cross sections				
[Composition 46]: Node (11,05), Non-fuel				
1.032220E+00	1.000000E+00	0.000000E+00	0.000000E+00	3.552610E-03
8.625670E-01	0.000000E+00	0.000000E+00	0.000000E+00	5.912640E-05
3.467690E-03				
0.000000E+00				
1.032220E+00	1.000000E+00	0.000000E+00	0.000000E+00	3.552610E-03
8.625670E-01	0.000000E+00	0.000000E+00	0.000000E+00	5.912640E-05
3.467690E-03				
0.000000E+00				
1.032220E+00	1.000000E+00	0.000000E+00	0.000000E+00	3.552610E-03
8.625670E-01	0.000000E+00	0.000000E+00	0.000000E+00	5.912640E-05

3.467690E-03				
0.000000E+00				
1.032220E+00	1.000000E+00	0.000000E+00	0.000000E+00	3.552610E-03
8.625670E-01	0.000000E+00	0.000000E+00	0.000000E+00	5.912640E-05
3.467690E-03				
0.000000E+00				
1.032220E+00	1.000000E+00	0.000000E+00	0.000000E+00	3.552610E-03
8.625670E-01	0.000000E+00	0.000000E+00	0.000000E+00	5.912640E-05
3.467690E-03				
0.000000E+00				
8.830343E-01	1.115989E+00	1.113831E+00	1.000000E+00	1.000000E+00
2.563519E+00	1.031130E+00	1.052487E+00	1.000000E+00	1.000000E+00
3.000000E+02	3.000000E+02	3.000000E+02	3.000000E+02	
<b>C...Cross sections</b>				
<b>[Composition 47]: Node (12,05), Non-fuel</b>				
1.017460E+00	1.000000E+00	0.000000E+00	0.000000E+00	4.437623E-03
8.581210E-01	0.000000E+00	0.000000E+00	0.000000E+00	6.137980E-05
4.364400E-03				
0.000000E+00				
1.017460E+00	1.000000E+00	0.000000E+00	0.000000E+00	4.437623E-03
8.581210E-01	0.000000E+00	0.000000E+00	0.000000E+00	6.137980E-05
4.364400E-03				
0.000000E+00				
1.017460E+00	1.000000E+00	0.000000E+00	0.000000E+00	4.437623E-03
8.581210E-01	0.000000E+00	0.000000E+00	0.000000E+00	6.137980E-05
4.364400E-03				
0.000000E+00				
1.017460E+00	1.000000E+00	0.000000E+00	0.000000E+00	4.437623E-03
8.581210E-01	0.000000E+00	0.000000E+00	0.000000E+00	6.137980E-05
4.364400E-03				
0.000000E+00				
1.017460E+00	1.000000E+00	0.000000E+00	0.000000E+00	4.437623E-03
8.581210E-01	0.000000E+00	0.000000E+00	0.000000E+00	6.137980E-05
4.364400E-03				
0.000000E+00				
9.357464E-01	1.199854E+00	9.667175E-01	1.000000E+00	1.000000E+00
1.042424E+00	3.059778E+00	1.015974E+00	1.000000E+00	1.000000E+00
3.000000E+02	3.000000E+02	3.000000E+02	3.000000E+02	
<b>C...Cross sections</b>				
<b>[Composition 48]: Node (06,06), Non-fuel</b>				
1.020810E+00	1.000000E+00	0.000000E+00	0.000000E+00	4.087970E-03
8.599620E-01	0.000000E+00	0.000000E+00	0.000000E+00	6.065490E-05
4.010910E-03				
0.000000E+00				
1.020810E+00	1.000000E+00	0.000000E+00	0.000000E+00	4.087970E-03
8.599620E-01	0.000000E+00	0.000000E+00	0.000000E+00	6.065490E-05
4.010910E-03				
0.000000E+00				
1.020810E+00	1.000000E+00	0.000000E+00	0.000000E+00	4.087970E-03
8.599620E-01	0.000000E+00	0.000000E+00	0.000000E+00	6.065490E-05
4.010910E-03				
0.000000E+00				
1.020810E+00	1.000000E+00	0.000000E+00	0.000000E+00	4.087970E-03
8.599620E-01	0.000000E+00	0.000000E+00	0.000000E+00	6.065490E-05

4.010910E-03				
0.000000E+00				
1.020810E+00	1.000000E+00	0.000000E+00	0.000000E+00	4.087970E-03
8.599620E-01	0.000000E+00	0.000000E+00	0.000000E+00	6.065490E-05
4.010910E-03				
0.000000E+00				
1.068608E+00	1.076973E+00	8.772770E-01	1.000000E+00	1.000000E+00
1.968325E+00	1.165940E+00	9.527737E-01	1.000000E+00	1.000000E+00
3.000000E+02	3.000000E+02	3.000000E+02	3.000000E+02	
C...Cross sections				
[Composition 49]: Node (07,06), Non-fuel				
1.044710E+00	1.000000E+00	0.000000E+00	0.000000E+00	3.032305E-03
8.675080E-01	0.000000E+00	0.000000E+00	0.000000E+00	5.720730E-05
2.932660E-03				
0.000000E+00				
1.044710E+00	1.000000E+00	0.000000E+00	0.000000E+00	3.032305E-03
8.675080E-01	0.000000E+00	0.000000E+00	0.000000E+00	5.720730E-05
2.932660E-03				
0.000000E+00				
1.044710E+00	1.000000E+00	0.000000E+00	0.000000E+00	3.032305E-03
8.675080E-01	0.000000E+00	0.000000E+00	0.000000E+00	5.720730E-05
2.932660E-03				
0.000000E+00				
1.044710E+00	1.000000E+00	0.000000E+00	0.000000E+00	3.032305E-03
8.675080E-01	0.000000E+00	0.000000E+00	0.000000E+00	5.720730E-05
2.932660E-03				
0.000000E+00				
1.044710E+00	1.000000E+00	0.000000E+00	0.000000E+00	3.032305E-03
8.675080E-01	0.000000E+00	0.000000E+00	0.000000E+00	5.720730E-05
2.932660E-03				
0.000000E+00				
1.044710E+00	1.000000E+00	0.000000E+00	0.000000E+00	3.032305E-03
8.675080E-01	0.000000E+00	0.000000E+00	0.000000E+00	5.720730E-05
2.932660E-03				
0.000000E+00				
1.159803E+00	8.465802E-01	1.200958E+00	1.000000E+00	1.000000E+00
9.772294E-01	2.388424E+00	1.159927E+00	1.000000E+00	1.000000E+00
3.000000E+02	3.000000E+02	3.000000E+02	3.000000E+02	
C...Cross sections				
[Composition 50]: Node (08,06), Fuel				
6.434310E-01	1.000000E+00	1.978040E-02	4.876720E-02	3.750225E-02
1.775450E-01	0.000000E+00	7.678480E-01	1.871010E+00	9.131460E-01
8.499220E-03				
0.000000E+00				
6.434310E-01	1.000000E+00	1.978040E-02	4.876720E-02	3.750225E-02
1.775450E-01	0.000000E+00	7.678480E-01	1.871010E+00	9.131460E-01
8.499220E-03				
0.000000E+00				
6.434310E-01	1.000000E+00	1.978040E-02	4.876720E-02	3.750225E-02
1.775450E-01	0.000000E+00	7.678480E-01	1.871010E+00	9.131460E-01
8.499220E-03				
0.000000E+00				
6.434310E-01	1.000000E+00	1.978040E-02	4.876720E-02	3.750225E-02
1.775450E-01	0.000000E+00	7.678480E-01	1.871010E+00	9.131460E-01
8.499220E-03				
0.000000E+00				
6.434310E-01	1.000000E+00	1.978040E-02	4.876720E-02	3.750225E-02
1.775450E-01	0.000000E+00	7.678480E-01	1.871010E+00	9.131460E-01
8.499220E-03				
0.000000E+00				
6.434310E-01	1.000000E+00	1.978040E-02	4.876720E-02	3.750225E-02
1.775450E-01	0.000000E+00	7.678480E-01	1.871010E+00	9.131460E-01

8.499220E-03				
0.000000E+00				
2.386298E+00	1.278651E+00	7.508314E-01	1.000000E+00	1.000000E+00
2.070959E-01	1.475668E+00	1.146490E+00	1.000000E+00	1.000000E+00
3.000000E+02	3.000000E+02	3.000000E+02	3.000000E+02	
C...Cross sections				
[Composition 51]: Node (09,06), Fuel				
6.697990E-01	1.000000E+00	1.842940E-02	4.551520E-02	3.447399E-02
1.811140E-01	0.000000E+00	7.403860E-01	1.804100E+00	8.809630E-01
7.626590E-03				
0.000000E+00				
6.697990E-01	1.000000E+00	1.842940E-02	4.551520E-02	3.447399E-02
1.811140E-01	0.000000E+00	7.403860E-01	1.804100E+00	8.809630E-01
7.626590E-03				
0.000000E+00				
6.697990E-01	1.000000E+00	1.842940E-02	4.551520E-02	3.447399E-02
1.811140E-01	0.000000E+00	7.403860E-01	1.804100E+00	8.809630E-01
7.626590E-03				
0.000000E+00				
6.697990E-01	1.000000E+00	1.842940E-02	4.551520E-02	3.447399E-02
1.811140E-01	0.000000E+00	7.403860E-01	1.804100E+00	8.809630E-01
7.626590E-03				
0.000000E+00				
6.697990E-01	1.000000E+00	1.842940E-02	4.551520E-02	3.447399E-02
1.811140E-01	0.000000E+00	7.403860E-01	1.804100E+00	8.809630E-01
7.626590E-03				
0.000000E+00				
8.418673E-01	8.430065E-01	-2.472672E+00	1.000000E+00	1.000000E+00
7.052960E-01	6.274263E-01	-1.790985E-01	1.000000E+00	1.000000E+00
3.000000E+02	3.000000E+02	3.000000E+02	3.000000E+02	
C...Cross sections				
[Composition 52]: Node (10,06), Fuel				
6.434990E-01	1.000000E+00	1.980790E-02	4.883560E-02	3.740915E-02
1.786620E-01	0.000000E+00	7.591320E-01	1.849770E+00	9.027050E-01
8.351600E-03				
0.000000E+00				
6.434990E-01	1.000000E+00	1.980790E-02	4.883560E-02	3.740915E-02
1.786620E-01	0.000000E+00	7.591320E-01	1.849770E+00	9.027050E-01
8.351600E-03				
0.000000E+00				
6.434990E-01	1.000000E+00	1.980790E-02	4.883560E-02	3.740915E-02
1.786620E-01	0.000000E+00	7.591320E-01	1.849770E+00	9.027050E-01
8.351600E-03				
0.000000E+00				
6.434990E-01	1.000000E+00	1.980790E-02	4.883560E-02	3.740915E-02
1.786620E-01	0.000000E+00	7.591320E-01	1.849770E+00	9.027050E-01
8.351600E-03				
0.000000E+00				
6.434990E-01	1.000000E+00	1.980790E-02	4.883560E-02	3.740915E-02
1.786620E-01	0.000000E+00	7.591320E-01	1.849770E+00	9.027050E-01
8.351600E-03				
0.000000E+00				
1.316089E+00	2.431484E+00	7.576988E-01	1.000000E+00	1.000000E+00
1.940100E+00	2.143294E-01	1.112948E+00	1.000000E+00	1.000000E+00

3.000000E+02	3.000000E+02	3.000000E+02	3.000000E+02	
C...Cross sections				
[Composition 53]: Node (11,06), Non-fuel				
1.046450E+00	1.000000E+00	0.000000E+00	0.000000E+00	2.975305E-03
8.648500E-01	0.000000E+00	0.000000E+00	0.000000E+00	5.795730E-05
2.874510E-03				
0.000000E+00				
1.046450E+00	1.000000E+00	0.000000E+00	0.000000E+00	2.975305E-03
8.648500E-01	0.000000E+00	0.000000E+00	0.000000E+00	5.795730E-05
2.874510E-03				
0.000000E+00				
1.046450E+00	1.000000E+00	0.000000E+00	0.000000E+00	2.975305E-03
8.648500E-01	0.000000E+00	0.000000E+00	0.000000E+00	5.795730E-05
2.874510E-03				
0.000000E+00				
1.046450E+00	1.000000E+00	0.000000E+00	0.000000E+00	2.975305E-03
8.648500E-01	0.000000E+00	0.000000E+00	0.000000E+00	5.795730E-05
2.874510E-03				
0.000000E+00				
8.488028E-01	1.154077E+00	1.193382E+00	1.000000E+00	1.000000E+00
2.101261E+00	9.433977E-01	1.208368E+00	1.000000E+00	1.000000E+00
3.000000E+02	3.000000E+02	3.000000E+02	3.000000E+02	
C...Cross sections				
[Composition 54]: Node (12,06), Non-fuel				
1.021220E+00	1.000000E+00	0.000000E+00	0.000000E+00	4.150350E-03
8.615080E-01	0.000000E+00	0.000000E+00	0.000000E+00	6.003710E-05
4.074500E-03				
0.000000E+00				
1.021220E+00	1.000000E+00	0.000000E+00	0.000000E+00	4.150350E-03
8.615080E-01	0.000000E+00	0.000000E+00	0.000000E+00	6.003710E-05
4.074500E-03				
0.000000E+00				
1.021220E+00	1.000000E+00	0.000000E+00	0.000000E+00	4.150350E-03
8.615080E-01	0.000000E+00	0.000000E+00	0.000000E+00	6.003710E-05
4.074500E-03				
0.000000E+00				
1.021220E+00	1.000000E+00	0.000000E+00	0.000000E+00	4.150350E-03
8.615080E-01	0.000000E+00	0.000000E+00	0.000000E+00	6.003710E-05
4.074500E-03				
0.000000E+00				
1.021220E+00	1.000000E+00	0.000000E+00	0.000000E+00	4.150350E-03
8.615080E-01	0.000000E+00	0.000000E+00	0.000000E+00	6.003710E-05
4.074500E-03				
0.000000E+00				
1.073993E+00	1.087152E+00	8.666419E-01	1.000000E+00	1.000000E+00
1.157000E+00	2.482945E+00	9.862874E-01	1.000000E+00	1.000000E+00
3.000000E+02	3.000000E+02	3.000000E+02	3.000000E+02	
C..Core Top [alpha beta] + Bot [alpha beta] for each g (zero current)				
1.00 0.00		1.00 0.00		
1.00 0.00		1.00 0.00		

```

C..Perimeter Alpha(g=1,ng) for each k (zero incoming current)
  1.66998 1.78380
C..Perimeter Beta(g=1,ng) for each k (zero incoming current)
  1.00 1.00
C..n1max..n2max..deltati...itupdj...tphieps...tpkeps
  2000.0    5   1.00E-01     2   1.00E-06  1.00E-05
C...neutron speeds
  1.2500E+07
  2.5000E+05
C...delayed neutron fractions
  0.000247
  0.0013845
  0.001222
  0.0026455
  0.000832
  0.000169
C...precursor half lives
  0.0127
  0.0317
  0.115
  0.311
  1.40
  3.87
C...delayed spectrum
  1.0000E+00
  0.0000E+00
C..Cross Section Reduction
  Region 1
    5 100 3 -1 0 0
    0.00000E+00 0.00000E+00 0.00000E+00 0.00000E+00 0.00000E+00
    0.00000E+00 0.00000E+00 0.00000E+00 0.00000E+00-2.50000E-04
    0.00000E+00
    0.00000E+00
    1.00000E+00 1.00000E+00 1.00000E+00 1.00000E+00 1.00000E+00
    1.00000E+00 1.00000E+00 1.00000E+00 1.00000E+00 1.00000E+00

```